Development of an extended 2D porcine muscle cell culture system and impact of growth promoters on muscle's innate immune resistance

Sujith Sebastian

Thesis submitted to the University of Nottingham

for the degree of Doctor of Philosophy

September, 2015

The University of Nottingham

UNITED KINGDOM · CHINA · MALAYSIA

Abstract

Skeletal muscle comprises about half of the body weight in mammals and its diverse roles in metabolism and innate immune functions makes cultured muscle as a useful tool in biomedical research. In this thesis, some of the major technical obstacles in porcine primary muscle cell cultures such as inadequate differentiation of myoblasts into myotubes and the premature detachment of the formed myotubes have been overcome with the achievement of high differentiation and myotube fusion rate of over 85% along with prolonged maintenance of myotubes in excess of 70 days. Myosin heavy chain (MyHC) expression profile of differentiated myotubes recapitulated adult muscle fibres and displayed phenotypic plasticity of gene expression in response to different media. Growth factor ractopamine (Ract) treatment (1h and 6h) of myotubes followed with subsequent bioinformatics analysis of a stable isotope labelling by amino acids in cell culture (SILAC) based proteomics study suggested differential expression of proteins associated with anti-viral innate immune response and increased protein accretion. Porcine muscle cells were infected with influenza A viruses to evaluate their immune function. Porcine muscle cells expressed influenza virus sialic acid α-2,3 and α-2,6 receptors and were fully permissive to influenza virus infection. Myoblasts produced more virus particles than myotubes. Muscle cells expressed the pro-inflammatory genes tumor necrosis factor alpha (TNF-α) and antiviral gene *Mx-1* and the infected cells had elevated caspase 3/7 activity to indicate apoptosis. However myotubes pre-treated with Ract appeared to confer no reduction in influenza virus output. Evidence presented herein suggests that the functional myotubes developed by this work can be used as a tool to study the molecular mechanisms of growth and innate immune pathways in muscle.

Publications and other scientific achievements related to this thesis

Peer reviewed papers

Sebastian,S., Goulding,L., Kuchipudi,S.V. and Chang,K.C., 2015. Extended 2D myotube culture recapitulates postnatal fibre type plasticity BMC Cell Biol. 16, 23

Baquero-Perez,B., Kuchipudi,S.V., Ho,J., **Sebastian,S**., Puranik,A., Howard,W., Brookes,S.M., Brown,I.H. and Chang,K.C., 2015. Chicken and duck myotubes are highly susceptible and permissive to influenza virus infection J.Virol. 89, 2494-2506

Technology transfer

Biomedical and commercial applicability of the extended 2D myotube culture system succeeded in a technology transfer of this method to Zoetis

Acknowledgements

I would like to thank my supervisor Prof. Kin-Chow Chang, for his supervision and encouragement during the PhD. I also want to thank Dr Suresh Kuchipudi for the motivation he provided. I would like to thank University of Nottingham and Zoetis for providing funding for the PhD. I like to thank Dr. Julia Kydd for her sincere help with thesis corrections. I thank Dr. Zoe Redshaw for providing the porcine myoblasts that I used during my PhD and constructive advises. Also thanks to Dr. Belinda Baquero for training me for the myoblast isolation. I also received great support from Dr Janet Daly who propagated some of the influenza viruses used in this study. I thank Prof. Richard Emes and Dr. Tom Giles for the help they provided with bioinformatics support.

I cordially thank Dr. Pengxiang Chang for his help with PTEC isolation and culturing and also for the good company in lab and office. I must thank my friends and colleagues, Meenu Jassal, Jemima Ho, Seng Lai, Tessa Slater, Sanjeev Kumar, Norazalina Saad and especially Leah Goulding who is successfully continuing the porcine muscle culture work.

I thank my best friend Maqsud Hossain for the blessed friendship and for being there in my hardships. I cordially thank him for the helps he did from day one until the very last minute of my PhD and for the best ever tea times. Alongside I thank our friend Sudhakar Bhandare for the good time we spent together.

I thank Mr Jais Mathew Narikatte for his brotherly support during the hardships.

I must thank my father and mother for their guidance, support and prayers towards this journey. I also thank my brother, sister and my in-laws for all the support they provided.

I thank my wife Neethu and our son Emmanuel for their patience and support during the hard times of PhD.

Declaration

I hereby declare that this thesis has been composed by myself and has not been, or will be, submitted for any other degree elsewhere. The work presented herein is my own and all work of other authors and material from other sources is duly acknowledged. Collaboration with other persons during this work has been fully acknowledged.

Sujith Sebastian

Abbreviations

°C	-	Degree Celsius
µl	-	Microliter(s)
µm	-	Micrometer(s)
µM	-	Micromolar
cDNA	-	Complementary *DNA*
CEE	-	Chick embryo extract
CO_2	-	Carbon dioxide
CPE	-	Cytopathic effect/damage
cRNA	-	Complementary RNA
DAB	-	3,3'-diaminobenzidine- chromogen
DAPI	-	4',6-diamidino-2-phenylindole
DEPC	-	Diethylpyrocarbonate
DM	-	differentiation media
DM1	-	0.4% UG containing DMEM
DM2	-	2% HS conatainig DMEM
DMEM	-	Dulbecco's Modified Eagle Medium
DMSO	-	Dimethyl sulfoxide
DNA	-	Deoxyribonucleic acid
dNTPs	-	Deoxynucleotide triphosphates
dsRNA	-	Double stranded
DTT	-	Dithiothreitol
EDTA	-	*E*thylenediaminetetraacetic acid
FCS	-	Fetal calf serum
GH	-	Growth hormone
h	-	Hour(s)
H&E	-	Haematoxylin and Eosin
h.p.i/hpi	-	Hours Post Infection
HPAI	-	High pathogenic avian influenza virus
HRP	-	Horseradish peroxidase
HS	-	Horse serum
IFN	-	Interferon
IGF-1	-	Insulin like growth factor-1
IL	-	Interleukin
LPAI	-	Low pathogenic avian influenza virus
LPAI	-	Low pathogenic avian influenza
M	-	Matrix
MAA	-	*Maackia amurensis lectin*
MC	-	1:1 mix of Maxgel and Collagen
MC+	-	Maxgel and collagen coating agent dried on the cell culture dish

MC+ method	-	Muscle cellc ulture method developed by this work (combination of MC+ coating,proliferation media and differentiation media conditions)
MC^{+}/MC+ coating	-	MC dried onto cell culture vessel
MDCK	-	Madin-Darby canine kidney
mg	-	Milligram(s)
min	-	Minute(s)
ml	-	Milliliter(s)
mM	-	Millimolar
MOI	-	Multiplicity of infection
mRNA	-	Messenger RNA
MX1	-	Myxovirus (Influenza) Resistance, Homolog Of Murine
NA	-	Neuraminidase
ng	-	Nanogram
nm	-	Nanometer(s)
nM	-	Nanomolar
NP	-	nucleoprotein
NPTr cells	-	Neonatal pig tracheal epithelial cells
O_2	-	Oxygen
p.i.	-	Post-infection
P/S	-	penicillin streptomycin
P/S	-	Penicillin and streptomycin
PBS	-	Phosphate buffered saline
PCR	-	Polymerase chain reaction
Penstrep	-	Penicillin and streptomycin
PM	-	proliferation media
PRRs	-	Pattern-recognition receptors
qPCR	-	quantitative real-time PCR
Ract	-	Ractopamine
RLU	-	Relative Light Unit
RNA	-	Ribonucleic acid
RNase	-	Ribonuclease
rRNA	-	Ribosomal RNA
RT-PCR	-	Reverse transcriptase polymerase chain reaction
SA	-	Sialic acid
sec	-	Second(s)
SILAC	-	Stable isotope labelling by amino acids in cell culture
SNA	-	*Sambucus nigra lectin*
ssRNA	-	Single stranded RNA
TBS	-	Tris buffered saline
TBST	-	Tris-Buffered Saline and Tween 20
TLR-4	-	Toll like receptor 4
TNF-α	-	Tumor necrosis factor-α
tRNA	-	Transfer RNA
UG	-	Ultroser-G; serum replacement

vmRNA	-	Viral messenger RNA
vRNA	-	Viral RNA
vRNP	-	Viral ribonucleoproteins
x g	-	Relative *centrifugal force*

Contents

Abstract ..... **i**

Publications and other scientific achievements related to this thesis ii

Acknowledgements iii

Declaration ..... **v**

Abbreviations ..... **vi**

List of Figures xx

List of Tables xxiv

Chapter 1 Introduction **1**

1.1 Origin and development of muscle 2

1.2 Classification of muscles 2

1.3 Skeletal muscle structure and function 4

1.3.1 Major structural proteins for muscle contraction in the sarcomere 8

1.4 Skeletal muscle differentiation 9

1.4.1 Myogenic regulatory factors (MRF) 9

1.4.2 Postnatal maintenance of skeletal muscle 10

1.5 Skeletal muscle regeneration 11

1.5.1 Satellite cells in skeletal muscle regeneration 12

1.5.2 Role of extra cellular matrix (ECM) in muscle function 13

1.5.3 Molecular markers of skeletal muscle satellite cells 15

1.5.4 Common markers used for satellite cell detection 16

1.6. Skeletal muscle fibre types in mammals 16

1.6.1 Skeletal muscle fibre type classification based on contractile properties .. 17

1.6.2 Skeletal muscle fibre typing based on biochemical properties 19

1.6.3 Skeletal muscle fibre typing based on MyHC expression 20

1.6.4 Myosin heavy chain isoforms expressed in fibres of mammalian skeletal muscle 20

1.6.5 Expression pattern of MyHC isoforms during embryonic and post-natal development 21

1.7 Skeletal muscle fibre plasticity 22

1.7.1 Effect of neuromuscular activity on muscle fibre types 23

1.7.2 Effect of hormones on muscle fibre types 24

1.8 Role of muscle fibre types in muscle quality and quantity 24

1.8.1 Myosin heavy chains and their role in meat quality 25

1.9 Current *in vitro* muscle culture systems- advantages and disadvantages 26

1.9.1 ECM components used in traditional in vitro muscle cultures 27

1.9.2 Porcine muscle cell culture systems 28

1.9 Role of muscle cells in innate immune regulation 29

1.10 Muscle cell culture as a model to study the effects of growth factors on growth and disease resistance 31

1.10.1 Role of growth promoters in growth and immunity 31

1.10.2 IGF-1 in skeletal muscle growth promotion 31

1.10.3 Testosterone in growth promotion 32

1.10.4 Role of Ractopamine in growth promotion 32

1.11 Influenza virus infection as a model to study innate immune regulation of muscle cells 34

1.12 Influenza A virus 34

1.12.1 Structure of influenza virus 35

1.12.2 Influenza virus life cycle 36

1.12.3 Receptors of Influenza virus 37

1.12.4 Influenza infection in pigs 37

1.12.5 Innate immune response to influenza virus infection 38

Hypothesis 39

Aims and objectives 39

Chapter 2 40

General Materials and Methods 40

2.1 Cell culture media 41

2.1.1 Proliferation media for pig myoblasts 41

2.1.2 Differentiation media for pig myoblasts, DM1 41

2.1.3 Differentiation media for long term maintenance of pig myotubes, DM2 42

2.1.4 HSMM cell growth media 42

2.1.5 HSMM fusion (differentiation) media 42

2.1.6 PTEC proliferation media 42

2.1.7 Cell culture media for MDCK cells 43

2.1.8 Cell culture media for NPTr cells 43

2.1.9 Cryopreservation media 43

2.1.10 Infection media 43

2.2 Method of primary cells and cell lines 43

2.2.1 Porcine Primary Myoblast isolation 43

2.2.2 Human Skeletal Muscle Myoblast Cell (HSMM) culture 45

2.2.3 HSMM cell culture 45

2.2.4 Primary Pig Tracheal Epithelial cells (PTECs) isolation and culture 45

2.2.5 Madin-Darby Canine Kidney (MDCK) cells 46

2.2.6 Newborn Pig Tracheal Epithelial (NPTr) cell culture 47

2.3 Extra Cellular Matrix (ECM) coating for pig muscle cell culture 47

2.3.1 Maxgel-Collagen (MC+) surface coating reagent stock solution 47

2.3.2 Procedure to prepare the MC+ coated cell culture vessel 48

2.3.3 Final preparation of MC+ coated flasks or plates 48

2.4 Porcine muscle cell culture 49

2.4.1 Revival of frozen pig myoblasts 49

2.4.2 Passage of pig myoblasts 50

2.4.3 Cryopreservation of pig myoblasts 51

2.4.4 Differentiation of pig myoblasts to myotubes 51

2.4.5 Long term maintenance of differentiated pig myotubes 51

2.4.6 Long term maintenance of porcine myotubes to induce postnatal muscle fibre type 52

2.5 Human skeletal muscle myoblast cells (HSMM) cell culture 52

2.5.1 Revival of cryopreserved HSMM cells 52

2.5.2 Sub culturing and passage of HSMM cells 52

2.5.3 Differentiation of HSMM cells 53

2.5.4 Long term maintenance of HSMM cell differentiated myotubes 53

2.6 Comparison of HSMM myotube fusion rate between standard and MC+ methods 53

2.6.1 Differentiation of HSMM cells using MC+ method 54

2.6.2 Comparison of HSMM fusion rate using MC+ differentiation method 54

2.6.3 Long term maintenance of HSMM myotubes using MC+ method 55

2.7.1 Growth promoter treatment of myotubes 55

2.7.2 Cell fixation and immunocytochemistry 57

2.7.3 Haematoxylin and Eosin (H&E) staining 57

2.7.4 Adenoviral mediated GFP expression in myotubes to examine structural integrity long term 58

2.7.5 Myoblast fusion index of porcine and human skeletal muscle cells 58

2.8 Influenza virus infection of cells 59

2.8.1 Influenza virus subtypes 59

2.8.2 Influenza virus receptor detection using lectin specific immunocytochemistry 60

2.8.3 Calculation of multiplicity of infection (MOI) 60

2.8.4 Influenza virus infection of muscle cells treated with growth promoters .. 61

2.8.5 Quantification of infectious virus released into the culture supernatants .. 62

2.9.1 Measurement of caspase 3/7 activation 63

2.9.2 Cell viability measurement by MTS assay 63

2.9.3 Quantitative real-time reverse transcriptase PCR (qRT- PCR) 64

2.9.3.1 RNA extraction, cDNA reverse transcription and qRT-PCR 64

2.9.3.2 Normalization of qRT-PCR 66

2.10 Statistical analysis 68

Chapter 3 69

Optimisation and characterisation of a long term, 2D myotube culture that recapitulates postnatal fibre plasticity 69

3.1 Abstract 70

3.2 Introduction 71

3.3 Results 74

Part 1: Optimisation of porcine myoblast culture conditions 74

3.3.1 Initial attempts to differentiate porcine myoblasts 75

3.3.2 Further optimisation of myoblast proliferation and differentiation into myotubes 77

a) Media and supplements 77

b) Extracellular matrices 78

c) Combination of collagen and Maxgel ECM extracellular matrices 83

3.3.3 MyHC gene expression of porcine myotubes cultured on different extracellular matrices 87

3.3.4 Enhanced differentiation of myoblasts by MC+ coating 88

3.3.5 Temporal change in myosin heavy chain expression upon differentiation of porcine myoblasts 90

3.3.6 Extended maintenance of porcine myotubes using MC+ method 91

3.3.7 Partial replacement of differentiation media allows prolonged maintenance of myotubes in culture 93

Temporal effect of the partial replacement of DM on myotube integrity 93

3.3.8 Effect of serum withdrawal on myotubes 95

Part 2: Characterisation of porcine myotubes differentiated and maintained using MC+ method 97

3.4.1 MC+ method significantly improved porcine myoblast differentiation 98

3.4.2 Characterisation of differentiated porcine myotubes maintained in culture for 70 days 99

3.4.3 Porcine myotubes maintained viability and expression of muscle protein α-actin during prolonged culture periods 101

3.4.4 Adeno viral mediated GFP marker to demonstrate long term persistence of the formed myotubes 103

..... 104

3.4.5 Differentiated porcine myotubes from different anatomical locations express muscle proteins 104

3.4.6 Differentiated porcine myotubes form actin-myosin striations 106

3.4.6 Porcine myotubes cultured using the MC+ method retain their differentiation for several passages..... 107

3.4.7 Differentiated porcine myotubes cultured for extended periods express MyHC isoforms based phenotypic plasticity and postnatal phenotype..... 109

3.4.8 Differentiated porcine myotubes reflect the MyHC isoform expression of adult muscle fibres..... 113

3.4.9 Myotubes differentiated using MC+ method spontaneously twitch in the culture 114

Part 3: Application of the porcine myotube MC+ culture method to muscle and epithelial cells from other species 115

3.5 Human skeletal muscle myoblasts (HSMM) cells 116

3.5.1 The MC+ muscle culture method significantly improved proliferation and differentiation of HSMM..... 116

3.5.2 MC+ method improved HSMM myoblast fusion..... 118

3.5.3 Maintenance of HSMM myotubes using a modified MC+ culture method over 13 days..... 120

3.5.4 MC+ coating improves mouse skeletal muscle C2C12 cells proliferation 122

3.5.5 MC+ coating improved pig tracheal epithelial cell (PTECs) proliferation 124

3.4 Discussion 126

Chapter 4 131

Towards the identification of early effector targets of ractopamine signalling in primary porcine muscle cells..... 131

Abstract..... 132

4.1 Introduction 133

4.2 Methods 136

4.2.1 SILAC preparation of porcine muscle cells..... 136

4.2.2 Processing of SILAC samples 137

4.2.3 Data analysis..... 139

4.3 Results 140

4.3.1 SILAC compatible media resulted in limited myotube differentiation ... 140

4.3.2 Trends in phosphoprotein and protein expression in response to Ract treatment 141

4.3.3 Differentially expressed proteins and phosphor proteins by Ract treatment 144

4.3.4 Ract treatment of muscle cells possibly induce protein synthesis and fatty acids metabolism..... 145

4.3.5 Ract treatment affected eIF2 signalling pathway by 1h and 6h of stimulation 147

4.3.6 Ract treatment inhibited MAPK/ERK signalling 149

4.3.7 Ract treatment on muscle cells induced changes in innate immune response 151

4.4 Discussion 156

Chapter 5 160

Impact of growth promoters on susceptibility of porcine muscle cells to influenza virus infection 160

Objectives 161

Abstract 161

5.1 Introduction 162

5.2 Results 165

5.2.1 Pig muscle cells express avian and mammalian sialic acid receptors and pig muscle cells are susceptible to influenza virus infection 165

5.2.2 Viral NP from swine H1N1 and pandemic H1N1 viruses accumulated in pig myoblasts in a time dependent manner. 167

5.2.3 Time dependent increase of viral NP expression in pig myotubes infected with pandemic H1N1 and swine H1N1 viruses 169

5.2.4 Higher influenza virus output from pig myoblasts than myotubes 171

5.2.5 Extended infection with swine H1N1 and pandemic H1N1 viruses results in greater cytopathic damage in myoblasts than myotubes 173

5.2.6 Influenza virus activates caspase 3/7 in pig myoblasts and myotubes 175

5.2.7 Ractopamine pre-treatment of myoblasts and myotubes does not affect the pandemic H1N1 virus production 178

5.2.8 Growth promoter ractopamine treatment of pig muscle and epithelial cells prior to influenza virus infection does not reduce progeny virus production ... 181

5.2.9 IGF- 1 and testosterone do not affect influenza virus production in pig myoblasts and myotubes 183

5.2.10 Ractopamine pre-treatment does not affect innate immune gene expression in myoblast or myotubes 184

5.3 Discussion 187

Porcine muscle cells are susceptible and permissive to influenza A virus 187

Effect of growth factors in influenza virus replication in porcine muscle cells 191

Effect of ractopamine in influenza virus replication in pig cells 191

Chapter 6 194

Discussion 194

Future perspectives 207

References 209

List of Figures

Figure 1.1 Graphical representation of a sarcomere (Richfield 2014). 5

Figure 1.2 Structural details of the sarcomere to show myosin and actin striations 7

Figure 1.3. Electron micrograph of a satellite cell (SC) 13

Figure 1.4 Electron micrograph of the structural arrangement of ECM around muscle fibres (Trotter and Purslow, 1992) 14

Figure 1.5. Structure of influenza A virus 36

Figure 3.1 Isolated pig myoblasts expressed Pax3 and Pax7 markers 75

Figure 3.2 Limited myotube formation capacity of porcine myoblasts 76

Figure 3.3 Maxgel ECM provides better differentiation capacity for porcine myoblasts 83

Figure 3.4 Maxgel-collagen surface coating improve myoblast differentiation 86

Figure 3.5 MyHC gene expression in porcine myotubes is influenced by the extracellular matrix coating on which the cells were differentiated. 87

Figure 3.6 Phase contrast micrographs of myotube formation at different time points in differentiation. 89

Figure 3.7 mRNA expression of MyHC isoforms in early stages of porcine myoblast differentiation on MC+ coated plates over 5 days 91

Figure 3.8 Porcine myotubes remain attached to the plate until 28 days of differentiation with some loss of myotubes 92

Figure 3.9 Partial replacement of differentiation media with DM2 allowed improved morphology and maintenance of myotubes or 28 days 94

Figure 3.10 Effect of replacement medium containing charcoal stripped FBS 96

Figure 3.11 The MC+ method improved differentiation capacity of porcine myoblasts compared with the standard culture method 99
Figure 3.12 MC+ method allowed extended culture of differentiated porcine myotubes for up to 70 days 100
Figure 3.13 Porcine myotubes maintained in excess of 50 days remain viable, metabolically functional and show expression of the muscle protein α-actin 102
Figure 3.14 Adeno virus mediated GFP marker expression demonstrated the persistence of intact myotubes in excess of 28 days in culture..... 104
Figure 3.15 Muscle protein expression in myotubes differentiated from myoblasts of different pig muscles 105
Figure 3.16 Differentiated porcine myotubes from LD and diaphragm muscles form acto-myosin striations at 5 and 42 days of differentiation 107
Figure 3.17 Porcine myoblasts cultured using MC+ method maintain their proliferation and differentiation capacity over seven passages..... 108
Figure 3.18 Extended myotube cultures exhibited phenotype plasticity 111
Figure 3.19 Differentiated porcine myotubes maintained in DM1 medium recapitulates adult pig muscle fibre type MyHC expression 113
Figure 3.20 MC+ method improved proliferation and differentiation of HSMM cells 117
Figure 3.21 The MC+ muscle culture method improved the number of HSMM fusion and differentiation into myotubes 119
Figure 3.22 Modified MC+ method allowed extended maintenance of HSMM myotubes in excess of16 days. 121
Figure 3.23 MC+ coating improved the proliferation of the C2C12 cell line 123

Figure 3.24 MC+ coating improves PTECs proliferation compared with Maxgel extracellular matrix. 125
Figure 4.1 Intracellular signaling pathways of the β-adrenergic receptor. 134
Figure 4.1 SILAC analysis flow chart showing the key steps in the process. 139
Figure 4.2 Use of SILAC-compatible culture reagents produced limited porcine myotubes. 140
Figure 4.3 Overview of the SILAC proteomics expression data 142
Figure 4.4 Representation of details such as peptides identified and quantified for each protein and the percentage coverage of protein sequence as shown in the protein file (Analysis Results Z1-10) 143
Figure 4.6 Comparisons of fold change in phosphoproteins and corresponding proteins at 1h (A) and 6h (B) of Ract treatment. 145
Figure 4.7 Most significant phosphoprotein networks detected were linked to (A) RNA modifications and protein synthesis, and (B) fatty acids metabolism. 146
Figure 4.8 eIF2 signalling was the most significant canonical pathway affected by Ract at 1h and 6h of stimulation (IPA derived). 148
Figure 4.9 Ractopamine treatment on porcine muscle cells inhibited ERK/MAPK signalling. 150
Figure 4.10 Ract treatment regulates host proteins to inhibit viral infection. 152
Figure 4.11 IFNA2 was identified as an upstream regulator using IPA algorithm.. 153
Figure 4.12 Ractopamine induced changes in viral sensors and anti-viral response. 155
Figure 5.1 Pig myoblasts and myotubes express sialic acid receptors and are susceptible to avian and mammalian influenza virus infection 166

Figure 5.2 Pig myoblasts infected with pandemic H1N1 virus and swine H1N1 viruses accumulated viral NP in a time dependent manner 168
Figure 5.3 Pig myotubes infected with pandemic H1N1 or swine H1N1 virus accumulated viral NP in a time dependent manner..... 170
Figure 5.4 Infected pig myoblasts released more infective virus than corresponding myotubes 172
Figure 5.5 Extended infection of pig myotubes with swine H1N1 and pandemic H1N1 influenza viruses produced less cytopathic damage than corresponding myoblasts 174
Figure 5.6 Influenza virus infected pig muscle cells displayed elevated caspase 3/7 activity..... 178
Figure 5.7 Ractopamine pre-treatment did not affect the subsequent production of pandemic H1N1 virus in pig myoblasts and myotubes..... 180
Figure 5.8 Ractopamine treatment of pig myotubes and NPTr cells led to increased H2N3 virus production..... 183
Figure 5.9 IGF-1 and testosterone did not affect pandemic H1N1 virus production from infected myoblasts and myotubes..... 184
Figure 5.10 Ractopamine treatment did not affect innate immune gene expression or influenza M gene expression in myoblasts and myotubes infected with swine H1N1 or pandemic H1N1 virus 186

List of Tables

Table 1.1 Properties of slow and fast skeletal frog muscle fibres 19

Table 1.2 Myosin heavy chain isoforms expressed in mammals and the genes encoding these proteins 21

Table 2.1 Volume of MC+ coating reagent required for different tissue culture vessels 48

Table 2.2 Volume of cell suspension in proliferation media recommended for different tissue culture flasks or multiwall plates. 50

Table 2. 3 Details of the growth promoter concentrations used on myotubes cultures 56

Table 2.4 Influenza virus subtypes used in this study 59

Table 2.5 Components of the qRT-PCR master mix 65

Table 2.6 Cycling conditions for taqman qRT-PCR 66

Table 2.7 Selected genes and their PCR primers and probes used to assess muscle cells, influenza virus and innate immune response 67

Table 3.1 Proliferation media and supplements used to improve myoblast differentiation 78

Table 3.2 Media supplements used in proliferation and differentiation of porcine myoblasts grown on collagen or Maxgel ECM as coating agent 80

Table 3.3 Media supplements used for myoblasts grown on Maxgel or Maxgel-Collagen (1:1) coated plates 84

Table 3.4 Cell culture media supplements used for the optimisation of myoblast cultures on MC+ coated plates 88

Table 4.1 Summary SILAC experimental design and Ract treatment. 137

Table 4.2 Detection summary of proteins and phosphoproteins 145

Chapter 1 Introduction

1.1 Origin and development of muscle

Muscle as a soft tissue comprises around half of the body weight in mammals. Primary function of muscle is to provide support in body posture, maintain joint structure and also to help in actions such as the movement of an organism. Muscle also supports vital functions such as the contraction of the heart which circulates movement of blood through the arteries and veins (Joseph Hill 2012) .

During embryogenesis, muscle originates from the mesodermal layer as a thin layer of tissue called a primary myotome. Highly coordinated cell proliferation (Gros et al. 2004), migration (Cinnamon et al. 1999) and movements (Holtzer et al. 1957) helps to arrange the muscle cells in the early embryo. Progressively the mononucleated myoblasts differentiate and fuse into multinucleated myofibrils (Holtzer et al., 1957).

1.2 Classification of muscles

Major characteristic of a muscle tissue is its ability to contract and assist in movements. Movements can be such like the movement of the whole organism or intra organ functions such moving blood through a blood vessel. Muscle can be classified into three types, based on its specialised functions.

Skeletal muscle

Skeletal muscle is the most abundant type of muscle present in mammals and its primary role is to support movements of the organism and provide fine motor skills. Such movements are possible due to the ability of muscle to contract and relax. A fundamental unit of contractile muscle tissue is a sarcomere where parallel fibres of myosin and actin interact or cross-bridge which results in contraction. Due to the arrangement of myosin, which is a thick filament and a thin filament of actin, skeletal

muscle appears to be striped. Each sarcomere is about 2.5µm in length and thousands of them are arranged linearly to form a long muscle. During embryogenesis, skeletal muscle is formed by the differentiation and fusion of multiple myoblasts into a myotube or a syncytial structure with multiple nuclei in a tubular form. A description of the detailed structure of skeletal muscle is given in Section 1.5

Cardiac muscle

In the muscular walls of the heart, the myocardium is made up of involuntarily contractile muscle tissue which controls the blood circulation throughout the body's organs and tissues. Myocardium is composed of repeating sarcomere units and microscopically, has striations due to the actin-myosin cross-bridging within the sarcomeres. Contraction of the myocardium is involuntary and the beats of the heart are synchronized. Although the cells appear striated, they remain as single unfused cells with a single nucleus and are tightly connected by intercalated discs.(Lin et al. 1997).

Smooth muscle

Smooth muscle is present in the walls of most blood vessels and organs which have a tubular structure, such as intestines. Unlike the striated appearance of skeletal or cardiac muscles, smooth muscle has no stripes, because the actin-myosin filaments in these cells are arranged randomly (Dominguez et al. 1998). Smooth muscle cells remain as mononuclear cells, but are connected to each other by special cell junctions called gap junctions. Smooth muscle contraction is controlled involuntarily during functions such as blood flow through a vein or movement of food through the intestine (Somlyo & Somlyo 1994).

1.3 Skeletal muscle structure and function

Skeletal muscle fibre appears striated when seen under higher magnification. The striations are formed of the repeating units of sarcomeres which are the functional units of skeletal muscle. Microstructure of the skeletal muscle from different species were illustrated by William Bowman in 1840 (Bowman 1840). He defined that the skeletal muscle fibril is covered by a membrane or sheath called sarcolemma. Detailed structure of the sarcolemma was elucidated by electron micrographic imaging(Mauro & Adams, 1961). These striations are formed due to the longitudinally arranged structural proteins, mainly the thick band of myosin heavy chains and light bands of sarcomeric α-actin. Graphical representation of a sarcomere is shown below (Figure 1.1).

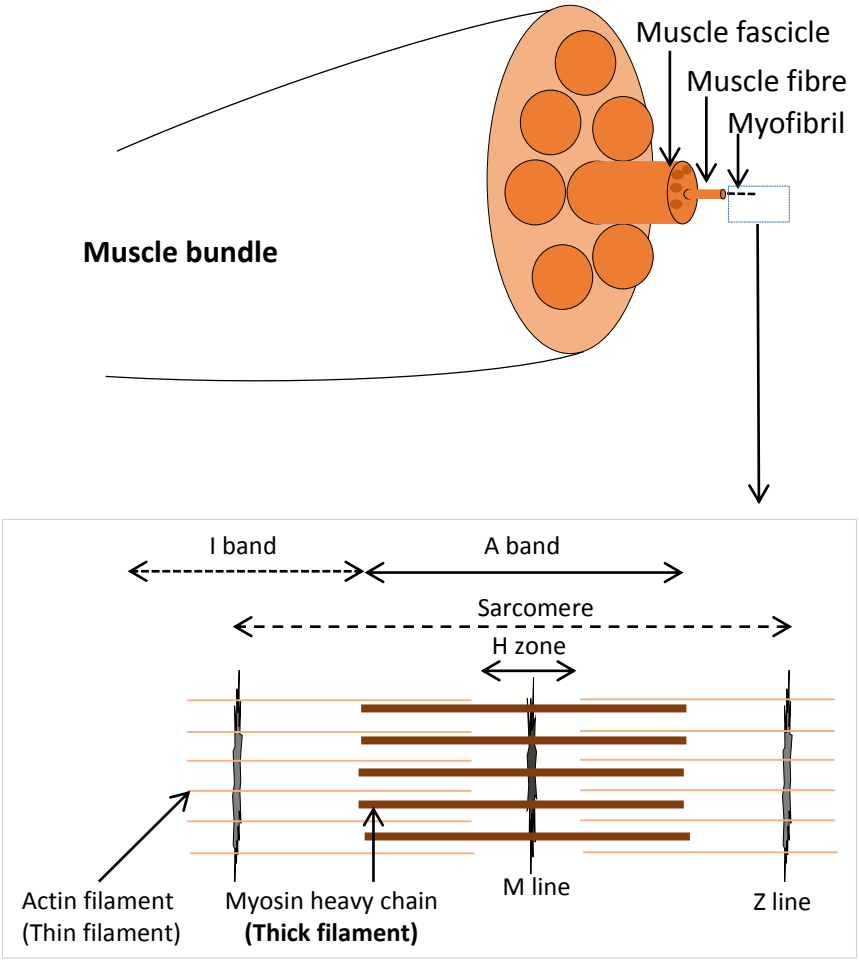

Figure 1.1 Graphical representation of a sarcomere (Richfield 2014).

A graphical representation of the structural details of a sarcomere. A muscle that is attached to the bone by tendons is formed of several fascicles of muscle and each fascicle contains several muscle fibres within it. Each muscle fibre is composed of many myofibrils that are composed of the longitudinally arranged think myosins and light actin filaments which essentially make the muscle fibre to be striated.

Sarcomeres are repeating units of contractile machinery which is composed of number of proteins. Major functional components of the sarcomere composed of thick myosin filament and thin actin filament. These two proteins cross link to initiate contraction. Both ends of a sarcomere contain Z-discs and the actin-myosin filaments arranged between these Z-dics. The region within a sarcomere that contains actin filaments that are not superimposed by myosin think filaments is known as I band or isotropic band

which is referred as light band. The region within a sarcomere where myosin filament is present an also appear darker in colour is called A band or anisotropic band. Presence of these alternative dark and light bands in sarcomere gives the striated appearance for myotubes. H zone is the central area where the thick myosin filament present not superimposed with actin filament thus appear paler within the A band. M line is a disc like region in the middle a sarcomere where the myosin filaments cross connected to the cytoskeleton (Campbell & Reece 2002). Number of myofibrils present in a muscle fibre varies between different muscles and species. Some studies using mice biceps branchii showed that the number of myofibrils increases from about 75 to 1200 in postnatal condition and with a diameter of 0.2-1.2 µm and average myofibrils had about 0.5 µm diameter(Goldspink, 1970). Electron microscopic analysis of myofibres revealed the ultrastructure of sarcomere. Although the *in vitro* differentiated myotubes are not fully comparable to in vivo myofibres, striations are visible by light microscope and myotubes that were generated as a part of this is shown here to compare to the electron micrograph of a sarcomere. Myotubes that were generated by the present study demonstrated the presence of striations. Myotubes within the sarcomere are striated as shown in Figure 1.2 which employed immunohistochemistry to reveal a myosin heavy chain fast isoform.

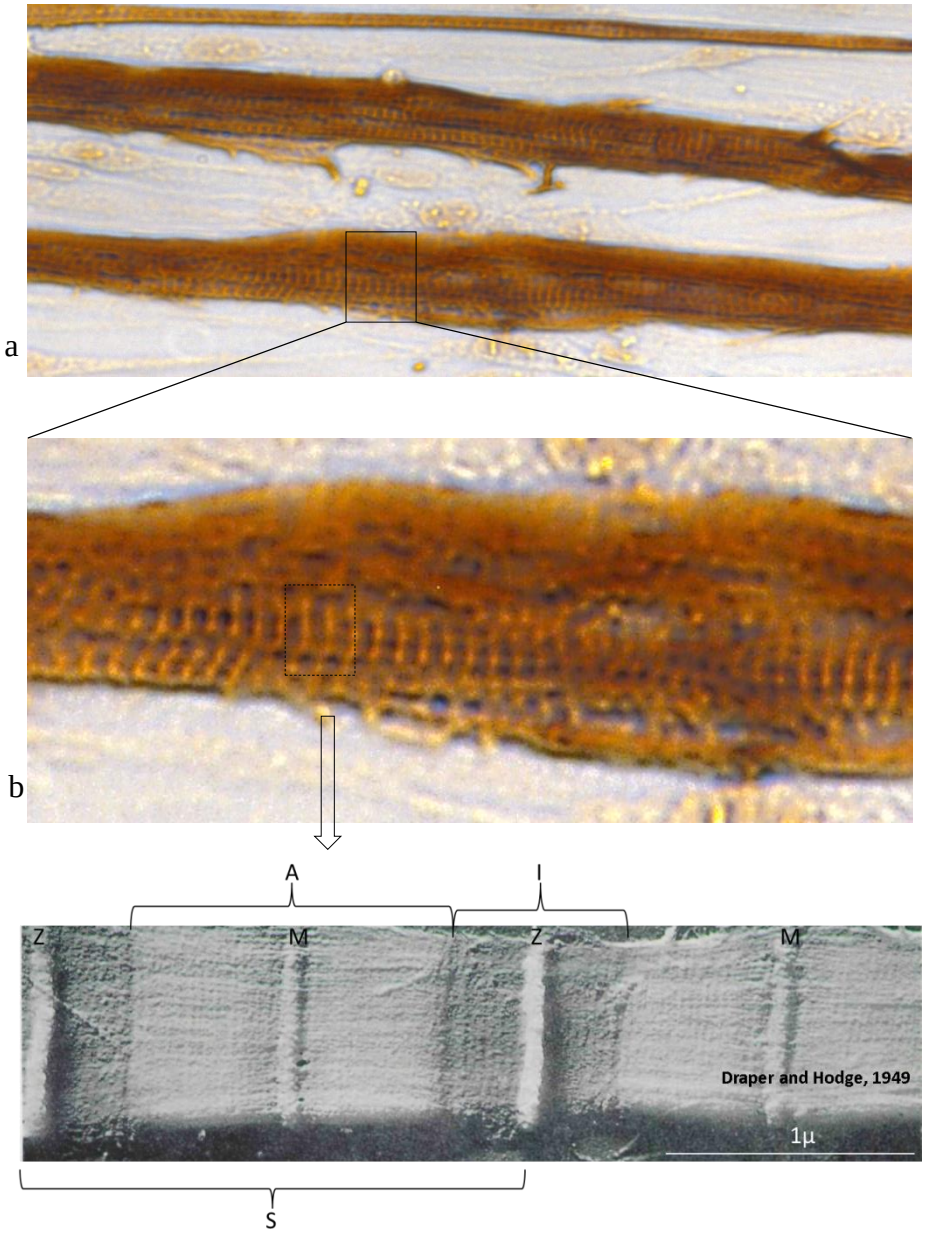

Figure 1.2 Structural details of the sarcomere to show myosin and actin striations

a) and b) porcine myotubes cultured *in vitro* then immunostained with an antibody specific for a myosin heavy chain fast isoform. Image was zoomed to the presented stage, no scale bar shown. Electron micrograph of a sarcomere to illustrate the sarcomeric (S) structure involving M line (M), A band (A), I band (I) and Z disc (Z) within I band. Image taken from Draper and Hodge 1949.

1.3.1 Major structural proteins for muscle contraction in the sarcomere

A major proportion of proteins present in the sarcomere consist of myosin and actin filaments. Myosin is a member of the myosin gene family which contains thirteen genes which are differentially expressed within separate muscles. Myosin is a mechanochemical enzyme or motor protein (Oplatka et al. 1974) and is found in a dimeric form with a head , neck and a tail regions . Biochemically, myosin acts as an ATPase enzyme, converting the chemical energy of ATP into mechanical energy to use for motor functions. For myosin to function as a motor protein during muscle contraction, it interacts with actin filaments (Krans 2010).

Along with myosin and actin, other proteins are involved in muscle contraction, including tropomyosin and troponins which are bound to the actin filament. Upon motor neuron stimulation, sarcoplasmic reticulum releases Ca^{++} which binds to troponin and leads tropomyosin to make a conformational change in the actin filament, resulting in exposure of the myosin binding sites. Subsequently myosin binds to actin to form crossbridges, which results in muscle contraction (Brenner & Eisenberg 1987). As a new ATP molecule binds onto the myosin, it releases the crossbridge and initiates another round of actin binding to make the contraction if Ca^{++} is present. Titin is another protein that keeps the myosin protein in place by binding to the Z line. Alpha actinin also expressed at the Z line and myomesins help the myosin to maintain at the M line. Nebulin is another actin binding protein which can bind to about 200 actin monomers. Myosin light chain is also present in the sarcomere.

1.4 Skeletal muscle differentiation

In vitro, characterisation of cells isolated from early embryos revealed that the isolated myoblasts can differentiate into two diverse fibre types which can contract either fast or slowly (Miller & Stockdale 1986). This indicates the capacity of myoblasts to differentiate into different types of muscle fibres.

Another milestone in the characterisation of skeletal muscle differentiation was that the overexpression of a basic-helix-loop-helix protein MyoD converts fibroblasts and adipoblast cell lines into myogenic cells (Tapscott et al. 1988). MyoD is expressed exclusively in active satellite cells or myoblasts and not in non-muscle cells and although other muscle regulatory factors exist, MyoD is considered to be the master regulator of skeletal muscle differentiation. In a quiescent satellite cell, the expression level of MyoD is very low, but exercise or muscle damage can induce MyoD in a dose dependent manner to commit the satellite cells' differentiation into myoblasts. Thus MyoD expression was observed to be upregulated by the denervation of a muscle or small cut in a tendon (Koishi et al. 1995). Further evidence for the critical role of MyoD in skeletal muscle differentiation was provided by the production of $MyoD^{-/-}$ knockout mice which showed reduced muscle differentiation potential (Koishi et al. 1995).

1.4.1 Myogenic regulatory factors (MRF)

In addition to MyoD, other proteins contribute to skeletal muscle differentiation. Myogenin, Myf-5 and MRF4 were found to induce myogenesis in different cell types (Perry & Rudnick 2000). These four proteins are considered to be the main myogenic regulatory factors or MRFs. These proteins form homo or heterodimers with each other

or with other proteins to regulate myogenesis (Funk et al. 1991). In a quiescent satellite cell, Myf-5 expression occurs initially to commit the cell to myogenesis and subsequently MyoD is activated, followed by the activation of MRF4 (Buckingham & Rigby 2014). Upon differentiation of myoblasts, muscle specific proteins are expressed in a highly coordinated manner and as a result, the expression of some of the contractile proteins such as myosins heavy chains (MyHCs) increases by several hundred fold (Devlin & Emerson 1978). Among the MRFs, Myf5 and MyoD are considered to be the myogenic determination factors since the null mutants for these genes failed to generate any muscle (Rudnicki et al. 1993).

1.4.2 Postnatal maintenance of skeletal muscle

An enormous increase in satellite cell proliferation occurs soon after birth and the increased number of satellite differentiate and fuse into muscle fibres (Chiakulas & Pauly 1965) which results in an increase in muscle fibre number postnatally. The resultant muscle fibre numbers within an individual muscle may be maintained into adulthood or may reduce with age (Picard et al. 2002) . Studies showed that the total nuclei in skeletal muscle fibres in a new born rat increases up to 100s to thousand fold from the first weeks to the first few months of growth (Enesco & Puddy, 1964). Although the satellite cells have the capacity to proliferate and maintain the skeletal muscle mass, a proportion of the satellite cells remains non-proliferative and avoids cell division. This preserves the satellite cell stock (Schultz 1996). Several factors can affect the non-proliferative state of the satellite cells. It was postulated that some unknown growth factors which diffuse through the muscle fibres from damaged muscle are highly potent inducers for proliferation of satellite cells (Schultz & McCormick 1994; Bischoff 1986a). Quiescent muscle satellite cells respond to chick

embryo extracts or fibroblast growth factor by proliferating actively and myoblasts fuse into multinucleated myotubes (Bischoff 1986b). Treatment of satellite cells with extracts from damaged muscle cells with serum induced and maintained the proliferation of satellite cells in culture. This suggests that factors are required from the damaged muscle to induce proliferation and the factors from serum is required to maintain the cell division (Bischoff 1990)

Satellite cells are recruited to repair the muscle tissue that has undergone a trauma, proliferation and fusion of myoblasts were detected in degenerating muscle fibres (Church et al. 1966; Shafiq et al. 1967) . Along with the differentiation of the satellite cells into myoblasts, a part of the cells were maintained as satellite cell reservoir upon this regeneration process(Church 1970). By using H^3-thymidine as a DNA integration marker for cell division it was showed that the satellite cells incorporate it and after few cycles the cells reduce the replication capacity subsequently increased number of nuclei were observed in myotubes (Moss & Leblond 1970; Moss & Leblond 1971).

1.5 Skeletal muscle regeneration

Skeletal muscle tissue can undergo a significant amount of damage following injury and trauma, ischemia or as a result of disease. Fortunately, muscle has a considerable capacity to regenerate compared with other tissues and this has been shown experimentally. Thus, in damaged or degenerating muscle tissue, inflammation, characterised by heat, pain and swelling develops. As the flow of lymph and blood and accompanying white blood cells to the damaged area increases, vascular permeability increases, permitting migration of white cells into the damaged area. Thus damaged myotubes are ingested by infiltrating phagocytes within one to two days of damage if the cells are nearer to blood vessels. Degenerating myotubes which are most distant

from blood vessels undergo necrosis and are eventually phagocytosed within a few days to few weeks (O'steen 1963; Carlson & Faulkner 1983; Carlson 1973). The unique regeneration capacity of muscle is mainly due to the availability of satellite cells. However, other cells such as bone marrow derived mesenchymal stem cells also migrate to the area of muscle damage and participate in regeneration (Ferrari 1998). Muscle tissue of the hind limb was irradiated with X-ray to denature the DNA of myofibre and satellite cells resulted in no regeneration, even with the help of circulating mesenchymal stem cells (Wakeford et al. 1991). Thus satellite cells appear to be the principle cell population involved in skeletal muscle regeneration (Partridge 2002).

1.5.1 Satellite cells in skeletal muscle regeneration

Early reports suggested that skeletal muscle regeneration involved the accumulation of muscle protein within the myotubes, since no apparent cell division was observed (Lewis & Lewis 1917). Later observations of the regeneration of skeletal muscle in the absence of cell division suggested that many mononucleated myoblasts fuse to form multinucleated structures (Lash et al. 1957). Progenitor cells isolated from different tissue of origin lost the capacity to differentiate in to the parental tissue after several rounds of sub culturing (Holtzer et al. 1960), this points to the innate differentiation deficiency of myoblasts when culturing *in vitro*. Experiments which blocked DNA synthesis and subsequent cell division showed that the multinucleated structure of myotubes were formed by the fusion of several myoblasts into a ribbon like structure, that can contract spontaneously (Konigsberg, Mcelvain, Tootle, & Herrmann, 1960) . At the same time, satellite cells were discovered (Figure 1.1) which led to a better understanding of the mechanisms underlying postnatal muscle maintenance and

regeneration. These quiescent cells reside within the myotubes, between the basal lamina and sarcolemma of skeletal muscle (Mauro 1961; Katz 1961).

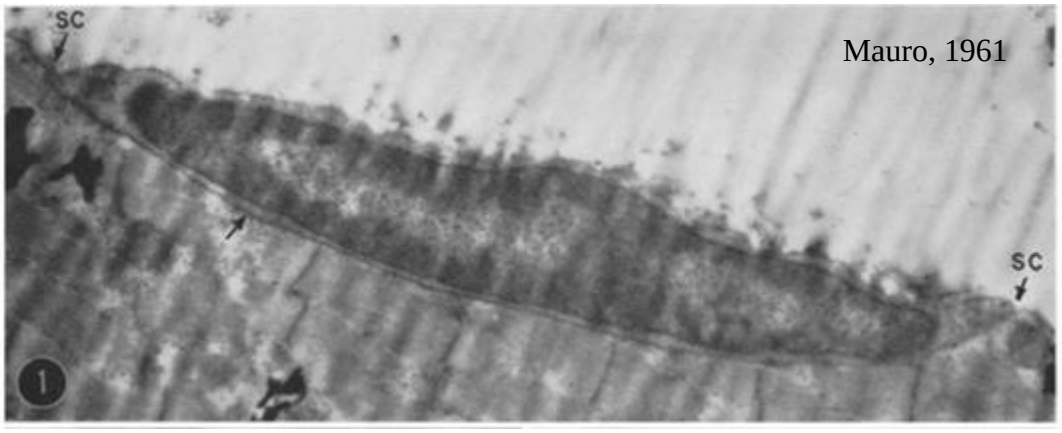

Figure 1.3. Electron micrograph of a satellite cell (SC)
Satellite cell situated at the periphery of basal lamina (image from Mauro, 1961). SC indicates the periphery of the satellite cell and arrows show the plasma membrane boundary between the satellite cell and the myofibril. Magnification10,000x.

The embryonic origin of the satellite cells involves a self-renewing population of myoblasts with stem cell like properties in the developing dermomyotome (Venters & Ordahl 2002). After embryogenesis, the satellite cells or the muscle progenitor cells remain in muscle and contribute to muscle mass maintenance in fetal and postnatal conditions (Gros et al. 2005). Both the adult skeletal muscle tissue and the tissue resident satellite cells were originated from the early embryonic somites (Armand et al. 1983).

1.5.2 Role of extra cellular matrix (ECM) in muscle function

Since skeletal muscle is mainly a contractile tissue and its main role is to facilitate motor function, the extra cellular matrix that supports the passive weight of the muscle at rest and cells within it, affect the normal maintenance of muscle and the repair damaged muscle tissue by satellite cells (Gillies & Lieber 2011). Individual muscle

fibres are surrounded with highly structured ECM components that adapt efficiently to the changing plasticity of the muscle fibre itself. The ECM supports the muscle fibre by providing a complete and firm sheath with structural arrangement to manage the shear force when the muscle fibres contract or relax (Trotter & Purslow 1992). Figure 1.4 shows the ECM structure that was obtained after the removal of myotubes with NaOH treatment and demonstrates the intimate relationship between myotubes and the ECM.

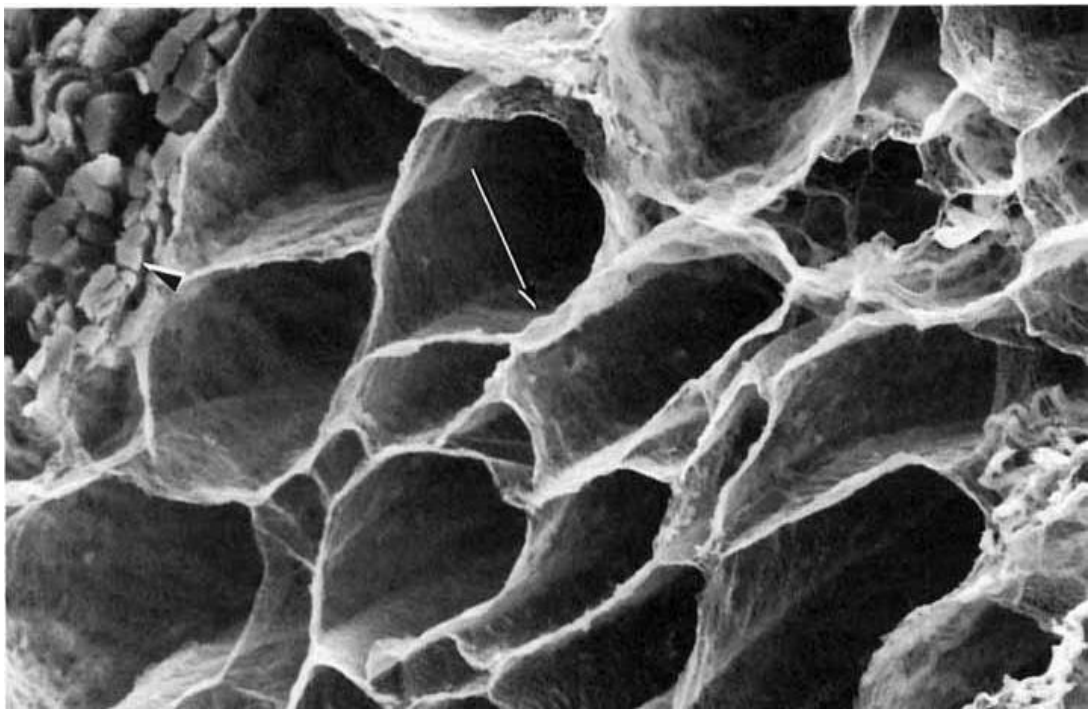

Figure 1.4 Electron micrograph of the structural arrangement of ECM around muscle fibres (Trotter and Purslow, 1992)
De-cellularized muscle tissue dispaly the structural features of ECM around myotubes. The arrow indicates the layer of ECM around the endomysium and the arrow head indicates the thick collagen fibres that support a bundle of myotubes (perimysium). Taken from Trotter and Purslow 1992.

The endomycial ECM (the ECM layer that is present around a muscle fibre) components and the structure help the transmission of contractile forces of muscle fibres by providing a firm but elastic support for the muscle fibre (Purslow & Trotter

1994). Although the structural arrangement of the ECM around muscle fibres is known, the formulation development or the formulation of ECM is unknown. This knowledge gap severely affects the development of muscle culture models in vitro. Immunohistochemical analyses have detected the presence of laminin, fibronectin and heparin sulfate as components of muscle ECM (Bayne et al. 1984) as well as. proteoglycans (PGs) including chondroitin sulfate and dermatan sulfate, glycosamino glycans chains (GAGs such as decorin and biglycan (Brandan & Inestrosa 1987; Gillies & Lieber 2011). Thus these components may be crucial in the development of improved culture systems for skeletal muscle.

1.5.3 Molecular markers of skeletal muscle satellite cells

Since the discovery of skeletal muscle satellite cells by Mauro (1961), further understanding of the structural organisation of the myofibre and the satellite cells followed. Electron microscopy revealed the structural arrangement of satellite cells in the myofibre and their abundance. It was estimated that less than five percent of the total nucleated cells in a myofibril are satellite cells and the rest reside within the sarcomere.

Pioneering work by Richard Bischoff using an isolated, single muscle fibre showed that a relatively low number of stem or satellite cells that reside within the basic lamina of the myotubes proliferate and differentiate into muscle fibres (Bischoff 1975; Bischoff 1986b). It was initially thought that thought that the mitogens secreted from the myotubes can activate the proliferation and differentiation of satellite cells (Bischoff 1986a).

1.5.4 Common markers used for satellite cell detection

Molecular techniques have detected an array of markers for satellite cells. For example, Syndecan 3–4, Integrin-7, c-Met, Caveolin-1 and Vcam1 are cell membrane proteins that are expressed in nearly all satellite cells. Following satellite cell differentiation another commonly used marker for myoblasts is Desmin. Transcription factors Pax3 and Pax7 are also present in satellite cells, Pax7 is detected in nearly all satellite cells, so is used commonly as a bona fide satellite cell marker (Seale et al. 2000). However, during differentiation of satellite cells to myoblasts, the expression level of Pax7 declines and increased expression of the myogenic regulatory factors such as myogenin, MyoD and Myf5 is observed (Halevy et al. 2004; Biressi & Rando 2010)

In vitro and *in vivo* studies have investigated the function of transcriptions factors Pax3 and Pax 7 in satellite cells (Relaix et al. 2005). Failure to express these transcription factors resulted in growth arrest or a change the fate of the satellite cells in the muscle. Muscle fibre interstitial space residing cells that lacked expression of Pax7 failed to differentiate into skeletal muscle and the same cells expressed Pax 7 before they turned into muscle (Mitchell et al. 2010). *In vivo*, a mouse deficient for Pax 7 resulted in a reduced satellite cell population in muscles collected post-natally and the size and number of myofibrils were smaller compared to neonatal mice born to mothers with Pax7 expression (Oustanina et al. 2004).

1.6. Skeletal muscle fibre types in mammals

Mammalian skeletal muscle exists in two different colours, dark red and pale red or white. Every muscle is composed of varying proportions of red and white muscle

fibres. Early skeletal muscle biologists such as Kühne in 1865 observed that the red and pale red / white colours are based the abundance of haemoglobin. Later on Ray Lankester (Lee 1958) suggested that muscles which undergo persistent and prolonged activity are red and twitch more slowly than white (Wells 1965). This led to the general classification of muscles into slow twitch red muscle and fast twitch white forms. The skeletal muscle system is highly heterogeneous and the presence of different proportions of myofibre types affects the contractile and metabolic properties as well as the muscle or meat quality for consumption.

1.6.1 Skeletal muscle fibre type classification based on contractile properties

Early studies tried to classify mammalian muscle based on the muscle twitch properties observed in different isolated muscles. For example, a muscle's different biological properties were considered including the Ca^{++} response and contraction/relaxation properties such as the velocity of contraction and spread of the contraction and relaxation. These features helped to classify the skeletal muscles into two broad classes, namely fast twitch and slow twitch types of muscle. The characteristic features of fast and slow twitch frog muscles are summarised in Table 1.1 using data from (Costantin et al., 1967).

Fast type muscle fibres	Slow type muscle fibres
Response to administration of Ca++	
• Twitch like contractions near the site of calcium administration • Contraction time is less than 5 sec (1 mM Ca, 50µl diameter drop) • Reversible contraction	○ Slower contraction ○ Spreads extensively to the bulk of the fibre upon low conc. from the confined small area of admin. ○ Small volume of 1mM Ca^{++} caused very little relaxation from 3 sec, increased Ca^{++} resulted in no relaxation
Fibre type identification criteria	
	○ Relative scarcity of sarcoplasmic reticulum
Velocity of contraction	
• Needed 3mM Ca^{++} , 50µ diameter volume • Initial sarcomere length- 2.8-3.5µ • Mean velocity- 6-12µ/sec • Sarcomere length reduced by at least 1µ/130ms	○ 30mM Ca^{++} ○ Initial sarcomere length- 3 µ ○ Mean velocity- 1 µ/sec ○ Sarcomere length reduced by at least 0.8-1.5µ/sec
Spread of contraction @ 0.25mM and 0.5mM Ca^{++}	
• Less contraction occurred at the site of Ca^{++} application(0.25mM) • Extensive spread at 0.5mM Ca^{++}	○ Extensive contraction ○ Extensive and more penetrant contraction in slow than fast at 0.5mM Ca^{++}
Relaxation	
• Fast relaxation occurred in fibres challenged with 2mM Ca^{++}	○ Little or no contraction even as low 0.5mM Ca^{++} conc. (may be due to calcium persistence in the myofilament space)

Table 1.1. Properties of slow and fast skeletal frog muscle fibres

(Constanin et al 1967)

The skeletal muscle of mammals is composed of different proportions of muscle fibre types. These types of muscle fibres were based on different parameters such as histochemical staining patterns and physiological properties, electron microscopic studies, immunohistochemistry studies based on myosin ATPase and biochemical characteristics of muscle fibres based on the abundance of oxidative or glycolytic enzymes. Peter *et al* classified muscle fibres into 3 different classes based on their biochemical properties using phosphorylase, lactate dehydrogenase, and succinate dehydrogenase. Thus class 1 muscles had oxidative metabolism with a slow twitch, class 2 muscles were fast twitch with oxidative metabolism and class 3 were fast twitch with a glycolytic metabolic activity (Peter et al. 1972).

1.6.2 Skeletal muscle fibre typing based on biochemical properties

Three biochemical methods are used to classify muscles and muscle fibres. Early skeletal muscle fibre studies by Brooke and Kaiser using Myosin ATPase classified muscle fibre types into Type-I, IIA and IIB (Brooke & Kaiser 1970). This myosin ATPase (mATPase) assay measures the ATPase capacity of myosins that enables the myosin to hydrolyse an ATP molecule into ADP and phosphate to catalyse the actin-myosin cross bridging. The assay relies on washing the muscle section in either an acid solution (pH~4) which inhibits the mATPase activity in the fast fibres without affecting the slow fibres. Conversely washing the muscle section with a basic solution inhibits the mATPase activity in slow but not in fast twitches fibres.

Another biochemical classification system involves succinate dehydrogenase (SDH) activity. SDH is an inner mitochondrial membrane enzyme that functions in the oxidative phosphorylation pathway and can thus be used to indicate the oxidative capacity of the muscle fibres. SDH activity is higher in slow twitch muscle fibres but lower in fast twitch fibres

A third biochemical classification system involves α-glycerophosphate dehydrogenase (αGPD) which is an enzyme involved in the glycolytic pathway. Thus αGPD activity is higher in fast twitch fibres but lower in slow twitch fibres, so this assay is used to detect the fast twitch muscle fibres.

1.6.3 Skeletal muscle fibre typing based on MyHC expression

MyHC proteins represent one of the most ubiquitously expressed proteins present in eukaryotes and they play a major function in different types of movements, including muscle contraction. During muscle contraction, MyHC proteins are also abundant and essential, usually present as various isoforms which contribute to muscle fibre heterogeneity.

1.6.4 Myosin heavy chain isoforms expressed in fibres of mammalian skeletal muscle

Muscle fibres were previously considered to be slow twitch or fast twitch based on their contractile properties. However, identification of new MyHC isoforms in muscle led to the identification of more fibre types which is classified as type 1, type 2A, type 2X and type 2B (Schiaffino & Pierobon Bormioli 1975; Hanzlíková et al. 1970). Although all these types of muscle fibre are present in most mammals, type 2B muscle

fibre is absent in human muscle (Smerdu et al., 1994). MyHC isoforms expressed in mammals are shown in Table 1.2 with the genes encoding the specific isoforms

Myosin heavy chain isoforms	**Genes**
Embryonic myosin heavy chain	*MYH3*
Perinatal myosin heavy chain	*MYH8*
Myosin heavy chain slow (type 1)	*MYH7*
Myosin heavy chain fast twitch 2A (type 2a)	*MYH2*
Myosin heavy chain fast twitch 2X (type 2x)	*MYH1*
Myosin heavy chain fast twitch 2B (type 2b)	*MYH4*

Table 1.2. Myosin heavy chain isoforms expressed in mammals and the genes encoding these proteins

1.6.5 Expression pattern of MyHC isoforms during embryonic and post-natal development

The relative expression of MyHC isoforms is a reliable method to characterise the developmental stage and maturity of muscle fibres *in vivo* and is also important in their function. During embryonic development, the most prevalent MyHC isoforms

expressed are embryonic MyHC and neonatal/perinatal MyHC (Whalen et al. 1981; Hoh & Yeoh 1979) which are encoded by genes MYH 3 and 8 respectively. Soon after birth, fast twitch MyHC expression is detected, for which neural activity is required MyHC isoform expression changes dramatically postnatally, with a shift from the predominant embryonic and perinatal MyHCs to fast twitch type MyHC isoforms (Allen & Leinwand 2001). Depending on the function of specific muscles, varied MyHC isoform expression occurs in different muscles (Agbulut et al. 2003)

Developmental myosin heavy chains are predominantly embryonic and perinatal MyHCs which are known to be expressed highly in the embryonic stages and the expression levels fall after the birth but the expression of these MyHCs becomes apparent as the myoblasts differentiate into new myotubes (Schiaffino et al. 2015).

1.7 Skeletal muscle fibre plasticity

Muscles retain a high degree of plasticity in terms of their functional ability. For example, their contractile characteristics, ability to manage load, time to fatigue and metabolic properties can all change according the demands placed on them, including neurological activity. The plasticity of muscle is mainly due to a shift in MyHC composition. Any shift in muscle fibre type is sequential, so a Type 1 slow twitch fibre will change to a fast twitch type 2A then to type 2X and finally to type 2B but the shift can happen in reverse order as well. Different factors are known to affect the plasticity of the muscle fibres' phenotype, including neuromuscular activity and hormones etc. (Pette 2002; Matsakas & Patel 2009).

1.7.1 Effect of neuromuscular activity on muscle fibre types

Differences in the motor neurone activity used by red and white myofibres which lead to muscle contraction were studied as early as 1874 by Ranvier, as cited in (Eccles, Eccles, & Lundberg, 1958) Thus slow and fast twitch muscles differ in their number and type of motor neuron units in a specific muscle. For example, in a rat soleus muscle (SOL), out of 30 motor neuron units, 27 are slow and 3 are fast. In contrast, in the extensor digitorum longus muscle (EDL) there are about 40 fast motor neuron units (Close 1967). Thus the contraction characteristics of red or white muscle fibres depend on the motor neuron activity exerted on that specific muscle. However, the muscle's entire characteristic can be changed by denervation. In rabbit and rat skeletal muscle, denervation results in de-differentiation of the muscle fibres by changing the activity of glycolytic and oxidative enzymes (Hogan et al. 1965). Furthermore, cross-uniting of a fast twitch nerve unit onto a slow muscle fibre converts the muscle to a fast twitch muscle and vice versa (Buller et al. 1960). At the time, it was postulated that the switch in muscle fibre type happens because of a substance that passes through the neuromuscular junction to the muscle fibre which transforms the muscle type. More recent in vivo studies show that a nerve impulse increases the MyHC-slow twitch gene expression and the MyHC gene's promoter activity can be blocked by cyclosporine (CsA), an inhibitor of a phosphatase calcineurin. Proteomics profiling and mass spectrometry experiments on chronic, low-frequency stimulated, fast twitch fibres revealed that the switch between fast and slow twitch fibre type resulted in the up regulation of muscle proteins such as cofilin-2, transgelin, SERCA-2, FABP-3 along with already known myosin heavy and light chains. Cofilin-2 and transgelin expression can be used as marker for the fast- slow fibre type switch (Donoghue et al.

2007) .Therefore it appears that the number and type of neurones which innervate a muscle can influence the types of twitch fibres.

Muscle plasticity is also demonstrated when mechanical loading and unloading of muscle fibres induce switches between fast and slow twitch types. Thus stretch-overload of fast twitch myofibres resulted in a shift to slow twitch type, with an associated increase in the expression of the slow twitch MyHC isoform (Goldspink 1999). The inverse effect was observed with mechanical unloading, when the slow twitch type myofibre shifted to fast twitch type (Caiozzo et al. 1996; Caiozzo et al. 1994).

1.7.2 Effect of hormones on muscle fibre types

Hormones are known to affect the muscle fibre's characteristics. For example administration of testosterone to female rats resulted in development of the levator ani muscle, which is usually vestigial in females (Hanzlíková et al. 1970). Thyroid hormone also has potent effects on muscle fibre phenotype, where hypothyroidism and low levels of thyroid hormone cause a shift from fast to slow twitch type (Fitts et al. 1980). In contrast, hyperthyroidism and high levels of thyroid hormone lead to a predominance of fast twitch fibres (Larsson et al. 1994).

1.8 Role of muscle fibre types in muscle quality and quantity

The complex cellular and tissue heterogeneity of skeletal muscle makes it difficult to identify the precise factors which affect muscle and therefore meat quality (Lefaucheur 2010). It is known that differences in the composition of muscle fibres determines the quality of meat (Karlsson et al. 1999). Since the number of myotubes present in a

muscle is determined primarily during embryonic development, any potential to improve the muscle's quality such as more oxidative and improvement of quantity is restrained by an ability to modify these features in the post-natal period (Montarras et al. 2013). Thus studies on food animal production have attempted to identify the desirable characteristics of muscle to ensure good quality and quantity for human consumption. For example, muscles with oxidative type fibres not only have higher metabolism but as a consequence good sensual (taste) qualities (Chang 2007).

1.8.1 Myosin heavy chains and their role in meat quality

Previous studies have shown that muscles composed predominantly of oxidative fibres led to a better meat quality in pigs (Chang et al. 2003). MyHC protein expression profiles in different pig muscles showed variation in the proportion of MyHC isoforms expressed. For example, in a fast twitch longissimus muscle with predominant glycolytic metabolism, an imposed stimulus resulted in a major shift of MyHC 2B expression to MyHC 2X isoform with only very limited change in MyHC 2A expression. This sequential change in MyHC isoform expression did not affect the type 1 MyHC isoforms. Such shifts in MyHC isoform expression also resulted in a reduced fat content in the muscle (Lefaucheur et al. 2004). In pigs, meat quality features such as pH, drip loss, succulence, intramuscular fat and the sensory quality of pork correlates positively with the MyHC expression profile where oxidative slow type MyHC isoform expression produced better meat quality (Kang et al. 2011). Additional meat qualities such as dark, firm and dry (DFD) are high value and pig meat with a high proportion of oxidative type muscle fibres, either from the slow or fast twitch type makes DFD pork (Kim et al. 2013). Therefore, depending on the qualities of meat required, the nature and metabolic activity of muscle differs, but by

exploiting the plasticity of muscle, can be modified during the animals' production process.

1.9 Current *in vitro* muscle culture systems- advantages and disadvantages

Swine are considered to be a model for humans in biomedical research, due to the genetic and structural similarity of their organs and comparable organ size. According to current information around 1.3 billion pigs were consumed worldwide for food which indicates the economic importance of pig production, along with its significance as a source of protein. Pork is the most consumed meat in world (FAO 2012). However, pigs are affected with over 140 diseases (Pigsite 2015) and this results in production loss with an associated economic impact. These important features show that pigs are an important target species to study the mechanisms of muscle growth and the factors which may have a negative impact.

It is advantageous to develop a reliable, representative and repeatable *in vitro* culture system for porcine skeletal muscle. These include a deeper understanding and knowledge of muscle growth for meat production and its modulation by growth factors, the physiology of healthy muscle, the pathology of muscle diseases, myokines and immune responses, metabolic diseases and the biological processes of muscle cells. Although some *in vitro* culture systems exist for porcine muscle, probably due to the technical difficulties in differentiation of these cells, there are very few published studies. Even then, there are advantages and disadvantages. Major disadvantages of the current porcine muscle culture systems are the poor differentiation and capacity and the spontaneous detachment of the fused myotubes

from the culture plate. A recent study showed that the pig muscle cells are the worst performers in terms of myoblast fusion to myotubes when compared with avian, equine and bovine muscle cells (Baquero-Perez et al. 2012). Another study using a porcine muscle culture system showed that the MyHC expression was mainly of embryonic isoforms (Zhu et al. 2013). The authors argued that the reason for such expression is probably because porcine muscle cells in culture resemble the MyHC expression profile of the original muscle from which the myoblasts isolated. The embryonic MyHC isoforms probably indicate immature myotubes.

1.9.1 ECM components used in traditional in vitro muscle cultures

Several studies have attempted to optimise in vitro muscle culture by using ECM components such as collagen type I, fibronectin, laminin, gelatin and Matrigel as surface coatings (Mau et al. 2008; Doumit & Merkel 1992) (Wilschut et al. 2010a). However, many of these studies used only a single ECM protein for coating the cell culture vessel surface and the results showed suboptimal growth and differentiation capacity. Another study used de-cellularized, homogenised tissue specific ECM (skin and skeletal muscle) to coat the cell culture vessel and this resulted in better proliferation and growth of the cells (Zhang et al. 2009). Similarly de-cellularized ECM tissues which contain different polysaccharides supported skeletal myoblasts growth and differentiation (DeQuach et al. 2010). A different approach combined fibrous ECM components such as entactin, laminin and collagen with glycosamino glycans from cod fish generated better growth of cells (Rønning et al. 2013).

More recently, coating plates with matrigel and laminin provided better growth and differentiation of pig muscle cells (Wilschut et al. 2010a). Thus it appears that

inclusion of multiple components of ECM in the culture of porcine muscle cells may aid not only proliferation, but also differentiation.

1.9.2 Porcine muscle cell culture systems

A variety of culture systems have been reported for porcine skeletal muscle cells. For example, the first ever porcine skeletal myoblasts isolation and proliferation followed with differentiation was performed on gelatin coated cell culture plates (Doumit & Merkel 1992), who used the model to study muscle biology. Further studies showed that the satellite cells existed as small and larger sizes, with the small satellite cells increasing in size upon proliferation to become myoblasts. Since this phenomenon was similar to cultures of human skeletal myoblast, the relevance of cultured porcine muscle cells as a large animal model for humans received much attention (Blanton et al. 1999).

In an attempt to recreate the extra cellular matrix for porcine satellite cells, plates coated with different extracellular matrix (ECM) components such as collagen type I, fibronectin, laminin, gelatin and Matrigel were compared, using cell proliferation and differentiation as the measure of success. The authors found that gelatin and matrigel provided the most efficient growth environment (Wilschut et al. 2010a). Unfortunately, although myoblasts growing on gelatin and matrigel ECM differentiated, the myoblast fusion rate was only about 30%, with 70% of cells remaining as unfused myoblasts. This technical difficulty probably resulted in a low number of published studies using porcine muscle culture system compared with models in other species such as mouse or avian systems (Sebastian et al. 2015).

Not only is the rate of myoblast fusion low *in* vitro but the differentiation of myoblasts into myotubes is s slow, taking almost 7 days to detect the characteristic expression of embryonic and perinatal MyHC. Furthermore there is no expression of postnatal MyHCs such as slow or fast twitch isoforms (Perruchot et al. 2012). Thus, the myotubes formed are very immature and not terminally differentiated, so this method is unsuitable to study skeletal muscle of adult pigs which predominantly express the fast twitch isoform of MyHCs.

The distinction between the expressions of different MyHC isoforms in muscle satellite cells of embryonic or postnatal condition was analysed in another study using isolated, embryonic rat muscle satellite cells. These muscle satellite cells expressed only embryonic isoforms of MyHCs such as embryonic and perinatal whereas the satellite cells from muscles of new born rats expressed MyHC 2A along with embryonic and perinatal MyHCs (Balan et al. 2009). This study sheds light on the expression pattern of MyHCs in embryonic condition and neonatal condition.

1.9 Role of muscle cells in innate immune regulation

There is increasing evidence of an association between muscles and the body's immune status, including the ability of muscle cells to produce cytokines or myokines. The identification of a muscle derived interleukin, IL15 as an anabolic inducing cytokine of muscle (Quinn et al. 1995) opened up a new path about the significance of muscle in innate immune regulation. IL15 is produced by muscle cells and not only induces hypertrophy (important in meat quantity) but also regulates natural killer cells (NK), which are often part of the lymphocyte subpopulation with anti-viral effector functions. IL15 also induces skeletal muscle differentiation (Quinn et al. 1997). Muscle cells can also secrete other cytokines such as IL-6, which was identified as an

exercise factor, later found to be a myokine that acts as an anti-inflammatory agent (Petersen & Pedersen 2005). Other evidences also suggest that there is an association between muscle and the body's immune status. For example, cyclosporine A, a drug used in organ transplant patients to suppress rejection of their transplanted organ by their own immune system, can lead to a loss of muscle mass. Cyclosporin A also results in other side effects caused by the drug blocking T-cell activation (Yousry & Kanitakis 1991).

Muscle contraction during exercise results in an increased expression of IL-6, along with other pro and anti-inflammatory cytokines such as tumour necrosis factor alpha (TNF□), IL-1, IL-1 receptor antagonist, TNF receptors, IL-10, IL-8 and macrophage inflammatory protein-1 (Pedersen 2000; Paula et al. 2015). Strenuous exercise also led to immune suppression (Hiscock & Pedersen 2002). Although IL-6 is known for its pro-inflammatory action, it is also involved in anti-inflammatory function (Pedersen 2006; Pereira et al. 2013). Myokines may also act on other cell types and tissues in a paracrine manner to control the function of those tissues (Bente Klarlund Pedersen 2011). One recent study identified over 50 myokines expressed by human skeletal muscle following stimulation *in vitro* with an electrical pulse (Raschke et al. 2013). Current studies show that the skeletal muscle-dependent myokines have multiple physiological functions. These include a reduction in adipogenesis but an increase in lipolysis, muscle hypertrophy and regeneration and glucose uptake by cells. The latter function may reduce the chances of developing type 2 diabetes (So et al. 2014)

1.10 Muscle cell culture as a model to study the effects of growth factors on growth and disease resistance

Skeletal muscle is an important tissue in the regulation of innate immunity and has a significant role in maintaining health, metabolic diseases and metabolism, skeletal muscle can be used as a convenient system to study the effect of different growth factors to understand the molecular mechanisms of their action on cells. Due to the already established evidences to support the role of skeletal muscle in innate immune modulation, skeletal muscle can be used to study the innate immune regulation upon treating with different conditions.

1.10.1 Role of growth promoters in growth and immunity

As their names suggest, growth hormone (GH) and insulin like growth factor-1 (IGF-1) can be used to promote muscle growth (Park et al. 2014; Yoshida et al. 2010). However, growth factors can also act as cytokines to induce proliferation and differentiation of immune cells and thus play a role in host immunity (van Buul-Offers & Kooijman 1998)

1.10.2 IGF-1 in skeletal muscle growth promotion

Along with the known effects of insulin like growth factor 1 (IGF-1) in growth promotion it is also known to be involved with innate immune function. IGF-1 is a small polypeptide with a molecular weight of about 7.6kDa (Rinderknecht & Humbel 1978) which possesses mitogenic activity (Kurtz et al. 1982). IGF-1 acts in a similar manner to insulin in its downstream signalling pathway and promotion of glucose uptake capacity in muscle (Poggi et al. 1979). IGF-1 treatment of fetal rat brain cell

cultures increased DNA synthesis (Lenoir & Honegger 1983) which is the precursor step for cell proliferation.

Exposure of cells to physiological concentrations of IGF-1 *in vitro*, block the expression of cytokines (Hunt & Eardley 1986). IGF1 treatment provided an immunosuppressive effect on mouse gut epithelial cells (Ge et al. 2015). The effects exerted by IGF1 may also act indirectly through other mechanisms (Valtorta et al. 1990). Exogenous administration of IGF1 is found to increase host longevity and resistance against the malaria parasite (Drexler et al. 2013).

1.10.3 Testosterone in growth promotion

Administration of testosterone as an anabolic inducer helps to increase the body size in humans (Kelley & Ruvalcaba 1982) and is also known to affect the muscle growth in birds (Balthazart et al. 1984).

1.10.4 Role of Ractopamine in growth promotion

Since animal meat is used as a source of protein for human consumption, effective production of animal meat deserves utmost importance. Different endogenous anabolic agents such as sex hormones which are the natural steroids including testosterone progesterone and estrogen were known to affect the growth positively (Velle 1976). Other than the endogenous sex hormones, steroids foreign to the body (e.g. estradiol benzoate, testosterone propionate with a modified steroid structure) and other compounds foreign to the body (e.g. stilbene derivatives and zeranol) were used to improve the animal growth (Hoffmann & Karg 1976). One of the major challenges in the efficient production of animal meat is the ability of the farm animal to convert the feed into meat. The feed to meat conversion rate generally falls when the animal

grows older, which reduces the animal's overall productivity As a result, growth promoters are frequently used in farm animal production (VanderWal 1976; Smith & Shelver 2002; Yaeger et al. 2012) but not all countries support the use of such growth promoters (Stephany 2010).

Beta-adrenergic agonists or beta agonists are a class of sympathomimetic agents that act upon the beta-adreno receptors to relax smooth muscle and also relax airways of the lung. Beta agonists act like epinephrine/nor-epinephrine on heart muscles to increase the heart rate and blood pressure (Phillips et al. 1980). Based on the specificity of this agonist for different receptors, it exerts different biological effects which may be beneficial or adverse. Beta agonists activate the adenylate cyclase that results in the increase of cyclic adenosine monophosphate (cAMP) levels in the cells which leads to the relaxation of smooth muscles. Ractopamine is used in the farm animal production the Unites States of America. Finishing pigs are treated with ractopamine for about 2 weeks prior to culling and these results in increased lean meat production. This was confirmed by the down regulation of lipogenic genes (Halsey et al. 2011). Treatment of pigs with ractopamine resulted in increased lean meat percentage (Kutzler et al. 2011). Although the use of beta adrenergic agents/ beta agonists induces growth in farm animals, consumption of such meat may be harmful to human health. Thus the usage of beta agonists in meat producing animals is illegal in Europe (Kuiper et al. 1998).

A detailed understanding of the mechanism of action underlying the success of ractopamine or other anabolic inducers in growth promotion will make them safe to use in animals. The resultant benefits will help to improve animal welfare, along with increased meat production.

1.11 Influenza virus infection as a model to study innate immune regulation of muscle cells

Studies to understand the molecular mechanism of growth factors such as Ract, IGF-1 and testosterone showed that number of innate immune genes was differentially regulated by the treatment of these factors on cultured myotubes (un published data, Chang. K.C). Several proteins associated with anti-viral response, including interferon A2 (IFNA2), *Mx-1*, interleukins and STAT1 found to be upregulated and this fascinating discovery led to investigate the potential innate immune effect of growth factors on muscle cells. Since skeletal muscle cells are known to support influenza virus infection (Baquero-Perez et al. 2015; Desdouits et al. 2013), it is a valid approach to use porcine skeletal muscle cells as a model to understand the innate immune response elicited by growth factor treatment in muscle cells against influenza infection.

1.12 Influenza A virus

Influenza A virus is the causative microorganism of common 'flu and is responsible for health problems in humans, pigs and other mammals and avians. Influenza infection in humans has caused very high mortality rates during pandemics, and the Spanish 'flu outbreak in 1918 was the worst pandemic in recorded history. Today, according to the World Health Organisation's (WHO) calculations, annually, about 3-5 million people are infected by this virus and the mortality is about 250,000-500,000.

This enveloped virus belongs to the family of *Orthomyxoviridae* with a segmented, single-stranded negative sense RNA genome (Lamb & Choppin 1983). Influenza virus is subtyped further based on two glycoproteins present on the envelope, namely

hemagglutinin (HA) and neuraminidase (NA). At the present time 18 different HAs and 11 NAs have been identified (Tong et al. 2013). The virus strain responsible for the 1918 influenza pandemic was H1N1. Due to the polymorphic nature of the HA and NA glycoproteins, Influenza A virus remains hard to control because antibodies fail to cross react. The common strains of Influenza A viruses cause low pathogenicity (LPAI) but although less frequent, highly pathogenic strains of avian Influenza (HPAI) cause high mortality in chickens. Influenza infection has a significant economic impact on the poultry and pig industries, as the clinical signs of infection may be so severe that euthanasia is needed, resulting incomplete loss of the production animals or if clinical signs are less severe, weight loss and therefore reduced production and lost time (Basuno et al. 2010).

1.12.1 Structure of influenza virus

Influenza virions exist in pleomorphic forms but the most common are spherical or filamentous (Noda 2011). Spherical virions have an approximate diameter of 80-120 nm whereas filamentous virions are about 20 μm in length. Influenza virus is composed of eight viral proteins such as P1, P2, P3, HA , NP, NA, M, and NS (Figure 1.6) which can be separated using 2 dimensional gel electrophoresis (Privalsky & Penhoet 1978) . The transmembrane proteins such as HA and NA and matrix protein 2 (M2) are inserted onto the outer layer membrane of the virion, which is formed of the host cell membrane.

The influenza virus genome is composed of eight segments of single stranded RNA which encode the following proteins; HA, NA, nucleoprotein (NP), matrix protein (M), polymerase basic protein 1 (PB1), polymerase basic protein 2 (PB2), polymerase acidic protein (PA), non-structural protein (NS). The genetic material of influenza

virus forms virus ribonucleoprotein complexes (vRNPs). Each RNA segment is wrapped around NP and form together with PB1, PB2 and PA (Hutchinson et al. 2010; Noda & Kawaoka 2010; Noda et al. 2006).

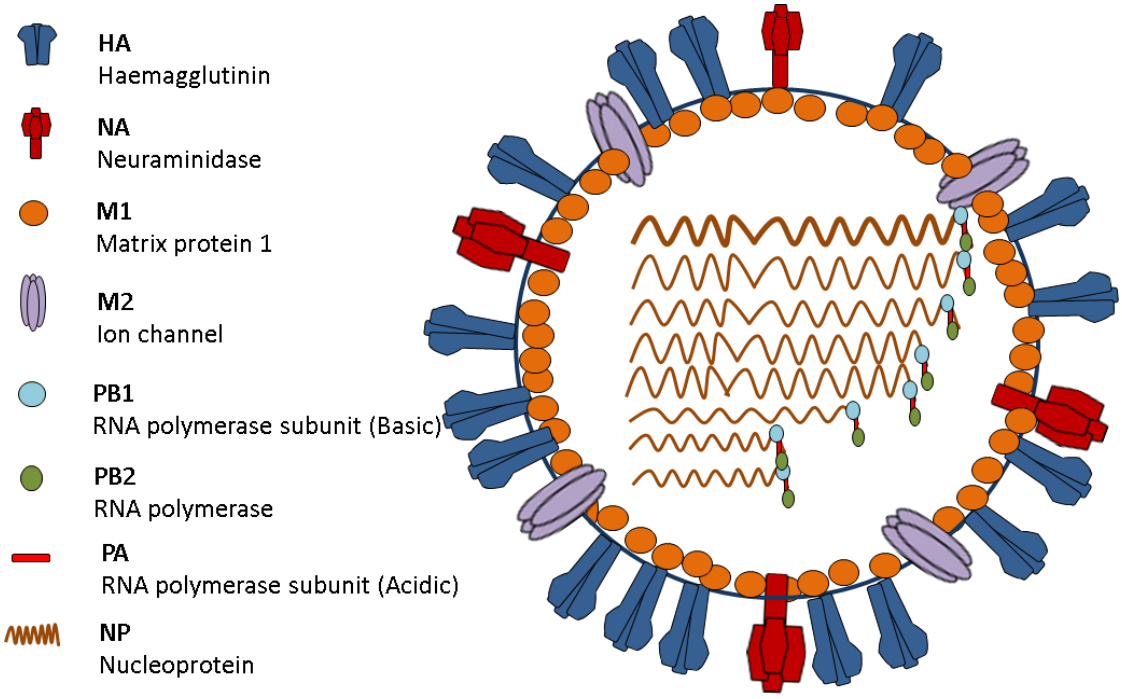

Figure 1.5. Structure of influenza A virus .

1.12.2 Influenza virus life cycle

The influenza virus life cycle proceeds through several steps; i) the attachment of virus to the cell membrane receptors and subsequent entry; ii) transfer of the vRNPs into the host cell's nucleus iii) transcription of the negative RNA strand to make the intermediate stage; iv) , translation and replication of the virus genome) the vRNPs are exported from the nucleus to the cytoplasm of the host cell; vi) virus assembly, budding and release (Nayak et al. 2004; Samji 2009).

1.12.3 Receptors of Influenza virus

Influenza virus attaches to host cells by binding to the membrane sialic acid (SA) receptors. Several human and animal viruses, including porcine sapovirus (Kim et al. 2014) use the sialic acid linked glycoproteins on the cell surface as a receptor for virus attachment (Matrosovich et al. 2015). Human influenza virus preferentially binds to SA-α2,6-galactose (Gal) whereas avian and equine influenza viruses preferentially recognise SA-α2,3-Gal, (Leung et al. 2012).Swine influenza virus binds to SA-α2,6-Gal and SA-α2,3-Gal (Kimble et al. 2010). Although the SA receptors are considered to be the primary route of influenza virus attachment, other receptors may also be involved (Lakdawala et al. 2013)

1.12.4 Influenza infection in pigs

Experimental infection studies showed that 27 out of a possible 38 virus strains can infect pig cells (Kida et al. 1994). Pigs are susceptible to both LPAI and HPAI strains and various LPAI strains have been detected in pigs (Ninomiya et al. 2002). Swine influenza (H3N2) has been reported to infect humans (Piralla et al. 2015). Influenza infection in post-weaning pigs causes increased mortality (Alvarez et al. 2015). A recent outbreak of swine influenza A (H3N2) virus in pigs caused a decreased interferon (IFN) and increased pro-inflammatory cytokine responses in myeloid dendritic cells which lead to a reduced antiviral capacity (Cao et al. 2015). Thus influenza virus does not just cause pyrexia and respiratory disease, but is also associated with a complex cytokine response in the host.

1.12.5 Innate immune response to influenza virus infection

As a first line of defence against any pathogens, most of the cells use the innate immune response. Subsequently the innate immune system stimulates the adaptive immune response to provide longer lasting and specific protection against the invaded organism. Pattern-recognition receptors (PRRs) in the cells (Akira et al. 2006) detect the invasion of virus particles (Beutler et al. 2007). PRRs detect the structural and genomic parts of viruses, such as genomic DNA (gDNA), single-stranded RNA (ssRNA), double-stranded RNA (dsRNA) and viral proteins. Influenza, as a ss RNA virus will be detected by PRRs such as toll like receptors (TLRs) including TLR 7 and 8 and retinoic acid-inducible gene I (RIG-I)-like receptors (Opitz et al. 2007). The host cells' response is to elicit type I interferons (IFNs) and various pro-inflammatory cytokines, eicosanoids and chemokines (Wolff et al. 2008; Iwasaki & Pillai 2014). IFNs induce the expression of the antiviral gene Mx-1 (Koerner et al. 2007) which is known to act as an anti-influenza factor.

Since muscle cells got an innate immune mechanism respond to invading infectious agent, and the growth factors got an intermediate role in providing enhanced growth with possible effect on host immune system, a study to understand the molecular mechanisms of enhanced growth and innate immune regulation upon muscle cells stimulated with growth factors deserves utmost importance.

Hypothesis

1. An *in vitro* porcine skeletal muscle cell model can be developed, in which cells multiply and differentiate into myotubes equivalent to adult muscle fibres.

2. An *in vitro* porcine skeletal muscle model can be used to assess the effect of growth promoters on:

a) Selected innate immune responses to influenza virus infection
b) Improvement of muscle quality

Aims and objectives

1. To develop a porcine muscle cell culture system that functionally resembles skeletal muscle *in vivo*.

2. To use the *in vitro* muscle model to:

a) Study the effect of growth promoters on innate immunity and muscle quality using a high throughput proteomics approach.
b) Evaluate muscle cells as a suitable model to study the impact of influenza virus infection and their potential immune response
c) Assess the effect of growth promoters on the anti-influenza virus innate immune responses

Chapter 2

General Materials and Methods

2.1 Cell culture media

This study utilised several primary cells and cell lines. Details about the cell culture media used for the culturing and method of cell culture is described in this section. Composition of cell culture media used in this study is shown below based on individual cell type.

2.1.1 Proliferation media for pig myoblasts

Porcine myoblasts isolated from the skeletal muscle was proliferated in the following proliferation media.

SKGM-2 with supplements and growth factors (Lonza) which contains the following proprietary supplements for the optimum myoblast proliferation- 10% FCS, 2mM L-glutamine, epidermal growth factor, dexamethasone and antibiotics. The above media was supplemented with 10% FCS, heat inactivated (Invitrogen), and 2% Chick Embryo Extract (CEE, Egg Tech-UK)

2.1.2 Differentiation media for pig myoblasts, DM1

Pig myoblasts that were proliferated over 90 percentage of confluence were differentiated into myotubes using the following differentiation media which is referred as DM1 with the following components DMEM high glucose (Invitrogen), 0.4% Ultroser™ G (UG), serum substitute (Pall Corporation), 1% penicillin-streptomycin (Invitrogen).

2.1.3 Differentiation media for long term maintenance of pig myotubes, DM2

Pig myotubes were optimised for the long term maintenance in the following differentiation media which is denoted as DM2 that is composed of DMEM high glucose (Invitrogen), 2% horse serum (HS), heat inactivated (Gibco), 1% Penicillin-streptomycin (Invitrogen).

2.1.4 HSMM cell growth media

SKGM2 media kit contains SKBM 2 basal media (Lonza) and the following supplements at given volume to add with the 500ml of the SKBM2 basal media, concentration of each supplement was not revealed by the manufacturer due to proprietary rights Human Epidermal Growth Factor (hEGF) 0.5 ml, Dexamethasone 0.5 ml, L-glutamine 10.0 ml, Fetal Bovine Serum (FBS) 50.0 ml Gentamicin/ Amphotericin-B (GA) 0.5ml.

2.1.5 HSMM fusion (differentiation) media

Differentiation of the cells were obtained by the addition of fusion media with the following composition DMEM:F-12 (Lonza), 2% horse serum (Lonza), 1% Penicillin-Streptomycin (Invitrogen).

2.1.6 PTEC proliferation media

Bronchial epithelial cell growth media with the supplements (BEGM, Lonza)

2.1.7 Cell culture media for MDCK cells

High glucose DMEM-Glutamax I (invitrogen) growth medium supplemented with 10% FCS and 1% Penicillin-Streptomycin.

2.1.8 Cell culture media for NPTr cells

RPMI 1640 (Sigma) medium supplemented with 10% FCS and 1% Penicillin-Streptomycin.

2.1.9 Cryopreservation media

Cryopreservation of cells was conducted using the following cryopreservation media composed of 40% proliferation media, 50% FBS and 10% Dimethyl sulfoxide Hybri-Max™ (DMSO, Sigma Aldrich)

2.1.10 Infection media

Influenza virus infection of the cells were carried using the serum free media which is composed of DMEM:F12 (Invitrogen) supplemented with 2% Ultroser G (Pall Corporation), 1% Penicillin-Streptomycin, and 250 ng/ml TPCK trypsin (Sigma-Aldrich).

2.2 Method of primary cells and cell lines

This study utilised a number of primary cell types and cell lines.

2.2.1 Porcine Primary Myoblast isolation

Pig myoblasts used in this study were isolated by Zoe Redshaw, a group member who kindly provided the cells for this study. Briefly, the method of muscle cells isolation

involved the following muscle; longissimus dorsi (LD), psoas, semimembranosus (SM) and diaphragm muscles from a 4 week old female Camborough 12 (Landrace X duroc X large white) pig. The excised muscle tissue was placed immediately into in ePBS (enhanced phosphate buffered saline; ePBS, 25mM glucose, 14mM sucrose, 100µg/ml streptomycin and 100IU/ml penicillin (same concentration was used for other cell types thus referred as 1% Penicillin-Streptomycin), 3µg/ml ampicillin B and 2mM L-glutamine). In the tissue culture hood, connective tissue was removed from the muscle and the muscle tissue was chopped into pieces as small as possible using a sterile scalpel and scissors. Around 5g of tissue was re-suspended in a 50 ml Falcon tube with 1.4 mg/ml pronase (Manufacturer) in ePBS. The tissue was incubated for 1 h at 37 °C in a water bath with occasional gentle agitation. Cells that were dissociated was centrifuged at 500g for 5min, then the supernatant (SN) discarded. Cells were resuspended in ePBS and re-centrifuged. A volume of 15ml α-MEM supplemented with 20% fetal bovine serum (FBS, Invitrogen, UK), 2 mM L-glutamine (Sigma), 100 IU/ml penicillin, 100 µg/ml streptomycin(Invitrogen), 3 µg/ml amphotericin B (Invitrogen) was added into the pellet and triturated with a 25ml pipette for 5min or until the cells were free of clumps. ePBS was added to 50ml before centrifugation at 150g for 5min. The supernatant containing cells was filtered through a 40uM cell strainer (Corning). The filtered cells were resuspended in ePBS and centrifuged at 150g for 10min. The SN was removed and the cells were resuspended in α-MEM containing, 20% (v:v) heat inactivated fetal bovine serum (FBS), 100µG/ml streptomycin, 100IU/ml penicillin, 3µg/ml ampicillin B and 2mM L-glutamine.

2.2.2 Human Skeletal Muscle Myoblast Cell (HSMM) culture

HSMM were cultured using the same conditions as porcine myoblasts (MC+ method-details given in later part of the methods) to compare the suitability of the MC+ culture method for HSMM cells

2.2.3 HSMM cell culture

HSMM cells were purchased from Lonza as a frozen vial which contained approximately 500,000 cells. The cells were revived according to the manufacturer's instruction, briefly, the frozen vial with the cells was immersed at 37ºC water bath without immersing the cap. When the vial was thawed almost 90%, it was taken out and sprayed with 70% industrially methylated spirit (IMS) and allowed to dry at room temperature. The vial was further wiped with IMS and transferred into the tissue culture hood. The contents of the vial (1 ml) was transferred into a 15ml falcon tube that contained 9 ml of SkGM 2 media (SkGM™-2 SingleQuots™ Kit, Lonza) that was pre-warmed to room temperature (RT), cells were then transferred into a T25 flask.

2.2.4 Primary Pig Tracheal Epithelial cells (PTECs) isolation and culture

Pig trachea was dissected out of four weeks old pigs in an aseptic manner and the trachea was placed directly in a 500 ml bottle containing enough collection media (300-350 ml) to cover the trachea. Collection media was composed of Dulbecco's Modified Eagle Medium (DMEM) (Gibco) supplemented with amphotericin B (3.75µg/ml) (Gibco) and 1% Penicillin-Streptomycin. The trachea was transferred into the cell culture hood and rinsed 3-4 times with PBS. Using a sterile scalpel and forceps, excess connective tissue was removed, the trachea rinsed again with PBS and cut

transversely into small fragments, to produce 3-4 pieces from one trachea. The trachea was then cut longitudinally as strips with about 2cm width. The inner most layer of the trachea, comprising the single cell epithelial layer was gently removed using a scalpel. This epithelial layer was minced into small pieces using a scissors and incubated in dissociation medium (DMEM-F12 (Gibco) supplemented with 0.06 U per ml pronase (Sigma), 1% Penicillin-Streptomycin and 3.75 µg/ml amphotericin B) overnight at 4°C on a tube rocker. After overnight incubation, the cell suspension was triturated very gently and filtered through a cell strainer (40µm) (BD Biosciences). The resultant flow through was centrifuged at 150g for 5 min and the cells were collected. The cell pellet was then rinsed three times with DMEM supplemented with 10% fetal calf serum (FCS) (Invitrogen), 1% Penicillin-Streptomycin and 3.75 µg/ml amphotericin B to remove the pronase/protease residues. Cells were further rinsed twice with PBS to remove FCS. The cell pellet was resuspended bronchial epithelial cell growth media with the supplements (BEGM SingleQuot Kit Suppl. & Growth Factors, Lonza). The culture flasks (T75) were pre-prepared by coating with 1% MaxGel™ ECM (Sigma) diluted in DMEM and the cells were seeded directly in to the T75 cell culture flasks. Culture media was replaced with fresh media every other day.

2.2.5 Madin-Darby Canine Kidney (MDCK) cells

MDCK cells were cultured in DMEM-glutamax I (high glucose) growth medium supplemented with 10% FCS and 1% Penicillin-Streptomycin why in T75 flasks. For passage, cells were rinsed three times with PBS to remove culture medium and 5 ml of pre warmed trypsin 1X (Invitrogen) added. Trypsinization was continued until most of the cells detached from the flasks and the reaction was terminated by adding 5 ml of DMEM-glutamax I supplemented with 10% FCS and pen strep. Cells were

centrifuged at 300 g for 5 min. The cell pellet was re-suspended in DMEM-glutamax I supplemented with 10% FCS and Penicillin-Streptomycin and seeded onto 96-well flat bottomed plate for influenza virus titration.

2.2.6 Newborn Pig Tracheal Epithelial (NPTr) cell culture

Newborn Pig Tracheal epithelial (NPTr) cells were maintained as a cell line and were cultured in RPMI 1640 (Sigma) medium supplemented with 10% FCS and 1% Penicillin-Streptomycin.

2.3 Extra Cellular Matrix (ECM) coating for pig muscle cell culture

Usage ECM at a specific combination and coating procedure resulted to a significant improvement to the muscle cell culture. The procedure to prepare the ECM coated cell culture dish is described below.

2.3.1 Maxgel-Collagen (MC+) surface coating reagent stock solution

Rat tail collagen solution (Sigma) was warmed up for few minutes at room temperature and a stock solution of 2% (v/v) made using PBS (e.g. 1ml collagen + 49 ml PBS). The solution was filtered through a 0.22uM syringe filter (Millipore). The sterile stock solution of Maxgel ECM was diluted 1:100 using DMEM (e.g. 100ul of Maxgel ECM in 10ml of DMEM). The coating solution (MC+) was made by adding 1:1 volume of Maxgel and collagen stock solutions and mixed well. The required volume of the coating solution was pipetted on to the culture flasks/plates as shown in Table 2.1.

Flask/Plate	Volume of MC^{+} solution
T75	4ml
T25	2ml
6 well plate	800ul / per well
12 well plate	400ul / per well
24 well plate	200ul / per well
48 well plate	100ul / per well
96-well plate	50ul / per well

Table 2.3 Volume of MC+ coating reagent required for different tissue culture vessels

2.3.2 Procedure to prepare the MC+ coated cell culture vessel

The MC+ coating reagent was transferred into the required cell culture vessel and swirled gently to cover the surface. The lid or cap was lifted slightly from the vessel and left in the tissue culture hood for at least 24hours to allow the coating to dry.

2.3.3 Final preparation of MC+ coated flasks or plates

Flasks/plates coated with MC+ reagent, were rinsed with DMEM first, followed by PBS as described here. Initially 5ml of DMEM was added into a T75 flask (proportional volume of DMEM was used to rinse other cell culture vessels of varying size), the cell culture vessel was gently swirled for few times and the media removed using a pipette. The same procedure was repeated with PBS and any trace of PBS was removed using a pipette. Plates were then either used immediately or stored for a few weeks to three months.

2.4 Porcine muscle cell culture

Steps involved with the porcine muscle cell culture is detailed below

2.4.1 Revival of frozen pig myoblasts

Vials of cells cryopreserved in LN were thawed quickly by incubating in a 37˚C water bath. When most of the frozen medium has melted, the cryovial was removed, decontaminated with 70% ethanol (EtOH) and dried. Cells (>0.5 $x10^6$) were gently pipetted into a tube containing 4 ml of proliferation media, spun down at 150g using a bench top centrifuge for 1-2 min and the supernatant was removed without disturbing the pellet. Cells were gently resuspended with 1ml of pig muscle cell proliferation media, then another 9ml of media was added into the tube and the complete volume transferred into a previously coated T75 flask.

At 24 hours post seeding, the proliferation media was replaced with fresh proliferation media and then subsequently every 48 hours. Revived frozen cells grew to about 60-70% confluence by 3-4 days post seeding when they were passaged and re-seeded into the required plate format. At 60-70% confluence, cells can be re-seeded into required plate format.

Myoblasts that were revived from cryopreservation were passaged when the T75 flask was about 65% confluent (2.5-2.8 million cells per T75 flask) and seeded into multiwell plates at approximately 0.8 million cells per 6 well plate as shown in Table 2.2. Cells were incubated at 37ºC incubator with 5% CO_2 and 5% O_2. The proliferation media was replaced at 24 hours post seeding. At 90-95% confluence, usually by 48-72 hours, cells were transferred into differentiation media.

Flask/Plate	Volume of suspended cells to use
T75	10-12ml
T25	4ml
Well of 6 well plate	2ml
Well of 12 well plate	1ml
Well of 24 well plate	0.5ml
Well of 48 well plate	0.25ml
Well of 96-well plate	0.1ml

Table 2.4 Volume of cell suspension in proliferation media recommended for different tissue culture flasks or multiwall plates.

2.4.2 Passage of pig myoblasts

Cryopreserved primary pig myoblasts were revived and allowed to proliferate for 2-3 passages in T75 flasks. The resultant cells were then re-frozen using the following protocol. Myoblasts at about 50-60% confluence were rinsed with 5ml of PBS twice then 4ml of pre-warmed (37°C) 0.5x trypsin (Invitrogen) in PBS was added. The flask was incubated at 37ºC for 1 min, then the flask was gently tapped with hand every 30 sec until most of the cells had detached from the surface, normally after 2min. Trypsin was inactivated by adding 5ml of pig muscle cell proliferation media, and the flask was gently swirled. The media containing the cells was then transferred into a 15ml falcon tube and centrifuged for 2 min at (150g) in a bench top centrifuge. Supernatant was removed and the cells were re-suspended in 1ml pig muscle cell proliferation

media prior to seeding onto three or four T75 flasks if required. For re-freezing the cells, follow the method given below.

2.4.3 Cryopreservation of pig myoblasts

Pig myoblasts were isolated and cryopreserved by Dr. Zoe Redshaw, details of the cryopreservation is given briefly here, the myoblasts that were isolated from pig muscles were initially proliferated to reach up to 60% confluence on collagen coated T75 flasks. Myoblasts were collected and resuspended in cryopreservation media. One T75 flask with about 60% confluent cells were enough to make three vials of cells for cryopreservation and each such vials contained about 0.5 million cells.

2.4.4 Differentiation of pig myoblasts to myotubes

To facilitate differentiation of myoblasts into myotubes pig myoblast proliferation media was removed, the cells were rinsed with a small volume of differentiation media then replaced with the required volume of differentiation media Table 2.2. The plate was incubated at 37ºC incubator with 5% CO_2 and 5% O_2. The cells were monitored for differentiation into myotubes using an inverted light microscope

2.4.5 Long term maintenance of differentiated pig myotubes

Several experiments were undertaken to assess the optimum volume of medium replacement to maintain myotube integrity and differentiated state for several weeks. The optimum method was to replace 25% of the total media volume in the well with fresh differentiation media (DMEM+2%HS+1% Penicillin-Streptomycin) every two days, starting from day 5-7 of differentiation.

2.4.6 Long term maintenance of porcine myotubes to induce postnatal muscle fibre type

For long term maintenance of the myotubes to allow the development of postnatal muscle fibre type, porcine myoblasts were allowed to differentiate for 7 days in pig myoblast differentiation media. From 7 days onwards 25% of the total media volume in the well was replaced with fresh differentiation media (DMEM+0.4%UG+1% Penicillin-Streptomycin), the partial replacement was continued and was able to maintain the myotubes in culture for over 7 weeks.

2.5 Human skeletal muscle myoblast cells (HSMM) cell culture

2.5.1 Revival of cryopreserved HSMM cells

Based on the manufacturer's instructions, the contents of the thawed vial were seeded onto a T25 cell culture flask directly, without centrifugation to avoid damage. Culture media (SKGM2, Lonza) was replaced with fresh culture media after 24 hours of incubation at 37°C, 5% CO_2, in a humidified incubator.

2.5.2 Sub culturing and passage of HSMM cells

Cells were passaged into new culture flasks when the revived HSMM cells achieved about 50%-70% confluence. Thus cells were rinsed with 10 ml of Dulbecco's Phosphate Buffered Saline (DPBS) followed by 2 ml of Trypsin/EDTA at RT. Once almost 90 percent of cells had detached from the flask, 4 ml of Trypsin Neutralizing Solution (TNS) was added. Contents were transferred into a 15 ml falcon tube and

centrifuged at 220 g for five minutes to pellet the cells. Cells were resuspended in the SKGM2 media with supplements at about one million cells per 75 cm^2.

2.5.3 Differentiation of HSMM cells

Differentiation of HSMM cells into multinucleated myotubes was carried out using manufacturer's instructions. Briefly the HSMM cells were cultured in growth media to 50-60% confluence. Differentiation of the cells was achieved by the addition of fusion media- (DMEM:F-12, Lonza supplemented with 2% horse serum) . Fusion media was replaced every other day and cells observed under an inverted microscope until the required differentiation was obtained, which normally took around 3-5 days.

2.5.4 Long term maintenance of HSMM cell differentiated myotubes

As per the manufacturer's instruction, long term (2-3 weeks) maintenance of differentiated HSMM myotubes was obtained by the replacement of fusion media with HSMM proliferation media every other day from one week of differentiation.

2.6 Comparison of HSMM myotube fusion rate between standard and MC+ methods

To assess the optimum method to achieve HSMM myotube fusion, the manufacturer recommended method was compared with the MC+ method (that was optimised for the pig myoblasts) differentiation method is described earlier in this section. The HSMM cells used for this study were passaged twice.

MC+ coated plates were prepared as previously described. HSMM cells which proliferated in SKGM 2 growth media were passaged using trypsin/EDTA and seeded onto MC+ coated multiwell plates at a cell density equivalent to 1 million cells per $75cm^2$.

2.6.1 Differentiation of HSMM cells using MC+ method

HSMM cells (equivalent to 1 million cells per $75cm^2$ surface area) were cultured and differentiated using the conditions applied to the porcine myoblasts cultures. Briefly, HSMM cells were seeded onto MC+ coated plates in SKGM2 media with supplements, 20% FCS and 2% chick embryo extract (CEE). Once the cells reached about 80-90% confluence, proliferation media was replaced with differentiation media that contained DMEM, 1% Penicillin-Streptomycin and 0.4% UG. Cells were incubated for 3-5 days in the same media at 37°C, 5% CO_2, 5% O_2 in a humidified incubator.

2.6.2 Comparison of HSMM fusion rate using MC+ differentiation method

To quantitatively measure the difference in fusion rate of HSMM between MC+ method and standard method, HSMM cells were cultured and differentiated using either MC+ method or manufacturer's method simultaneously on separate 96-well plates. Myotubes were fixed at five days of differentiation and fixed with 70% EtOH. Myotubes were immunostained for expression of fast twitch myosin heavy chain and counterstained with Harris- haematoxylin. Myoblast fusion rate was calculated as described later in this chapter.

2.6.3 Long term maintenance of HSMM myotubes using MC+ method

In order to evaluate the long term maintenance of the HSMM myotubes that were differentiated using the MC+ method, the myotubes that were formed by four to five days of differentiation using the MC+ method were maintained further by replacing the differentiation media with proliferation media on fifth day of differentiation. The resultant myotubes were maintained in the proliferation media for a further nine days and a second round of differentiation was induced by replacing the proliferation media with differentiation media (DM1- DMEM, 1% Penicillin-Streptomycin and 0.4% UG). During this second round of differentiation, the HSMM cells were allowed to differentiate for 2-3 days to obtain increased differentiation.

2.7.1 Growth promoter treatment of myotubes

DMEM media (DM1) with Ultroser G was removed from myotubes which had been differentiated for 5 days and replaced with 1% of charcoal stripped FCS (Gibco) containing DMEM with 1% Penicillin-Streptomycin. Charcoal stripped FCS was used to reduce the amount of growth factors present within the UG that was used in the DM1 for differentiation. Myotubes were maintained in this media for 24 hours until the growth promoter treatment. Relevant concentrations of growth promoters used is shown in the table below. The growth promoters were diluted in respective agents and stored at -80˚C prior to use at 1: 10,000 dilution (1ul of growth promoter per every 10 ml of growth media in the well, final concentration used is shown in table). To expose cells to the growth promoter, the existing media (DMEM+1% charcoal stripped FCS+ 1% Penicillin-Streptomycin) was removed from the relevant wells and 1 µl of each

growth promoter added per 10 ml of culture media. After mixing and the growth promoter supplemented medium was quickly placed back into the corresponding wells. Every treatment was conducted as triplicates. Due to the normal evaporation of media during culture, any deficiency in the volume of medium in each well (usually ~10%) was topped up to the optimum volume by the addition of DMEM+ 1% Penicillin-Streptomycin without out the addition of charcoal stripped FCS (to avoid the introduction of fresh serum). The myotubes were incubated in the media containing growth promoter supplements for the required time (stat range of hours) and at the end of treatment, media was removed and cells were rinsed three times with DMEM at RT. Following the rinses, cells were replenished with the DMEM with 1% charcoal stripped FCS and 1% Penicillin-Streptomycin until collection of the cells for lysis and extraction of DNA for molecular analysis.

Growth promoter	**Final conc. used**	**Vehicle**
Ractopamine	100µg/ml	DMSO
IGF-1	10ng/ml	10mM HCl
Testosterone	100nM	EtOH

Table 2. 5 Details of the growth promoter concentrations used on myotubes cultures

2.7.2 Cell fixation and immunocytochemistry

Myotubes or myoblasts were rinsed twice with PBS before fixation with 70% EtOH for 10 min at RT. The EtOH was removed and the cells were rinsed three times with PBS and once with tris buffered saline (TBS) for 10 mins. The plates were immunostained or the plates with TBS were stored at 4˚C until use. Immunostaining was performed using Dako EnVision+ System using a horseradish peroxidase-3,3'-diaminobenzidine (HRP-DAB) according to the manufacturer's recommendations. Briefly, the endogenous peroxidase blocking solution was added to the fixed cells for 10 min at RT then washed off with TBS at least 3 times. Primary mouse monoclonal antibodies were diluted in 1X TBS at 10 µg/ml concentration. The following dilutions were used respectively; Pax3 (1/100, Abcam); Pax7 (1/50- a kind gift from Dr. Dylan Sweetman, University of Nottingham); MyHC fast twitch (1/400, Sigma); MyHC slow twitch (1/4000, Sigma) and Alpha Actin (1/50, DAKO, clone Sr-1). After 40 min of incubation with primary antibody at RT, cells were rinsed 3 times with TBS. This step was followed by incubation with an HRP-labelled polymer conjugated anti-mouse secondary reagent for 40 min at RT. Unbound antibody was rinsed off with 3 rinses with TBS. After the antibody incubations, cells were incubated with DAB substrate for 6 min at RT. Once enough dark brown colour had developed, cells were washed with TBS and either imaged or stained with haematoxylin. Cells that were not incubated with the primary antibodies were treated as negative controls.

2.7.3 Haematoxylin and Eosin (H&E) staining

Cells were initially washed with generous amount of tap water and Harris' haematoxylin was applied for 6 min and then rinsed with running tap water several 3-5times. Acidified alcohol was added for 1 or 2 sec and was quickly removed. Cells

were washed with tap water 4-5 times and ammoniated water was added for 2 min. The cells were subsequently incubated with eosin solution for 2 min and rinsed with H_2O three times before imaging with a light microscope.

2.7.4 Adenoviral mediated GFP expression in myotubes to examine structural integrity long term

During long term cultures over 28 days, it was necessary to demonstrate that the integrity of myotubes was maintained. Therefore, pig myoblasts and myotubes were allowed to differentiate in the DM1 for 5 days in a 96-well plate before addition of an adenoviral expression system that contains a green fluorescent protein (GFP) expression construct under control of the cytomegalovirus (CMV) promoter (Adeno–X Expression System 2, BD Biosciences) GFP expression was observed after around 48 hours when myotubes were imaged using a fluorescent microscope. To ensure imaging of same set of myotubes, a region with identifiable patterns of myotubes was identified and manual reference points were made to repeatedly identify GFP in the same region of the well. A total of three replicates were performed in each experiment.

2.7.5 Myoblast fusion index of porcine and human skeletal muscle cells

The myoblast fusion rate was quantified for the porcine myoblast and human skeletal myoblast cells (HSMM- Lonza, CC-2580). Myoblasts were differentiated for 5 days and immunostained against α-sarcomeric actin followed by nuclear counterstaining with Harris' Haematoxylin. Images were obtained at 40X magnification and the nuclei of the unfused myoblasts and multinucleated myotubes were manually counted. The percentage of nuclei in the myotubes compared with the total number of nuclei in one

field was calculated. Around 1200 nuclei were counted for each differentiation condition from over 12 images for each condition. Myotubes were defined as cells with more than three nuclei in a fused state and myoblasts were defined as unfused cells with a single nucleus.

2.8 Influenza virus infection of cells

2.8.1 Influenza virus subtypes

The influenza-A virus subtypes used in this study are shown in table below. Embryonated chicken eggs that were 10 days old were inoculated with the respective virus subtype and the allantoic fluid was harvested at 48 h post inoculation. Viruses were aliquoted and stored at -80 °C until use.

species	Influenza A virus subtypes
avian	Low pathogenic influenza [LPAI] H2N3(A/mallard duck/England/7277/06)
human	USSR H1N1 (A/USSR/77)
swine	H1N1 (A/swine/England/117316/1986)
human	pandemic H1N1 2009 (A/California/07/2009)

Table 2.6 Influenza virus subtypes used in this study

2.8.2 Influenza virus receptor detection using lectin specific immunocytochemistry

Influenza virus can attach to host cells via receptors normally used by lectins (Baum & Paulson 1990). To detect the expression of lectin receptors on host cells and therefore their susceptibility to influenza attachment, immunocytochemistry was undertaken. Porcine myoblasts and myotubes were grown in the Nunc™ Lab-Tek™ II Chamber Slide™ System (10 wells) in which wells were pre-coated with MC+. Cells were rinsed with PBS and fixed with 70% EtOH. The streptavidin/biotin blocking kit (Vector Laboratories) was used to remove any endogenous biotin activity. Cells were incubated overnight at 4°C in the dark with fluorescein isothiocyanate (FITC)-labelled *Sambucus nigra agglutinin* (SNA) lectin and biotinylated *Maackia amurensis agglutinin* (MAA II) lectin (Vector Laboratories) with a final concentration of 10 µg/ml. The myoblast or myotube cells were washed three times with TBS before the addition of streptavidin-alexa-fluor 594 conjugate (Invitrogen) and a further incubation for 2h at RT. After washing 3 times with TBS, the gasket and the walls of the multiwell chamber were removed carefully using a scalpel blade. A drop of ProLong Gold anti-fade reagent with 4′, 6′ diamidino-2-phenylindole (DAPI) (Invitrogen) was used to mount the sample. Slides were then kept at RT in the dark to cure until image acquisition using a fluorescent microscope. Negative controls were samples without lectin MAA II.

2.8.3 Calculation of multiplicity of infection (MOI)

Approximately 40,000 MDCK cells in 100µl per well were seeded into a 96-well plate and the cells were allowed to form a confluent single cell layer for 24 hours. Cells

were then washed with PBS (Invitrogen) prior to the addition of the relevant influenza virus stock. Virus was added in two fold dilutions from 1 µl up to 50 µl per well as the maximum volume. Three replicate wells were used for every dilution pipette tip was changed for every dilutions. Virus stock was diluted in serum-free infection medium in which cells were incubated with virus for 2 hours at 37˚ C, 5% CO_2 then the medium was washed off and cells rinsed three times with PBS. Cells were replenished with 100 µl of fresh infection medium and incubated at 37˚C for a further 4 hours. At the end of this period, cells were rinsed with PBS and fixed with chilled acetone:methanol (1:1) and immunostained for viral NP protein using anti NP antibody (Abcam), diluted 1:200 with TBS as described earlier in the methods section. Wells which contained NP positive cells were described as focal forming unit (ffu). The dilution at which 95-100% of the cells in a well were stained positively for viral NP protein was considered as 1.0 MOI.

2.8.4 Influenza virus infection of muscle cells treated with growth promoters

Porcine myoblasts and myotubes were treated with growth promoters as described earlier using 12 well flat bottomed plate. Influenza virus stock was prepared at the required MOI in infection medium.

Muscle cells were rinsed with PBS and 50 µl of infection medium containing virus was added to the wells and incubated at 37˚C, 5%CO2 for 2 hours. After infection, cells were rinsed 3 times with PBS to remove the unbound viruses. Cells were incubated with DMEM containing 1% charcoal stripped FCS, 250 ng/ml TPCK trypsin, 1% Penicillin-Streptomycin and respective growth promoters for required duration until cell culture supernatant or cell lysate was collected for further analysis.

Influenza virus was carried out for the NPTr cells using infection media and infection was done for PTECs using BEGM media supplemented with 250ng/ml TPCK trypsin.

2.8.5 Quantification of infectious virus released into the culture supernatants

Culture supernatants from muscle cells, PTECs or NPTr cells were collected at specific times after infection with the respective virus subtypes and transferred into an Eppendorf tube. The supernatant was centrifuged at 500g for 5 min then transferred into a fresh sterile tube before storing at -80° C. To quantify the infectious virus released into the culture supernatant, the supernatant was thawed on ice. In the meanwhile a 96 well, flat bottomed plate containing confluent MDCK cells was washed three times with PBS and 50 µl was transferred into each well of the confluent MDCK cells. For every sample, 3 replicate wells were used. After 2 hours of virus binding, the wells were rinsed off with PBS and 100 µl of fresh infection medium was added into each well and further incubated for 4 hours at 37°C, 5% CO2. Cells were rinsed with PBS, fixed with cold acetone-methanol (1:1) for 10 min then rinsed again with PBS, followed by with a 10min incubation in TBS. incubation in TBS. Uninfected wells of MDCK cells were kept as negative controls.

Immunostaining for viral NP was performed as described earlier in this chapter. Light microscope images were acquired at 10X magnification. Focal forming units per ml (ffu/ml) of supernatant was calculated using the following formula (Adeno-X™ Rapid Titre Kit User Manual)

$$\frac{\text{(Infected cells/field) x (fields/well)}}{\text{Volume of virus (ml) x (dilution factor)}}$$

Since the images were captured at 10X magnification, the number of fields per well of a 96-well plate is considered as 12.6.

2.9.1 Measurement of caspase 3/7 activation

The activation of caspase 3/7 as an indication of apoptosis was measured using Caspase-Glo 3/7 Assay (Promega) according to manufacturer's instructions. In brief, muscle cells were grown in 96-well, flat bottomed plat s. Once the desired duration of infection was completed, 100 µl of Caspase-Glo 3/7 reagent was added to one well of 96-well plate containing 100 µl of medium. The reagent was mixed gently with the culture media followed by incubation at 37°C for 30 min. The mixture was subsequently transferred to a white-walled 96-well plate (Greiner Bio-One) and the luminescence was measured using Orion L microplate luminometer (Titertek-Berthold).

2.9.2 Cell viability measurement by MTS assay

CellTiter 96®, a non-radioactive cell proliferation assay (hereafter referred to as MTS) kit containing 3-(4,5-dimethylthiazol-2-yl)-5-(3-carboxymethoxyphenyl)-2-(4-sulfophenyl)-2H-tetrazolium (MTS) (Promega) was used to measure the cellular metabolic activity and thus indicate viability. Porcine myotubes were differentiated in several 96-well plates for 7 days and subsequently the myotubes in 96 well plates were used every week intervals for 50 days. For assay of viability, 20 µl of MTS reagent was added per well of a 96-well plate containing 100 µl of medium and mixed gently, followed by incubation in a 37°C, 5% CO_2 incubator for 1 h. Up to four replicate wells were used for each sample and the wells without any added MTS reagent were considered as negative control and the background reading obtained from these wells

was subtracted from the sample values. The absorbance was read at 490 nm using a luminometer (BMG Fluostar optima microplate Reader).

2.9.3 Quantitative real-time reverse transcriptase PCR (qRT- PCR)

The expression levels of a number of selected muscles, influenza virus and cytokine genes were quantified used quantitative real time polymerase chain reaction (qRT-PCR). A Taqman based qRT-PCR method was used and this was similar for the myosin heavy chain isoforms and the innate immune related genes.

2.9.3.1 RNA extraction, cDNA reverse transcription and qRT-PCR

Cells were lysed in Qiagen's RLT Plus buffer with 1% β- Mercaptoethanol containing buffer until RNA extraction. The total RNA was extracted using the established protocol obtained with the Qiagen's RNeasy Plus kit. Possible contamination of genomic DNA was eliminated using Qiagen's genomic DNA elimination columns, based on the manufacturer's protocol. The isolated total RNA (1 μg) was reverse transcribed using a SuperScript™ III First-Strand Synthesis System (Invitrogen) for RT-PCR.

qPCR was performed using a LightCycler® 96 Real-Time PCR System (Roche) with LightCycler 480 probes master mix (Roche). All the genes except the TNF-α were TaqMan hydrolysis probes (FAM TAMRA labelled probes) and their respective primer pairs. For TNF-α gene quantification, the SYBR green chemistry was used. For each sample, the PCR reaction was set up as shown in the table shown below.

qPCR master mix components	volume
probes master mix	10 µl
probe (final concentration 200 nM)	0.4 µl
primers mix (final concentration 600 nM)	0.6 µl
template cDNA (used at 1:25 dilution)	5 µl
Diethylpyrocarbonate (DEPC) treated water	3.4 µl

Table 2.7 Components of the qRT-PCR master mix

The cycling conditions for qPCR using TaqMan and SYBR green based qPCR are shown in shown below.

Step		**Temperature (°C)**	**Time (s)**	**Cycle**
Initial denaturation		95	600	1
Melting	Denaturation	95	10	45
	Annealing	60	30	
	Extension	72	10	
Cooling		4	Hold	1

Table 2.8 Cycling conditions for taqman qRT-PCR

qPCR conditions used for the SYBR green based qRT-PCR was; pre-incubation at 95 °C for 5 followed by 45 cycles of 95 °C for 30 sec, 60 °C for 30 sec and 72 °C for 10 sec. After PCR, a melting curve analysis was performed with continuous acquisition mode. All the qRT-PCR experiments were performed using three biological replicates with three technical replicates for each sample. The mean values from these replicates were used for calculation of gene expression.

2.9.3.2 Normalization of qRT-PCR

18S rRNA was used as the house-keeping gene for the normalization of target gene expression levels. Based on the relative standard curve method, expression of each gene of interest was calculated. A small volume (2 µl) from all cDNA stocks used in the experiment was pooled into an Eppendorf to make the cDNA pooled stock. From this, a 2-fold-serial dilution from 1:25 to 1:1600 was made to generate a standard curve. The Cq value of each standard and log concentration was used to calculate the equation for each gene using linear regression analysis. Interpolation of the Ct value corresponding to the standard curve was used to calculate the concentration of each

target gene. Normalisation of the target gene expression calculated by the formula: the gene expression concentration of the target gene / concentration of *18S rRNA*.

Primer	Sequence	Species
Embryonic MyHC	Forward - cccggctttggtctgattt	Porcine
	Reverse - ggtgtcggctgagagtca	
	Probe – tgctgctgtctgctgtcctctgcg	
Perinatal MyHC	Forward - cgagccctcctgctttatctc	Porcine
	Reverse - tgccagatgaaaatgcaggtt	
	Probe – ccaagagcccagagtgttaggcacttcc	
MyHC slow	Forward -ggccccttccagcttga	Porcine
	Reverse -tggctgcgccttggttt	
	Probe -cctctttcttctcccagggacattcga	
MyHC2a	Forward -ttaaaaagctccaagaactgtttca	Porcine
	Reverse -ccatttcctggtcggaactc	
	Probe –ttccaggctgcatcttctcacttgctaag	
MyHc2x	Forward - agcttcaagttctgccccact	Porcine
	Reverse - ggctgcgggttattgatgg	
	Probe – agcccagtcaaagacccttgagatgca	
MyHC2b	Forward -cactttaagtagttgtctgccttgag	Porcine
	Reverse -ggcagcagggcactagatgt	
	Probe -tgccaccgtcttcatctggtaacataagagg	
Alpha actin	Forward - ccagcaccatgaagatcaagatc	Porcine
	Reverse - acatctgctggaaggtggaca	
	Probe – ccccgccggagcgcaagt	
18S	Forward -acggctaccacatccaagga	Human/ Porcine
	Reverse -accaattacagggcctcgaaa	
	Probe -cgcgcaaattacccactcccga	
Influenza A – M gene	Forward - agatgagtcttctaaccgaggtcg	
	Reverse – tgcaaaaacatcttcaagtctctg	
	Probe - tcaggccccctcaaagccga	
TNF-α	Forward- cccgactatctggactttgct	Porcine
	Reverse- ccagcccctcattctctttct	
Mx-1	Forward - tgaacgaagaagacgaatggaa	Porcine
	Reverse - ccacctgcgaagcatctga	
	Probe - cagttaccgggacagcgagattgagc	

Table 2.9 Selected genes and their PCR primers and probes used to assess muscle cells, influenza virus and innate immune response

2.10 Statistical analysis

Statistical analysis was performed for the qRT-PCR results and the myotube fusion rate using GraphPad Prism 6 (GraphPad Software). Experiments were performed with a minimum of three replicates and the standard error was calculated. Student's t test was used to assign statistical significance. P values < 0.05 were considered statistically significant.

Chapter 3

Optimisation and characterisation of a long term, 2D myotube culture that recapitulates postnatal fibre plasticity

3.1 Abstract

Development of a long term sustainable myotube culture that simulates functional skeletal muscle will greatly contribute towards the reduction of animal use and help to study muscle biology in a convenient manner with high throughput. Skeletal muscle cultures of mammalian or avian species traditionally suffer from insufficient myotube differentiation capacity and short lifespan in culture. These technical limitations greatly restrict the ability of myotubes to undergo phenotypic maturation. This study established a simple and effective method of long term porcine myotube culture (beyond 50 days) in a two-dimensional format (2D) in which the cells retained key features of postnatal fibre types, predominantly fast MyHC isoforms. This was achieved by making a significant improvement to the culture conditions, such as the extracellular matrix components and an improved proliferation and differentiation method to maintain the myotubes for extended periods in culture. The presence of muscle specific genes and protein expression along with spontaneously twitching myotubes demonstrated the function of this muscle culture system. This culture method is a promising alternative for porcine myotubes which may be applied to other species, including human.

3.2 Introduction

Skeletal muscle satellite cells are progenitors of multinucleated muscle fibres, first identified by Mauro (1961) and are one of the earliest recognised cells with stem cell-like properties (Mauro 1961; Schalbruch & Hellhammer 1977). *In vitro,* isolated satellite cells are activated then undergo rapid proliferation as myoblasts, which then differentiate and fuse to form post-mitotic myotubes which are characteristic of early muscle fibres (Capers 1960) . Skeletal muscle fibres in animals display a high degree of phenotypic plasticity. They are highly adaptive to different internal and external signals such as physiological demands or response to disease, which results in phenotypic changes in size (hypertrophy or atrophy) and metabolic capacity (ranging from highly oxidative to enhanced glycolytic fibre type) (Schiaffino & Reggiani 2011). Examples which lead to changes in muscle fibres include neuromuscular signals, hormonal or nutritional changes and physical stress (Fitts & Widrick 1996; Fitts et al. 2001; Blaauw et al. 2013).

In vivo, newly formed myotubes undergo a maturation process of hypertrophy and metabolic remodelling during which the initial dominant embryonic and perinatal (neonatal) myosin heavy chain (MyHC) isoforms are replaced with the four main postnatal MyHC isoforms of slow, 2A, 2X and 2B, each sequentially corresponding to a fibre type of increasing glycolytic and decreasing oxidative capacity (Ecob-Prince et al. 1986)

Although muscle satellite cells of different host species have been used in adherent two-dimension (2D) cultures for many years, to date such cultures can primarily only undergo the early stages of myogenesis and myotube formation (Lauren Cornall 2012; Owens et al. 2013; Zhu et al. 2013). *In vitro,* myoblasts often show limited ability to

differentiate and fuse, and porcine myoblasts in particular show the least differentiation among mammalian and avian species (Baquero-Perez et al. 2012) . Since myotubes in culture are prone to rapid detachment and breakage, presumably through spontaneous contractions, their replacement by newly-formed myotubes perpetuates an immature phenotype (Kubis et al. 1997). Due to these limitations, muscle culture experiments are typically performed on immature myotubes over a narrow window of 3 to 7 days of differentiation (Abdul-Hussein et al. 2012).

Several attempts have been made to improve the myotube culture method by providing different extracellular matrix (matrigel and laminin) components (Wilschut et al. 2010b). Although some improvement in fusion was achieved, myotubes could not be sustained beyond five days. Other approaches utilised electro spun polymer coating (Sakar et al. 2012), which was reported to facilitate myoblast fusion and myotube attachment, but with limited success. In another approach, topology dependent myotube arrangement was used to generate myotubes for tissue engineering purposes (Zhao et al. 2009). A combination of mechanical stretching of the myotubes over microgrooves partially improved the differentiation but this was only sustained over several days (Huang et al. 2012).

Several three-dimension (3D) cultures have been developed using a specialised fabricated mould, with the help of a fibroblast co-culture (Kalman et al. 2015). Other attempts to extend the transient persistence of myotubes included the use of other 3D cultures. For example, murine C2C12 muscle cells were grown on silicon wafers (Sakar et al. 2012). Another approach used primary rabbit muscle cells cultured on gelatin microbeads in suspension and this resulted in prolonged myotube adherence and fibre maturation for up to five weeks, with the expression of adult fast twitch MyHCs (2A, 2X and/or 2B isoforms) (Kubis et al. 1997). Thus some of these attempts

improved the quality of the myotubes. Another study used a 3D collagen mould in a chamber slide which improved primary rat myotube formation and reduced loss over a three-week period (Smith et al. 2012). However, such culture methods and other similar approaches have limited practicalities requiring specialised culture platforms and as a consequence, have reduced flexibility to conduct routine cellular manipulations.

This chapter describes the development of a simple and highly reproducible method for the extended 2D culture of myotubes from primary porcine myoblasts. The pig is an excellent model species, owing to its physiological similarity to humans, easy availability of tissue, as well as its importance as target species in its own right. The method allowed efficient differentiation and fusion of myoblasts into myotubes that remained adherent to the 2D culture surface for over seven weeks. In addition, for the first time, myotubes matured into postnatal fibre types expressing MyHC 2x and 2b predominantly by three weeks of differentiation. This is a major technical advance which will permit to the study of plasticity in porcine muscle phenotype.

3.3 Results

Part 1: Optimisation of porcine myoblast culture conditions

3.3.1 Initial attempts to differentiate porcine myoblasts

Porcine myoblasts were isolated and cryopreserved by Dr. Zoe Redshaw using a modified myoblast isolation method (Baquero-Perez et al. 2012). Isolated myoblasts thawed, cultured on collagen coated plates and tested for their purity based on Pax3 and Pax7 molecular marker expression which showed that around 95% cells were positive for these markers (Figure 3.1).

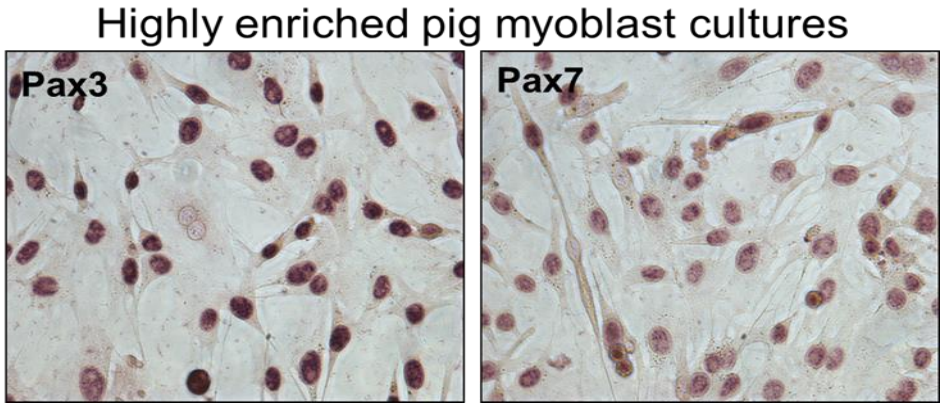

Figure 3.1 Isolated pig myoblasts expressed Pax3 and Pax7 markers
Pig myoblasts immunostained against Pax3 and Pax7 proteins.

Initially cells were cultured on rat tail collagen, type 1 (Sigma) using the widely followed method of skeletal muscle culture that was developed by Doumit (Doumit & Merkel 1992). Cells were cultured in minimum essential media-α (α- MEM media) supplemented with 10% fetal bovine/calf serum (FBS), and the cells were differentiated in DMEM supplemented with 2% horse serum (HS) prior to imaging using a light microscope. This method of differentiation resulted in very limited myoblast fusion by eight days of differentiation (Figure 3.2 a-c). To optimise the differentiation efficiency of porcine myoblasts, cells were cultured using the proliferation media (PM) composed of minimum essential media-α (α- MEM media)

and 10% fetal bovine/calf serum (FBS) until the cells reached about 80% confluence and differentiation was induced using the differentiation media (DM) that was composed of DMEM with 1% penicillin-streptomycin supplemented with horse serum as either 2% or 0.5% or 0%. No differentiation of myoblasts into myotubes was observed with this method (Figure 3.2 a-c). Next, the serum replacement Ultroser G (UG) which has been shown to induce better differentiation of the mouse skeletal muscle cell line C2C12 (Portiér et al. 1999), thus UG at 1, 0.4 and 0.2% was also used in the differentiation medium to compare its effects on porcine myoblast differentiation. The results showed that a small number of myotubes developed by five days of differentiation when cultured in 0.4% UG supplemented medium (Figure 3.2 e)

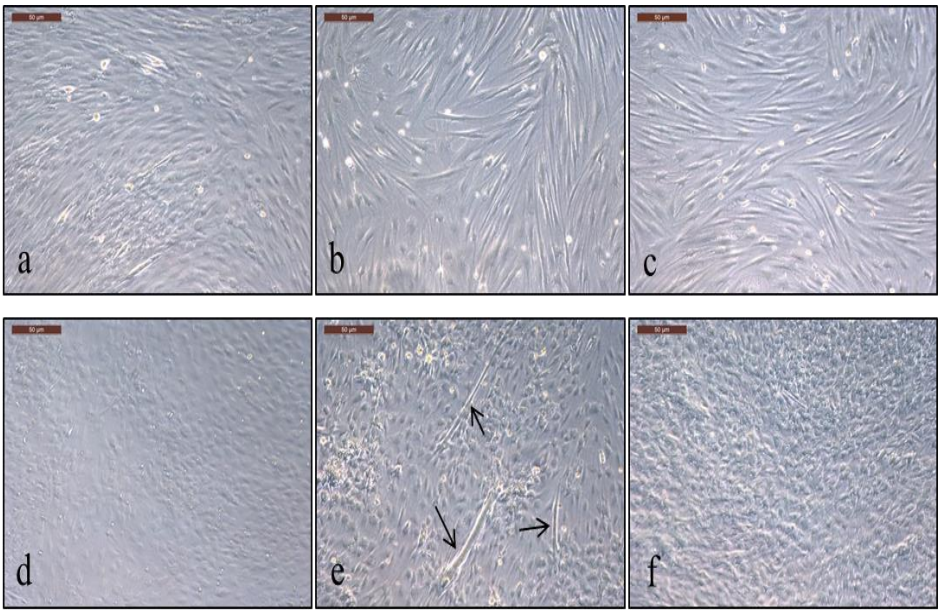

Figure 3.2 Limited myotube formation capacity of porcine myoblasts

Fusion capacity of porcine myoblasts cultured on collagen, type 1 coated plates in α-MEM media supplemented with 10% FBS and penicillin-streptomycin until 90% confluence then differentiated using DMEM supplemented with (a) 2% HS , (b) 0.5% HS (b) and (c) no HS followed by (d) 0.2% UG (e) 0.4% UG and (f) 1% UG (f). Arrows indicate the presence of myotubes (e).

3.3.2 Further optimisation of myoblast proliferation and differentiation into myotubes

a) Media and supplements

In order to optimise the differentiation capacity of porcine myoblasts, two proliferation media were used with the following supplements shown in Table 3.1. Cell were grown in collagen, type 1 coated plates. Since α- MEM is commonly used in myoblasts culture, α- MEM was used as one of the media for one set of cells and another set of cells were grown in a commercially formulated SKGM-2 skeletal myoblast culture media (Lonza). Cells were maintained in differentiation media for upto 10 days to observe the myotubes firmed (images not shown). Examination of the cultures demonstrated myotube formation under condition 11 using SKGM-2 media, with 4% chick embryo extract (CEE) and 20% HS and 0.4% UG in differentiation media (Figure 3.2 e). Thus future cultures used SKGM-2, supplemented with CEE as the proliferation media followed by UG supplementation in the differentiation media.

Conditions	Supplements and medium used at each stage		
	PM		DM
	α- MEM	SKGM-2	
1	20% FBS		DMEM+2% HS
2	20% FBS		DMEM+0.4% UG
3	4% UG		DMEM+0.4% UG
4	No serum		DMEM+2% HS
5	No serum		DMEM+0.4% UG
6	5% FBS		DMEM+2% HS
7	5% FBS		DMEM+0.4% UG
8	10% HS		DMEM+0.4% UG
9	5% HS		DMEM+0.4% UG
10	4% CEE+10%HS		DMEM+0.4% UG
11	**4% CEE+20%HS**		**DMEM+0.4% UG**
12	4%CEE+4% UG		DMEM+0.4% UG

Table 3.10 Proliferation media and supplements used to improve myoblast differentiation

Comparison between α- MEM and SKGM-2 media, supplemented with HS or UG or CEE at the final percentages (v:v) shown. Media supplement provided better differentiation (condition 11) is shown in red.

b) Extracellular matrices

Having optimised the best media for proliferation and differentiation using rat tail collagen type 1 as the extracellular matrix, further experiments were conducted to identify the best extracellular matrix (ECM) for differentiation of porcine myoblasts MaxGel™ ECM (Sigma) is composed of a number of extracellular matrix proteins including collagens, laminin, fibronectin, tenascin, elastin and a number of

proteoglycans and glycosaminoglycan which is known to improve the culture conditions for different cells types. Since SKGM2 was found as a better proliferation media and the presence of CEE and UG positively affected the myoblast differentiation, these components were provided in the media but further concentrations of the supplements were tested. Since 20% of HS resulted in better differentiation than 10% HS in proliferation media (condition 10), as shown in table 3.1, it was postulated that inclusion of nutrient rich FBS in the proliferation media to replace HS along with CEE and UG in differentiation media may result in better myoblast differentiation. CEE was previously shown to induce the myoblast proliferation (Bischoff 1986b).

Thus porcine myoblast cells were cultured on rat tail collagen type 1 or Maxgel coated plates using the f proliferation and differentiation media conditions shown in table 3.2.

Condition	PM	CEE (%)	HS (%)	FBS (%)	UG (%)	DM
1	SKGM	4	20			DMEM+0.4% UG
2	SKGM	2	20			DMEM+0.4% UG
3	SKGM	4		20		DMEM+0.4% UG
4	SKGM	2		20		DMEM+0.4% UG
5	SKGM	4	20			DMEM+0.3% UG
6	SKGM			10	2	DMEM+0.4% UG
7	SKGM		10		2	DMEM+0.4% UG
8	SKGM	4		10	2	DMEM+0.4% UG
9	SKGM	4	10		2	DMEM+0.4% UG
10	SKGM			10	2	DMEM+0.3% UG
11	SKGM		7.5	7.5	1	DMEM+0.4% UG
12	SKGM	4	7.5	7.5	1	DMEM+0.4% UG

Table 3.2 Media supplements used in proliferation and differentiation of porcine myoblasts grown on collagen or Maxgel ECM as coating agent

Along with the media supplements shown in table 3.2 other conditions were also used to optimise the myoblasts conditions mainly using varying concentrations of HS, FBS, CEE or UG in proliferation media and mainly by varying the concentration of UG in differentiation media.

As a measure of differentiation, the number of myotubes was assessed after three to five days of culture by expression of α-actin using antibodies described in Chapter 2. Differentiated myotubes were more abundant with collagen and Maxgel ECM extracellular matrices. The results also showed that CEE in proliferation media and

UG in differentiation media are key ingredients for differentiation capacity (Figure 3.3.b). Usage of Maxgel as a coating agent improved the proliferation rate which was assesses subjectively by the percentage of cell confluence in wells (Figure 3.3.e) and increased differentiation capacity (Figure 3.3.c). Even though the usage of Maxgel ECM improved myoblast proliferation and differentiation, the differentiated myotubes were sampled at 5, 8 and 12 days and showed detachment from the culture plates on day 8 (Figure 3.2, indicated by 8d and 12d).As a consequence of the relatively small number of differentiated myotubes and the detachment after a short period in culture, more optimisation steps were performed.

Collagen, type 1

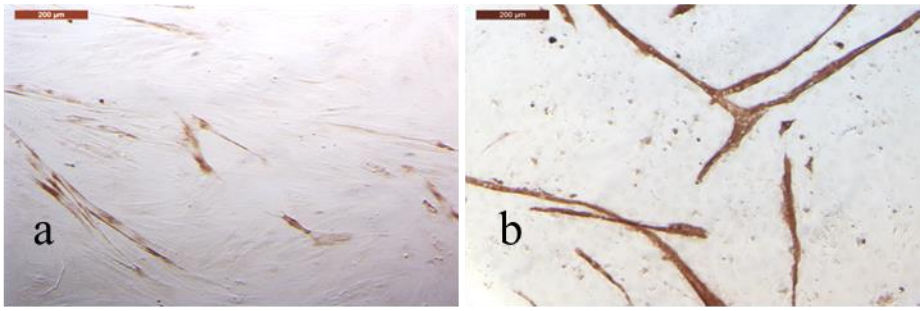

Maxgel

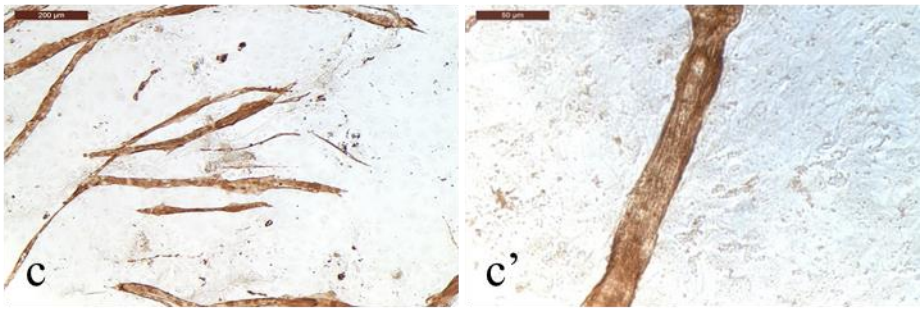

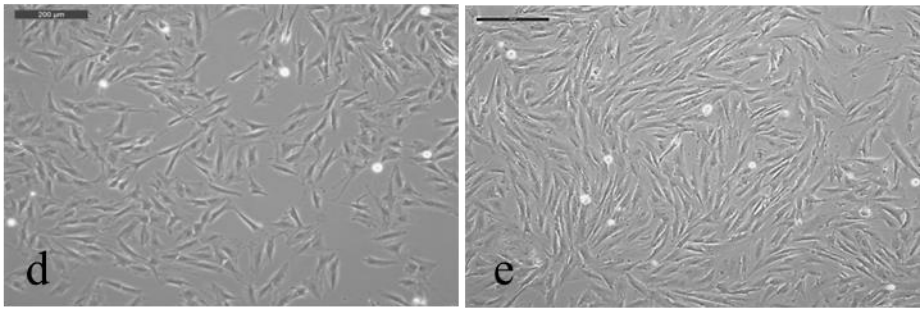

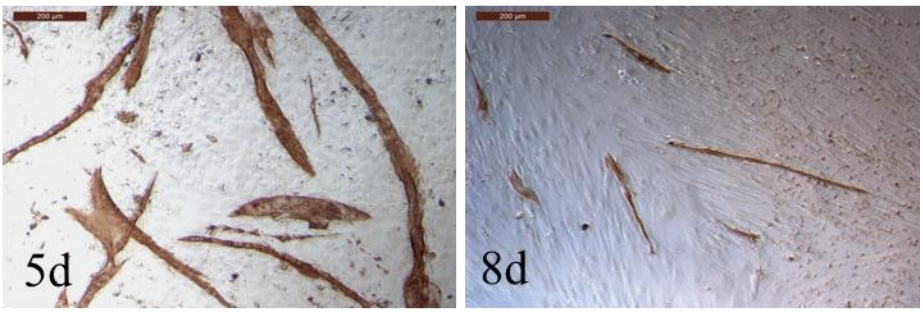



Figure 3.3 Maxgel ECM provides better differentiation capacity for porcine myoblasts

Expression of the muscle protein α-actin was detected in differentiated porcine myotubes using immunocytochemistry (dark brown). Cells cultured on collagen coated plates in SKGM 2 supplemented with 20%HS and differentiated in DMEM with 2% HS (a), myoblasts cultured on collagen coated plates in SKGM-2 with 4% CEE and 20% HS and differentiated for five days in DMEM supplemented with 0.4% UG provided better differentiation (c), a myotube that was cultured on Maxgel ECM is shown at 40X magnification (c'). Maxgel coating and usage of SKGM 2 media with 4% CEE and 20% HS significantly improved the proliferation rate of myoblasts (e) compared with the cells grown on Collagen coated plates using the same conditions (d). The limited number of myotubes formed by three to five days of differentiation under the Maxgel coated plates using SKGM 2 media with 4% CEE and 20%HS was not persistent, myotubes detached from culture plate thus a reduction in the amount of myotubes visible from five days of differentiation (5d) to 12 days of differentiation (12d).

c) Combination of collagen and Maxgel ECM extracellular matrices

In order to improve the proliferation and differentiation capacity of myoblasts along with prolonged maintenance and adhesion of myotubes, a new combination of coating was used. Collagen prepared at 2% v/v in PBS and Maxgel ECM diluted 1:100 in DMEM were prepared then mixed at 1:1 ratio (referred as MC – to indicate Maxgel-Collagen) and used as a coating agent in a 96 well plate as detailed in Chapter 2]. Separate plates were coated with Maxgel ECM alone or MC together with a combination of other supplements as shown in table 3.3. Myoblasts culture conditions (3, 4,5,8,9 and 12) resulted in improved myotube formation. Overall, the best myotube differentiation was obtained with condition 3 (images not shown), SKGM 2

supplemented with 2% CEE and 20% FBS for proliferation and DMEM with 0.4% UG as differentiation media.

Condition	Prol. media	CEE (%)	HS (%)	FBS (%)	UG (%)	Diff. med
1	SKGM2	4	20			DMEM+0.4% UG
2	SKGM2	2	20			DMEM+0.4% UG
3	SKGM2	4		20		DMEM+0.4% UG
4	SKGM2	2		20		DMEM+0.4% UG
5	SKGM2	4	20			DMEM+0.3% UG
6	SKGM2			10	2	DMEM+0.4% UG
7	SKGM2		10		2	DMEM+0.4% UG
8	SKGM2	4		10	2	DMEM+0.4% UG
9	SKGM2	4	10		2	DMEM+0.4% UG
10	SKGM2			10	2	DMEM+0.3% UG
11	SKGM2		7.5	7.5	1	DMEM+0.4% UG
12	SKGM2	4	7.5	7.5	1	DMEM+0.4% UG

Table 3.3 Media supplements used for myoblasts grown on Maxgel or Maxgel-Collagen (1:1) coated plates

Conditions used to compare the differentiation capacity of pig myoblasts on Maxgel or MC coated plates.

Combination of Collagen with Maxgel ECM (MC) at 1:1 ratio as a coating agent and supplementation of 20% FBS and 2% CEE in SKGM 2 as proliferation media and

0.4% UG containing DMEM as differentiation media significantly improved myotube formation. There was a significant improvement in proliferation rate of the myoblasts grown on MC coated plates (Figure 3.4.a') when compared with Maxgel ECM only (Figure 3.4.. a) coated plates. It was noted that the increased proliferation capacity of myoblasts under the 20% FBS condition allowed a uniform growth of the myoblasts on MC coated plates (Figure 3.4.a') but the cells on Maxgel ECM coated plates generally formed cells aggregated to a confined area (Figure 3.4.a). This aggregation continued during the differentiation and resulted in areas of densely packed cells (Figure 3.4.b),also shown as myotubes immunostained for muscle protein α actin (Figure 3.4.c). Areas of cell aggregation are marked by arrow marks (Figure 3.4.a) and such areas are circled in the images of differentiated myotubes (Figure 3.4. b and c). Myoblasts grown on MC coated plates grown as a homogeneous layer of cells (Figure 3.4. a') which differentiated to evenly arranged myotubes (Figure 3.4.b') by five days of differentiation. Evenly arranged myotubes grown on MC coated plates immunostained for MyHC fast is represented (Figure 3.4. c'). Myotubes formed by this method using both coatings suffered from non-persistent myotubes by eight to ten days of differentiation when most of the myotubes detached from the plate (Figure 3.4. d) as indicated by arrow. The differentiated myotubes detached as a layer from five days of differentiation (e). A layer of myotubes was immunostained for MyHC fast shown in the inset (f) to show that the detached layer of cells express muscle protein.

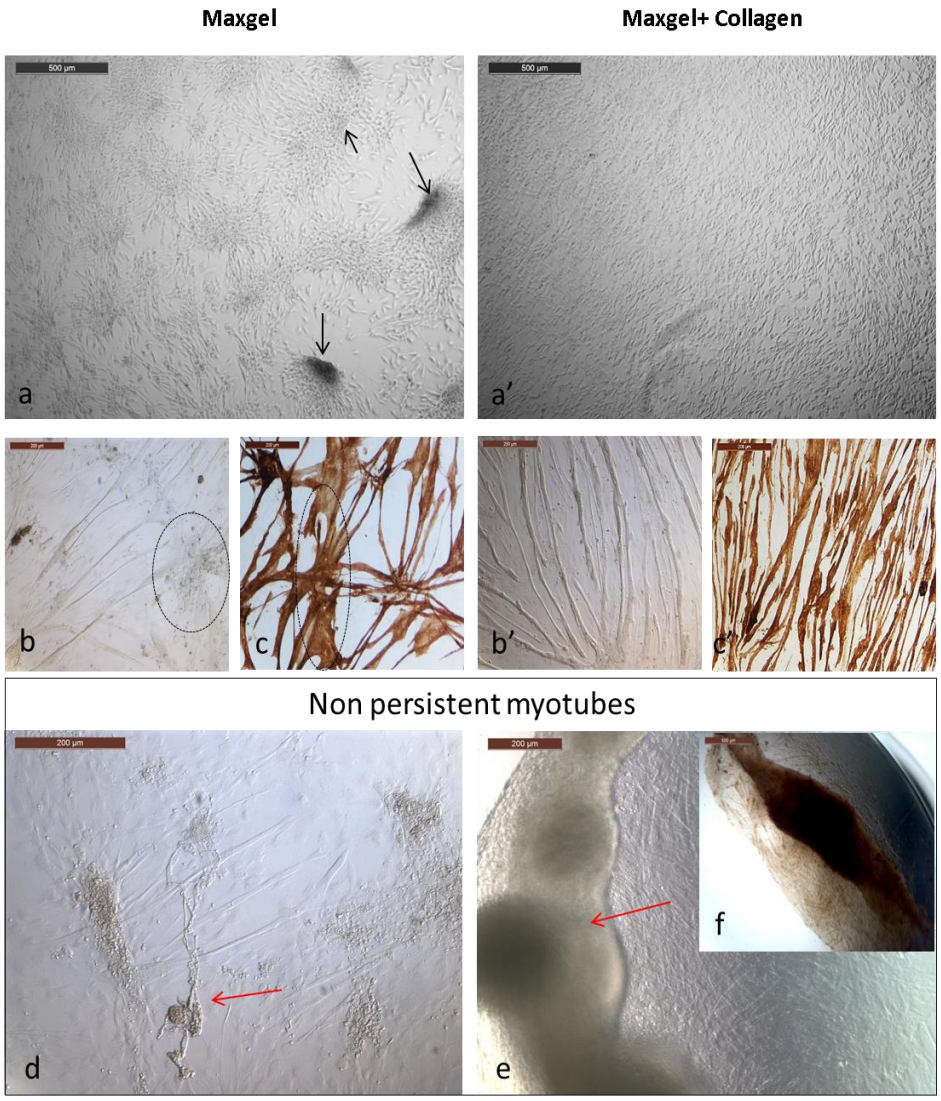

Figure 3.4 Maxgel-collagen surface coating improve myoblast differentiation

Myoblasts proliferated on Maxgel ECM coated plates grow as cell aggregates (a), myoblasts differentiated for five days on Maxgel ECM coated plates form few myotubes and cell aggregates (b), MyHC positive fast twitch myotubes reveals cell aggregates and myotubes which are circled with dotted lines. Myoblasts grown on MC coated plates grow evenly (a') and further differentiates into homogenously arranged myotubes (b') by five days of differentiation which is also presented as immunostained myotubes for MyHC fast twitch protein expression (c'). A myotube that has detached from the culture plate is indicated with red arrow (d). Myotubes detached from the well as a layer of cells from about five days of differentiation (e), similar detached layer myotubes immunostained for muscle protein MyHC fast (f).

3.3.3 MyHC gene expression of porcine myotubes cultured on different extracellular matrices

Myoblasts that had differentiated into myotubes after five days incubation on separate six well plates coated with Maxgel ECM or MC were collected and cDNA obtained as outlined in Chapter 2 . qRT-PCR results showed that myotubes cultured on Maxgel ECM had an increased MyHC slow expression compared with corresponding myotubes that were cultured on MC coated plates. (Figure 3.4 b and b' respectively) Fast type MyHCs- 2A, 2X and 2Bexpression was high in myotubes cultured on MC coated plates compared with myotubes cultured on Maxgel ECM. All gene expressions were normalised to the house keeping gene 18s rRNA expression. The results indicate that expression of the MyHC genes in porcine myotubes can be affected by the extracellular matrix on which they were cultured.

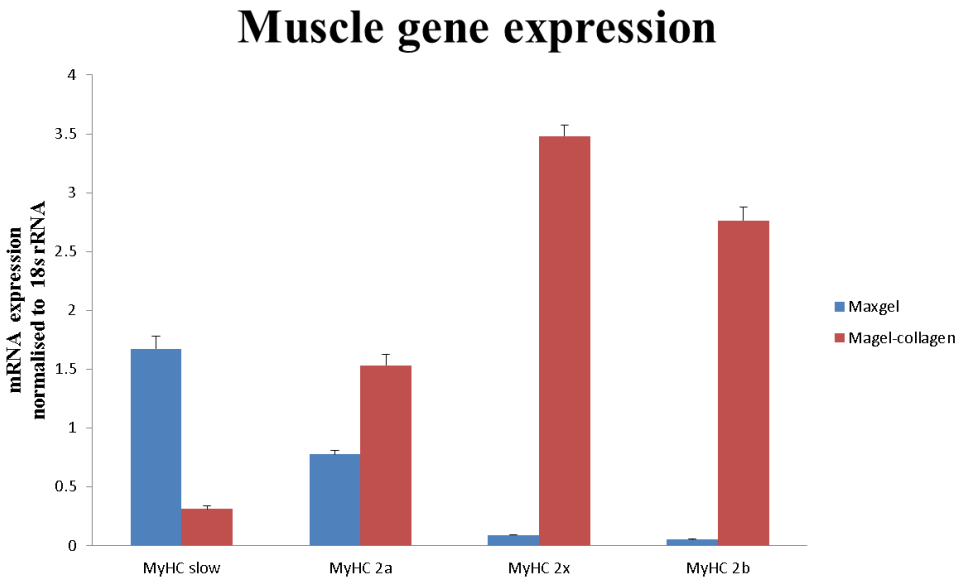

Figure 3.5 MyHC gene expression in porcine myotubes is influenced by the extracellular matrix coating on which the cells were differentiated.

Five day differentiated porcine myotubes expressed varying levels of MyHC genes on extracellular matrix specific manner

3.3.4 Enhanced differentiation of myoblasts by MC+ coating

Since the myotubes were detaching from the as a layer after a few days of differentiation, the Maxgel-collagen coating agent prepared at a 1:1 ratio was applied to 24 well plates and allowed to dry the solution in the culture well as outlined in Chapter 2, such ECM coating method was referred as MC+ coating. SKGM 2 supplemented with 20% FBS and 2% CEE (combination 3) was used as proliferation media and DMEM supplemented with 0.4% UG as differentiation media resulted in highest amount of myotube formation which succeeded to maintain the myotubes in culture plate without detaching from surface.

Conditions	Media	CEE (%)	HS (%)	FBS (%)	uG (%)	Diff. med
1	SKGM2	2	20			DMEM+0.4% uG
2	SKGM2	4		20		DMEM+0.4% uG
3	SKGM2	2		20		DMEM+0.4% uG
4	SKGM2	4		10	2	DMEM+0.4% uG
5	SKGM2	4	10		2	DMEM+0.4% uG
6	SKGM2	4	7.5	7.5	1	DMEM+0.4% uG

Table 3.4 Cell culture media supplements used for the optimisation of myoblast cultures on MC+ coated plates

Porcine myoblasts cultured on MC+ coated plates fused to myotubes at a high rate (Figure 3.6). By three days of differentiation, most of the myoblasts had differentiated into myotubes and by 5 days the maximum number of myotubes was visible.

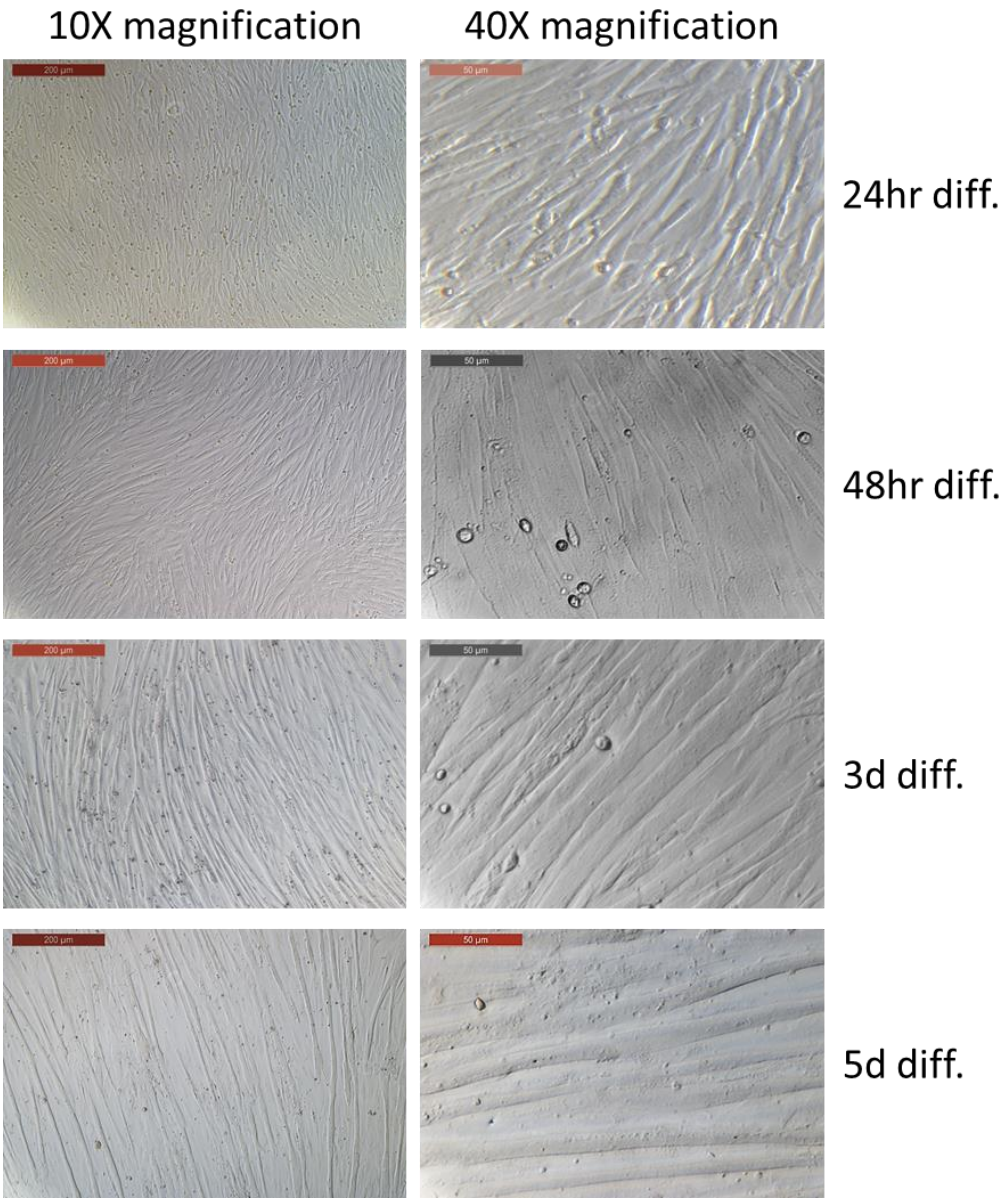

Figure 3.6 Phase contrast micrographs of myotube formation at different time points in differentiation.

Temporal differentiation capacity of myotubes cultured on MC+ coated plates are shown in micrographs at the magnifications shown. Time dependent changes happened to myoblasts was imaged at 24 hours of differentiation subsequently at 48h, 3days and 5 days of differentiation. The maximum number of well-formed myotubes

was visible by five days of differentiation. Formation of multinucleated (three or more nuclei) myotubes from the single myoblasts was considered as myoblasts fusion.

3.3.5 Temporal change in myosin heavy chain expression upon differentiation of porcine myoblasts

The expression of MYHC isoforms were monitored in porcine myoblast cultures after proliferation in SKGM2 medium supplemented with 20% FBS and 2% CEE and differentiation on MC+ coated plates using DMEM supplemented with 0.4% UG (DM1). After two days of proliferation (Figure 3.7a), prior to the initiation of differentiation, very low levels of MyHC isoforms were expressed. Embryonic MyHC was detected at highest, albeit very low levels and perinatal MyHC expression was just detectable. Very low amounts of MyHC slow, MyHC 2a and MyHC 2b were detected but MyHC 2x expression was absent. After two days of differentiation in DM1, all MyHC isoforms were detectable but embryonic MyHC expression remained predominant and at much higher levels compared with pre-differentiation stage (Figure 3.7 a). MyHC 2b expression was also abundant. A similar MyHC isoform expression pattern was observed over the five days (Figure 3.7 c-d) of differentiation, although with declining levels. mRNA expression levels of each gene was normalised against the expression of the housekeeping gene 18S rRNA.

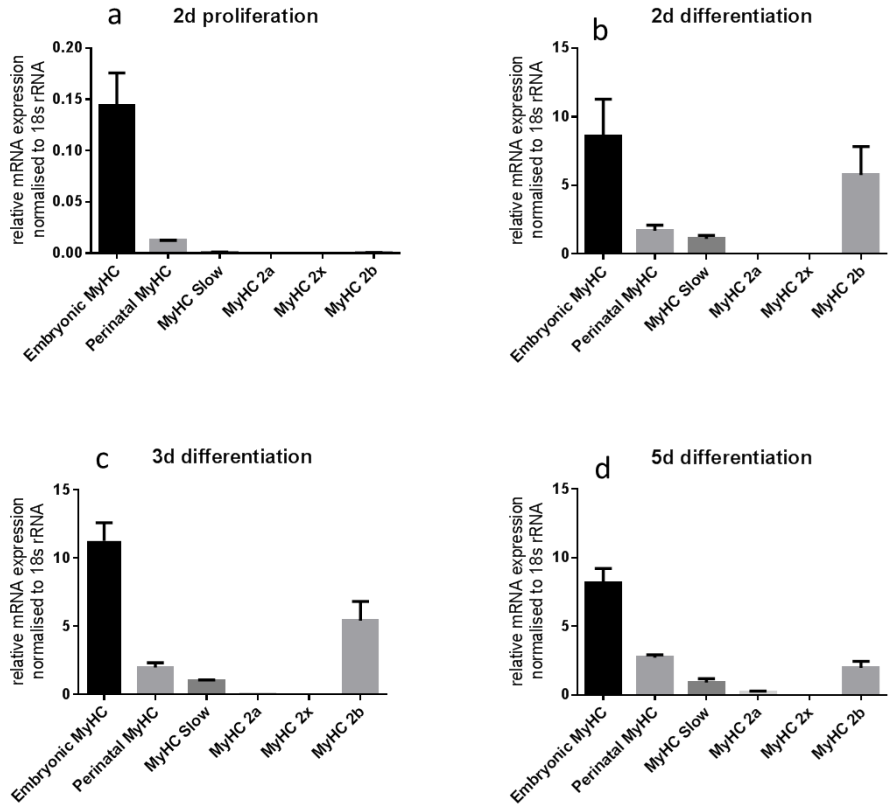

Figure 3.7 mRNA expression of MyHC isoforms in early stages of porcine myoblast differentiation on MC+ coated plates over 5 days

MyHC mRNA expression of porcine myoblasts cultured on MC+ coated plates quantified after two days in proliferation condition (a) and after two, three and five days of differentiation respectively (b-d) All the expression values were normalised to 18s rRNA expression and the experiments were performed in triplicate.

3.3.6 Extended maintenance of porcine myotubes using MC+ method

Significantly improved myotube formation was achieved by the MC+ coated plates in combination with SKGM 2 media supplemented with 20% FBS and 2% CEE as proliferation media followed by differentiation using DMEM supplemented with 0.4% UG. Combination of the above mentioned conditions was referred as MC+ method.

Next, the length of time which myotubes retained their differentiated state and remained adherent was investigated by differentiating myoblasts to myotubes in 24 well plates and monitoring their morphology under phase contrast microscopy every 3-4 days over 28 days. As shown in Figure 3.8 myotubes maintained their structure for over 15 days after differentiation but by 21 days, some myotubes rounded up and detached from the plate. By 28 days, more myotubes were detached and the remaining attached cells started to aggregate

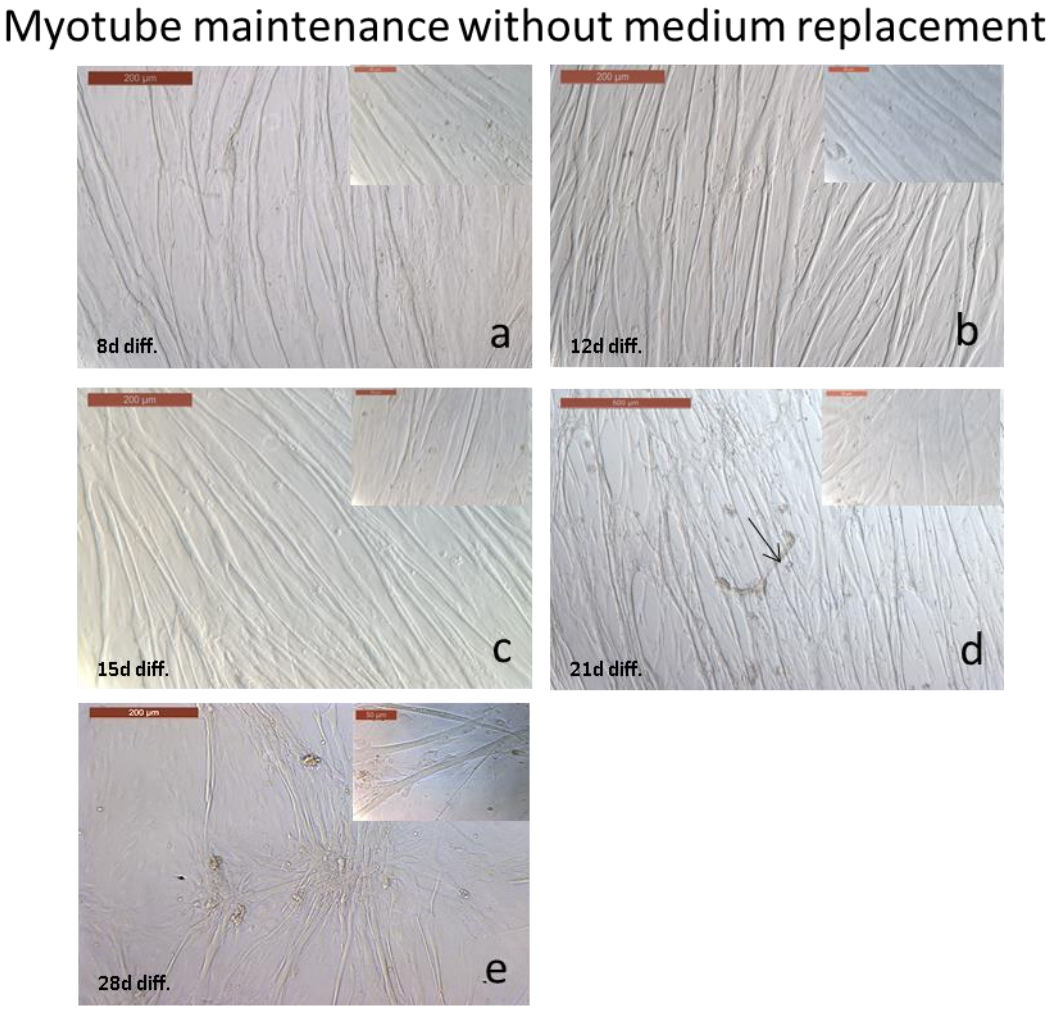

Figure 3.8 Porcine myotubes remain attached to the plate until 28 days of differentiation with some loss of myotubes

Micrographs acquired using a light microscope to show porcine myoblasts differentiated on MC+ coated plates for 28 days without replacing the differentiation

media. (a-c) at 8, 12 and 15 days of differentiation, myotubes maintained its structure. (d) Some myotubes were more granular and detached from the plate by 21 days of differentiation (arrow). (e) Myotubes continued to detach and aggregate by 28 days of differentiation. Scale bar = 200µm. Higher magnification images presented in the inset, scale bar = 50 µm.

3.3.7 Partial replacement of differentiation media allows prolonged maintenance of myotubes in culture

To maintain the structural integrity and attachment of the differentiated myotubes in culture more than 15 days, 25% of the total volume of media in the well was replaced with fresh differentiation media, either DM1 (0.4% UG-DMEM) or DM2 (2%HS-DMEM) at day 15 of differentiation (Figure 3.9. a and b respectively), differentiation media was partially replaced again at 18 and 21 days of differentiation and the cells were fixed at 28 days of differentiation. It was found that partial replacement with DM2 medium resulted in improved myotube morphology and attachment compared with DM1 supplementation after 28 days of differentiation

Temporal effect of the partial replacement of DM on myotube integrity

In order to determine the most appropriate starting time for the replacement of differentiation media to maintain the myotubes for long term in culture, partial replacement of differentiation media (DM2) was started at five days or seven days or 13 days or 15 days of differentiation. Partial replacement of DM2 was repeated every two days from the start of media replacement programme (e.g. five days of differentiation). Early replacement of medium resulted in better myotube maintenance and attachment of myotubes until 44 days without much detachment (Figure 3.9.c and

d) compared with partial replacement started at 13 or 15 days (Figure 3.9 e and f respectively). Therefore, for all future experiments, partial replacement of the DM2 differentiation media with 2%HS was started at seven days of differentiation and continued every two days until the end of the experiment.

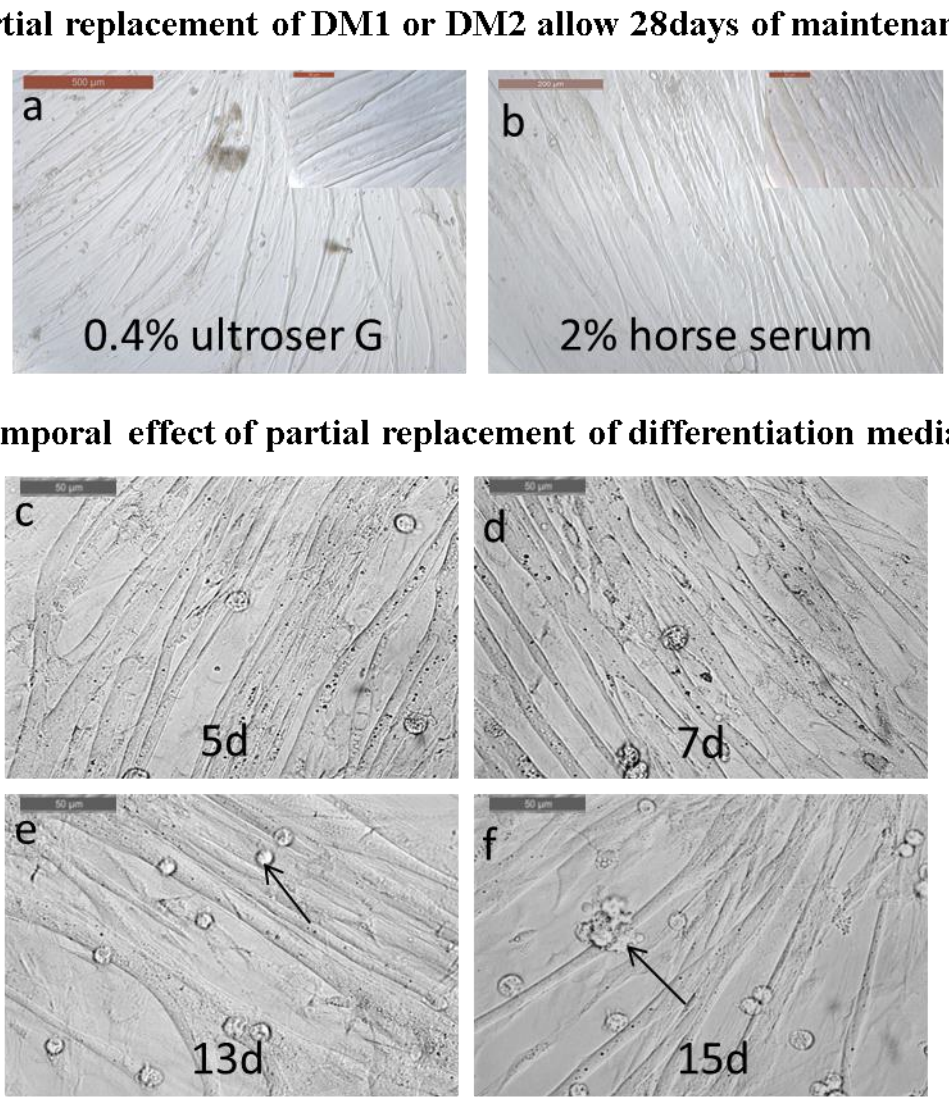

Figure 3.9 Partial replacement of differentiation media with DM2 allowed improved morphology and maintenance of myotubes or 28 days

Micrographs of myotubes maintained in differentiation media for 28 days following partial replacement of media with a) DM1 and b) DM2 at 15 days and media replacement repeated at every three days up to 21 days in differentiation. Partial

replacement of the media started at either five days (c) or seven days (d) or later at 13 or 15 days of differentiation. Myotubes for which medium replacement started at 5 or 7 days maintained their morphology and attachment better until 44 days (not shown) compared with the partial replacement started at 13(e) or 15 (f) days, when cell rounding (arrows) developed.

3.3.8 Effect of serum withdrawal on myotubes

For experimental purposes, it was necessary to maintain myotubes under conditions free of serum or a serum replacement for at least 24 hours prior to exposure to any growth promoters, in order to avoid any undesired effects caused by these supplements. Since myotubes cannot be maintained in completely serum free media, charcoal stripped FCS (Invitrogen), which is known to contain reduced levels of growth factors, was used at different concentrations to (0.3%, 0.6%, 1%, 2% and 3% in DMEM (v:v) to evaluate the effect on myotubes and compare their morphology and attachment with equivalent concentrations of standard FBS. The entire volume of the culture well was replaced with pre-warmed media. Media replacement, either charcoal stripped or normal FBS was performed at two different stages, namely at three or five days of differentiation and cells were cultured for a further 48 hours before microscopic examination. It was found that with the exception of 0.3% and 0.6% charcoal stripped FBS, myotubes cultured in charcoal stripped FBS medium from five days of differentiation sustained myotubes with good morphology and adhesion after 48 hours, when compared with the samples that had the charcoal stripped FBS media replacement at three days of differentiation (Figure 3.10). A minimum of 1% charcoal stripped FBS in DMEM was adequate to maintain myotubes in culture. In media containing 0.3% and 0.6% charcoal stripped FBS, most of the myotubes broke and detached. Myotubes maintained in DM1 with 0.4% UG was used as a positive control.

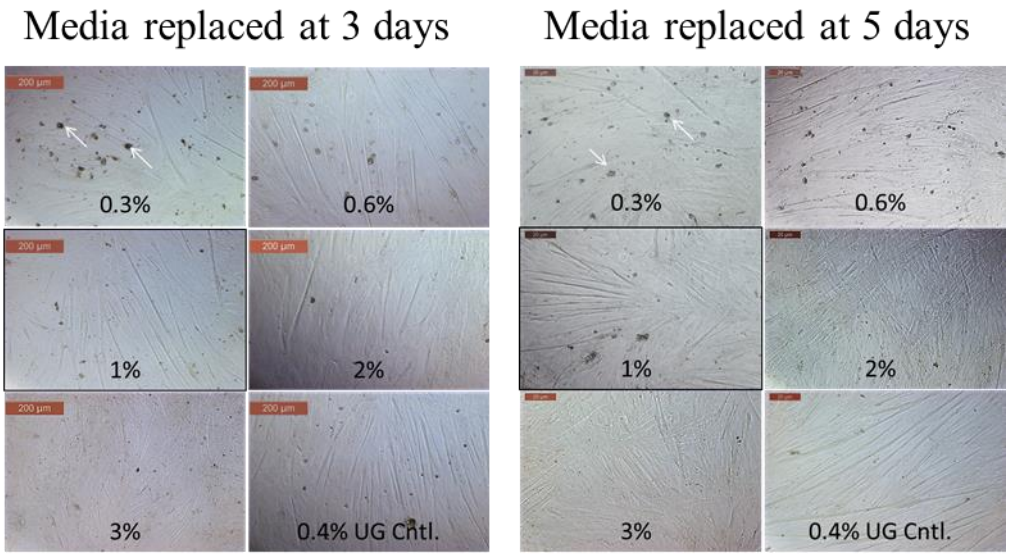

Figure 3.10 Effect of replacement medium containing charcoal stripped FBS

Micrographs of myotubes following replacement of the differentiation medium with either charcoal stripped FBS or standard FCS at various concentrations on days 3 (left panel) or 5 (right panel) post differentiation. Images are represented with the amount of charcoal stripped FCS present in the media (e.g. 0.3% or 3%) Cultures with 0.3% charcoal stripped FBS showed rounded and broken myotubes (white arrows). Therefore 1% charcoal stripped FBS found to be adequate to maintain myotubes which is outlined in black. A positive control of 0.4% UG containing media was used (bottom right corner of each panel)

Part 2: Characterisation of porcine myotubes differentiated and maintained using MC+ method

3.4.1 MC+ method significantly improved porcine myoblast differentiation

After the optimisation experiments, two methods (standard and MC+) were compared to assess which was optimum in differentiating myotubes which expressed α-actin and MyHC slow twitch isoform, both of this are characteristic of myotubes. significant improvement in porcine myoblast fusion and differentiation was achieved by the usage of MC+ method, namely 85% myoblast fusion into myotubes, compared with <20% fusion using other approaches (Figure 3.11. a). Immunohistochemical analysis of the expression of α-actin and MyHC slow isoform showed high levels of expression by all myotubes after 5 days using the MC+ differentiation method, compared with the standard method (Figure 3.11. c and b respectively). So to summarise, the MC+ method involves 1:1 ratio v/v Maxgel ECM and collagen, type 1 coating solution dried to the plate (MC+ coating) with SKGM 2 supplemented with 20% FBS and 2% CEE as proliferation media and DMEM supplemented with 0.4% UG as differentiation media (MC+ method) was used in all subsequent experiments.

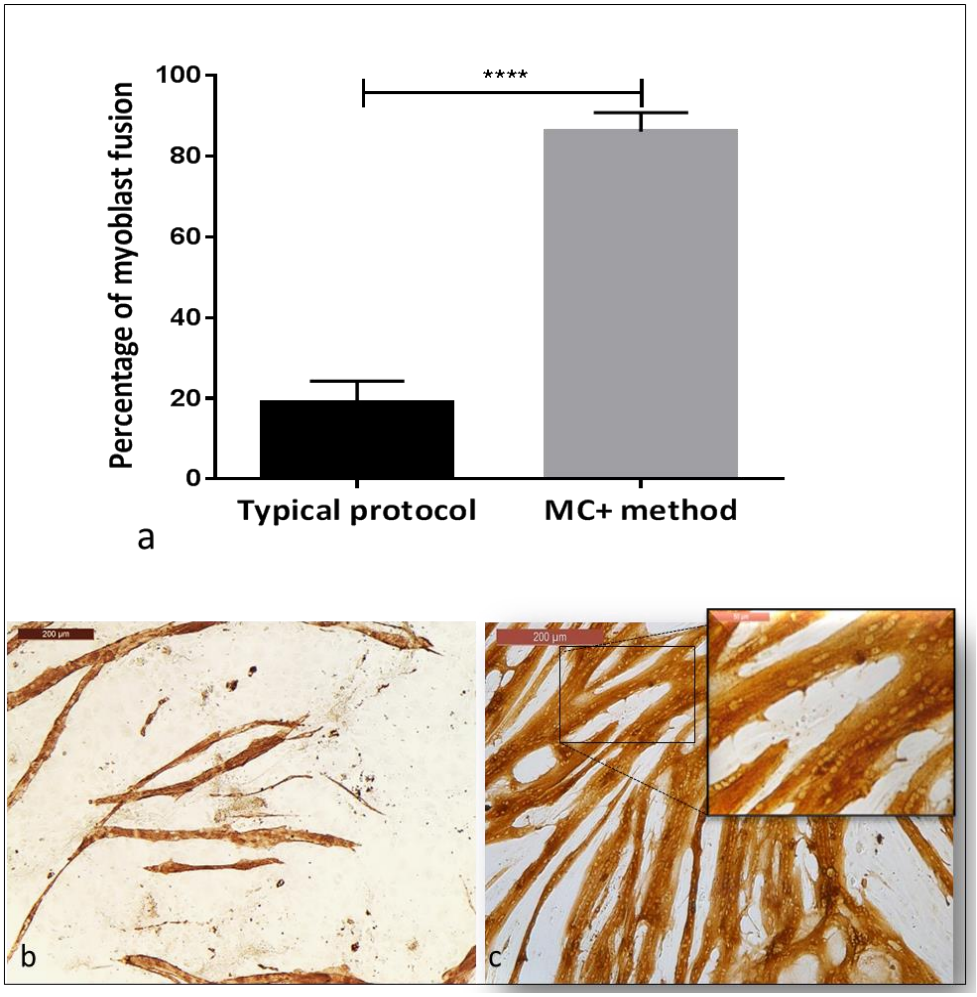

Figure 3.11 The MC+ method improved differentiation capacity of porcine myoblasts compared with the standard culture method

(a) Comparison of the percentage of myoblast fusions following differentiation in the standard protocol versus the MC+ method (b & c) Immunohistochemistry of myotubes differentiated for 5 days by the MC+ method to show expression of muscle protein α-actin (b) and MyHC slow twitch isoform(c). Scale bar = 200µm and 50 µm for the image presented in the inset.

3.4.2 Characterisation of differentiated porcine myotubes maintained in culture for 70 days

Using the optimal conditions summarised in Section 3.4.1 for porcine myoblast proliferation and differentiation into myotubes, cells were cultured for 70 days, with medium partially replaced with DM1 or DM2 at every two days from seven days of

differentiation and periodic microscopic examination conducted as indicated in respective images. Using this approach, it was possible to maintain the morphology and attachment of differentiated myotubes for up to 70 days (Figure 3.12). Based on these findings, this method was used in all future experiments, usually involving incubations of over 28 days.

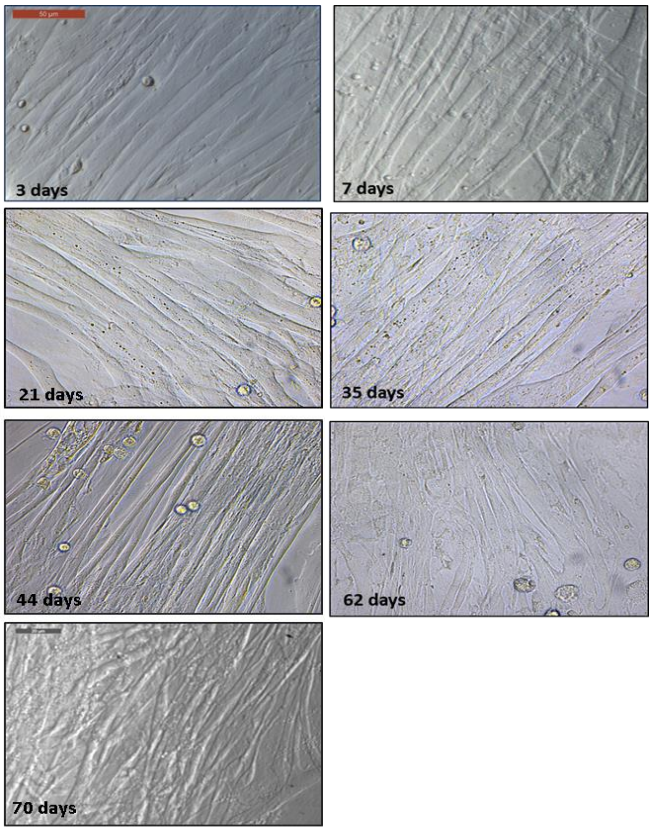

Figure 3.12 MC+ method allowed extended culture of differentiated porcine myotubes for up to 70 days

Micrographs of differentiated myotubes examined at the time points shown, from three days until 70 days. Throughout this period myotubes retained their characteristic morphology and remained attached.

3.4.3 Porcine myotubes maintained viability and expression of muscle protein α-actin during prolonged culture periods

To measure the viability and expression of α-actin by differentiated porcine myotubes which had been cultured for extended periods up to 50 days, the MTS assay and immunohistochemistry were used. Myotubes were cultured on 96 wells plates in four replicates. The MTS assay data showed that differentiated porcine myocytes remained viable and expressed α-actin protein when sampled at weekly intervals over a 50 day period (Figure 3.13)

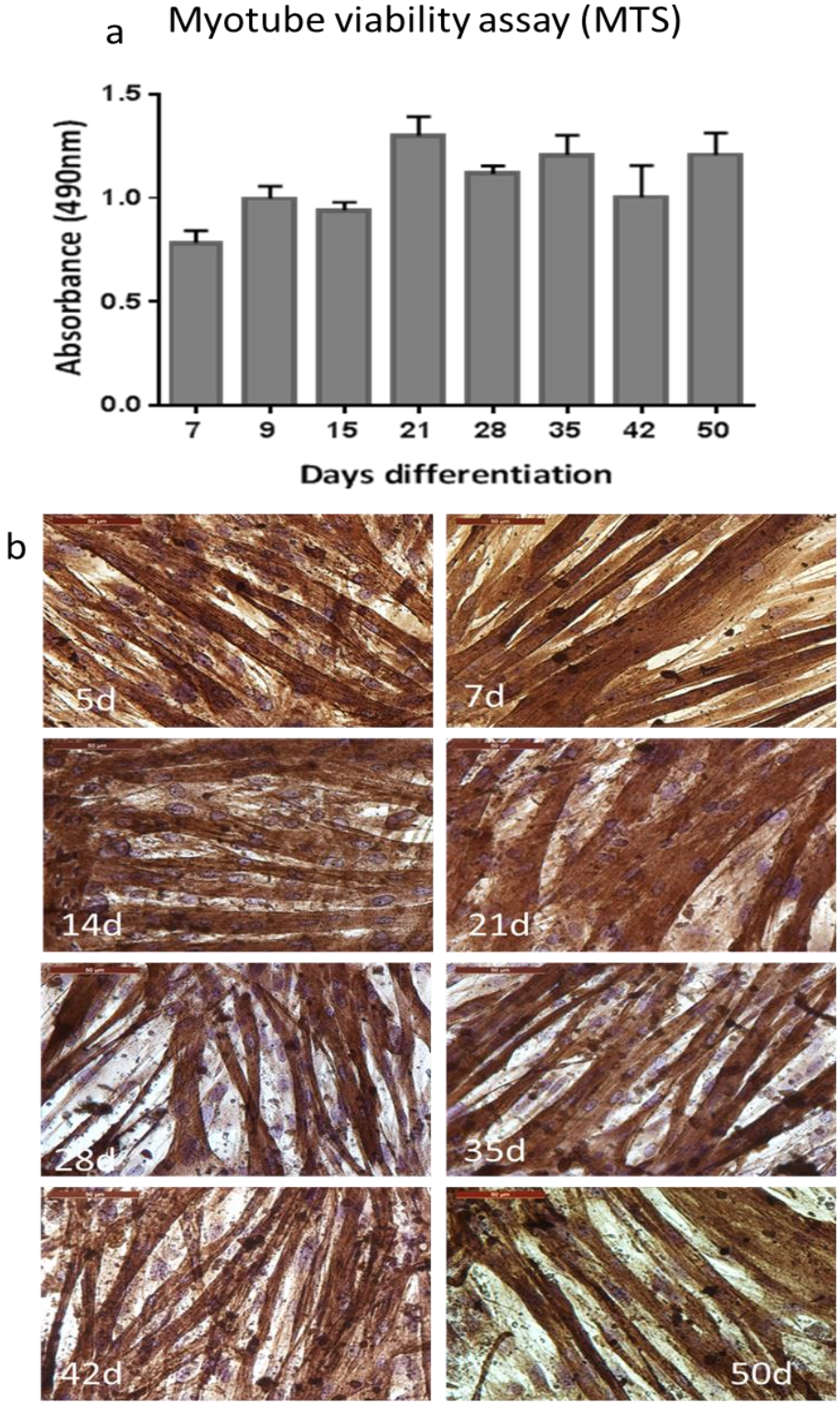

Figure 3.13 Porcine myotubes maintained in excess of 50 days remain viable, metabolically functional and show expression of the muscle protein α-actin

Myotube viability was measured using the MTS assay which showed that cells remained viable over 50 days of culture. (a). Myotubes expressed muscle protein α-actin at all time points up to 50 days as detected by immunohistochemistry (b).

3.4.4 Adeno viral mediated GFP marker to demonstrate long term persistence of the formed myotubes

In order to demonstrate that the same myotubes formed earlier in the culture (about 3-5 days of differentiation) remained unaltered during the entire span of the culture, an adenoviral GFP expressing vector was used as a marker. Myotubes differentiated for 5 days were infected with the adeno virus vector and the differentiation media was partially replaced from 7 days of differentiation during the entire duration of the culture. Expression of GFP protein marker from a replication deficient adeno virus vector by 8 days of differentiation helped to identify areas of fully formed myotubes in the culture well. Sequential fluorescence imaging of the same area of myotubes allowed to demonstrate that the myotubes originally formed earlier in the differentiation process remained in the culture without significant loss of myotubes. All the myotubes remained fluorescent during the full span of cell culture (imaged until 28 days in differentiation) which indicated that no further fusion of undifferentiated myoblasts in the well to the originally formed myotubes had happened (figure 3.14). Cell morphology and attachment was also observed throughout.

This evidence also indicates the possibility to overexpress a gene of interest in cultured porcine myotubes. Adeno virus mediated transduction is a commonly used gene expression tool for hard to transfect cells such as muscle cells. This result showed that the myotubes were susceptible to adeno virus vector infection and the myotube morphology was maintained for 28 days.

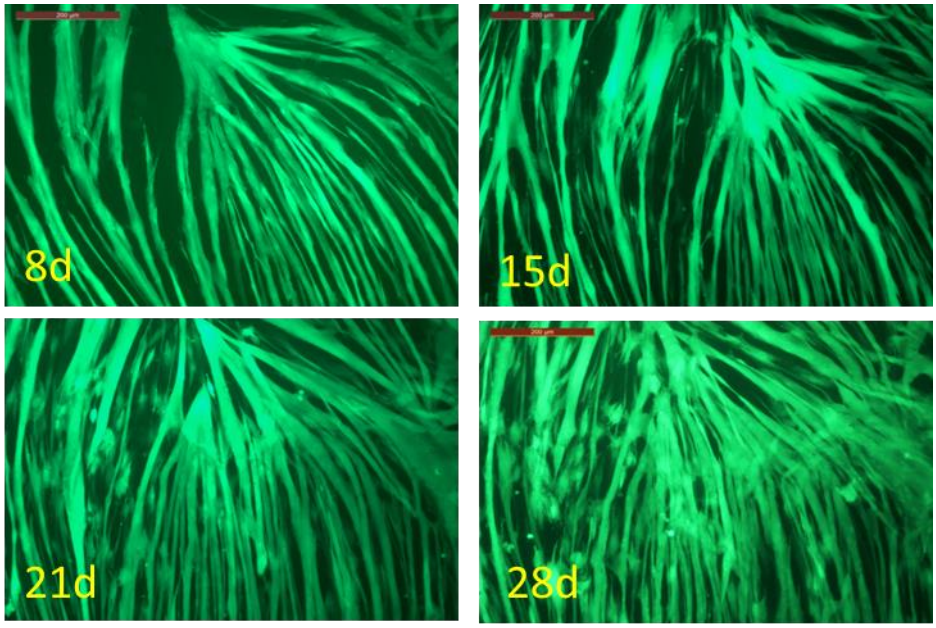

Figure 3.14 Adeno virus mediated GFP marker expression demonstrated the persistence of intact myotubes in excess of 28 days in culture

Myotubes differentiated for five days were infected with AAV that express GFP as a marker. GFP expression was detected in myotubes at 8, 15, 21 and 28 days of differentiation and myotubes retained their morphology and attachment to the plate.

3.4.5 Differentiated porcine myotubes from different anatomical locations express muscle proteins

Having optimised the MC+ method to differentiate porcine myotubes from muscle over 5 days, the same method was used to assess its suitability for other sources of muscle myoblasts, namely LD, SM and psoas. Figure 3.15 shows that myotubes could be differentiated successfully from these muscle sources. These cells were also screened for expression of muscle specific proteins, MyHC slow and MyHC fast twitch expression using immunohistochemistry and the results showed expression of both proteins in all cells types which were tested at five days of differentiation (Figure 3.15).

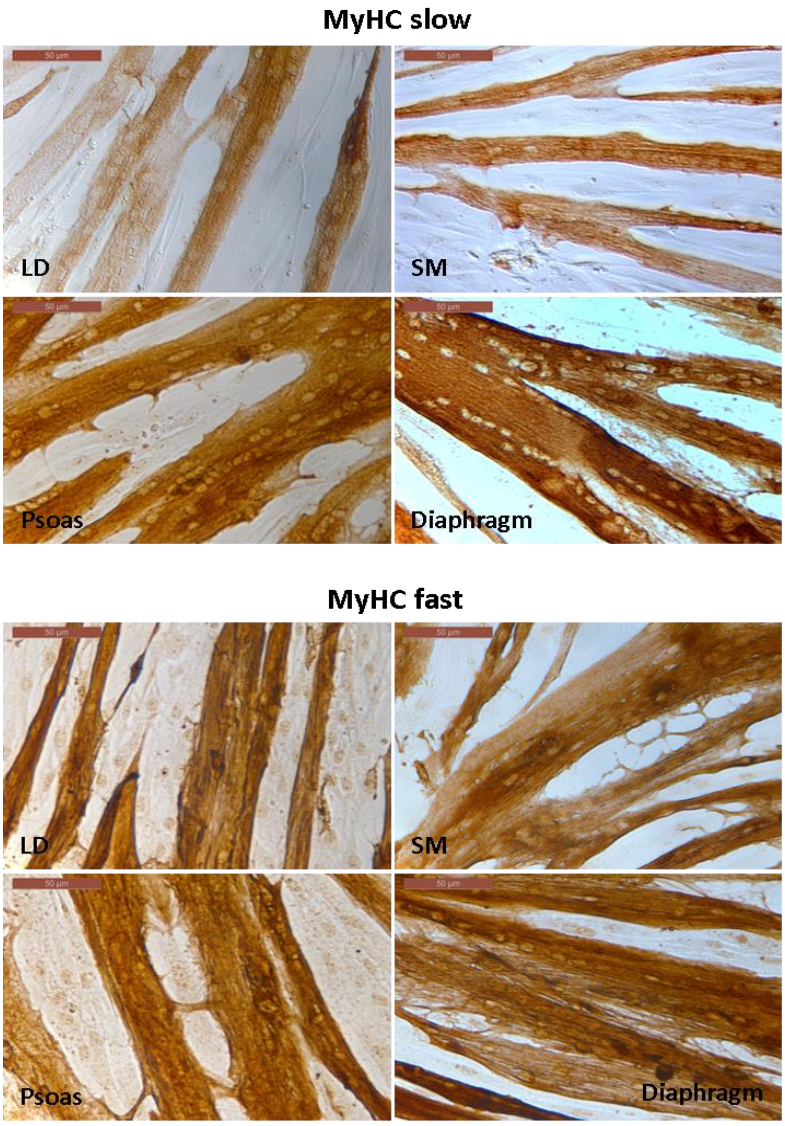

Figure 3.15 Muscle protein expression in myotubes differentiated from myoblasts of different pig muscles

Myoblasts isolated from different pig muscles (denoted on micrographs) were differentiated for five days using the MC+ method and subsequently fixed for immunostaining. The expression of muscle proteins MyHC slow (top panel) and MyHC fast twitch (bottom panel) were detected in myotubes isolated from different muscles.

3.4.6 Differentiated porcine myotubes form actin-myosin striations

The functional ability of *in vitro* differentiated myotubes can be demonstrated by the presence of actin- myosin cross striations, which are a fundamental unit of motor function. Therefore, as shown in Figure 3.16, pig LD myotubes that had been differentiated for either five days (a) or 42 days (b) were immunostained with antibodies specific for α-actin to visualise actin- myosin striations. In addition, myoblasts isolated from the diaphragm and LD were differentiated for five days then immunostained with antibodies specific for MyHC fast (c -f). Actin- myosin striations were visible in all muscles, although striations were abundant in myotubes cultured for less than 10 days.

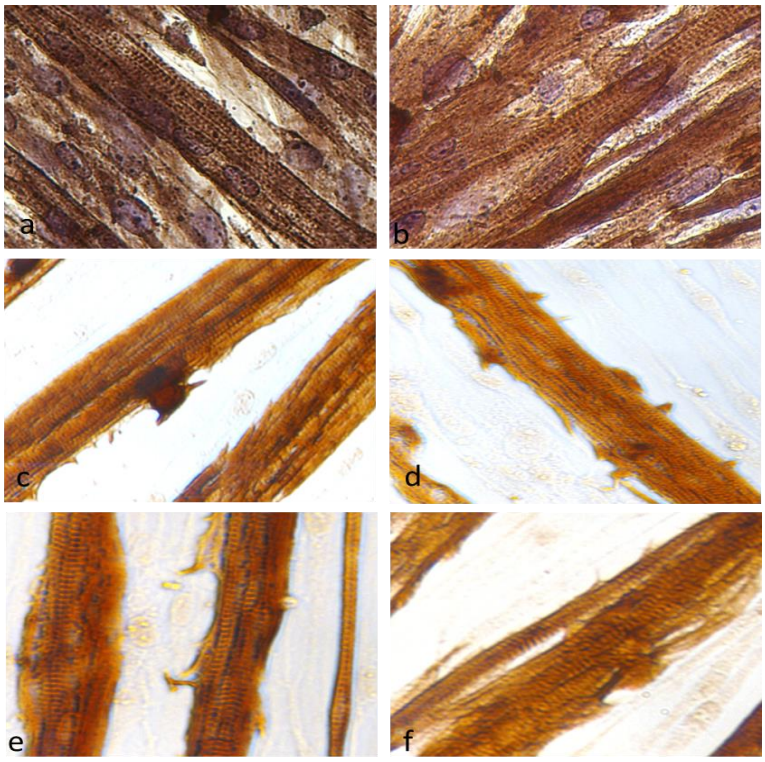

Figure 3.16 Differentiated porcine myotubes from LD and diaphragm muscles form acto-myosin striations at 5 and 42 days of differentiation

Actin-myosin striations were detected in myotubes immunostained for α-actin (a and b- LD muscle) and MyHC fast (c and d- diaphragm and e and f - LD).

3.4.6 Porcine myotubes cultured using the MC+ method retain their differentiation for several passages

In general, primary cells lose their differentiation capacity after a few rounds of cell division *in vitro*, but maintenance of the differentiation capacity is important for experimental purposes. Therefore the ability of porcine myoblasts to continue proliferation and remain differentiated was assessed over seven passages prior to H&E staining. Myoblasts were first differentiated into myotubes for five days and cultured using the MC+ method then passaged as described in Chapter 2. Representative

micrographs of H& E stained myotubes with their respective passage number are shown in Figure 3.17.

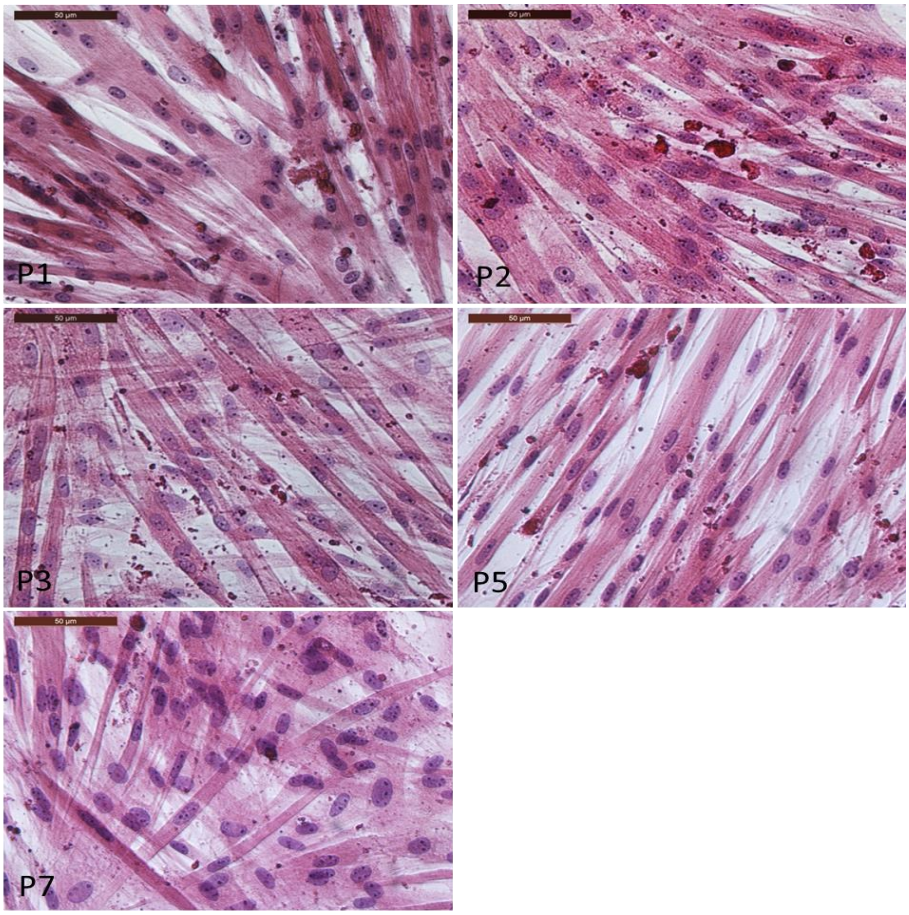

Figure 3.17 Porcine myoblasts cultured using MC+ method maintain their proliferation and differentiation capacity over seven passages

Myotubes differentiated from sequentially passaged myoblasts are H&E stained and imaged using light microscope. Respective passage number is denoted on the micrographs. P= passage.

3.4.7 Differentiated porcine myotubes cultured for extended periods express MyHC isoforms based phenotypic plasticity and postnatal phenotype

The expression profile of different MyHC isoforms plays an important role in the muscle's function and meat quality, such as the size of the muscle, (Wimmers et al. 2008). In response to neuromuscular activity, hormonal control or physical stimuli, muscle is known to change its phenotype by transition of the MyHC expression from slow (MyHC slow) to fast twitch (MyHC 2a, MyHC 2x and MyHC 2b) (Schiaffino & Reggiani 1994). Such a change in MyHC isoform expression leads to a metabolic change in the muscle which affects the muscle quality (Pette 2002). Therefore, the ability to replicate the desired MyHC isoform expression pattern in cultured muscle cells is of utmost importance due to its invaluable potential to study the effect of any pharmaceutical interventions to modulate the MyHC expression and thus the muscle quality. In these experiments, differentiated myotubes were cultured for 28 days in DM1 (0.4% UG) or DM2 (2% HS) medium and the level of MyHC isoforms analysed by qRT-PCR at weekly intervals as described in Chapter 2. The results showed that differentiated porcine myotubes maintained in culture for 28 days adapted the MyHC isoform depending on the differentiation media provided. Myotubes maintained in DM1 (0.4% UG) predominantly expressed glycolytic fast type MyHCs at 21 and 28 days of differentiation (Figure 3.18). On the other hand, myotubes maintained in DM2 (2% HS) had a predominant expression of oxidative fast MyHC (MyHC 2a) and also significantly higher expression of MyHC slow, embryonic and perinatal MyHC isoforms were detected at 21 and / or 28 days of differentiation (Fig 3.18). This data demonstrate that the differentiated porcine myotubes possess plasticity in MyHC

isoform expression according to the culture medium. This information may be exploited for specific future studies including studies to improve meat quality.

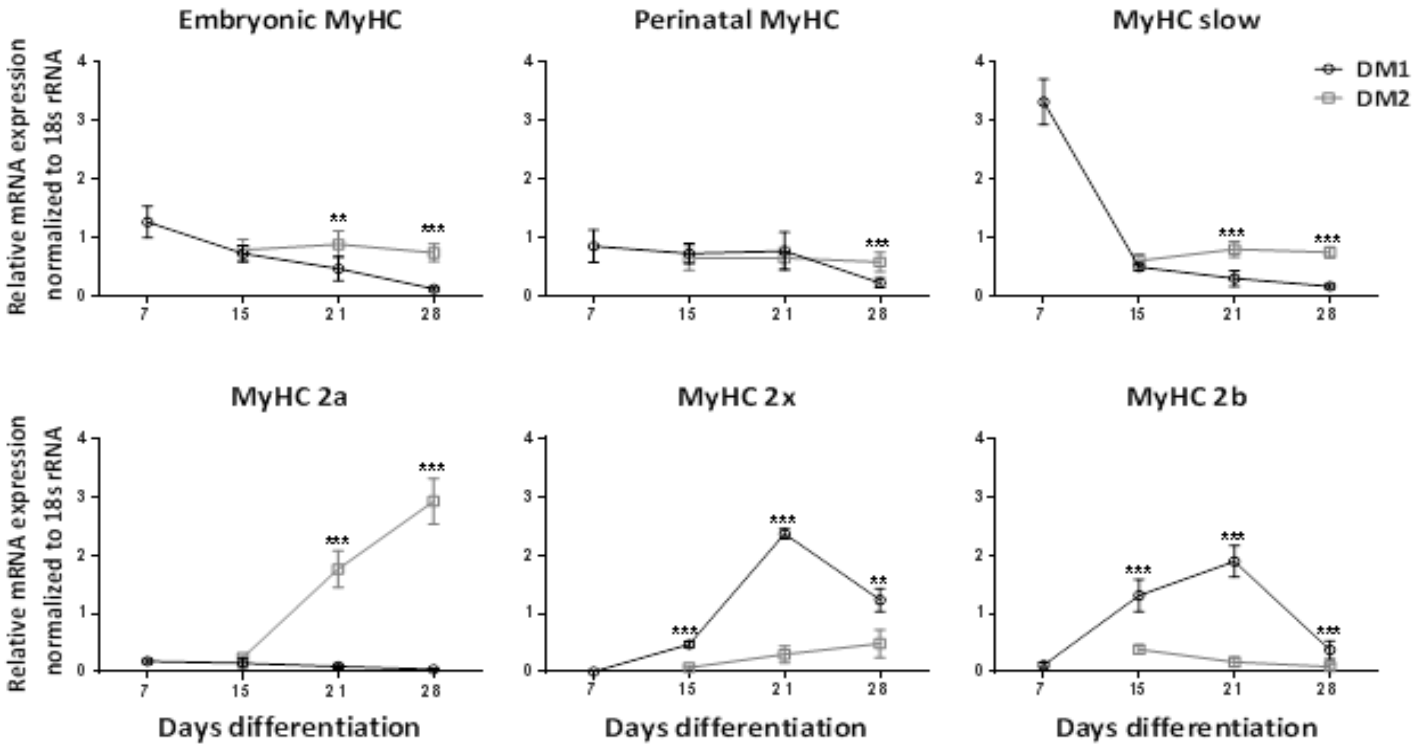

Figure 3.18 Extended myotube cultures exhibited phenotype plasticity

The type of DM media used to culture differentiated myotubes over 28 days profoundly affected the profiles of MyHC expression. Myotubes maintained in DM1 (0.4% UG) had significantly higher expression levels of MyHC 2x and 2b at 15, 21 and 28 days of differentiation whereas

cells cultured in DM2 (2% HS) showed significantly higher oxidative fast twitch MyHC 2a isoform expression at 21 and 28 days). ** = $p \leq 0.01$, ***= $p \leq 0.001$.

3.4.8 Differentiated porcine myotubes reflect the MyHC isoform expression of adult muscle fibres

Pig adult muscle shows a predominantly fast type MyHC expression profile. To determine if porcine myotubes expressed a similar phenotype, myotubes were differentiated using DM1 media and maintained for 21 or 28 days using the partial replacement of differentiation medium every two days before comparison of their MyHC isoform phenotype with LD muscle from an adult pig using qRT-PCR. As shown in Figure 3.19, the expression pattern of MyHC isoforms was similar in adult muscle cells and porcine myotubes at both 21 and 28 days. However, the levels of MyHC 2x and 2b expression were considerably higher in adult LD muscle compared with the myotubes (Figure 3.19).

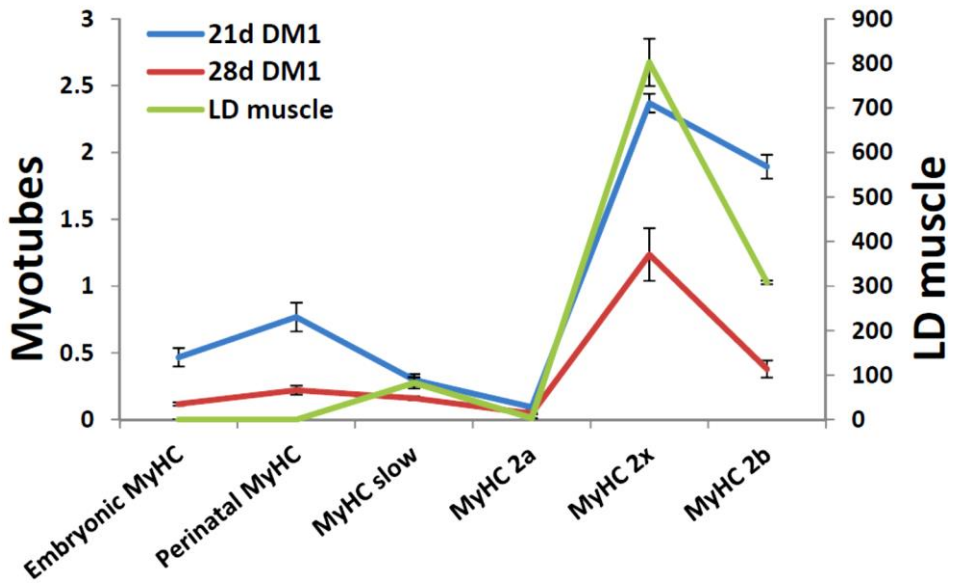

Figure 3.19 Differentiated porcine myotubes maintained in DM1 medium recapitulates adult pig muscle fibre type MyHC expression

Myotubes differentiated for 21 and 28 days using partial replacement of DM1 expressed MyHC 2x and 2b isoforms in a comparable ratio with adult pig LD muscle, but levels of expression differed considerably.

3.4.9 Myotubes differentiated using MC+ method spontaneously twitch in the culture

Myotubes obtained by the MC+ method were spontaneously twitching in the culture well. This phenomenon was observed more in the myotubes that were differentiated from about three days to over 60 days. Relatively abundant number of twitching myotubes observed in myotubes differentiated between 4 days and 15 days. Recorded videos of such myotubes differentiated to different duration are presented on the compact disc attached with this thesis (Additional files – twitching myotube videos).

Part 3: Application of the porcine myotube MC+ culture method to muscle and epithelial cells from other species

3.5 Human skeletal muscle myoblasts (HSMM) cells

3.5.1 The MC+ muscle culture method significantly improved proliferation and differentiation of HSMM

In order to assess the suitability of the MC+ muscle culture method for myoblasts of human primary skeletal muscle myoblasts (HSMM), cells (Lonza) were cultured using the manufacturer's recommended method and compared with the MC+ method in terms of proliferation and differentiation over 3 days each. The proliferation ability of HSMM cells using the MC+ method was compared with the manufacturer's recommended method, at three days the MC+ method showed improvement in cell proliferation (Figure 3.20. a-d). In addition, the HSMM cells differentiated for three days using the MC+ method (Figure 3.20. h) showed improved differentiation by comparison with the cells differentiated using manufacturer's recommended method (Figure 3.20. f).

Impact of SKGM 2 media in MC+ method on HSMM cell proliferation and differentiation

In order to evaluate the effects of the proliferation media's ingredients on HSMM differentiation, cells were proliferated and differentiated on MC+ coated plates using Lonza's recommended proliferation media (SKGM 2 with 10% FBS) or SKGM 2 supplemented with 20% FBS and 2% CEE (the same combination used in porcine myoblast proliferation).Both sets of the cells were then differentiated using DM1 medium. Microscopic observation of the cells showed an improved differentiation of the HSSM cells using MC+ method (figure 3.20.j) compared with the manufacturer's method (figure 3.20.i) This indicates the beneficial effect which proliferation media can have on the further differentiation of the HSMM myoblasts.

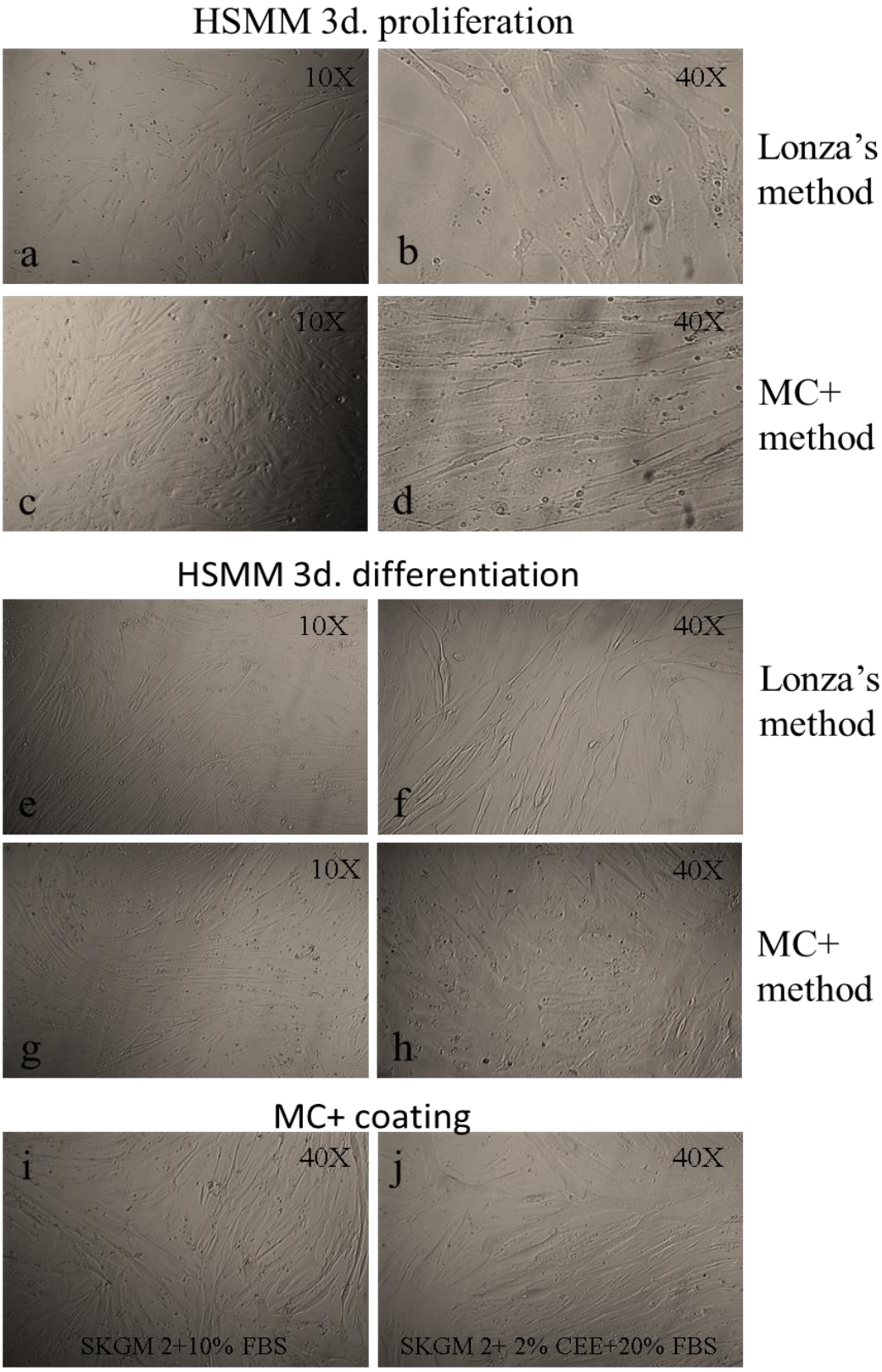

Figure 3.20 MC+ method improved proliferation and differentiation of HSMM cells

Micrographs of HSMM cells and porcine myoblasts proliferated (a-d) or differentiated (e-h) using Lonza's recommended or MC+ conditions for three days). HSMM cells proliferated on MC+ coated plates using either SKGM 2 supplemented with 10% FBS (recommended by

Lonza) and differentiated for three days using DMEM supplemented with 0.4% UG (i) and HSMM were proliferated and differentiated using MC+ method at three days of differentiation (j).

3.5.2 MC+ method improved HSMM myoblast fusion

Fusion rate was calculated for the HSMM myotubes differentiated for five days using either the manufacturer's (Lonza) or MC+ culture methods. The MC+ method significantly improved the differentiation of HSMM at five days when compared with the manufacturer's method. Calculation of fusion rate was performed in a similar method to porcine myoblast fusion rate as explained in Chapter 2. More than 1000 nuclei were counted from more than 10 images of both culture methods to calculate the fusion rate. To assess the presence of MyHC slow and fast isoforms as a measure of differentiation, immunohistochemistry was performed. The MC+ method significantly improved the number of differentiated myotubes and the expression of MyHC slow and fast isoforms indicates their potential functional capacity of the myotubes. However, unlike pig myotubes at an equivalent stage of differentiation, no twitching was observed in HSMM cells and the myotubes started to detach from the plate after five to seven days of differentiation. No replacement of medium or passage was performed on these cells. This result suggests that further optimisation of the method will be required for HSMM myotubes to attain function.

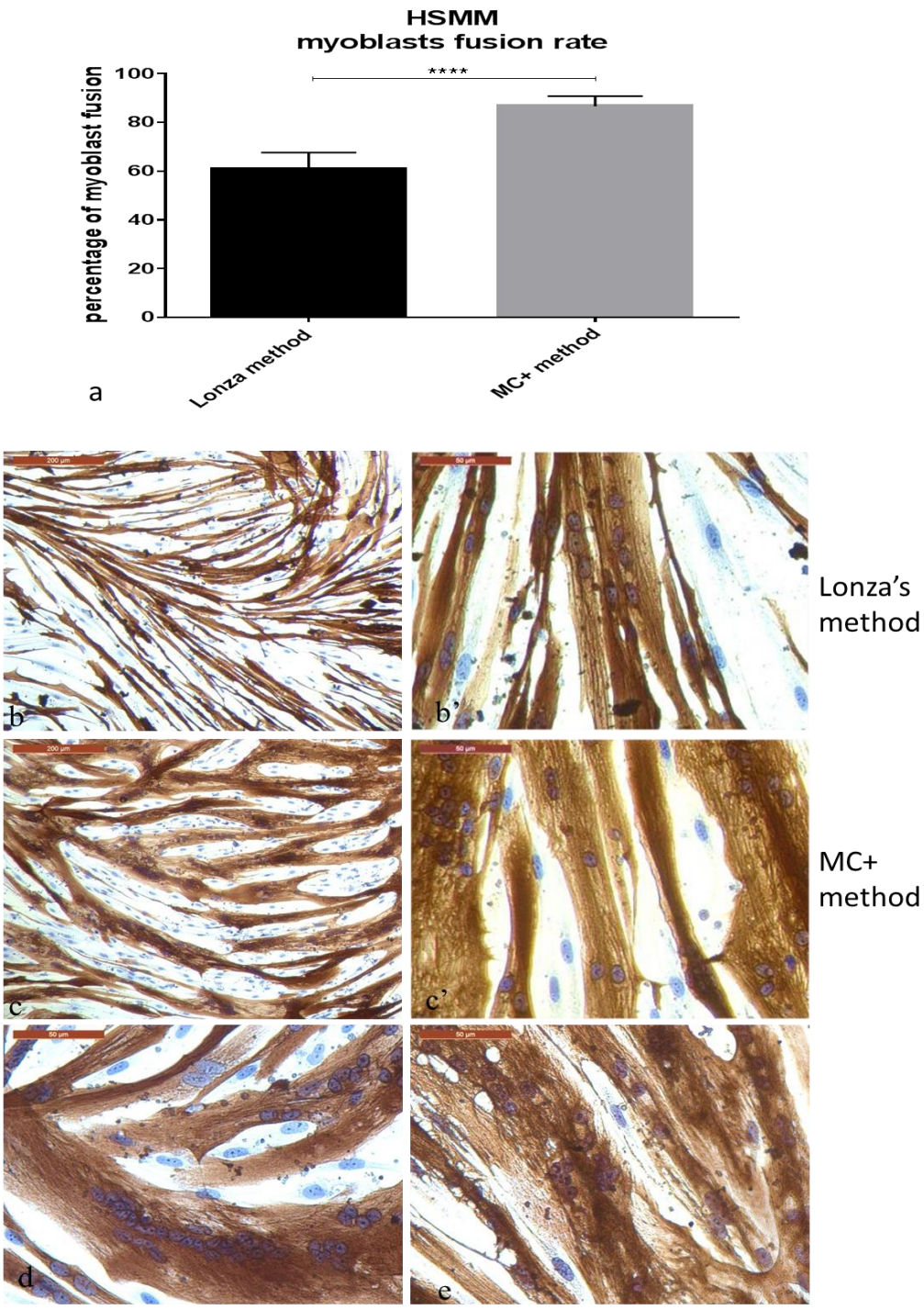

Figure 3.21 The MC+ muscle culture method improved the number of HSMM fusion and differentiation into myotubes

HSMM myoblast fusion when cultured using the MC+ method was significantly higher compared with the Lonza method (a). Unpaired t-test **** = $p \leq 0.0001$. HSMM myotubes were immunostained against MyHC slow at five days of differentiation and the nuclei were counter stained with haematoxylin images reveal the expression of muscle specific MyHC Slow (d) and MyHC fast (e) isoforms in both Lonza and MC+ culture conditions.

3.5.3 Maintenance of HSMM myotubes using a modified MC+ culture method over 13 days

Despite of the significantly improved differentiation capacity of HSMM at day 3 using the MC+ rather than the manufacturer's method, myotubes detached from the plate after about five to seven days of differentiation. Lonza recommends replacement of the differentiation medium with fresh proliferation medium after initial set of myoblast fusion occurred to allow long term maintenance. To assess the optimum conditions for longer term maintenance of HSMM myotubes, one set of myotubes were differentiated using manufacturer's method and another set using the MC+ method for five days, when then differentiation media was replaced with proliferation media. Myotubes initially cultured using manufacturer's method used SKGM 2 with 10% FBS for the replacement, every day until day 13. For the cells initially cultured and differentiated using MC+ method, the proliferation media consisted of SKGM2 + 2% CEE + 20% FBS. Cells maintained until 13 days by the proliferation media replacement had a notable loss of myotubes for both the manufacturer's method (Figure 3.22.a) and MC+ methods (Figure 3.22.b).

In a second experiment, HSMM cells were maintained in the same way until day 13 and a second round of differentiation was applied by replacing the proliferation media with DM1, referred to as the modified MC+ method. The results showed that increased numbers of myotubes was detected after the second round of differentiation, 16 days after the initial differentiation. Significantly increased myotube formation was observed in the wells maintained using the MC+ method (Figure 3.22.b') compared with the cells maintained using Lonza's method (Figure 3.22.a')

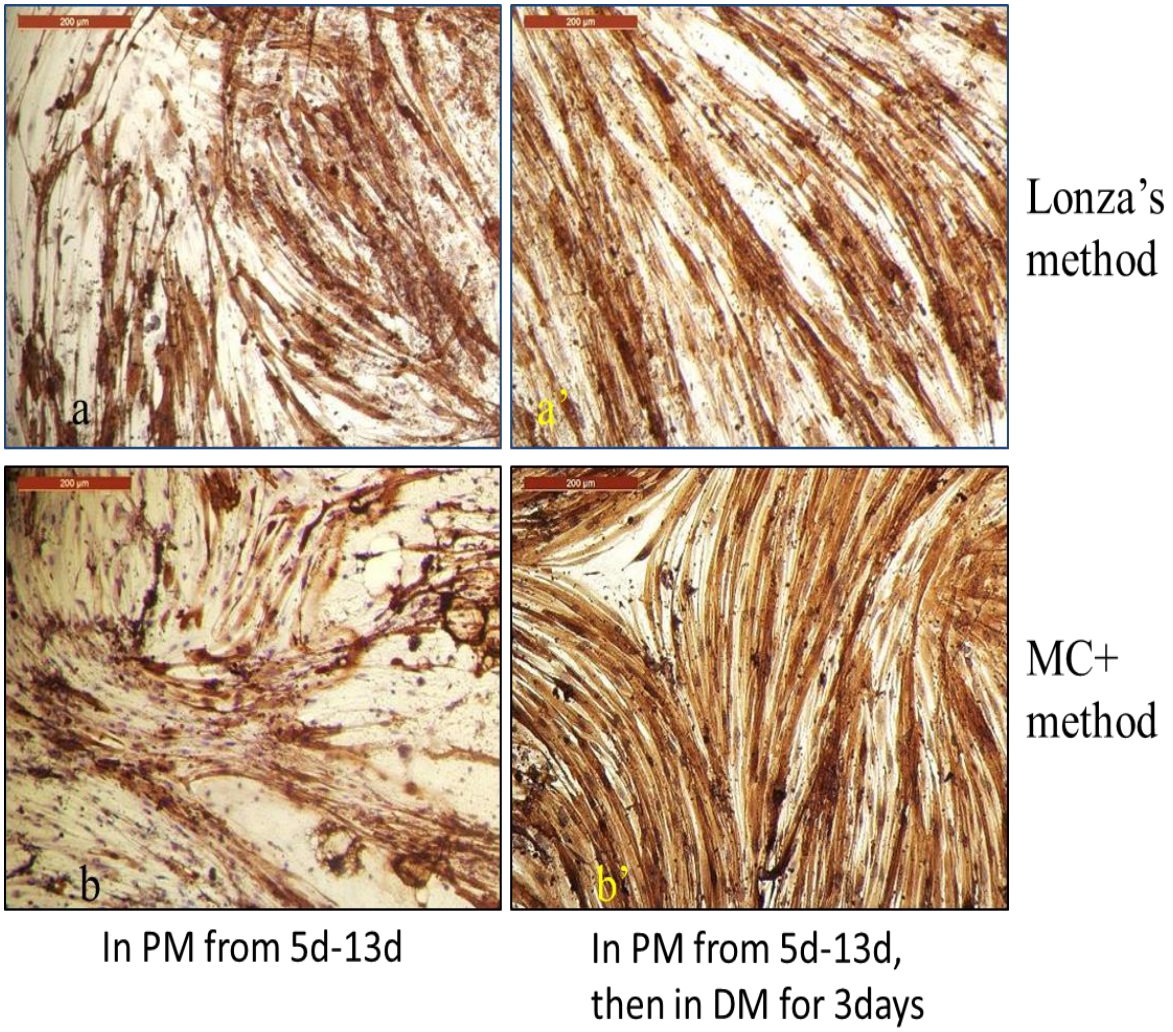

Figure 3.22 Modified MC+ method allowed extended maintenance of HSMM myotubes in excess of16 days.

HSMM myotubes maintained for 13 days by the replacement of differentiation media with proliferation media partially extended the life of myotubes cultured using manufacturer's method (a) and MC+ methods (b). Myotubes maintained using the modified MC+ method significantly improved the maintenance of myotubes (b') compared with manufacturer's method recommended method (a'). PM = proliferation media, DM = differentiation media.

3.5.4 MC+ coating improves mouse skeletal muscle C2C12 cells proliferation

In order to test the ability of the MC+ coating to improve proliferation of muscle cells from different species, a mouse skeletal muscle cell line C2C12 was used. These experiments compared three growth conditions using 96 well plates: i), uncoated plates with Glutamax I medium, supplemented with 10% FBS, ii) MC+ coated plates using Glutamax I media with 10% FBS and iii) MC+ coated plates using SKGM 2 media supplemented with 10% FBS. The data showed a significant improvement in proliferation for C2C12 cells cultured on MC+ coated plates with Glutamax I media compared with uncoated plates (Figure 3.23.b). Comparison of the Glutamax I and SKGM2 media on coated plates showed a further improvement in proliferation of C2C12 cells (Figure 3.23.c). Differentiation of C2C12 cells cultured on MC+ coated plates using DMEM supplemented with 0.4% UG resulted in increased number of differentiated cells, but the myotubes started detaching from the plate after about five days of differentiation (data not shown).

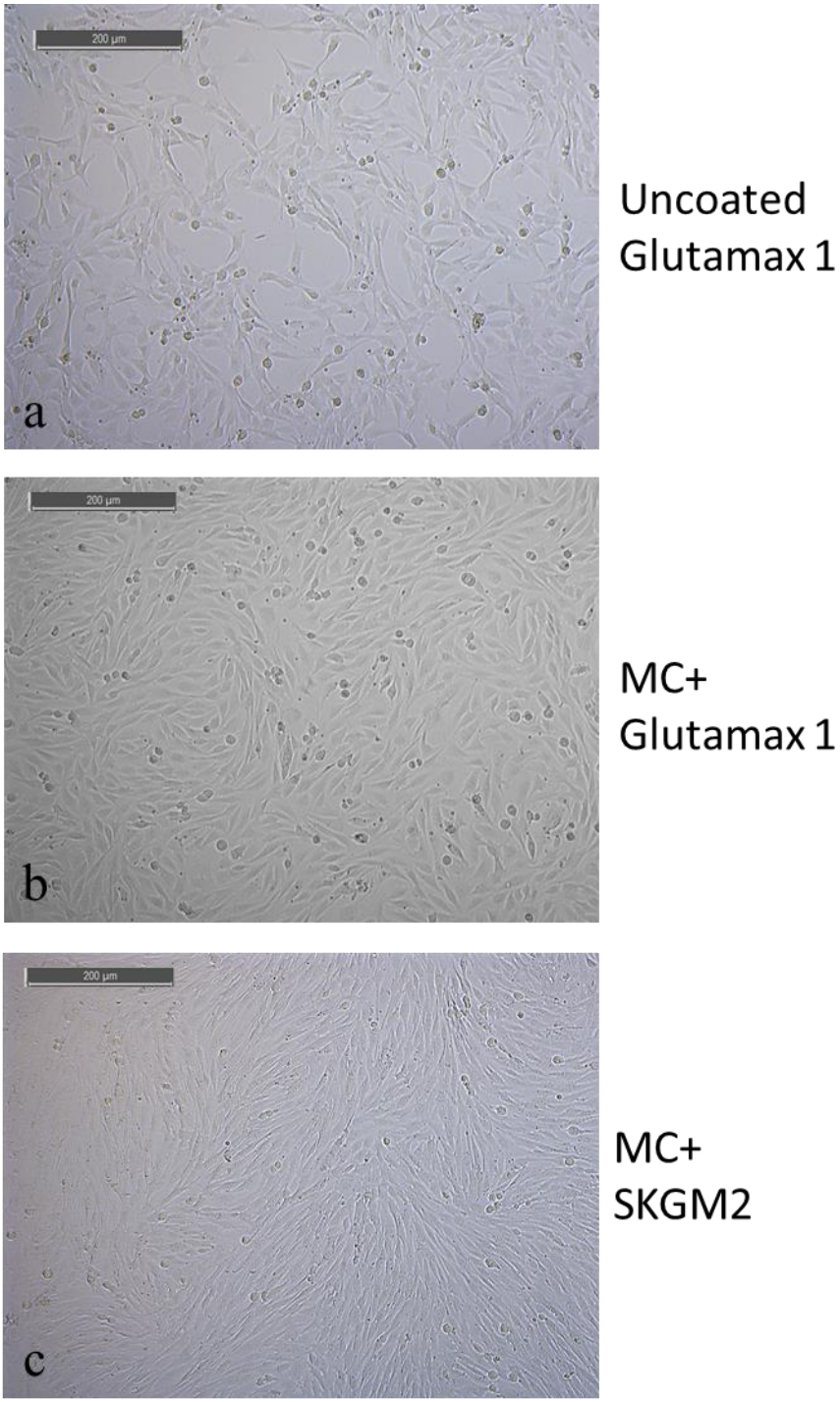

Figure 3.23 MC+ coating improved the proliferation of the C2C12 cell line

Proliferation of C2C12 myoblasts cultured for 48 hours on uncoated plates using Glutamax I media (a), MC+ coated and Glutamax media (b) and MC+ coating and SKGM 2 media (c).

3.5.5 MC+ coating improved pig tracheal epithelial cell (PTECs) proliferation

Maxgel ECM is the recommended extracellular matrix for PTECs but the cells take a long time to start proliferation. Therefore proliferation and differentiation of freshly isolated, primary PTECs in T75 flasks, coated with either MC+ or Maxgel extracellular matrix was compared. Using the MC+ method, a significant improvement in cell survival and proliferation was observed at 30 and 60 hours after seeding compared with cells in the Maxgel ECM (Figure 3.24).

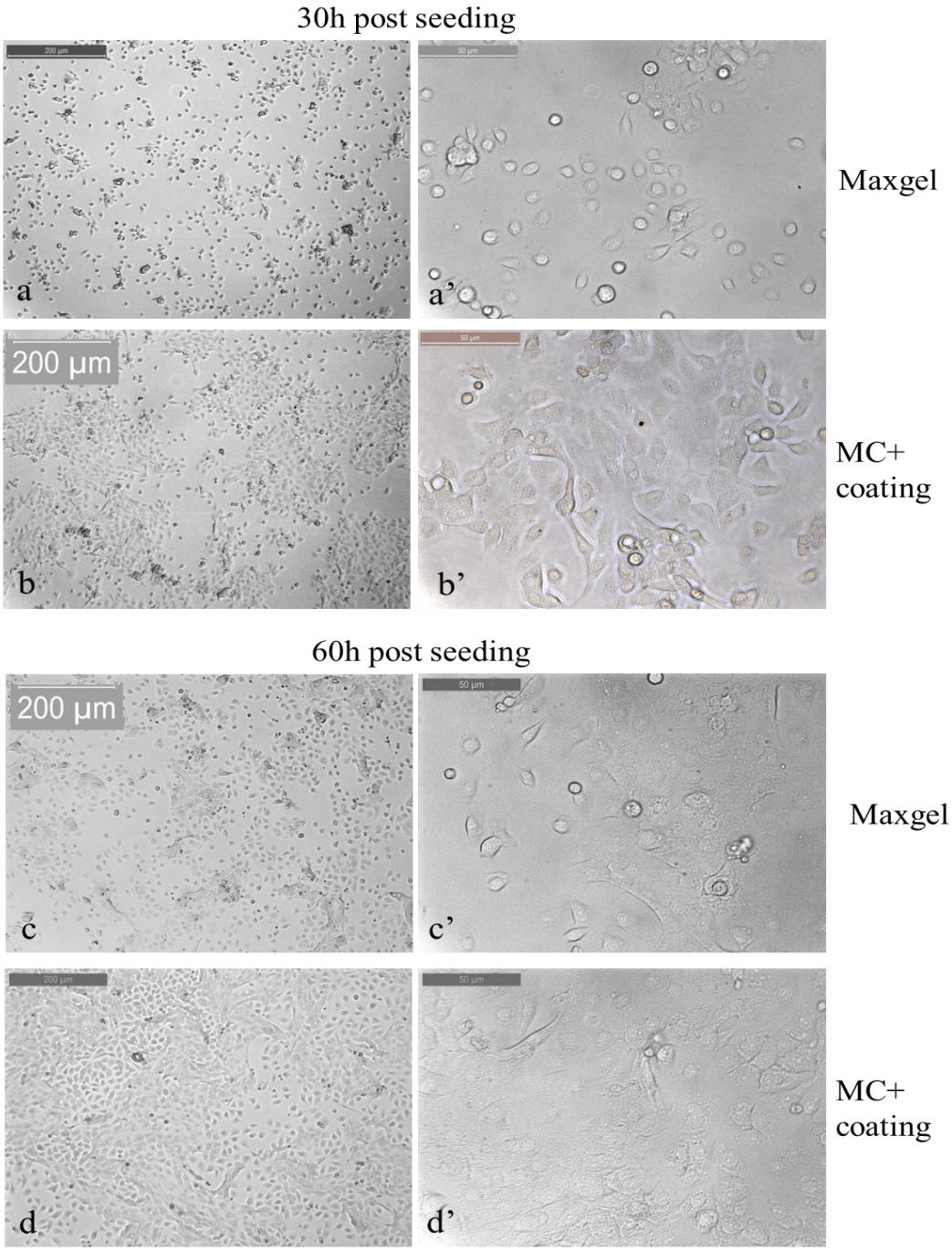

Figure 3.24 MC+ coating improves PTECs proliferation compared with Maxgel extracellular matrix.

Micrographs of PTECs proliferated on MC+ or Maxgel ECM coated flasks for 30 or 60 hours.

3.4 Discussion

The ability to maintain cultured and differentiated skeletal myotubes in the laboratory is a useful model for several reasons. First, it can be used to reduce the use of animals in research and to study the molecular mechanisms of skeletal muscle related biology and function. Secondly, recent advances in regenerative medicine are making progress towards developing engineered muscle which can theoretically replace damaged muscle tissue (Merceron et al. 2015) or rectify muscle related disease conditions (Roca et al. 2015) through gene regulation therapy. Thirdly, an increasing number of attempts are being made to make meat *in vitro* (Pandurangan & Kim 2015) after the first ever demonstration of the production of *in vitro* beef burger which aims ultimately to contribute to sustainable food production. To date, several methods have been developed to culture skeletal myotubes *in vitro* using two dimensional (2D) (Murray & Pogogeff 1946; Szepsenwol 1946; Demestre et al. 2015) or three dimensional (3D) culture systems (Cerino et al. 2015). However, the success and practicality of such muscle culture systems need simplicity, and ability to differentiate myoblasts into multinucleated myotubes with relevant gene and protein expression and ultimately a fully functional skeletal myotube.

Despite of the increase in the development of muscle culture systems, most of them are either very complex for routine work, need highly specialised equipment and expertise or are suboptimal due to the immature state of myotubes or the inability to maintain the myotubes in culture for the desired duration. Several studies have generated *in vitro* cultured myotubes derived from a range of mammals including human, pig, rabbit, cow, horse, mouse and rat (Lauren Cornall 2012; Owens et al. 2013; Partridge 1997; Abdul-Hussein et al. 2012; Baquero-Perez et al. 2012; Doumit & Merkel 1992; Zhu et al. 2013) and avian; chicken and duck (Baquero-Perez et al. 2012) species.

Expression of muscle specific MyHC genes and proteins in the cultured myotubes is vital to prove their functional relevance and thus correlate their function to adult muscle. Due to inadequate differentiation of myotubes , none of the studies (Li et al. 2015; Lewis et al. 2014; Zhu et al. 2013) reported the expression profile of all MyHC isoforms that are known to be expressed in adult pig muscles (Chang et al. 1995; da Costa et al. 2002; Lefaucheur et al. 2004). Most published experiments on myotubes are performed within about a week of differentiation, at a stage when adult MyHCs (namely MyHC 2X and 2B) are largely lacking. The principal reasons for this predicament are limited efficiency in myotube formation and continual loss of newly formed myotubes through fragmentation and detachment. The ability to culture myotubes long term in 2D to resemble the postnatal phenotype is therefore of high biomedical value (Che et al. 2013; Aas et al. 2013; D'Amico et al. 2013; Oldfors & Lamont 2008). The most important biomedical or veterinary muscle conditions such as muscle hypertrophic growth (Glass 2005; Pallafacchina et al. 2013), muscle wasting or atrophy (Glass 2003), changes in fibre type composition affecting muscle performance or meat quality (Chang 2007; Chang et al. 2003), and obesity related insulin resistance (Zierath & Hawley 2004; Kahn et al. 2006) all involve skeletal muscle in the postnatal fibre state. Therefore, a well characterised and repeatable *in vitro* muscle culture platform is clearly advantageous to examine the basic mechanisms and underlying changes in this cell type. Until now such a platform has been elusive in that myotube differentiation and maturation were major limiting factors.

The present work reports on a technical breakthrough that enables porcine myotube differentiation and accommodates spontaneous myotube contractions without detachment over a period of several weeks. This method should facilitate the *in vitro* study of all aspects of postnatal muscle fibre biology. This study investigated a variety of extracellular matrices, medium and supplements and ultimately succeeded in developing and optimising a model that allows short term differentiation and long term maintenance of porcine myotubes. The

characterisation demonstrated that the developed method allowed maintenance of differentiation capacity of myoblasts for over seven passages. Terminally differentiated myotubes exhibited actin-myosin striations and the myotubes maintained the capacity to spontaneously twitch for over 60 days in culture. Such properties of the myotubes indicate that the provided ECM coating and possible expression of required cell adhesion molecules by differentiated myotubes may have formed an elastic surface for the myotubes to remain attached and twitch (Friedrich et al. 2011). Tracking of the formed myotube using a GFP marker showed that the myotubes that were initially formed in the culture well remained in culture during the entire duration of culture without much loss or deformity to myotube appearance. The persistence of myotubes for long terms may have helped them to mature into a striated form. Viability determination of the myotubes using MTS assay also confirmed that the myotubes remained in the culture well were metabolically active. Furthermore, the method is transferable to the myotube cultures of other species (human and mouse) and proliferation of tracheal epithelial cells of pigs.

In the first weeks of postnatal development in rats and mice, there is typically a progressive loss of embryonic and perinatal MyHCs and accumulation of MyHC 2A, 2X and 2B isoforms in designated fast fibre populations (Schiaffino & Reggiani 2011). The extended porcine myotube culture system developed by this work showed a predominant pre-natal MyHC isoform (embryonic and perinatal MyHCs) expression in the early stages of differentiation which is comparable with neonatal pig muscles. Extended maturation of myotubes in DM1 showed that a reduction in embryonic and perinatal MyHC expression was accompanied by dominant expression of MyHC 2X and 2B. Furthermore, the pattern of relative MyHC expression at day 21 and 28 of differentiation in DM1 resembled the MyHC expression profile of a 22 week old pig longissimus dorsi muscle (da Costa et al. 2002). The difference in MyHC profiles between DM1 and DM2 is biologically significant as it demonstrates the expression

plasticity of postnatal MyHC genes stimulated by different culture media. *In vivo*, early postnatal changes in MyHC gene expression that lead to the formation of adult fibre types are dependent on the establishment of corresponding fast and slow motor units, load bearing after birth, and in the case of fast MyHC induction, a thyroid hormone surge (Schiaffino & Reggiani 2011). The ability of the myotubes developed by this work to adopt a fast or slow MyHC profile in the absence of innervation indicates that the nutritional environment and choice of particular culture conditions are also important phenotype determinants. The DM1 myotube culture over several weeks also showed a fast-like postnatal pattern of MyHC expression. A 2D culture platform has therefore been established that is conducive to the study of coordinated gene changes that govern fibre type and associated phenotypic alterations.

The MC+ method of muscle culture that successfully extended the pig myotubes also improved the differentiation of HSMM into myotubes and partially improved their extended maintenance. It also improved the proliferation of the murine skeletal C2C12 cell line and primary porcine tracheal epithelial cells. These results indicate the potential application of this protocol to other species. This finding also raises questions about the role of potentially novel and shared key regulators of myoblast differentiation in addition to the currently known genes (Jansen & Pavlath 2008; Srinivas et al. 2007; Kim et al. 2015) . Identification of key factors associated with the improved differentiation will contribute to future research on the skeletal muscle model.

It is known that the ECM coating plays major role in providing the most suitable niche for the functional replication of differentiated myotubes *in vitro*. Identification of the expression of ECM components and other cell adhesion molecules such as intercellular adhesion molecule 1 (ICAM-1), vascular cell adhesion molecule-1 (VCAM-1), and E-selectin (Chopra et al. 2012; Zhang et al. 2011; Beauchamp et al. 1992) which are upregulated during the differentiation process will contribute further to improvement of the culture conditions (Larsen et al. 2006).

Since the interaction between ECM and cells is known to regulate the differentiation of cells (Globus et al. 1995), it is a critical research aspect to understand the ECM expression profile during the differentiation of the currently developed muscle culture system. Ultra-structural imaging of the ECM coating using scanning electron microscopy (SEM) may also provide a better understanding of the structural organisation of the MC+ coating and its interaction with the myotubes.

The MC+ method for porcine muscle cell differentiation presented here succeeded to overcome the major technical difficulties in muscle cell culture such as inadequate differentiation and early detachment of myotubes from culture vessel. This technical breakthrough helped to utilise the porcine muscle cells in studies to understand the molecular mechanisms of growth factors such as beta agonist ractopamine in increased growth performance and its potential role in innate immune regulation.

Chapter 4

Towards the identification of early effector targets of ractopamine signalling in primary porcine muscle cells

Abstract

This chapter describes about the identification of early protein targets of ractopamine (Ract) signalling in primary porcine muscle cells by the use of stable isotope labelling by amino acids in cell culture (SILAC) based on quantitative mass spectrometry. This allowed the detection and quantification of differentially expressed 1100 proteins and 650 phosphopeptides. Ract induced metabolic changes consistent with the promotion of fatty acids turnover, glycogen synthesis and protein synthesis. Inhibition (dephosphorylated) of a key proliferation and growth control pathway mitogen-activated protein kinase/extracellular signal-regulated kinase (MAPK/ERK) signalling was observed. More interestingly, Ract treatment induced changes in muscle cell innate immunity predicted to promote viral sensing and anti-viral response.

4.1 Introduction

Ractopamine (Ract) and other related β-adrenergic agonists are known for their ability to increase lean mass and decrease fat deposition through of repartitioning nutrients from adipose tissue to skeletal muscle (Ryall et al. 2008; Stoller et al. 2003). The β2-agonists have additional applied uses in the induction of bronchodilation in asthma treatment, and in the counteraction of muscle wasting conditions (Ryall et al. 2008; Busquets et al. 2004). Ract is thought to signal through the adenylate cyclase (AC)-protein kinase A (PKA) pathway (Kume et al. 1994; Torphy 1994). Upon Ract binding to transmembrane β-adrenergic receptor (βAR), activates the guanine nucleotide-binding protein (G protein). G proteins are heterotrimers that consist of Gα and tightly associated Gβγ subunits; in its inactive form, the Gα subunit is coupled with guanosine diphosphate (GDP). Binding of β-agonists to βAR leads to the replacement of GDP with guanosine triphosphate (GTP). The activated Gα subunit then dissociates from the Gβγ dimer and activates AC, which catalyses the conversion of adenosine triphosphate (ATP) to cyclic adenosine monophosphate (cAMP) that then binds to the regulatory subunits of cAMP-dependent PKA, causing a conformational change that releases and activates the catalytic PKA subunits. These activated subunits can then phosphorylate various enzymes to mediate cellular responses (Figure 4. 1).

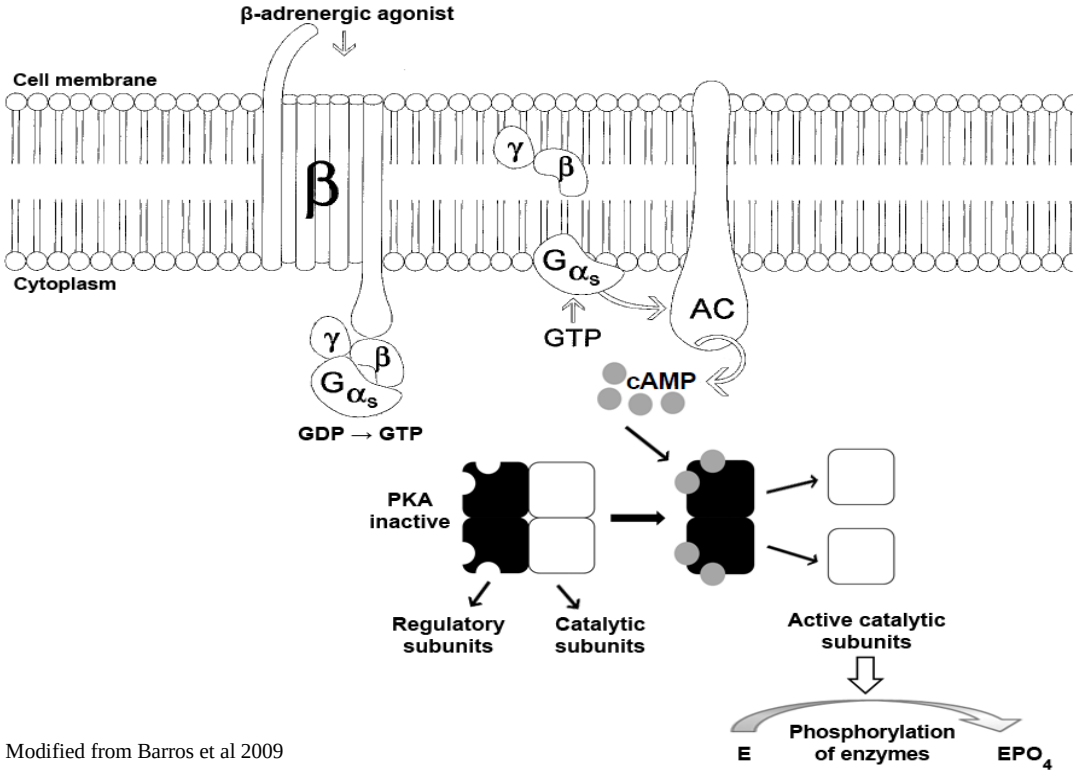

Modified from Barros et al 2009

Figure 4.1 Intracellular signaling pathways of the β-adrenergic receptor.

β, β-adrenergic receptor; γ/β, γ and β subunits of the G protein; Gα, α subunit of the G protein; GTP, guanosine triphosphate; AC, adenyl cyclase; ATP, adenosine triphosphate; cAMP, cyclic adenosine monophosphate; PKA, cAMP-dependent PKA; E, enzyme; and EPO4, phosphorylated enzyme (Barros et al. 1999).

Ract is known to exert different actions in skeletal muscle such as the coordinated re-programming of muscle genes that leads to a more glycolytic muscle phenotype (Gunawan et al. 2007; Shi et al. 2007). The downstream molecular components or signalling intermediates of Ract that mediate its various phenotypic effects are not well understood. Previous work by several research groups on β-agonist mediated differential muscle expression *in vitro* and *in vivo* has not been able to identify or fully explain the early causal molecular interactions that lead to the eventual steady-state outcome of β-agonist treatment. The early induction events of Ract are likely to be

responsible for the subsequent transformation of muscle phenotype. Understanding the early signalling events of target activation could potentially provide new basic and applied understanding of muscle growth and facilitate the identification of key effector targets that mediate the beneficial effects of Ract which in turn would provide new opportunities for pharmaceutical targeting. Additionally, the identification of early targets of Ract signalling could provide clues on mediators of less desired or side effects, such as reduced meat quality associated with increased glycolytic muscle fibres (Depreux et al. 2002), and smooth muscle relaxation(Colbert et al. 1991) leading to hypotension or myocardial toxicity (Yaeger et al. 2012). Such information could generate new awareness of certain signalling intermediates that could be responsible for or associated with possible unwanted effects.

RNA expression profiling by high throughput RNA sequencing or microarray analysis would enable to identify the changes in gene expression but is unable to identify early or transient changes at the protein level that could be responsible for subsequent downstream events. It is known that the mRNA expression of genes may not correlate to their protein expression (Gry et al. 2009; Greenbaum et al. 2003) This research aimed to use a high throughput proteomic approach to detect quantitative protein and phosphoprotein changes in porcine muscle cells in early response to Ract treatment (1 and 6h). Reversible phosphorylation and dephosphorylation of proteins is a principal mode of intracellular signalling (Schreiber et al. 2008). The approach adopted is based on the use of stable isotope labelling by amino acids in cell culture (SILAC) (Ong et al. 2002; Harsha et al. 2008) to conduct quantitative mass spectrometry. By correlating the functional relationships between the changes in whole protein expression and the phosphorylation status of individual proteins, it may be possible to identify and characterise novel early targets of Ract signalling in muscle growth.

4.2 Methods

4.2.1 SILAC preparation of porcine muscle cells

The SILAC preparation of primary porcine skeletal muscle cells was conducted by Dr. Zoe Redshaw. Briefly, primary myoblasts (satellite cells) were generated from *psoas major* of three 4-6 weeks old pigs as previously described (Baqureo-Perez et al. 2012). All SILAC culture reagents were supplied by Dundee Cell Products. Porcine satellite cells that were stored as frozen vials was seeded in a collagen-coated T75 flask containing one of three different types of amino acid isotopes in Dulbecco's Modified Eagle Media (DMEM) with 20% dialysed fetal calf serum (FCS, MWCO 10 000 Da, cat. no. DS1003), 2mM L-glutamine, and 100U/ml penicillin and streptomycin. Following SILAC DMEM media were, (1) unlabelled arginine and lysine (light/control, R0K0, cat. no. LM014), (2) ^{13}C labelled arginine and ^{2}D labelled lysine (medium, R6K4, cat. no. LM016) and (3) ^{13}C and ^{15}N labelled arginine, and ^{13}C and ^{15}N labelled lysine (heavy, R10K8, cat. no. LM015). Myoblasts isolated from different pigs were separately grown in the three different SILAC DMEM. When cells reached 70-80% confluence, they were transferred to a T175 flask and subsequently into two final T175 flasks. At this stage cells were at passage 3 and the cells were assumed to have undergone 5-7 rounds of cell division which would have allowed the incorporation of the corresponding isotopes into the entire cellular proteins. When the myoblasts reached to almost confluent stage, satellite cells were differentiated for 2 days in DMEM with 0.4% Ultroser G- UG (Pall Corporation), 2mM L-glutamine, and 100U/ml penicillin and streptomycin. UG has previously been shown to enhance myotube formation in human and rodent skeletal muscle cells (Benders et al. 1991; Sultan et al. 2006). The resultant cell population that contained differentiated

myoblasts/myotubes were subjected to three treatment conditions (untreated control, 1h with 10^{-5} M Ract, and 6h with 10^{-5} M Ract) (Santa Cruz, cat. no. sc-205832) (Table 1). Subsequently, all cells were harvested by trypsinisation and the cell pellet was dispatched in dry ice to Dundee Cell Products for quantitative mass spectrometry. Details of the samples are shown in Table 4.1.

Pooled sample 1 (3 technical replicate runs)				
	Pig 1 (phosphoproteins)	R0K0 control	R6K4 1h ractopamine	R10K8 6h ractopamine
	Pig 2 (phosphoproteins)	R0K0 control	R6K4 1h ractopamine	R10K8 6h ractopamine
	Pig 3 (phosphoproteins)	R0K0 control	R6K4 1h ractopamine	R10K8 6h ractopamine
Pooled sample 2 (single run)				
	Pig 1 (total proteins)	R0K0 control	R6K4 1h ractopamine	R10K8 6h ractopamine
	Pig 2 (total proteins)	R0K0 control	R6K4 1h ractopamine	R10K8 6h ractopamine
	Pig 3 (total proteins)	R0K0 control	R6K4 1h ractopamine	R10K8 6h ractopamine

Table 4.1 Summary SILAC experimental design and Ract treatment.

4.2.2 Processing of SILAC samples

High resolution mass spectrometry that isotopically resolves, quantify and identify proteins and phosphoproteins separately was performed by Dundee Cell Products. Briefly, cells from the cultures were lysed and the protein was extracted. Equal

quantities of proteins were pooled for all pigs and the pooled samples were subjected to sodium dodecyl sulphate polyacrylamide gel electrophoresis (SDS PAGE) (NuPAGE, Invitrogen) (Figure 4.2). Multiple regions of the gel that contains separated protein was excised which was followed by in-gel trypsin digestion (Trypsin, Roche) to obtain a full spectrum of peptides for analysis by nLC MS/MS (Emmott et al. 2010) (Dionex U3000 coupled to a Thermo Scientific LTQ-Orbitrap velos). Phosphoproteomics analysis was carried out in the following manner, the cell lysates were treated according to the previously published protocol (Weintz et al. 2010) except that the trypsinised peptides were fractionated by HILIC chromatography prior to titanium dioxide (TiO2) enrichment of phosphopeptides. Protein analysis was carried out in the following manner; pooled lysates were subjected to one run; for phosphoprotein analysis pooled lysates were subjected to three technical-repeat runs (Table 4.1). Multiple peptides of each protein were resolved and the relative amounts of each isotopic form quantified (Fig. 4.2). MaxQuant, a quantitative proteomics software package, was used to analyse the mass-spectrometric data sets.

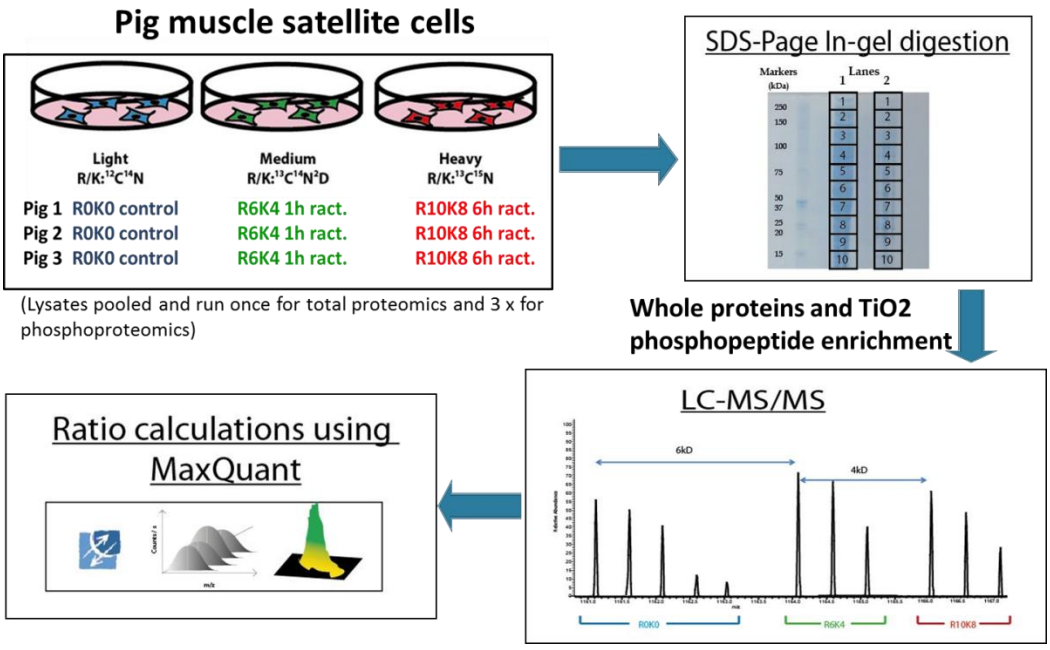

Figure 4.1 SILAC analysis flow chart showing the key steps in the process.

4.2.3 Data analysis

Data sets of differentially expressed proteins and phosphoproteins were analysed with Ingenuity Pathway Analysis (IPA, Qiagen) and Metacore (Thomson Reuters) software.

4.3 Results

4.3.1 SILAC compatible media resulted in limited myotube differentiation

Myoblasts were proliferated in specialised SILAC-compatible DMEM and dialysed FCS to allow the incorporation of the stable isotype labelled amino acids to the proteins. Due to this reason, the improved MC+ muscle culture method was not been used for this experiment and the culture conditions were not optimal for the differentiation of porcine muscle cells (Figure 4.3, courtesy Zoe Redshaw). Therefore, the porcine muscle cells used in SILAC-quantitative proteomics contained largely porcine myoblasts than myotubes. Relatively less number of myotubes were visible at different duration of differentiation but the culture was predominantly composed of myoblast

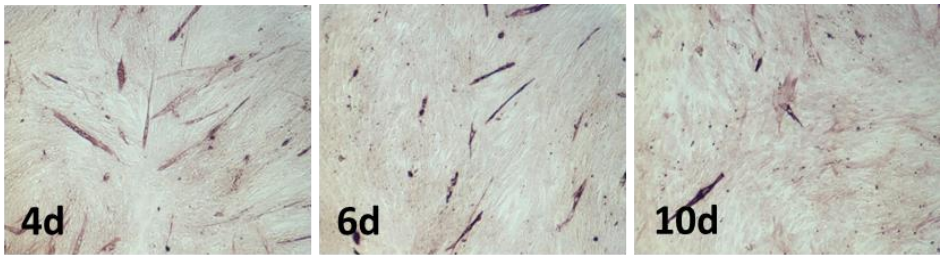

Figure 4.2 Use of SILAC-compatible culture reagents produced limited porcine myotubes.

Muscle cells differentiated for 4d, 6d and 10d were immunostained for the presence of sarcomeric α-actin. Limited myotubes was detected at 4d which showed further reduction with extended culture, presumably due to contraction loss.

4.3.2 Trends in phosphoprotein and protein expression in response to Ract treatment

Quantitative proteomic data were derived from pooled muscle cell samples of three pigs. Muscle cells of each pig were cultured separately in three different isotopic media (R0K0 [L], R6K4 [M] and R10K8 [H]) and subsequently exposed to 10^{-5}M Ract for 0h (no Ract treatment), 1h and 6h respectively (Table 1). Two primary sets (Excel files) of results were generated by Dundee Cell Products: quantitative phosphoprotein analysis ("Analysis Results ZR1-3 Phospho" file) and quantitative protein analysis ("Analysis Results Z1-10" file). The data files are added with the thesis as an attached compact disk. All listed proteins were within acceptable posterior error probability (PEP) threshold for a SILAC experiment (set at $\leqslant$ 0.1 for phosphopeptides and $\leqslant$ 0.01 for standard peptides). PEP (Käll et al. 2008) or false discovery rate was calculated using Bayesian statistics as a probability of a false hit using peptide identification score and length of peptide. According to the PEP score method to ensure the accurate identification of protein peptides, the smaller the PEP score, the more certain is the identification of a peptide. Longer peptides are automatically accepted with lower PEP scores.

Representative views of the phosphoprotein file (Analysis Results ZR1-3 Phospho) are shown in Figure 4.4 A and B. Columns highlighted in yellow indicate fold change in phosphorylation (M/L = 1h and H/L = 6h) of corresponding peptides. Since the protein samples used in phosphoprotein analysis were phosphoprotein enriched samples, these data were not normalised. Another reason for not normalising the data was due to the presence of multisite phosphorylation or dephosphorylation events within an identified

peptide. Additional details such as PEP, location of phosphorylation site(s), amino acid sequence of identified peptide and gene symbols are indicated (red boxes).

A.

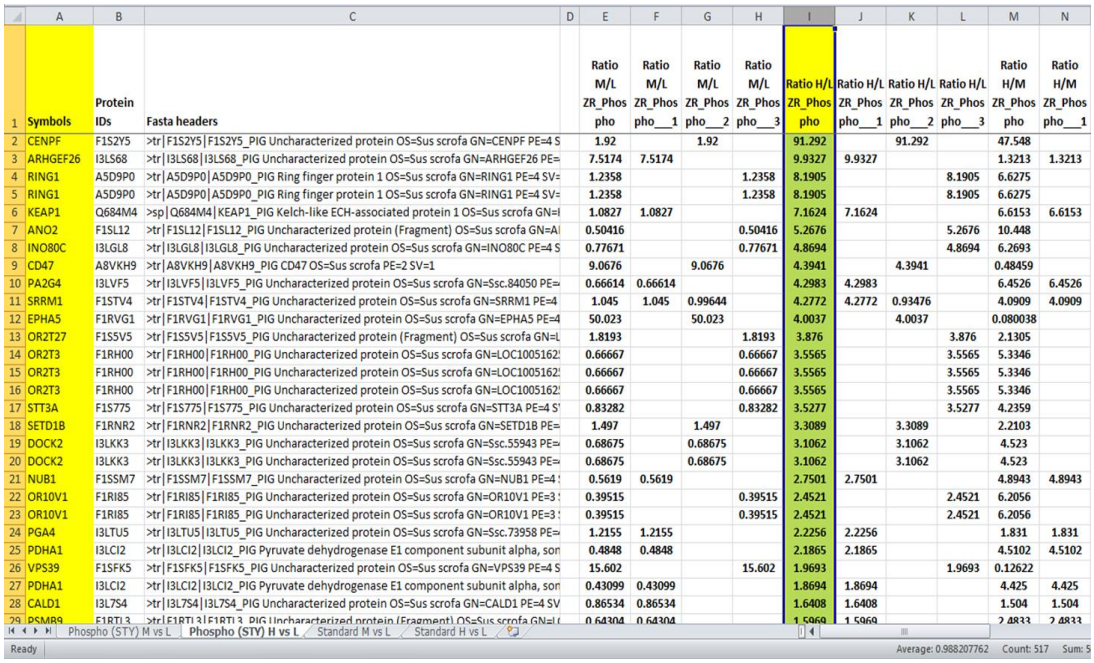

	A	B	C	D	E	F	G	H	I	J	K	L	M	N
1	Symbols	Protein IDs	Fasta headers		Ratio M/L ZR_Phospho	Ratio M/L ZR_Phospho__1	Ratio M/L ZR_Phospho__2	Ratio M/L ZR_Phospho__3	Ratio H/L ZR_Phospho	Ratio H/L ZR_Phospho__1	Ratio H/L ZR_Phospho__2	Ratio H/L ZR_Phospho__3	Ratio H/M ZR_Phospho	Ratio H/M ZR_Phospho__1
2	CENPF	F1S2Y5	>tr|F1S2Y5|F1S2Y5_PIG Uncharacterized protein OS=Sus scrofa GN=CENPF PE=4 S		1.92		1.92		91.292		91.292		47.548	
3	ARHGEF26	I3LS68	>tr|I3LS68|I3LS68_PIG Uncharacterized protein OS=Sus scrofa GN=ARHGEF26 PE=		7.5174	7.5174			9.9327	9.9327			1.3213	1.3213
4	RING1	A5D9P0	>tr|A5D9P0|A5D9P0_PIG Ring finger protein 1 OS=Sus scrofa GN=RING1 PE=4 SV=		1.2358			1.2358	8.1905			8.1905	6.6275	
5	RING1	A5D9P0	>tr|A5D9P0|A5D9P0_PIG Ring finger protein 1 OS=Sus scrofa GN=RING1 PE=4 SV=		1.2358			1.2358	8.1905			8.1905	6.6275	
6	KEAP1	Q684M4	>sp|Q684M4|KEAP1_PIG Kelch-like ECH-associated protein 1 OS=Sus scrofa GN=I		1.0827	1.0827			7.1624	7.1624			6.6153	6.6153
7	ANO2	F1SL12	>tr|F1SL12|F1SL12_PIG Uncharacterized protein (Fragment) OS=Sus scrofa GN=A		0.50416			0.50416	5.2676			5.2676	10.448	
8	INO80C	I3LGL8	>tr|I3LGL8|I3LGL8_PIG Uncharacterized protein OS=Sus scrofa GN=INO80C PE=4 S		0.77671			0.77671	4.8694			4.8694	6.2693	
9	CD47	A8VKH9	>tr|A8VKH9|A8VKH9_PIG CD47 OS=Sus scrofa PE=2 SV=1		9.0676		9.0676		4.3941		4.3941		0.48459	
10	PA2G4	I3LVF5	>tr|I3LVF5|I3LVF5_PIG Uncharacterized protein OS=Sus scrofa GN=Ssc.84050 PE=		0.66614	0.66614			4.2983	4.2983			6.4526	6.4526
11	SRRM1	F1STV4	>tr|F1STV4|F1STV4_PIG Uncharacterized protein OS=Sus scrofa GN=SRRM1 PE=4		1.045	1.045	0.99644		4.2772	4.2772	0.93476		4.0909	4.0909
12	EPHA5	F1RVG1	>tr|F1RVG1|F1RVG1_PIG Uncharacterized protein OS=Sus scrofa GN=EPHA5 PE=4		50.023		50.023		4.0037		4.0037		0.080038	
13	OR2T27	F1S5V5	>tr|F1S5V5|F1S5V5_PIG Uncharacterized protein (Fragment) OS=Sus scrofa GN=L		1.8193			1.8193	3.876			3.876	2.1305	
14	OR2T3	F1RH00	>tr|F1RH00|F1RH00_PIG Uncharacterized protein OS=Sus scrofa GN=LOC1005162		0.66667			0.66667	3.5565			3.5565	5.3346	
15	OR2T3	F1RH00	>tr|F1RH00|F1RH00_PIG Uncharacterized protein OS=Sus scrofa GN=LOC1005162		0.66667			0.66667	3.5565			3.5565	5.3346	
16	OR2T3	F1RH00	>tr|F1RH00|F1RH00_PIG Uncharacterized protein OS=Sus scrofa GN=LOC1005162		0.66667			0.66667	3.5565			3.5565	5.3346	
17	STT3A	F1S775	>tr|F1S775|F1S775_PIG Uncharacterized protein OS=Sus scrofa GN=STT3A PE=4 S		0.83282			0.83282	3.5277			3.5277	4.2359	
18	SETD1B	F1RNR2	>tr|F1RNR2|F1RNR2_PIG Uncharacterized protein OS=Sus scrofa GN=SETD1B PE=		1.497		1.497		3.3089		3.3089		2.2103	
19	DOCK2	I3LKK3	>tr|I3LKK3|I3LKK3_PIG Uncharacterized protein OS=Sus scrofa GN=Ssc.55943 PE=		0.68675		0.68675		3.1062		3.1062		4.523	
20	DOCK2	I3LKK3	>tr|I3LKK3|I3LKK3_PIG Uncharacterized protein OS=Sus scrofa GN=Ssc.55943 PE=		0.68675		0.68675		3.1062		3.1062		4.523	
21	NUB1	F1SSM7	>tr|F1SSM7|F1SSM7_PIG Uncharacterized protein OS=Sus scrofa GN=NUB1 PE=4		0.5619	0.5619			2.7501	2.7501			4.8943	4.8943
22	OR10V1	F1RI85	>tr|F1RI85|F1RI85_PIG Uncharacterized protein OS=Sus scrofa GN=OR10V1 PE=3		0.39515			0.39515	2.4521			2.4521	6.2056	
23	OR10V1	F1RI85	>tr|F1RI85|F1RI85_PIG Uncharacterized protein OS=Sus scrofa GN=OR10V1 PE=3		0.39515			0.39515	2.4521			2.4521	6.2056	
24	PGA4	I3LTU5	>tr|I3LTU5|I3LTU5_PIG Uncharacterized protein OS=Sus scrofa GN=Ssc.73958 PE=		1.2155	1.2155			2.2256	2.2256			1.831	1.831
25	PDHA1	I3LCI2	>tr|I3LCI2|I3LCI2_PIG Pyruvate dehydrogenase E1 component subunit alpha, sor		0.4848	0.4848			2.1865	2.1865			4.5102	4.5102
26	VPS39	F1SFK5	>tr|F1SFK5|F1SFK5_PIG Uncharacterized protein OS=Sus scrofa GN=VPS39 PE=4 S		15.602			15.602	1.9693			1.9693	0.12622	
27	PDHA1	I3LCI2	>tr|I3LCI2|I3LCI2_PIG Pyruvate dehydrogenase E1 component subunit alpha, sor		0.43099	0.43099			1.8694	1.8694			4.425	4.425
28	CALD1	I3L7S4	>tr|I3L7S4|I3L7S4_PIG Uncharacterized protein OS=Sus scrofa GN=CALD1 PE=4 SV		0.86534	0.86534			1.6408	1.6408			1.504	1.504
29	PSMB9	F1RTL3	>tr|F1RTL3|F1RTL3_PIG Uncharacterized protein (Fragment) OS=Sus scrofa GN=I		0.64304	0.64304			1.5969	1.5969			2.4833	2.4833

Phospho (STY) M vs L | Phospho (STY) H vs L | Standard M vs L | Standard H vs L

Ready | Average: 0.988207762 | Count: 517 | Sum: 5

B.

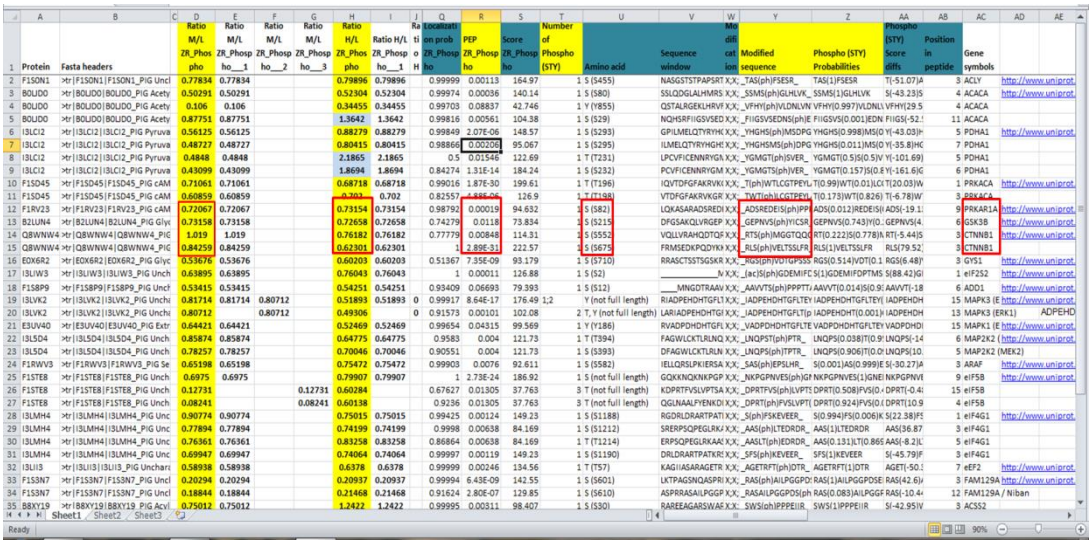

	A	B	C	D	E	F	G	H	I	J	Q	R	S	T	U	V	W	Y	Z	AA	AB	AC	AD	AE
1	Protein	Fasta headers		Ratio M/L ZR_Phospho	Ratio M/L ZR_Phospho__1	Ratio M/L ZR_Phospho__2	Ratio M/L ZR_Phospho__3	Ratio H/L ZR_Phospho	Ratio H/L ZR_Phospho__1	Ra tio H	Localization prob ZR_Phospho	PEP ZR_Phospho	Score ZR_Phospho	Number of Phospho (STY)	Amino acid	Sequence window	diffcat ion	Modified sequence	Phospho (STY) Probabilities	Phospho (STY) Score diffs	Position in peptide	Gene symbols		
2	F1SON1	>tr|F1SON1|F1SON1_PIG Uncl		0.77834	0.77834			0.79896	0.79896		0.99999	0.00113	164.97	1	S (S455)	NASGSTSTPAPSRT	X;X;_	_TAS(ph)FSESR_	TAS(1)FSESR	T(-51.07)A	3	ACLY		http://www.uniprot.
3	B0LID0	>tr|B0LID0|B0LID0_PIG Acety		0.50291	0.50291			0.52304	0.52304		0.99974	0.00036	140.14	1	S (S80)	SSLQDGLALHMRS	X;X;_	_SSMS(ph)GLHLVK_	SSMS(1)GLHLVK	S(-43.23)S	4	ACACA		http://www.uniprot.
4	B0LID0	>tr|B0LID0|B0LID0_PIG Acety		0.106	0.106			0.34455	0.34455		0.99703	0.08837	42.746	1	Y (Y855)	QSTALRGEKLHRVF	X;X;_	_VFHY(ph)VLDNLVN	VFHY(0.997)VLDNL	VFHY(29.5	4	ACACA		
5	B0LID0	>tr|B0LID0|B0LID0_PIG Acety		0.87751	0.87751			1.3642	1.3642		0.99816	0.00561	104.38	1	S (S29)	NQHSRFIIGSVSED	X;X;_	_FIIGSV\SEDNS(ph)E	FIIGSV\S(0.001)EDN	FIIGS(-52.5	11	ACACA		
6	I3LCI2	>tr|I3LCI2|I3LCI2_PIG Pyruva		0.56125	0.56125			0.88279	0.88279		0.99849	2.07E-06	148.57	1	S (S293)	GPILMELQTYRYHC	X;X;_	_YHGHS(ph)MSDPG	YHGHS(0.998)MS(0	Y(-43.03)H	5	PDHA1		http://www.uniprot.
7	I3LCI2	>tr|I3LCI2|I3LCI2_PIG Pyruva		0.48727	0.48727			0.80415	0.80415		0.98866	0.00208	95.067	1	S (S295)	ILMELQTYRYHGHC	X;X;_	_YHGHSMS(ph)DPG	YHGHS(0.011)MS(0	Y(-35.8)HC	7	PDHA1		
8	I3LCI2	>tr|I3LCI2|I3LCI2_PIG Pyruva		0.4848	0.4848			2.1865	2.1865		0.5	0.01546	122.69	1	T (T231)	LPCVFICENNRYGA	X;X;_	_YGMGT(ph)SVER_	YGMGT(0.5)S(0.5)V	Y(-101.69)	5	PDHA1		
9	I3LCI2	>tr|I3LCI2|I3LCI2_PIG Pyruva		0.43099	0.43099			1.8694	1.8694		0.84274	1.31E-14	184.24	1	S (S232)	PCVFICENNRYGM	X;X;_	_YGMGTS(ph)VER_	YGMGT(0.157)S(0.8	Y(-161.6)G	6	PDHA1		
10	F1SD45	>tr|F1SD45|F1SD45_PIG cAM		0.71061	0.71061			0.68718	0.68718		0.99016	1.87E-30	199.61	1	T (T196)	IQVTDFGFAKRVKI	X;X;_	_T(ph)WTLCGTPEYL	T(0.99)WT(0.01)LCI	T(20.03)W	1	PRKACA		http://www.uniprot.
11	F1SD45	>tr|F1SD45|F1SD45_PIG cAM		0.60859	0.60859			0.702	0.702		0.82557	1.88E-06	126.9	1	T (T198)	VTDFGFAKRVKGR	X;X;_	_TWT(ph)LCGTPEYL	T(0.173)WT(0.826)	T(-6.78)W	3	PRKAC		
12	F1RV23	>tr|F1RV23|F1RV23_PIG cAM		0.72067	0.72067			0.73154	0.73154		0.98792	0.00019	94.632	1	S (S82)	LQKASARAQSREDI	X;X;_	_ADSREDEIS(ph)PP	ADS(0.012)REDEIS(	ADS(-19.1	9	PRKAR1A		http://www.uniprot.
13	B2LUN4	>tr|B2LUN4|B2LUN4_PIG Glyc		0.73158	0.73158			0.72658	0.72658		0.74279	0.0118	73.834	1	S (S215)	DFGSAKQLVRGEP	X;X;_	_GEPNVS(ph)YICSR	GEPNVS(0.743)Y(0.	GEPNVS(4.	6	GSK3B		http://www.uniprot.
14	Q8WNW4	>tr|Q8WNW4|Q8WNW4_PIG		1.019	1.019			0.76182	0.76182		0.77779	0.00848	114.31	1	S (S552)	VQLLVRAHQDTQF	X;X;_	_RTS(ph)MGGTQQI	RT(0.222)S(0.778)A	RT(-5.44)S	3	CTNNB1		http://www.uniprot.
15	Q8WNW4	>tr|Q8WNW4|Q8WNW4_PIG		0.84259	0.84259			0.62301	0.62301		1	2.89E-31	222.57	1	S (S675)	FRMSEDKPQDYKR	X;X;_	_RLS(ph)VELTSSLFR	RLS(1)VELTSSLFR	RLS(79.52)	3	CTNNB1		
16	E0X6R2	>tr|E0X6R2|E0X6R2_PIG Glyc		0.53676	0.53676			0.60203	0.60203		0.51367	7.35E-09	93.179	1	S (S710)	RRASCTSSTSGSKR	X;X;_	_RGS(ph)VDTGPSSS	RGS(0.514)VDT(0.1	RGS(6.48)T	3	GYS1		http://www.uniprot.
17	I3LIW3	>tr|I3LIW3|I3LIW3_PIG Unch		0.63895	0.63895			0.76043	0.76043		1	0.00011	126.88	1	S (S2)	_____N	X;X;_	_(ac)S(ph)GDEMIFC	S(1)GDEMIFDPTMS	S(88.42)GI	1	eIF252		http://www.uniprot.
18	F1S8P9	>tr|F1S8P9|F1S8P9_PIG Unch		0.53415	0.53415			0.54251	0.54251		0.93409	0.06693	79.393	1	S (S12)	___MNGDTRAAV	X;X;_	_AAVVTS(ph)PPPTI	AAVVT(0.014)S(0.9	AAVVT(-18	6	ADD1		http://www.uniprot.
19	I3LVK2	>tr|I3LVK2|I3LVK2_PIG Unchi		0.81714	0.81714	0.80712		0.51893	0.51893	0	0.99917	8.64E-17	176.49	1;2	Y (not full length)	RIADPEHDHTGFLT	X;X;_	_IADPEHDHTGFLT(p	IADPEHDHTGFLT(0.001)	IADPEHDH	15	MAPK3 (E		http://www.uniprot.
20	I3LVK2	>tr|I3LVK2|I3LVK2_PIG Unchi		0.80712		0.80712		0.49306		0	0.91573	0.00101	102.08	2	T, Y (not full length)	LARIADPEHDHTGF	X;X;_	_IADPEHDHTGFLT(p	IADPEHDHTGFLT(0.001)	IADPEHDH	13	MAPK3 (ERK1)		ADPEHD
21	E3UV40	>tr|E3UV40|E3UV40_PIG Extr		0.64421	0.64421			0.52469	0.52469		0.99654	0.04315	99.569	1	Y (Y186)	RVADPDHDHTGFL	X;X;_	_VADPDHDHTGFLT	VADPDHDHTGFLT	VADPDHDI	15	MAPK1 (E		http://www.uniprot.
22	I3LSD4	>tr|I3LSD4|I3LSD4_PIG Unch		0.85874	0.85874			0.64775	0.64775		0.9583	0.004	121.73	1	T (T394)	FAGWLCKTLRLNQ	X;X;_	_LNQPST(ph)PTR_	LNQPS(0.038)T(0.9	LNQPS(-14	6	MAP2K2 (		http://www.uniprot.
23	I3LSD4	>tr|I3LSD4|I3LSD4_PIG Unch		0.78257	0.78257			0.70046	0.70046		0.90551	0.004	121.73	1	S (S393)	DFAGWLCKTLRLN	X;X;_	_LNQPS(ph)TPTR_	LNQPS(0.906)T(0.0	LNQPS(10.	5	MAP2K2 (MEK2)		
24	F1RWV3	>tr|F1RWV3|F1RWV3_PIG Se		0.65198	0.65198			0.75472	0.75472		0.99903	0.0076	92.611	1	S (S582)	IELLQRSLPKIERSA	X;X;_	_SAS(ph)EPSLHR_	S(0.001)AS(0.999)E	S(-30.27)A	3	ARAF		http://www.uniprot.
25	F1ST E8	>tr|F1ST E8|F1ST E8_PIG Unch		0.6975	0.6975			0.79907	0.79907		1	2.73E-24	186.92	1	S (not full length)	GQKKNQKNKPGP	X;X;_	_NKPGPNVES(ph)GI	NKPGPNVES(1)GNE	NKPGPNVI	9	eIF5B		
26	F1ST E8	>tr|F1ST E8|F1ST E8_PIG Unch		0.12731			0.12731	0.60284			0.67627	0.01305	37.763	3	T (not full length)	KDPRTPVSLVPTSA	X;X;_	_DPRTPVS(ph)LVPTS	DPRTPVS(0.508)PVS(0.4	DPRT(-0.4(	15	eIF5B		
27	F1ST E8	>tr|F1ST E8|F1ST E8_PIG Unch		0.08241			0.08241	0.60138			0.9236	0.01305	37.763	3	T (not full length)	QGLNAALFYENKDI	X;X;_	_DPRT(ph)PVSLVPT	DPRT(0.924)PVS(0.(	DPRT(10.9	4	eIF5B		
28	I3LMH4	>tr|I3LMH4|I3LMH4_PIG Unc		0.90774	0.90774			0.75015	0.75015		0.99425	0.00124	149.23	1	S (S1188)	RGDRLDRARTPATI	X;X;_	_S(ph)FSKEVEER_	S(0.994)FS(0.006)K	S(22.38)FS	1	eIF4G1		http://www.uniprot.
29	I3LMH4	>tr|I3LMH4|I3LMH4_PIG Unc		0.77894	0.77894			0.74199	0.74199		0.9998	0.00638	84.169	1	S (S1212)	SRERPSQPEGLRKA	X;X;_	_AAS(ph)LTEDRDR_	AAS(1)LTEDRDR	AAS(36.87	3	eIF4G1		
30	I3LMH4	>tr|I3LMH4|I3LMH4_PIG Unc		0.76361	0.76361			0.83258	0.83258		0.86864	0.00638	84.169	1	T (T1214)	ERPSQPEGLRKAAT	X;X;_	_AASLT(ph)EDRDR_	AAS(0.131)LT(0.865	AAS(-8.2)L	5	eIF4G1		
31	I3LMH4	>tr|I3LMH4|I3LMH4_PIG Unc		0.69947	0.69947			0.74064	0.74064		0.99997	0.00119	149.23	1	S (S1190)	DRLDRARTPATKRT	X;X;_	_SFS(ph)KEVEER_	SFS(1)KEVEER	S(-45.79)F	3	eIF4G1		
32	I3LII3	>tr|I3LII3|I3LII3_PIG Unchar		0.58938	0.58938			0.6378	0.6378		0.99999	0.00246	134.56	1	T (T57)	KAGIIASARAGETR	X;X;_	_AGETRFT(ph)DTR_	AGETRFT(1)DTR	AGET(-50.5	7	eEF2		http://www.uniprot.
33	F1S3N7	>tr|F1S3N7|F1S3N7_PIG Uncl		0.20294	0.20294			0.20937	0.20937		0.99994	6.43E-09	142.55	1	S (S601)	LKTPAGSNQASPRI	X;X;_	_RAS(ph)AILPGGPDS	RAS(1)AILPGGPDSE	RAS(42.6)A	3	FAM129A		http://www.uniprot.
34	F1S3N7	>tr|F1S3N7|F1S3N7_PIG Uncl		0.18844	0.18844			0.21468	0.21468		0.91624	2.80E-07	129.85	1	S (S610)	ASPRRASAILPGGP	X;X;_	_RASAILPGGPDS(ph	RAS(0.083)AILPGGF	RAS(-10.4	12	FAM129A / Niban		
35	B8XY19	>tr|B8XY19|B8XY19_PIG Acyl		0.75012	0.75012			1.2422	1.2422		0.99995	0.00311	98.407	1	S (S30)	RAREEAGARSWAE	X;X;_	_SWS(ph)PPPEIIR_	SWS(1)PPPEIIR	S(-42.95)W	3	ACSS2		

Sheet1 | Sheet2 | Sheet3

Ready | 90%

Figure 4.3 Overview of the SILAC proteomics expression data

Key parameters such as protein symbols, protein IDs, posterior error probabilities, location of phospho- amino acids and peptide sequences are found in Analysis Results ZR1-3 Phospho. The layout of the protein file (Analysis Results Z1-10) file is similar to the phosphoprotein file (Fig. 4.5). Protein fold change (M/L = 1h and H/L = 6h)

values were normalised (Normalisation formula = (1/median value for all column ratios x protein ratio). The number of peptides identified and quantified for each protein, and the percentage coverage of protein sequence are highlighted.

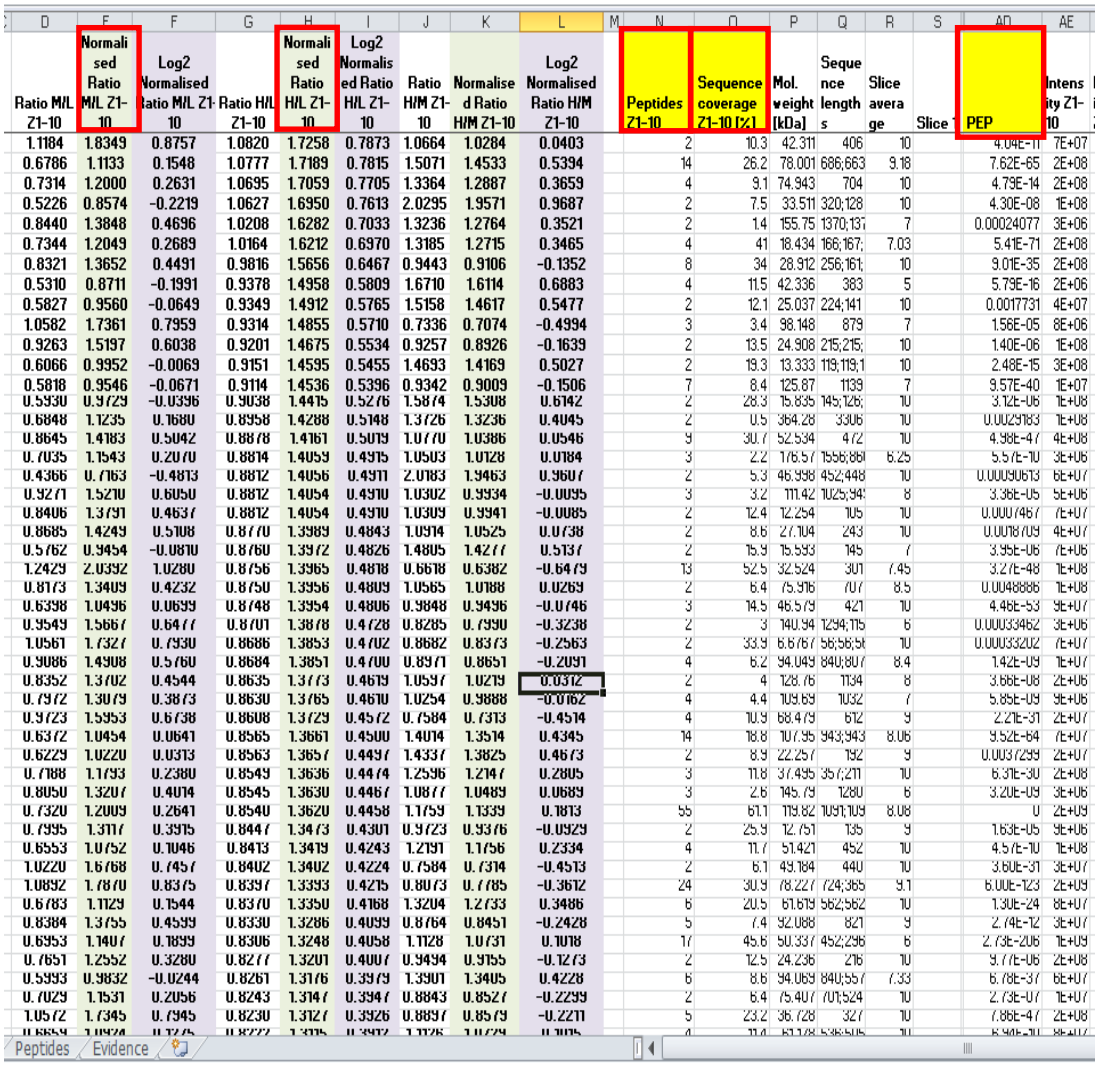

D	F	F	G	H	I	J	K	L	M	N	O	P	Q	R	S	AD	AE
Ratio M/L Z1-10	Normalised Ratio M/L Z1-10	Log2 Normalised Ratio M/L Z1-10	Ratio H/L Z1-10	Normalised Ratio H/L Z1-10	Log2 Normalised Ratio H/L Z1-10	Ratio H/M Z1-10	Normalised Ratio H/M Z1-10	Log2 Normalised Ratio H/M Z1-10		Peptides Z1-10	Sequence coverage Z1-10 [%]	Mol. weight [kDa]	Sequence lengths	Slice average	Slice 1	PEP	Intensity Z1-10
1.1184	1.8349	0.8757	1.0820	1.7258	0.7873	1.0664	1.0284	0.0403		2	10.3	42.311	406	10		4.04E-11	7E+07
0.6786	1.1133	0.1548	1.0777	1.7189	0.7815	1.5071	1.4533	0.5394		14	26.2	78.001	686;663	9.18		7.62E-65	2E+08
0.7314	1.2000	0.2631	1.0695	1.7059	0.7705	1.3364	1.2887	0.3659		4	9.1	74.943	704	10		4.79E-14	2E+08
0.5226	0.8574	-0.2219	1.0627	1.6950	0.7613	2.0295	1.9571	0.9687		2	7.5	33.511	320;128	10		4.30E-08	1E+08
0.8440	1.3848	0.4696	1.0208	1.6282	0.7033	1.3236	1.2764	0.3521		2	1.4	155.75	1370;137	7		0.00024077	3E+06
0.7344	1.2049	0.2689	1.0164	1.6212	0.6970	1.3185	1.2715	0.3465		4	41	18.434	166;167;	7.03		5.41E-71	2E+08
0.8321	1.3652	0.4491	0.9816	1.5656	0.6467	0.9443	0.9106	-0.1352		8	34	28.912	256;161;	10		9.01E-35	2E+08
0.5310	0.8711	-0.1991	0.9378	1.4958	0.5809	1.6710	1.6114	0.6883		4	11.5	42.336	383	5		5.79E-16	2E+06
0.5827	0.9560	-0.0649	0.9349	1.4912	0.5765	1.5158	1.4617	0.5477		2	12.1	25.037	224;141	10		0.0017731	4E+07
1.0582	1.7361	0.7959	0.9314	1.4855	0.5710	0.7336	0.7074	-0.4994		3	3.4	98.148	879	7		1.56E-05	8E+06
0.9263	1.5197	0.6038	0.9201	1.4675	0.5534	0.9257	0.8926	-0.1639		2	13.5	24.908	215;215;	10		1.40E-06	1E+08
0.6066	0.9952	-0.0069	0.9151	1.4595	0.5455	1.4693	1.4169	0.5027		2	19.3	13.333	119;119;1	10		2.48E-15	3E+08
0.5818	0.9546	-0.0671	0.9114	1.4536	0.5396	0.9342	0.9009	-0.1506		7	8.4	125.87	1139	7		9.57E-40	1E+07
0.5930	0.9729	-0.0396	0.9038	1.4415	0.5276	1.5874	1.5308	0.6142		2	28.3	15.835	145;126;	10		3.12E-06	1E+08
0.6848	1.1235	0.1680	0.8958	1.4288	0.5148	1.3726	1.3236	0.4045		2	0.5	364.28	3306	10		0.0029183	9E+06
0.8645	1.4183	0.5042	0.8878	1.4161	0.5019	1.0770	1.0386	0.0546		9	30.7	52.534	472	10		4.98E-47	4E+08
0.7035	1.1543	0.2070	0.8814	1.4059	0.4915	1.0503	1.0128	0.0184		3	2.2	176.57	1556;861	6.25		5.57E-10	3E+06
0.4366	0.7163	-0.4813	0.8812	1.4056	0.4911	2.0183	1.9463	0.9607		2	5.3	46.998	452;448	10		0.0009613	6E+07
0.9271	1.5210	0.6050	0.8812	1.4054	0.4910	1.0302	0.9934	-0.0095		3	3.2	111.42	1025;943	8		3.36E-05	5E+06
0.8406	1.3791	0.4637	0.8812	1.4054	0.4910	1.0309	0.9941	-0.0085		2	12.4	12.254	105	10		0.0007467	7E+07
0.8685	1.4249	0.5108	0.8770	1.3989	0.4843	1.0314	1.0525	0.0738		2	8.6	27.104	243	10		0.0018709	4E+07
0.5762	0.9454	-0.0810	0.8760	1.3972	0.4826	1.4805	1.4277	0.5137		2	16.9	16.593	145	7		3.95E-06	7E+06
1.2429	2.0392	1.0280	0.8756	1.3965	0.4818	0.6618	0.6382	-0.6479		13	52.5	32.524	301	7.45		3.27E-48	1E+08
0.8173	1.3409	0.4232	0.8750	1.3956	0.4809	1.0565	1.0188	0.0269		2	6.4	75.916	707	8.5		0.0048886	1E+08
0.6398	1.0496	0.0699	0.8748	1.3954	0.4806	0.9848	0.9496	-0.0746		3	14.5	46.579	421	10		4.46E-53	9E+07
0.9549	1.5667	0.6477	0.8701	1.3878	0.4728	0.8285	0.7990	-0.3238		2	3	140.94	1294;115	6		0.0003462	3E+06
1.0561	1.7327	0.7930	0.8686	1.3853	0.4702	0.8682	0.8373	-0.2563		2	33.9	6.6767	56;56;5	10		0.0003202	7E+07
0.9086	1.4908	0.5760	0.8684	1.3851	0.4700	0.8971	0.8651	-0.2091		4	6.2	94.049	840;807	8.4		1.42E-09	1E+07
0.8352	1.3702	0.4544	0.8635	1.3773	0.4619	1.0597	1.0219	0.0312		2	4	128.76	1134	8		3.66E-08	2E+06
0.7972	1.3079	0.3873	0.8630	1.3765	0.4610	1.0254	0.9888	-0.0162		4	4.4	109.69	1032	7		5.85E-09	9E+06
0.9723	1.5953	0.6738	0.8608	1.3729	0.4572	0.7584	0.7313	-0.4514		4	10.9	68.479	612	9		2.27E-31	2E+07
0.6372	1.0454	0.0641	0.8565	1.3661	0.4500	1.4014	1.3514	0.4345		14	18.8	107.95	943;943	8.06		9.52E-64	7E+07
0.6229	1.0220	0.0313	0.8563	1.3657	0.4497	1.4337	1.3825	0.4673		2	8.9	22.257	192	9		0.0037299	2E+07
0.7188	1.1793	0.2380	0.8549	1.3636	0.4474	1.2596	1.2147	0.2805		3	11.8	37.495	357;211	10		6.31E-30	2E+08
0.8050	1.3207	0.4014	0.8545	1.3630	0.4467	1.0877	1.0489	0.0689		3	2.6	145.79	1280	6		3.20E-09	3E+06
0.7320	1.2009	0.2641	0.8540	1.3620	0.4458	1.1759	1.1339	0.1813		55	61.1	119.82	1091;109	8.08		0	2E+09
0.7995	1.3117	0.3915	0.8447	1.3473	0.4301	0.9723	0.9376	-0.0529		2	25.9	12.751	135	9		1.63E-05	9E+06
0.6553	1.0752	0.1046	0.8413	1.3419	0.4243	1.2191	1.1756	0.2334		4	11.7	51.421	452	10		4.57E-10	1E+08
1.0220	1.6768	0.7457	0.8402	1.3402	0.4224	0.7584	0.7314	-0.4513		2	6.1	49.184	440	10		3.60E-31	3E+07
1.0892	1.7870	0.8375	0.8397	1.3393	0.4215	0.8073	0.7785	-0.3612		24	30.9	78.227	724;365	9.1		6.00E-123	2E+09
0.6783	1.1129	0.1544	0.8370	1.3350	0.4168	1.3204	1.2733	0.3486		6	20.5	61.619	562;562	10		1.30E-24	8E+07
0.8384	1.3755	0.4599	0.8330	1.3286	0.4099	0.8764	0.8451	-0.2428		5	7.4	92.088	821	9		2.74E-12	3E+07
0.6953	1.1407	0.1899	0.8306	1.3248	0.4058	1.1128	1.0731	0.1018		17	45.6	50.337	452;296	6		2.73E-206	1E+09
0.7651	1.2552	0.3280	0.8277	1.3201	0.4007	0.9494	0.9155	-0.1273		2	12.5	24.236	216	10		9.77E-06	2E+08
0.5993	0.9832	-0.0244	0.8261	1.3176	0.3979	1.3901	1.3405	0.4228		6	8.6	94.069	840;557	7.33		6.78E-37	6E+07
0.7029	1.1531	0.2056	0.8243	1.3147	0.3947	0.8843	0.8527	-0.2299		2	6.4	75.407	701;524	10		2.73E-07	1E+07
1.0572	1.7345	0.7945	0.8230	1.3127	0.3926	0.8897	0.8579	-0.2211		5	23.2	36.728	327	10		7.86E-47	2E+08
1.0859	1.0924	0.1275	0.8222	1.3115	0.3913	1.1726	1.1309	0.1705		4	11.4	51.178	536;505	10		6.94E-31	8E+07

Peptides | Evidence

Figure 4.4 Representation of details such as peptides identified and quantified for each protein and the percentage coverage of protein sequence as shown in the protein file (Analysis Results Z1-10)

4.3.3 Differentially expressed proteins and phosphor proteins by Ract treatment

In order to evaluate the fold change in in the context of fold change in corresponding proteins, the two data sets were integrated ("Phospho & std comparison ZR1-3" file). The findings are graphically presented in Figure 4.6. At both 1h (A) and 6h (B) of Ract treatment, phosphoproteins were mostly dephosphorylated and corresponded to reduced protein accumulation.

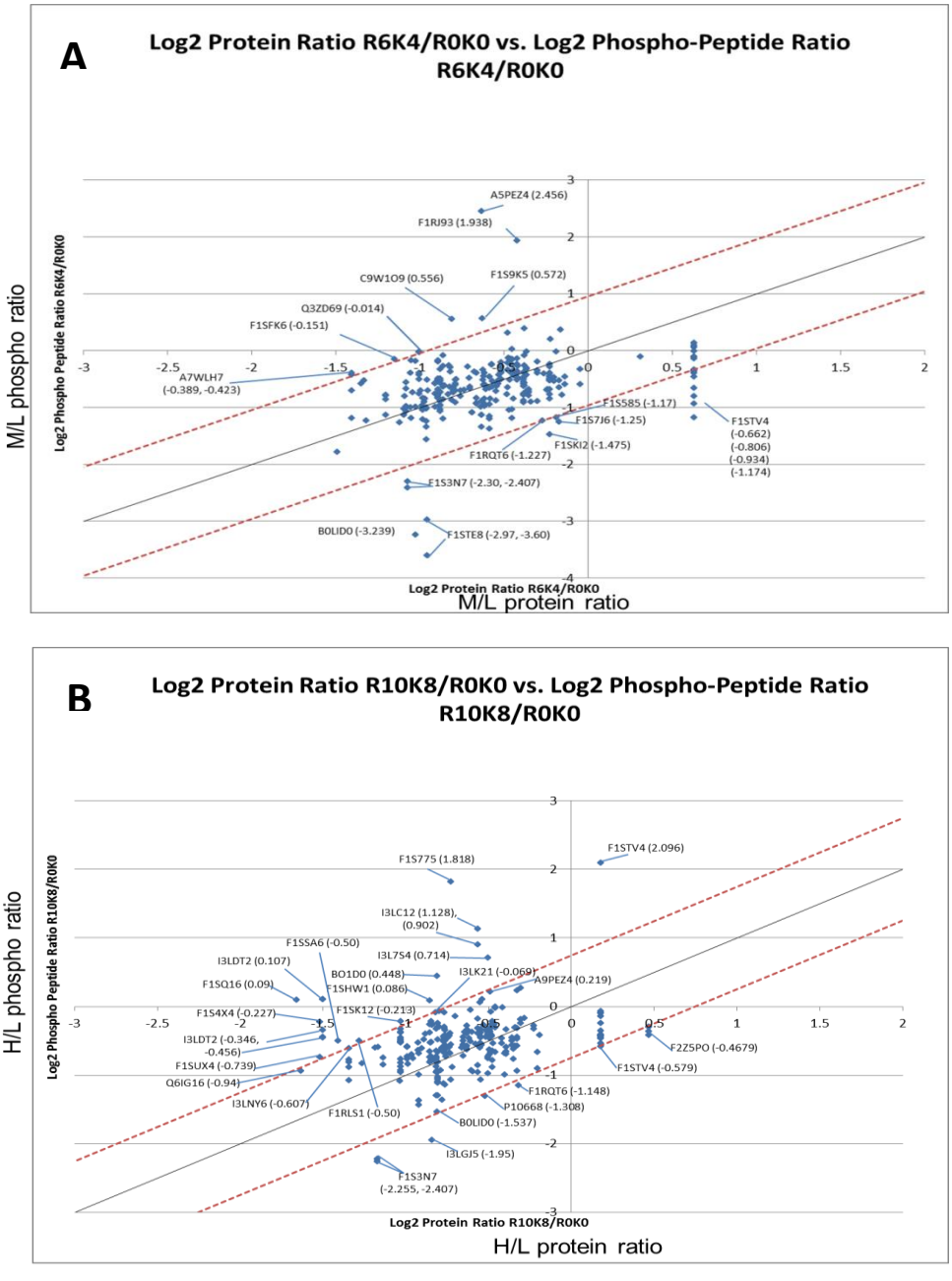

Figure 4.6 Comparisons of fold change in phosphoproteins and corresponding proteins at 1h (A) and 6h (B) of Ract treatment.

Standard proteins and phosphoproteins those were quantifiable and identifiable are displayed. Proteins that were not able to quantify (were detected) were not included. Dotted red line represents one standard deviation from midline.

Overall, over one thousand proteins and more than six hundred phosphopeptides were quantified and identified. The number of detected protein and phosphopetides were in line with current expectations of high throughput proteomics (Table 4.2).

	Identified	**Quantified**
No. of proteins	1314 (at both time pts)	1103 (at both time pts)
No. of phosphoproteins	815 (at one/both time pts)	649 (at one/both time pts)

Table 4.2 Detection summary of proteins and phosphoproteins

4.3.4 Ract treatment of muscle cells possibly induce protein synthesis and fatty acids metabolism

The statistically significant (PEP $\leqslant$ 0.1 for phosphopeptides and $\leqslant$0.01 for standard peptides) phosphoprotein and protein data sets were filtered for fold changes that were greater than 1.2 or less than 0.8 in differential expression. The four corresponding differential expression lists (phosphoprotein 1h, phosphoproteins 6h, proteins 1h and proteins 6h) are presented in the "Standard proteome and phosphoproteome shortlists" file. Each of the four lists was subjected to pathway analyses using the IPA and, to a lesser extent, Metacore software. Both software are designed for human and murine

data and do not provide biological interpretation on phosphorylation data. The most significant networks or pathways detected for differentially expressed phosphorylated proteins at both time points (1h and 6h) were those in connection with protein synthesis and fatty acids metabolism (Figure 4.7).

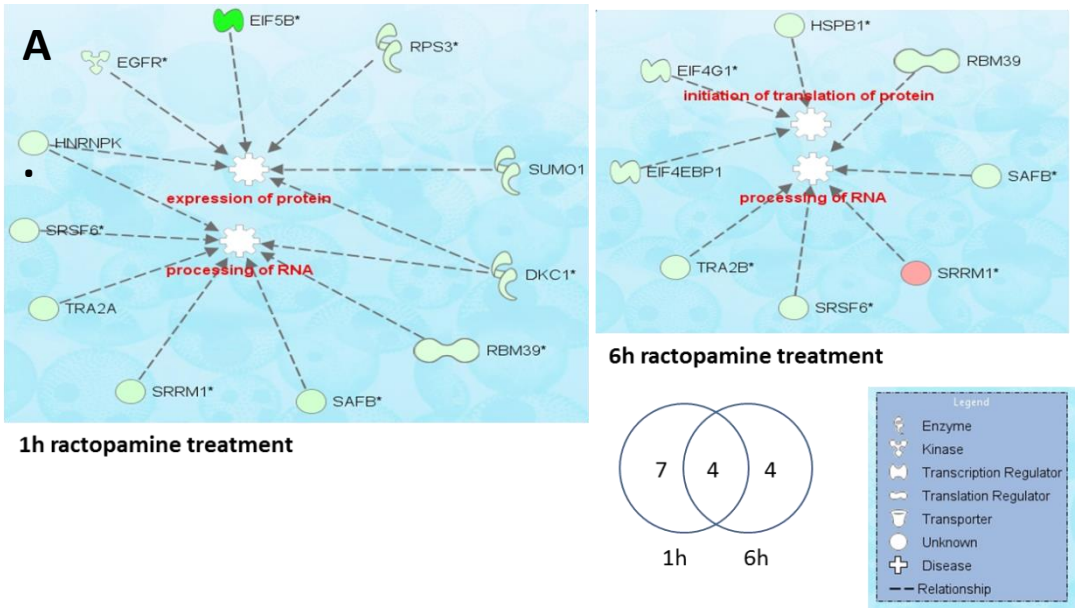

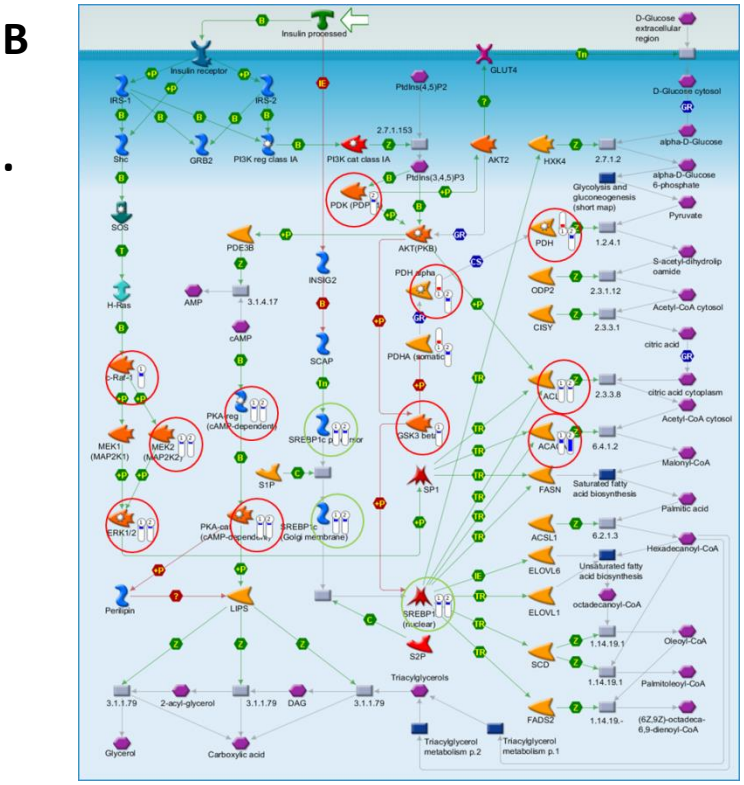

Figure 4.7 Most significant phosphoprotein networks detected were linked to (A) RNA modifications and protein synthesis, and (B) fatty acids metabolism.

Differentially phosphorylated proteins (green=downregulation/ dephosphorylation, red = up-regulation/phosphorylation) generated by IPA. Venn diagram shows overlap of four proteins between 1h and 6h Ract treatment. (B) Differentially phosphorylated proteins (circled) in fatty acids metabolism network generated by Metacore. Within each circle, 1 and 6 refer to 1h and 6h Ract treatment respectively, blue column signifies down-regulation (dephosphorylation) and red column indicates up-regulation (phosphorylation).

4.3.5 Ract treatment affected eIF2 signalling pathway by 1h and 6h of stimulation

Effect of Ract treatment on canonical pathways were analysed by IPA and was found that the most affected canonical pathway was eukaryotic translation initiation factor 2 pathway (eIF2) (Figure 4.8). Synthesis of protein or the initiation of translation in eukaryotes is a multistep process involved with several factors. One of the key steps in eukaryotic translation is the initiation of translation and eIF2 plays an important role in the addition of the first amino acid, methionine to the mRNA strand (Pain 1996; Voorma et al. 1994). Although more confirmation studies required to establish the accurate effect of the bioinformatics based prediction, an enhanced eIF2 pathway indicates increased protein synthesis and this effects is however consistent with the known phenotypic effects of Ract in skeletal muscle.

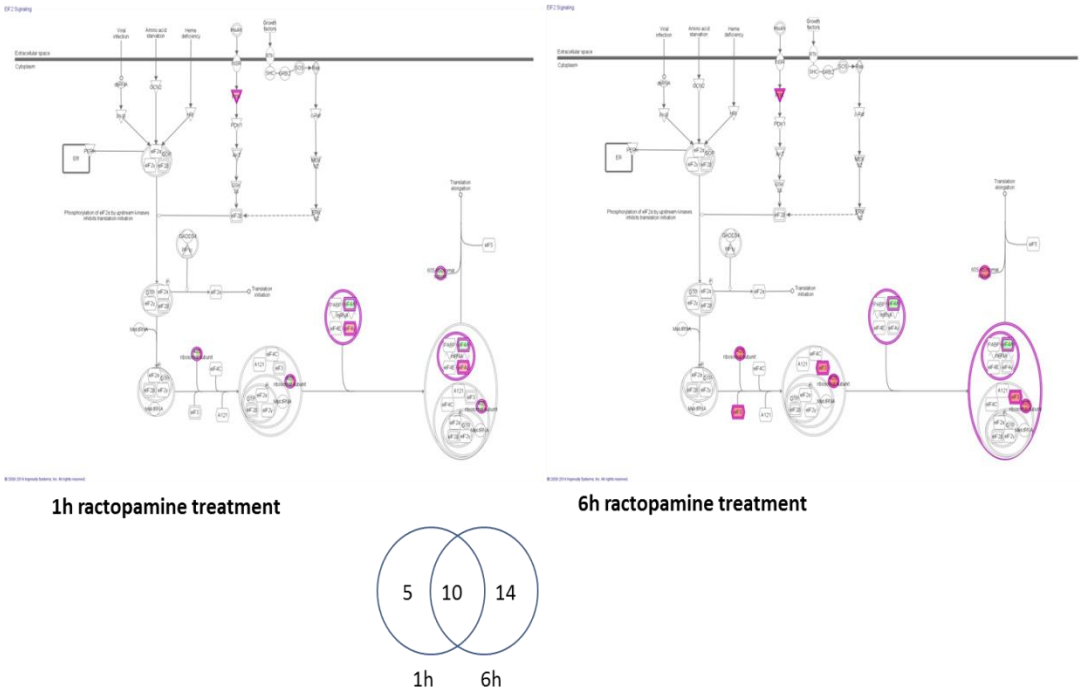

Figure 4.8 eIF2 signalling was the most significant canonical pathway affected by Ract at 1h and 6h of stimulation (IPA derived).

Differentially expressed proteins showed considerable overlap (10 proteins, venn diagram) between the two time points. Red = up-regulation. Green = down-regulation.

4.3.6 Ract treatment inhibited MAPK/ERK signalling

Extracellular signal-regulated kinase-mitogen activated protein kinase (ERK/MAPK) signalling has been shown to be involved in the transactivation of different gene such as c-Myc and also it activates translation initiation by phosphorylation of 40S ribosomal protein S6 kinases (S6Ks) (Pende et al. 2004). ERK/MAPK pathway plays a role in β2-agonist (Clenbuterol)-induced hypertrophy of fast muscles in mice (Shi et al. 2007). Since Ract is known to act as an anabolic inducer, it was expected that the ERK/MAPK may be activated, contrary to expectation, Ract treatment of porcine muscle cells resulted in an extensively dephosphorylated state of the ERK/MAPK pathway (Figure 4.9).

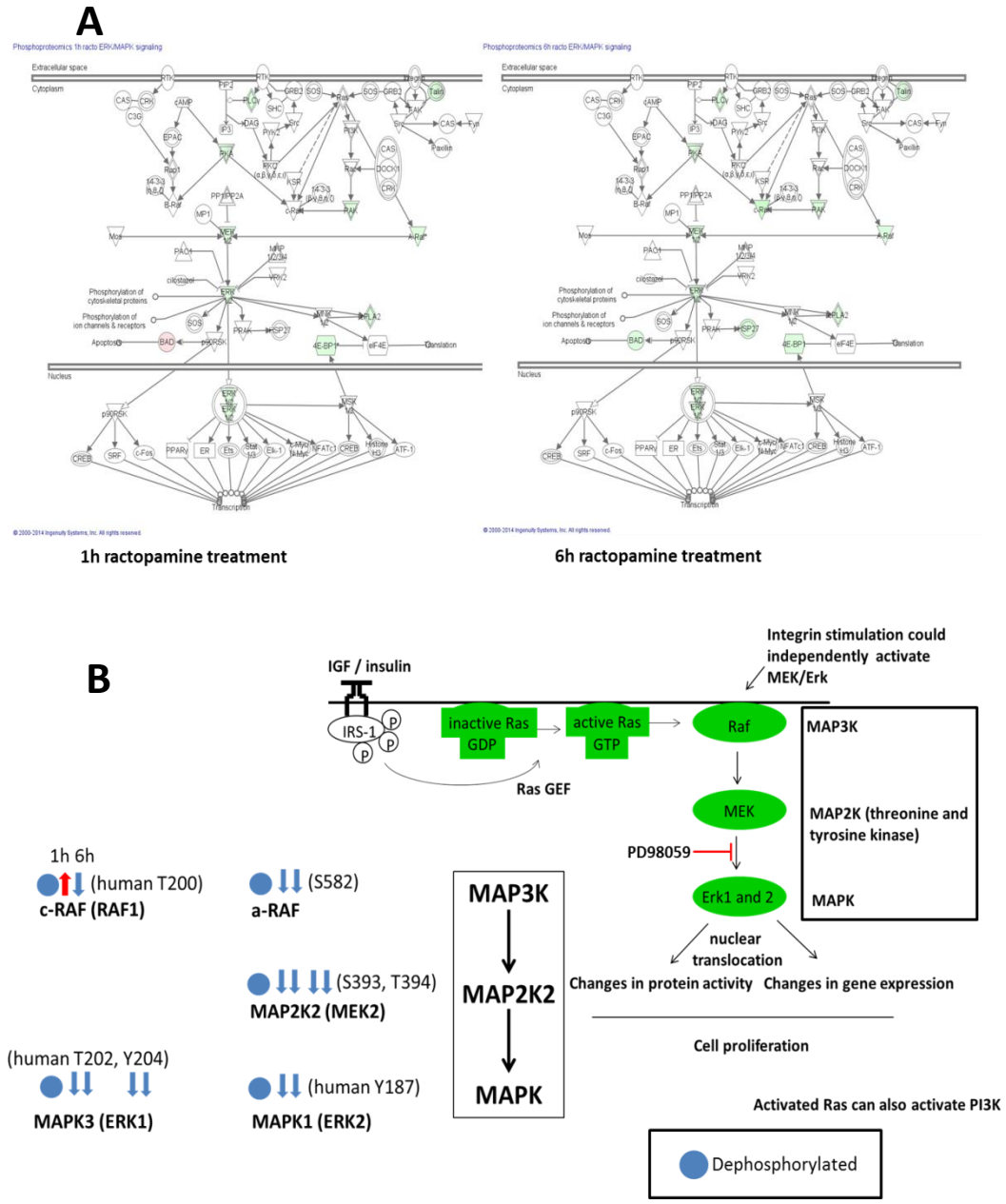

Figure 4.9 Ractopamine treatment on porcine muscle cells inhibited ERK/MAPK signalling.

Canonical ERK/MAPK pathway (A) showed consistent pattern of dephosphorylation (inactivation) at 1h and 6h of Rac stimulation (IPA generated). Red = increased phosphorylation, green = decreased phosphorylation. (B) All detected members of MAP3K, MAP2K and MAPK consistently showed reduced phosphorylation in response to Ract exposure.

4.3.7 Ract treatment on muscle cells induced changes in innate immune response

Ract stimulation of porcine muscle cells differentially regulated the innate immune proteins. Using an algorithm to predict functional effect (in IPA), Ract was predicted to inhibit viral infection (Figure 4.10) based on the differential expression of innate immune-related proteins and their known directional effect on viral infection. At 1h Ract stimulation, 39 out of the 69 innate immune-related proteins were directionally expressed in such a manner as predicted to inhibit viral infection. Likewise, at 6h Ract exposure, 26 out of 57 innate-immune-related proteins were regulated in a manner as to predict inhibition of viral infection. Z-score is an indication of prediction significance; score $\leqslant 2$ suggests that the prediction of viral inhibition is significant.

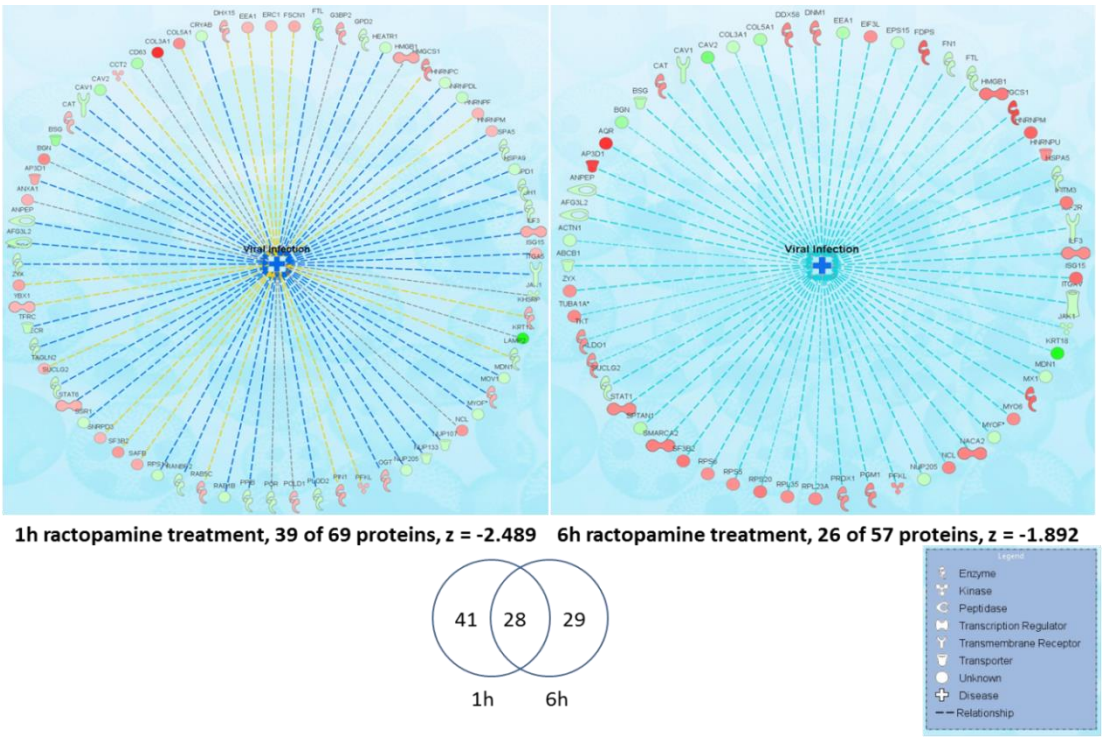

Figure 4.10 Ract treatment regulates host proteins to inhibit viral infection. Functional effects analysis using IPA indicate viral infection was affected with 69 proteins involved at 1 hour of Ract treatment. 57 protein associated with virus infection was affected by 6 hours of Ract treatment. Differentially expressed proteins showed considerable overlap (28 proteins, venn diagram) between the two Ract exposure time points. Red = up-regulation, green = down-regulation.

'Upstream Regulator' analysis using the IPA, an algorithm which can predict that the protein of interest were expressed under a particular upstream regulator protein. Analysis revealed that the differentially expressed innate immune proteins were regulated by interferon A2 (IFNA2), a type one IFN. This indicates that Ract may act through IFNA2 to activate the innate immune proteins. At 1h Ract stimulation, 5 out of the 8 innate immune-related proteins were directionally expressed in such a manner as to predict IFNA2 activation. Likewise, at 6h Ract exposure, 10 out of 11 innate-

immune-related proteins were regulated in a manner as to predict an activated IFNA2 (Figure 4.11).

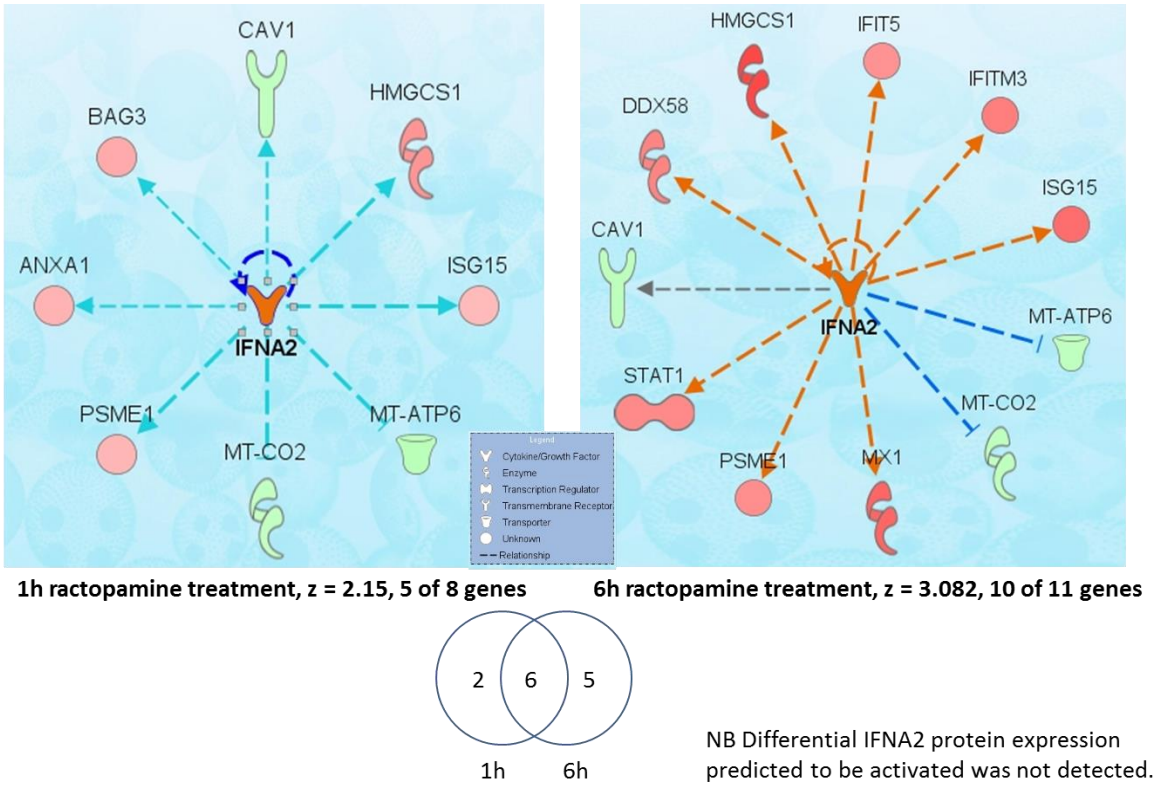

Figure 4.11 IFNA2 was identified as an upstream regulator using IPA algorithm
Innate immune proteins expressed at 1h or 6h of Ract stimulation under IFNA2 as upstream regulator. Z-score is an indication of prediction significance; score ≥ 2 suggests that the prediction of IFNA2 activation is significant. Differentially expressed proteins showed considerable overlap (6 proteins, venn diagram) between the two time points. Red = up-regulation, green = down-regulation.

Some of the differentially regulated proteins that mediate an anti-viral function are highlighted in Figure 4.12. . Ract treatment up-regulated the expression of STAT1 and 6, and several IFN-inducible proteins at one or both time points of stimulation. Protein including Mx1, IFITM3, RIG-I, IFIT5 and ISG15 were detected to be upregulated by Ract treatment. Type I IFN signals through the Janus kinase (JAK) and

Signal Transducer and Activator of Transcription (STAT) proteins to induce the transcription of IFN-inducible genes that mediate the anti-viral state (Schindler & Plumlee 2008). Interferon-induced proteins with tetratricopeptide repeats (IFITs) (Feeley et al. 2011; Katibah et al. 2014) and RIG-I (Errett & Gale Jr 2015; Rehwinkel & Reis e Sousa 2010) are RNA binding proteins, and along with Mx1 (Haller et al. 1998; Haller et al. 2015) are innate immune effectors against viruses such as influenza. Interleukin enhancer binding factor 3 (ILF3/NF90) is a double stranded RNA binding protein with potential to inhibit viral translation (Castella et al. 2015; Masuda et al. 2013). ILF3 forms a heterodimer with a 45 kDa transcription factor (NF45, ILF2) required for T-cell expression of interleukin 2. ILF3 is phosphorylated at Thr-188 and Thr-315 by PKR in response to certain RNA viruses which results in the dissociation of ILF2 from the ILF2-ILF3 complex resulting in a cytoplasmic sequestration of ILF3 where it can bind to viral RNAs and inhibit viral replication (translation). Overall, Ract appeared to promote an innate antiviral response in porcine muscle cells. The functional significance of ILF3 dephosphorylation is uncertain.

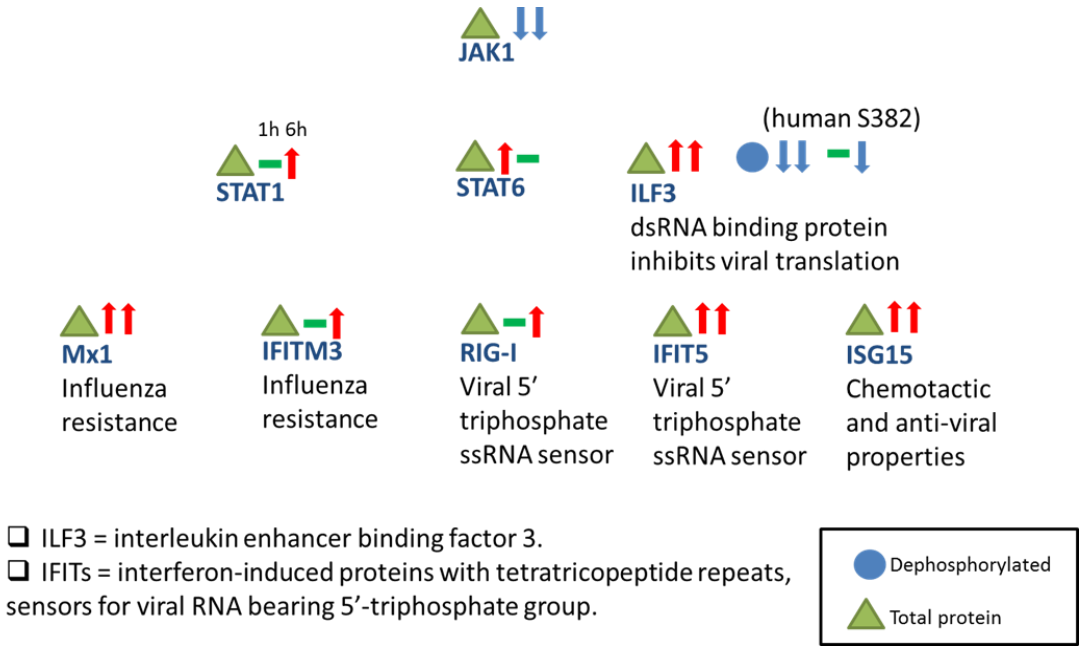

- ILF3 = interleukin enhancer binding factor 3.
- IFITs = interferon-induced proteins with tetratricopeptide repeats, sensors for viral RNA bearing 5′-triphosphate group.

Figure 4.12 Ractopamine induced changes in viral sensors and anti-viral response.

Innate immune proteins identified to express at 1h and 6h Ract stimulation of muscle cells. Triangle represents the total protein and the direction of arrow indicates up (red) or down (blue) regulation of protein expression. Green bar represents, protein undetected at a particular time point. Blue circle indicates phosphoprotein (ILF3) and the phosphorylation status of two sites at 1h and 6h Ract treatment.

4.4 Discussion

The early proteins and phosphoproteins targeted by Ract stimulation (for 1h and 6h) in primary porcine muscle cells were extensively characterised by quantitative mass spectrometry through the use of SILAC. About 1100 proteins and 650 phosphopeptides were successfully identified and quantified. As highlighted earlier, a major limitation of the use of SILAC in porcine myotube cultures was the poor rate of myotube formation. The MC+ method that was optimised to efficiently differentiate porcine myoblasts into myotubes was not readily compatible with the use of existing premade isotopic media. A high throughput mass spectrometry technique, iTRAQ (isobaric tags for relative or absolute quantification) was used which allows quantitative comparison of protein abundance by measuring peak intensities of reporter ions released from iTRAQ tagged peptides by fragmentation during MS/MS (Wiese et al. 2007). However, unlike SILAC, current labelling issues and data analysis techniques for iTRAQ struggle to report reliable estimates of relative protein abundance (Karp et al. 2010).

The complexity of protein expression is much greater than RNA expression and the following biological interpretation of protein changes are challenging. Besides the identified quantitative changes in whole protein, biological function, stability and activity are often regulated by post-translational changes such as phosphorylation and sumoylation (Santos-Rosa & Caldas 2005; Cain et al. 2014). Protein phosphorylation events could mean activation or inhibition of function(Roskoski 2015). Furthermore, different phospho-sites on the same protein may have opposing functions. For example, phosphorylation of GSK-3β at tyrosine-216 or GSK-3α at tyrosine-279 enhances the enzymatic activity of GSK-3, while phosphorlyation of serine-9 in GSK-

3β (by Akt) or serine-21 in GSK-3α significantly decreases active site availability (McCubrey et al. 2014). Ract treatment led to dephosphorylation of GSK3B at S215 (next to Y216) which speculatively could reduce its kinase activity. Although skeletal muscle and liver have the least complex transcriptomes among different organs, about 11K genes are expressed in skeletal muscle (Ramsköld et al. 2009). Since RNAs are alternatively spliced followed by extensive post-translational modifications, more proteins are expected to be produced than genes transcribed. Therefore in the muscle cell study it was estimated that only a small proportion of the total proteins were quantified which is an indication of the disparity in advances between RNA and protein detection technologies.

The changes in protein and phosphoprotein profiles in porcine muscle cells treated with Ract were highly consistent with the known effects of Ract as a β-adrenergic agonist. In some countries (such as the U.S.A.), Ract (marketed commercially as Paylean) is often used in pigs during the last 4 to 6 weeks of the fattening period of production, apparently to increase fat-free lean growth and reduce back fat thickness. The anabolic effects of Ract found in the present study firmly supported the claimed growth benefits of Ract. Even over a short duration (6h) of Ract stimulation, there was indication of raised protein and glycogen syntheses in muscle cells. The predicted increase in glycogen was in line with the finding that the hypertrophic effect of Ract is mediated through fast glycolytic fibres (Gunawan et al. 2007; Shi et al. 2007). The commercial use of Ract in pig production is not without side effects. The anabolic performance of Ract is short lived; its prolonged use (beyond 5 weeks) can cause poor growth and low conversion efficiency. Pigs on Ract could be highly agitated, difficult to handle and show tachycardia.

A convincing effect of Ract on porcine muscle cells was the extensive dephosphorylayion (inactivation) of the ERK signalling cascade, a central MAPK pathway that plays a role in the regulation of various cellular processes such as proliferation, differentiation, development, learning, survival and, under some conditions, also apoptosis (Shaul & Seger 2007). It was shown that the use of MEK1 inhibitor (PD98059) or over-expression of MAPK phosphatase -1 (MKP1/DUSP1) inhibited clenbuterol (β2-agonist)-induced skeletal muscle hypertrophy in fast murine muscles (Shi et al. 2007). In contrasts, PD98059 more recently was shown to prevent muscle wasting in tumour bearing mice, and promotes myogenic differentiation of C2C12 cells (Penna et al. 2010). These two apparently conflicting results are not easily resolved. However, they do point to the ERK/MAPK pathway as an important regulatory route of muscle growth. Further investigations are needed to clarify the role of a dephosphorylated ERK pathway in muscle hypertrophic growth.

One of the most interesting findings was the heightened innate immune response of porcine muscle cells to Ract treatment. Dozens of innate immune proteins were differentially regulated in a direction that was predicted by IPA, based on published data, to inhibit viral replication (Figure 4.10). Inspection of differentially regulated innate immune proteins identified viral sensors and type I IFN-inducible antiviral proteins that are known to target influenza A viruses (Figure 4.11 and 4.12). This key observation has opened up the possibility that Ract as a growth promoter could have significant modulatory effects on host innate immune response in muscle and indeed other cell types. Related questions that need to be addressed are the stability of the innate immune response to extended Ract stimulation, dose effects of Ract and the ability of Ract treated cells to resist virus challenge. An immediate need is to more

fully characterise the innate immune response of porcine myotubes to Ract treatment at both protein and RNA levels.

Chapter 5

Impact of growth promoters on susceptibility of porcine muscle cells to influenza virus infection

Objectives

Investigation of porcine muscle cells as targets of influenza virus infection in vitro

Evaluation of possible innate immune effects of growth promoters on porcine muscle cells

Abstract

Results presented in this chapter suggest that porcine muscle cells cultured in vitro closely represent fully functional skeletal muscle tissue. *In vitro* porcine muscle cells and NPTr cells could be infected with avian influenza virus and produced virus particles. Pig myoblasts and myotubes expressed avian and human influenza virus receptors, namely avian α-2, 3 and human α-2, 6-linked sialic acid receptors. Both myoblasts and myotubes infected with influenza virus produced infective virus particles. However, myoblasts were produced more virus particles compared with corresponding myotubes. These infected muscle cells responded by developing different innate immune responses as elevated caspase 3/7 activity which is a marker of apoptosis, displayed cytopathic effects and expressed pro-inflammatory cytokine TNF- α and *Mx-1* gene. Innate immune response for different growth promoters such as ractopamine, IGF-1 and testosterone was studied using pig muscle and tracheal epithelial cells, before and after influenza virus infection. The results showed that ractopamine promotes avian influenza H2N3 virus production in porcine myotubes and NPTr cells. In contrast, IGF-1 and testosterone had no effect on virus production. None of the selected growth promoters affected the expression of innate immune gene expression significantly.

5.1 Introduction

Skeletal muscle holds its importance as one of the earliest tissues to be used in experimental biology to primarily study the mechanism of muscle contraction and energy metabolism (Ringer 1887; Wilson 1809). Skeletal muscle comprises around fifty percent of total body weight in mammals and its role as a secretory and innate immune organ is becoming more evident from the recent studies(Pedersen 2013; Bente K Pedersen 2011) . System homeostasis is maintained by responding to different environmental and hormonal stimuli and skeletal muscle plays a major role (Frost & Lang 2012; Peake et al. 2005). Recent insights obtained from skeletal muscle research suggest that this tissue plays a major role in modulating the immune status of the organism, including anti- viral activity (Kakugawa et al. 2009).

Since meat of animal origin is the primary source of protein globally, its production has relevance in global food security, while continuing to ensure a high level of animal welfare. Two possible approaches to increase meat production are to enhance muscle growth and reduce the negative impact of infectious disease on meat production. Along with the commonly followed approaches of vaccination and improved diagnostic measures to control diseases, multiple strategies are used in farm animal production to increase meat yield and enhance disease resistance. One such approach to improve meat yield is the use of steroid hormones such as testosterone and their synthetic versions in beef cattle and sheep. Use of the beta adrenergic agonist ractopamine (Centner et al. 2014) is also a method accepted commercially by the U.S. Food and Drug Administration (FDA). IGF-1 is also used commercially as a growth promoter because it's known to induce cell proliferation by inducing cells to enter cell division (Yu et al. 2015). However there are disadvantages to the use of some growth

promoters. For example, IGF-1 is associated with abnormal cell growth like nasal polyps in pigs (Petruson et al. 1988). Nevertheless, to feed the world's growing human population, growth enhancement along with better disease resistance are desirable goals in food production animal farming.

Growth hormone (GH) affects the endocrine activity of the thymus and thus it affects adaptive immunity (Mocchegiani et al. 1990). The role IGF-1 as an autoimmune inducing factor was described earlier (Aguayo et al. 1994). IGF-1 is also involved with autoimmune diseases such as rheumatoid arthritis (Suzuki et al. 2014). In contrast IGF-1 also protects cells against a TNF-α induced cytotoxic condition (Pang et al. 2007).

Similarly, exposure of birds to high levels of testosterone suppresses the immune system (Andersson et al. 2004). Testosterone treatment of mice reduced the expression of toll like receptor 4 (TLR-4), which primarily enables the cells to detect bacterial infection and it thus acts as an immunosuppressive agent (Rettew et al. 2008). Testosterone also regulates cancer by acting upon antitumor genes and thus influences tumour specific immunity (Zhang et al. 2015). Since there is evidence to suggest that the growth enhancers are involved with cell growth and can influence the immune status of the organism, this study aimed to investigate the signalling mediators that coordinate growth and innate immune function.

Growth promoters predominantly exert their effect on skeletal muscle. However, skeletal muscle is not a major site of influenza A replication in pigs (Schaefer et al. 2015; Mooij et al. 2015) infection. Therefore first, it was important to validate the effects of influenza infection on myoblast and myotube cultures before studying the possible antiviral effects of growth promoters.

The first objective of this study was to test whether pig myoblasts and myotubes can be infected with avian influenza virus *in vitro*. It then examined the impact of three growth promoters, namely ractopamine, IGF-1 and testosterone on muscle cells which were subsequently infected with influenza virus. Evaluation of the host innate immune response in muscle cells treated with growth promoters which were later infected with influenza virus.

RNA-seq analyses and SILAC based proteomics analyses of porcine myotubes treated with ractopamine, IGF-1 and testosterone showed that several cytokines and proteins associated with host innate immune system are affected by these growth promoters. Several antiviral proteins including anti influenza factors were found to be upregulated by ractopamine treatment of myotubes. Since pigs are commercially important as food production animals and influenza virus infection is a major burden to the pig industry, this study addressed the effect growth enhancers on selected anti-viral responses in influenza virus infected pig muscle cells *in vitro*.

This study showed for the first time that the porcine myoblasts and myotubes muscle cells express both avian and mammalian sialic acid receptors, which make these cells susceptible to influenza virus infection. Thus when the pig myoblast and myotube muscle cells were experimentally infected with avian and mammalian influenza A virus, both cell types were permissive to infection. Both myoblasts and myotubes muscle cells responded to avian influenza virus infection by induction of apoptosis, secretion of pro-inflammatory cytokines and antiviral gene expression.

5.2 Results

5.2.1 Pig muscle cells express avian and mammalian sialic acid receptors and pig muscle cells are susceptible to influenza virus infection

Pig skeletal muscle cells (myoblasts and myotubes) expressed avian and mammalian type sialic acid receptors (Figure 5.1. a-b). The staining pattern demonstrated the expression of avian α-2, 3 and human α-2, 6-linked sialic acid receptors on the surface membrane of both myoblast and myotubes. The susceptibility of porcine myoblasts and MDCK cells to influenza virus infection was compared using swine H1N1 and pandemic H1N1 viruses. Infection was detected by expression of the NP protein using immunocytochemistry. Myoblasts were infected by all strains tested. In general, myoblasts required almost twice the amount of virus to obtain similar multiplicity of infection (MOI) obtained in MDCK cells (data not shown). To evaluate the ability of influenza virus to infect pig muscle cells, myotubes at seven days of differentiation were infected at an MOI of 1 with LPAI H2N3, human USSR H1N1, swine H1N1 and pandemic H1N1 viruses (Figure 5.1 c-f respectively). Viral nuclear protein (NP) was immunodetected in the myotubes after 6 hours of infection.

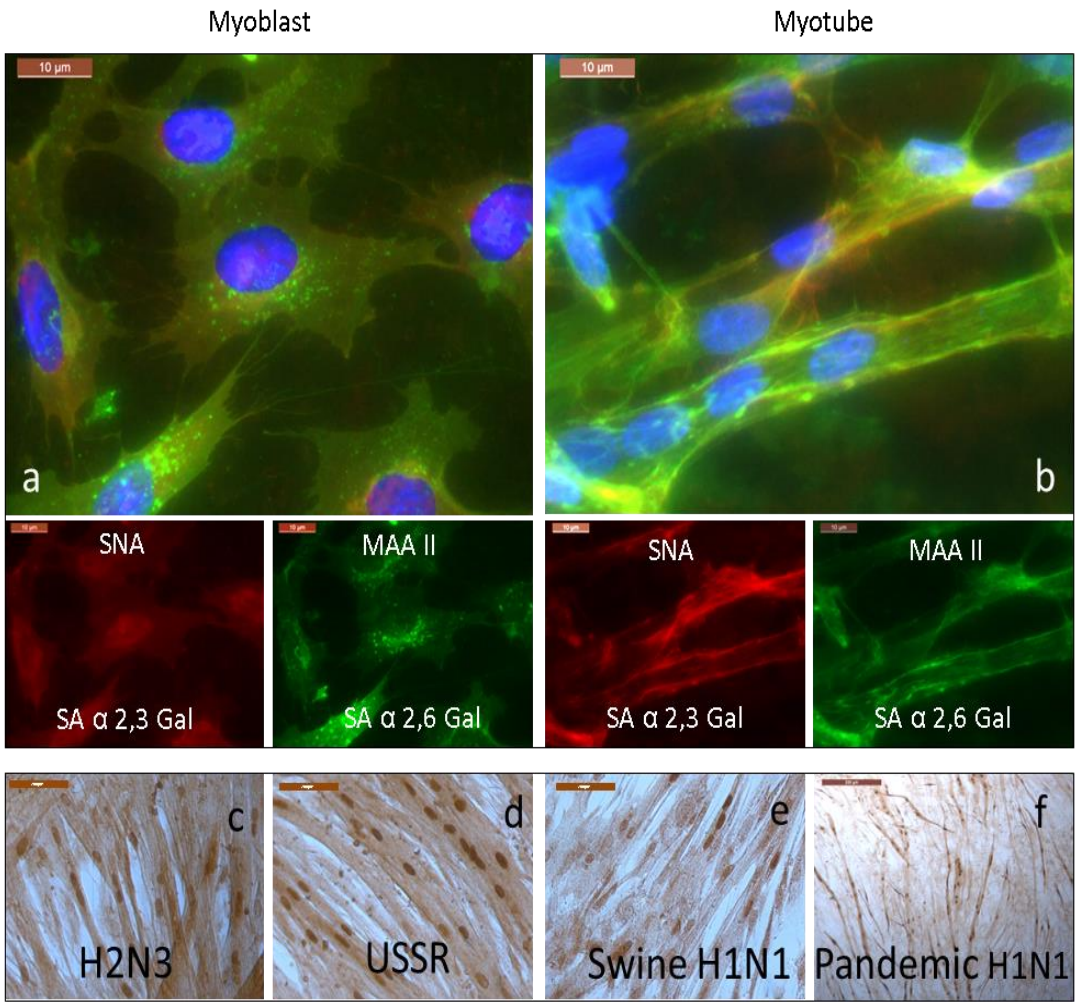

Figure 5.1 Pig myoblasts and myotubes express sialic acid receptors and are susceptible to avian and mammalian influenza virus infection

Pig myoblasts (a) and myotubes (b) expressed mammalian α-2,6-linked sialic acid receptor (green) and avian α-2,3-linked sialic acid receptor (red), DAPI was used for the nuclear counter staining shown in blue; *Sambucus nigra* 783 (SNA) and *Maackia amurensis* (MAA-II) lectins were used to detect the corresponding receptors. Influenza A NP protein was detected in myotubes, predominantly nuclear expression at 6 hours of infection at 1.0 MOI with the indicated virus strains (c-f). Expression of influenza A NP protein was detected by immunostaining against NP protein using EnVision+ System-HRP (DAB)

5.2.2 Viral NP from swine H1N1 and pandemic H1N1 viruses accumulated in pig myoblasts in a time dependent manner.

To establish the influenza virus replication dynamics in pig myoblasts, cells were separately infected with swine H1N1 virus and pandemic H1N1 virus at MOI of 0.1 and 1.0. Cells were fixed at 2h interval from 2 to 12 hours post-infection (hpi) (Figure 5.2). After four hours of infection with pandemic H1N1 virus at MOI of 0.1 and 1.0, myoblasts were stained positive for viral NP. In cells infected with swine H1N1 virus at MOI of 0.1 and 1.0 NP detection was evident only at 6 hpi. This indicates that pandemic H1N1 virus replicated faster in myoblasts than swine H1N1 virus.

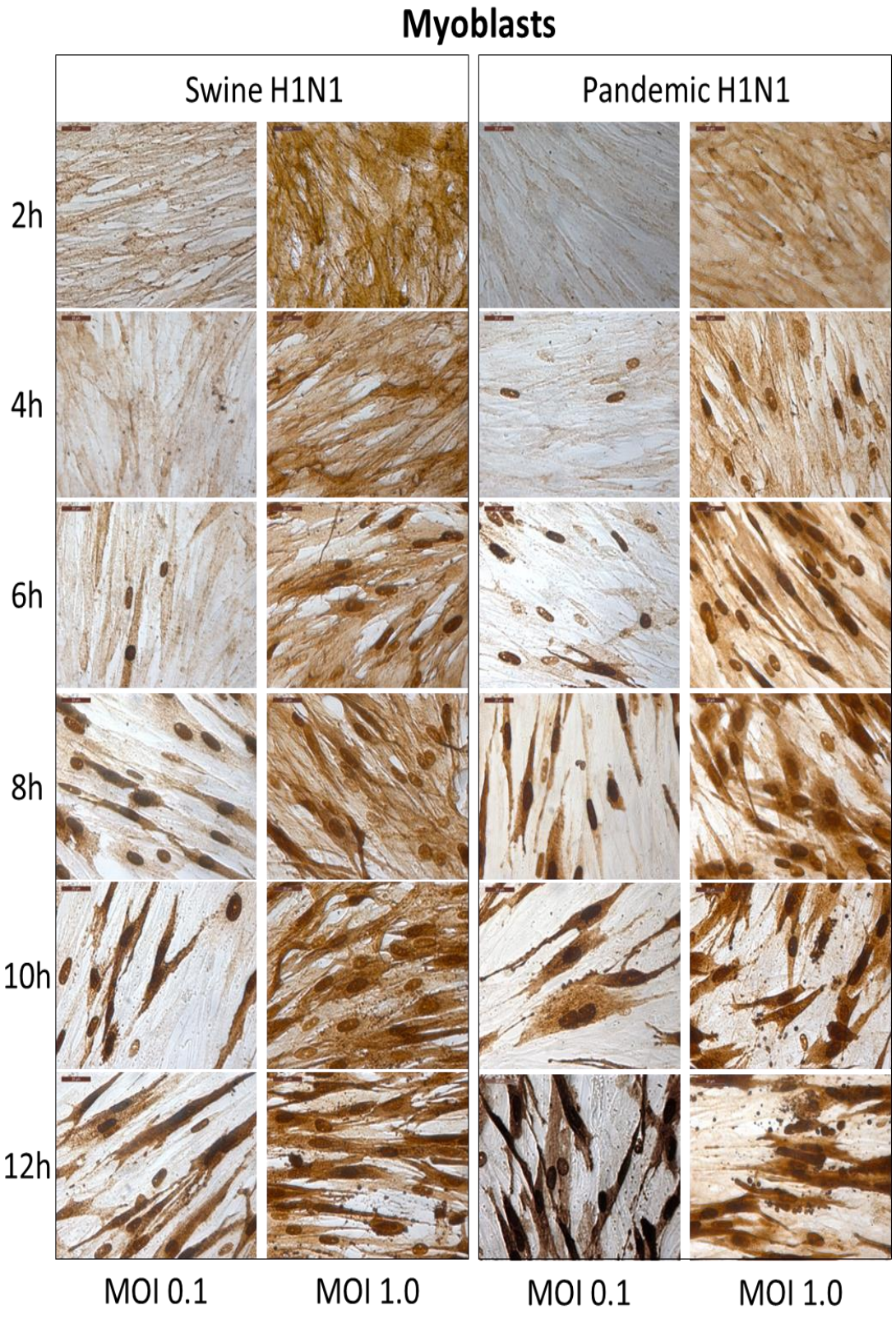

Figure 5.2 Pig myoblasts infected with pandemic H1N1 virus and swine H1N1 viruses accumulated viral NP in a time dependent manner

Myoblasts infected with swine H1N1 virus (left panel) and pandemic H1N1 virus (right panel) showed detectable viral NP expression at 6h and 4 hpi respectively. For

both viruses there was progressive accumulation of NP from initial nuclear detection to both nuclear and cytoplasmic accumulation at later time points.

5.2.3 Time dependent increase of viral NP expression in pig myotubes infected with pandemic H1N1 and swine H1N1 viruses

With pandemic H1N1 virus at 4 hpi, viral NP detection in myotubes was much weaker than corresponding myoblasts (Figure. 5.3). Like infected myoblasts, there was little visible cytopathic damage in myotubes at 12 hpi with either virus.

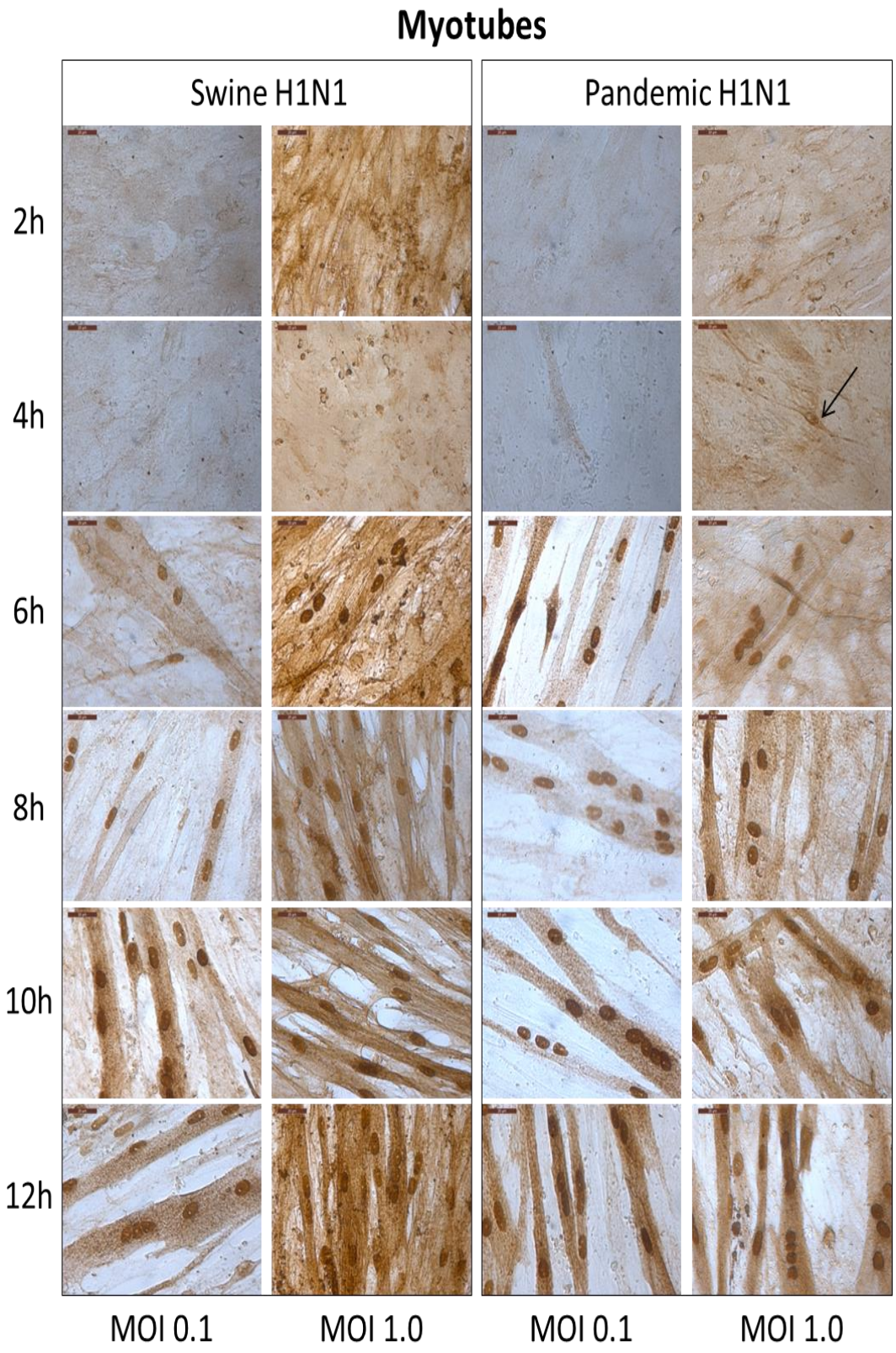

Figure 5.3 Pig myotubes infected with pandemic H1N1 or swine H1N1 virus accumulated viral NP in a time dependent manner

Myotubes infected with either virus showed clear nuclear NP detection from 6 hours of infection. Myotubes infected with pandemic H1N1 virus (right panel) showed weak detectable NP expression (arrow) from 4 hpi.

5.2.4 Higher influenza virus output from pig myoblasts than myotubes

Pig myoblast and myotubes were infected with MOI of 0.1 and 1.0 of swine H1N1 virus or pandemic H1N1 virus. Progeny virus output was determined as the amount of infective virus (as foci forming units [ffu] in MDCK cells) produced at 10, 20 and 30 hours of infection. At most time points for both viruses, myoblasts produced statistically more infective progeny virus than myotubes (Figure 5.4). Furthermore, at 1.0 MOI, swine H1N1 virus generated more progeny virus than pandemic H1N1 virus from both myoblasts and myotubes.

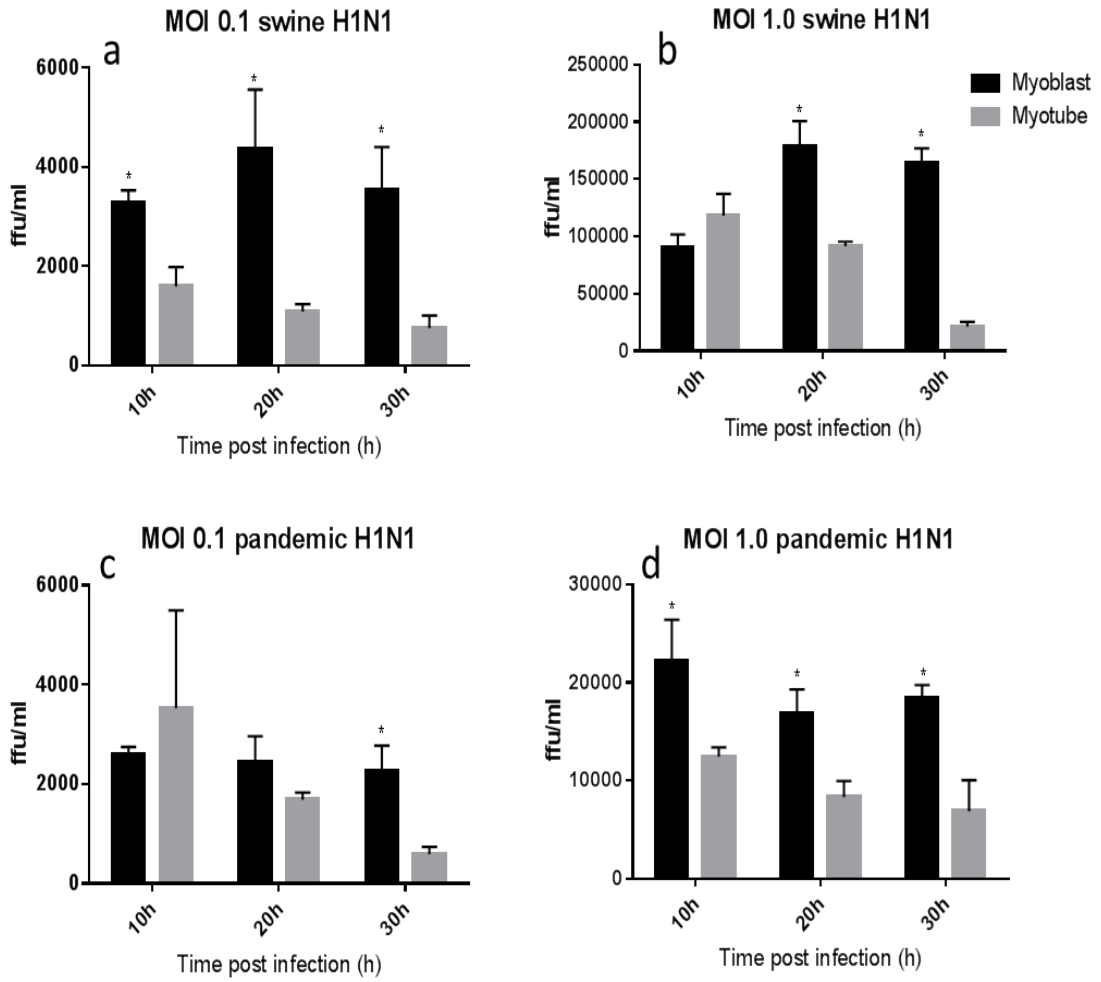

Figure 5.4 Infected pig myoblasts released more infective virus than corresponding myotubes

Pig muscle cells (myoblasts and myotubes) were infected with swine or pandemic H1N1 virus at 0.1 and 1.0 MOI over 30h. At most infection time points for either virus, more infective progeny virus was produced from myoblasts than myotubes. Virus output was determined as ffu/ml of infected supernatants. * indicates significant p-value ≤ 0.05 based on unpaired t test between myoblasts and myotubes. ffu = foci forming units.

5.2.5 Extended infection with swine H1N1 and pandemic H1N1 viruses results in greater cytopathic damage in myoblasts than myotubes

When pig muscle cells were infected over 20 or 30h with swine H1N1 and pandemic H1N1, more cytopathic damage was observed in myoblasts than myotubes with the same virus dose. Cytopathic damage of myoblasts found included gross structural fragmentation and formation cytoplasmic vacuoles (Figure 5.5). By 30 hpi, only few seemingly viable adherent cells remained. Infected myotubes showed little cytopathic damage or effect (CPE) at 20 hpi. By 30 hpi, only swine H1N1 virus caused some CPE in myotubes; pandemic H1N1 virus infected myotubes at 30 hpi showed no evidence of CPE (Figure 5.5 a'-d'). Taken together, both pig myoblasts and myotubes are susceptible and permissive to influenza virus infection. Myoblasts appear more prone to developing CPE from influenza virus infection than myotubes.

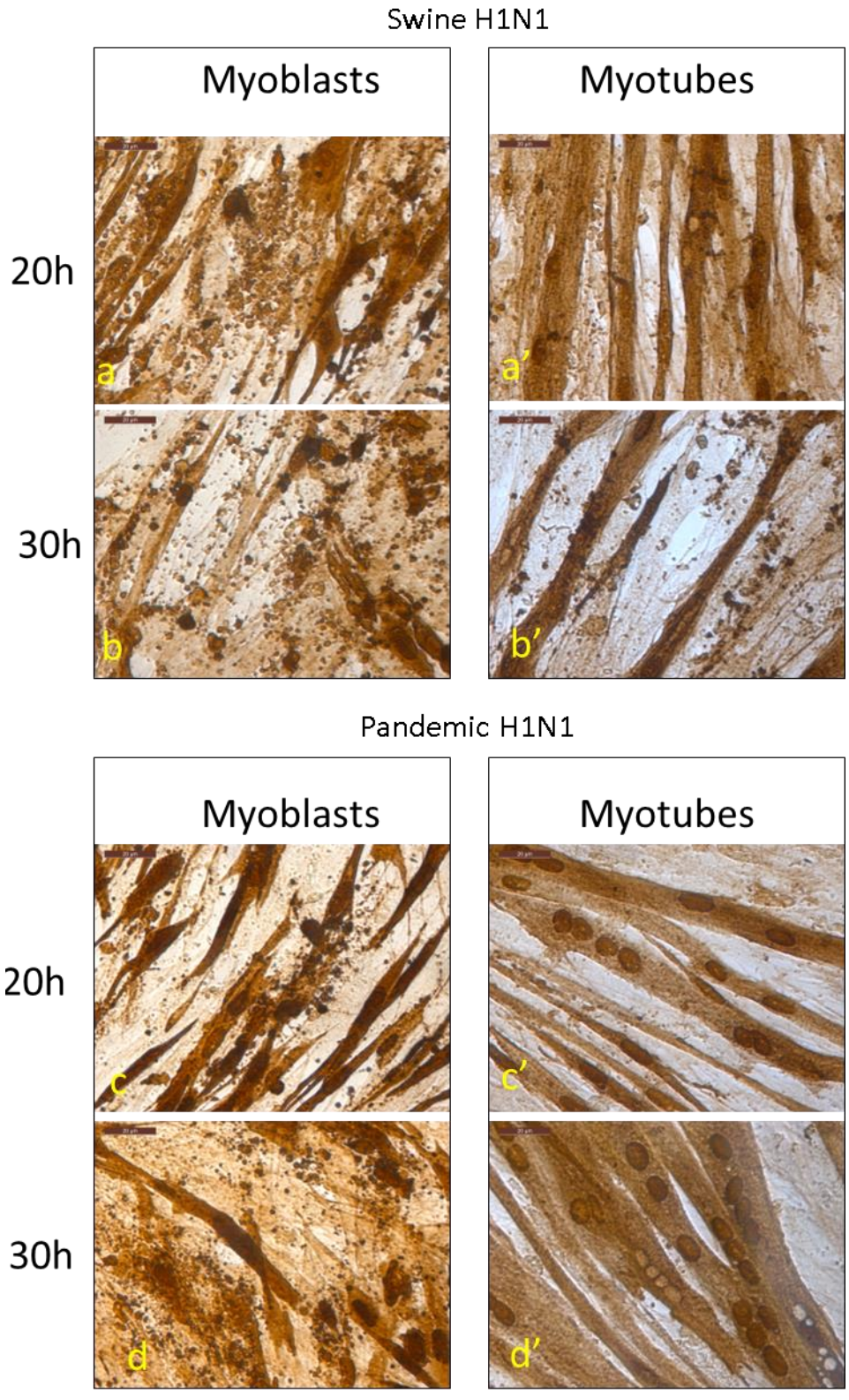

Figure 5.5 Extended infection of pig myotubes with swine H1N1 and pandemic H1N1 influenza viruses produced less cytopathic damage than corresponding myoblasts

Extended 20 to 30h infection of myoblasts and myotubes with 1.0 MOI of swine H1N1 virus and pandemic H1N1 virus caused more CPE in myoblasts than myotubes Top panels of myoblasts (a and b) and myotubes (a' and b') were infected with swine H1N1 at MOI 1.0. By 20 hpi, there was extensive and progressive myoblast destruction (a and b). Less CPE were evident with swine H1N1 virus infected myotubes (a' and b'). Bottom panels of pandemic H1N1 virus infection in myoblasts (c and d) and myotubes (c' and d') showed greater CPE in myoblasts than myotubes at 20 and 30 hpi. CPE in pandemic virus infected myotubes were relatively mild. Overall, swine H1N1 virus produced more severe CPE in myoblasts and myotubes than pandemic H1N1 virus. All panels were immunostained for viral NP protein (brown colour).

5.2.6 Influenza virus activates caspase 3/7 in pig myoblasts and myotubes

To evaluate the ability of pig muscle cells to respond to the influenza virus infection through apoptosis, a commercially available luciferase based caspase 3/7 activation kit was used. The activated caspase 3/7 present inside the cells upon influenza virus infection will cleave the substrate which is present in the reagent into an active form which will react to the luciferase provided in the buffer into light (Anon 2015). Pig myoblasts showed an increased caspase 3/7 activity upon infection with swine or pandemic H1N1 at MOI of 0.1 and 1.0 (Figure 5.6 a-d). The increase in caspase activity after infection was statistically significant with a p value less than or equal to 0.5 when an unpaired t test was carried out. Similarly myotubes also showed increased caspase 3/7 activation upon infection with the similar influenza viruses (Figure 5.6 e-h). Statistical significance of the difference between uninfected control and the myotubes infected with influenza virus was tested using unpaired t-test and the $p \leq 0.05$

is indicated with an asterisk. It is notable that at 10 hours of infection, caspase3/7 activity falls below the uninfected sample values for all samples other than the myoblast and myotubes infected with MOI of 1.0 with swine H1N1 (Figure 5.6. b&f).

Myoblasts

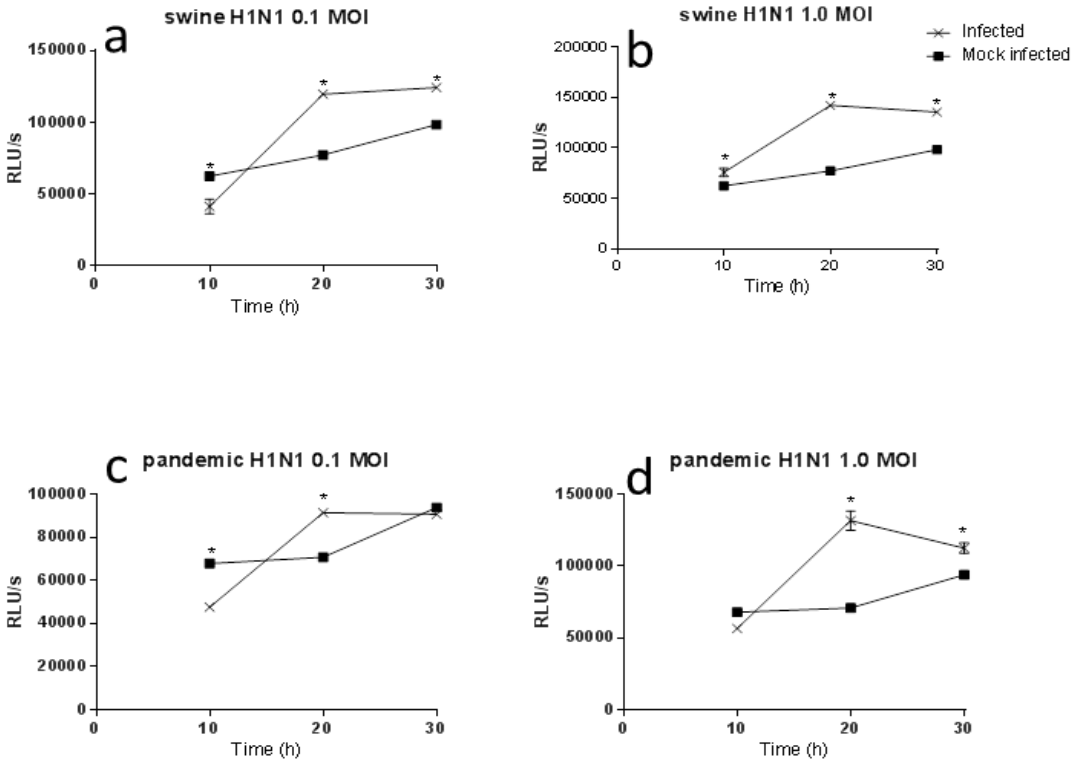

Myotubes

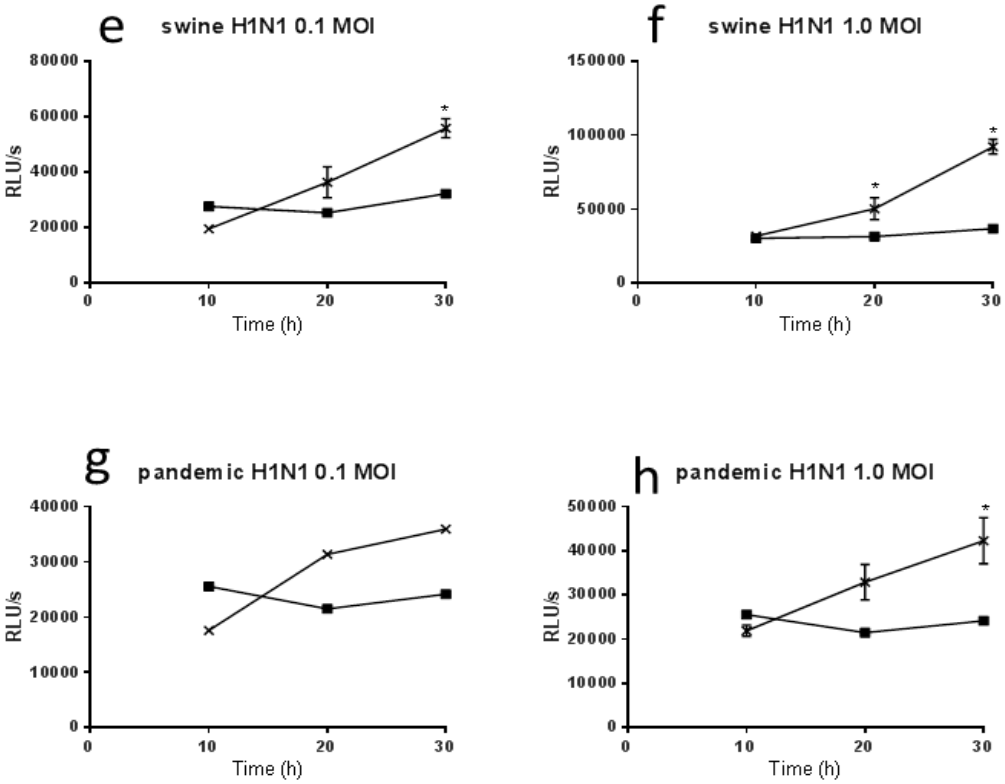

Figure 5.6 Influenza virus infected pig muscle cells displayed elevated caspase 3/7 activity

Pig myoblasts infected with swine H1N virus (a and b) or pandemic H1N1 virus (c and d) at MOI of 0.1 and 1.0 resulted in elevated caspase 3/7 activation by 20 and 30 hours of infection. Likewise, infection of myotubes with swine H1N1 virus (e and f) or pandemic H1N1 virus (g and h) at MOI of 0.1 and 1.0 resulted in elevated caspase 3/7 activation by 20 and 30 hours of infection. Asterisk indicates p value less than or equal to 0.05 of an unpaired t test.

5.2.7 Ractopamine pre-treatment of myoblasts and myotubes does not affect the pandemic H1N1 virus production

Ractopamine is used to increase the lean mass ration in pigs prior to slaughter (S. B. Smith et al. 1989; Gonzalez et al. 2007; Stites et al. 1991). The usage of ractopamine is not legal across the world but countries such as the U.S.A support its usage. Enhancement of growth and disease resistance are particularly desirable in food animal production.

Examination of SILAC based protein profiles and global gene expression changes of the myotubes treated with 10^{-5} M ractopamine for 1 and 6 hours revealed that different innate immune related intracellular signalling pathways are affected. Ractopamine treated myotubes showed upregulation of a number of different antiviral proteins. These observations suggest that growth promoters could affect signalling pathways that lead to increased growth and improved innate immunity and it was assumed that the ractopamine treatment may induce possible anti influenza effect.

Pig myotubes were differentiated for 5 days and incubated with 1% charcoal stripped FCS containing DMEM differentiation media for 24 hours before ractopamine

treatment. Myotubes were thence treated with ractopamine (10^{-5} M for 6 hours) in the same charcoal stripped FCS containing media. Then the myotubes were infected with influenza virus using the infection media without the presence of ractopamine for the initial 2 hours of infection or the virus attachment stage. Subsequently the myotubes were provided with fresh infection media supplemented with ractopamine. Progeny virus production from the resultant myotubes was assessed. Myoblasts cells had undergone the similar treatment except the initial differentiation step, instead they were used for the experiment after 48 hours of seeding and when the cells were about 80-90% confluent.

Pre-treatment of myoblasts or myotubes with ractopamine for 6h had no significant effect on progeny virus production over 36h of infection (Figure. 5.7.a)

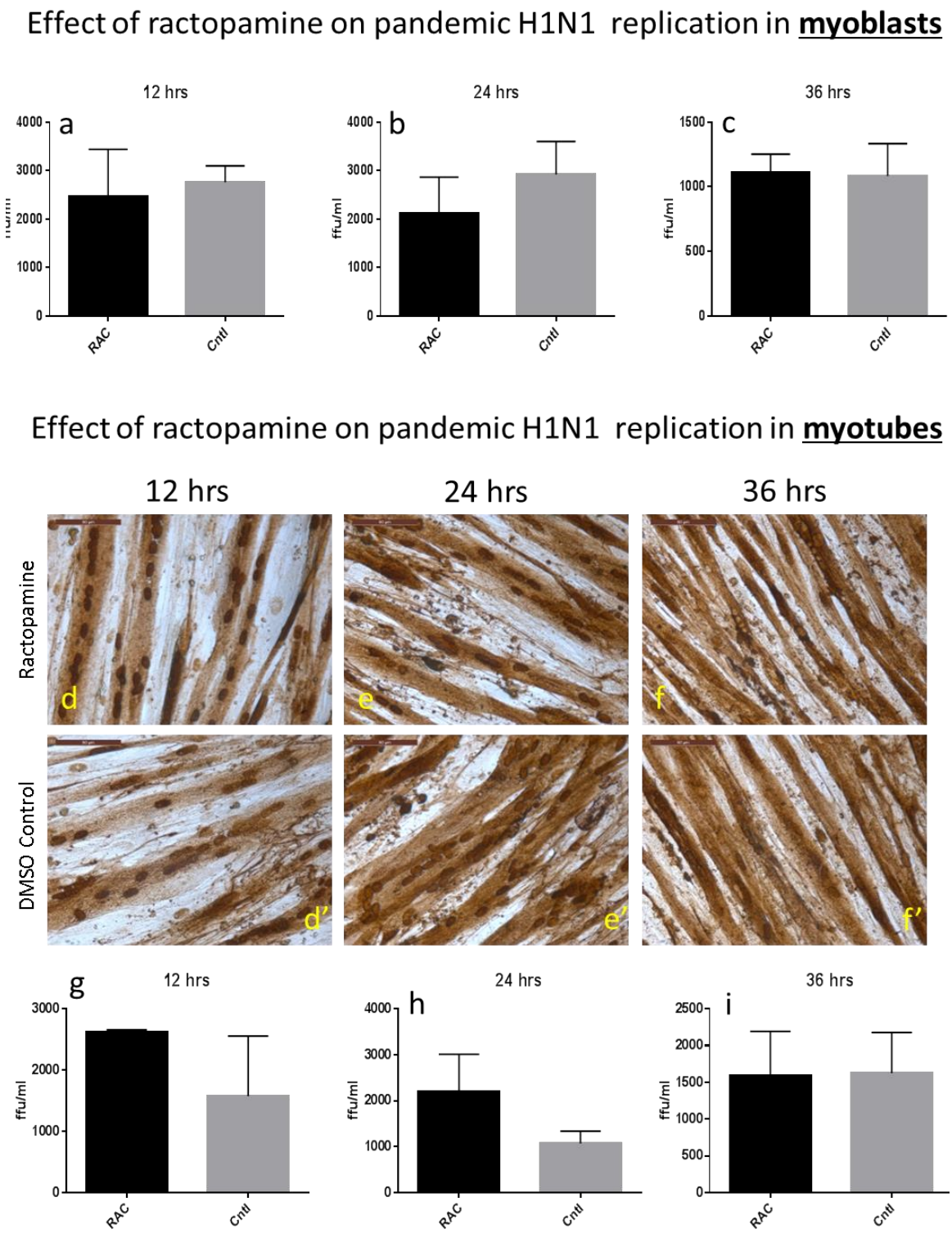

Figure 5.7 Ractopamine pre-treatment did not affect the subsequent production of pandemic H1N1 virus in pig myoblasts and myotubes

(a-c) Pig myoblasts pre-treated with ractopamine for 6 hours were infected with pandemic H1N1 virus at MOI of 0.1 over 36h to determine virus release, ractopamine was not used during initial two hours of infection. Similar to the progeny virus release from myoblast , viral NP immunodetection in myotubes showed no apparent difference

in staining intensity between ractopamine pre-treated and corresponding untreated controls over 36 of infection at 0.1 MO(d-f and d'-f-) I. There was no significant difference in progeny virus release over 36 of infection at 0.1 MOI from ractopamine treated and untreated control myotubes (g-i). ffu = foci forming units.

5.2.8 Growth promoter ractopamine treatment of pig muscle and epithelial cells prior to influenza virus infection does not reduce progeny virus production

Ractopamine treatment of myoblasts and myotubes was conducted in a similar manner as explained in the previous section (Figure 5.7). PTECs were cultured BEGM cell culture media and infected in the same media supplemented with 250 ng/ml TPCK trypsin. NPTr cells were treated in the same manner to muscle cells, primary PTECs and NPTr cells were used to examine the effect of ractopamine treatment on influenza replication. Ractopamine treated PTECs, for a duration of 6h, did not have any effect on avian H2N3 virus production at 12 and 18 hours of infection (Figure 5.8. a). Ractopamine treatment of NPTr cells resulted in a significant increase in progeny virus production at 18h of infection (Figure 5.8. b). Ractopamine treatment of myoblasts for 6h also had no effect on subsequent progeny H2N3 virus release (Figure 5.8. c). Pig myotubes (differentiated for 6 days) were treated with ractopamine for 6h or 20 hours prior to influenza virus infections. Twenty hour ractopamine treated myotubes followed by infection with swine H1N1 virus at MOI of 0.5, had no effect on virus production; however infection with avian H2N3 virus at 1.0 MOI of ractopamine treated myotubes produced significantly more progeny virus (Figure 5.8. d and f). Six hour ractopamine treatment of myotubes followed by infection with H2N3 virus at MOI of 1.0 caused no significant difference in virus production (Figure 5.8.e).

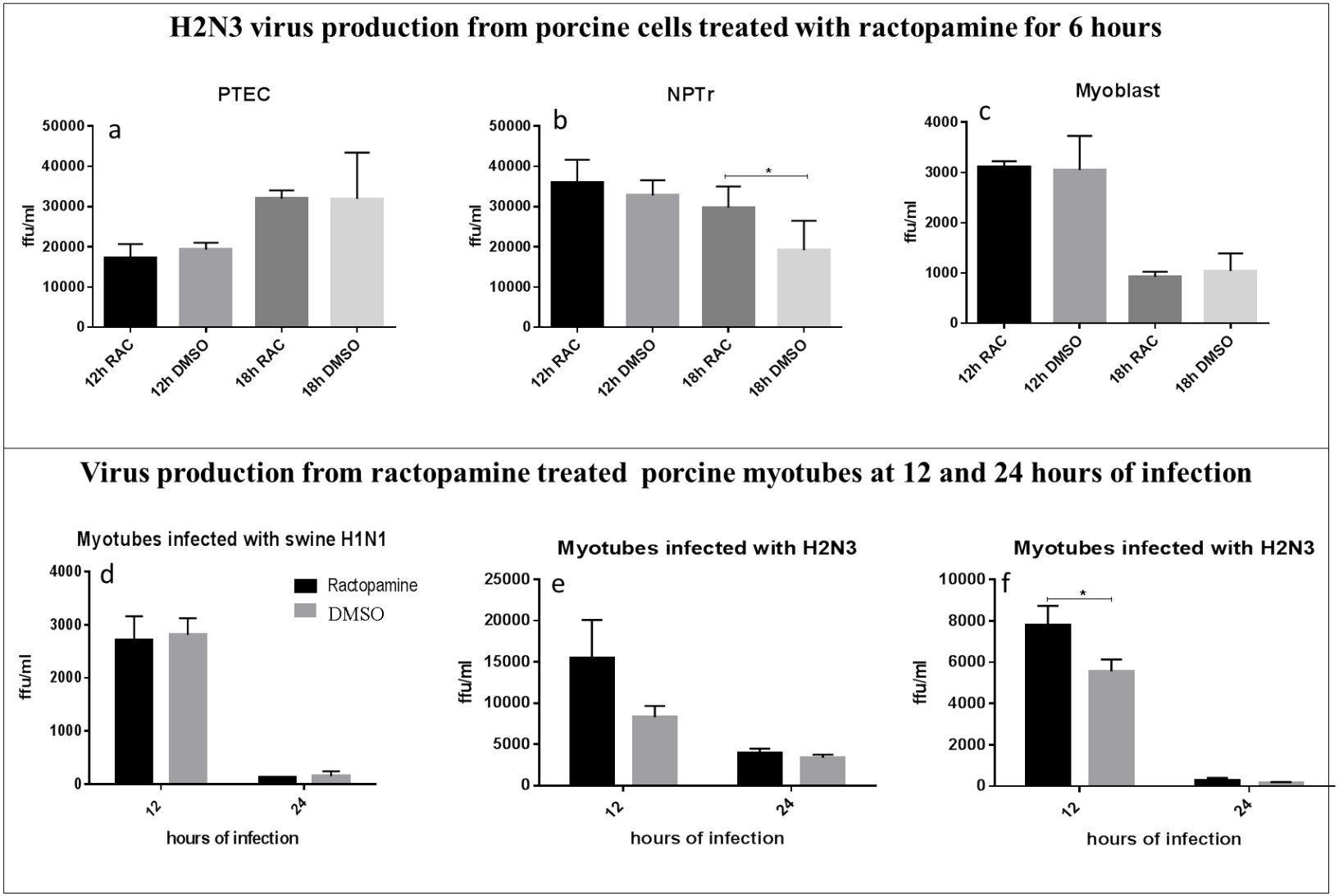
H2N3 virus production from porcine cells treated with ractopamine for 6 hours
PTEC
a
ffu/ml
50000
40000
30000
20000
10000
0
12h RAC
12h DMSO
18h RAC
18h DMSO
NPTr
b
*
Myoblast
c
4000
3000
2000
1000
Virus production from ractopamine treated porcine myotubes at 12 and 24 hours of infection
Myotubes infected with swine H1N1
d
Ractopamine
DMSO
hours of infection
Myotubes infected with H2N3
e
25000
15000
5000
Myotubes infected with H2N3
f
10000
8000
6000
12
24

Figure 5.8 Ractopamine treatment of pig myotubes and NPTr cells led to increased H2N3 virus production

Cells were treated with 10^{-5} M ractopamine and equal volume of DMSO was used as a vehicle control for all the cell types used in this study. Ractopamine (10^{-5} M) treatment of PTECs had no effect on progeny virus release. PTECs treated with ractopamine at 10^{-5} M for 6h or with DMSO were infected with avian H2N3 virus at 2.0 MOI for 12 and 18h. (b) NPTr cells were similarly treated with ractopamine and infected with H2N3 virus at MOI of 0.5. At 18h pi, significantly more viable virus was released relative to DMSO treated control. Likewise, ractopamine treated myoblasts (0.5 MOI) did not show any difference in (c) H2N3 virus progeny release. 7d differentiated myotubes treated with ractopamine for 20 hours (d) prior to swine H1N1 virus (0.5 MOI) infection did not result in a significant difference in virus progeny release when compared with its corresponding DMSO controls. (e) Myotubes treated with ractopamine for 6 hours prior to infection and infected with H2N3 virus at 0.5 MOI had no significant effect on virus output relative to DMSO treated control. (f) Myotubes treated with ractopamine for 20 hours and infected with 0.5 MOI of H2N3 virus resulted in significantly increased virus production. Asterisk indicates p value less than or equal to 0.05 based on unpaired t tests. ffu = foci forming units.

5.2.9 IGF- 1 and testosterone do not affect influenza virus production in pig myoblasts and myotubes

Pig myoblasts (Figure 5.9 a-c) and myotubes (Figure 5.9 a'-c') were pre-treated with IGF-1 (10ng/ml) or testosterone (10^{-5} M) for 6 hours followed by infection with pandemic H1N1 virus at MOI of 0.1. IGF-1 and testosterone were withdrawn during the initial 2 hours of infection to allow the virus attachment but was re-introduced with the infection medium at the same concentration after rinsing off the unbound viruses the growth promoters were present afterwards until the supernatant was collected at 12, 24 and 36 hpi to quantify the viable virus particles released by the cells. For both myoblasts and myotubes, pre-treatment with IGF-1 or testosterone and subsequent

infection with pandemic H1N1 virus had no significant effect on the progeny production as determined by foci forming assays on MDCK cells.

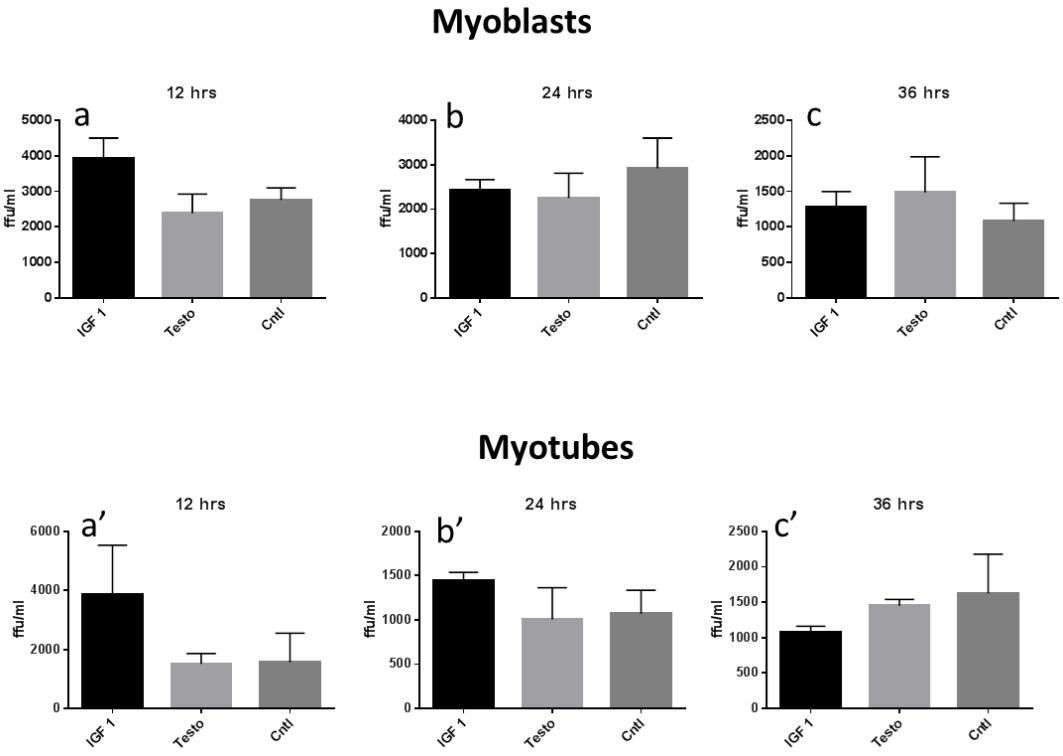

Figure 5.9 IGF-1 and testosterone did not affect pandemic H1N1 virus production from infected myoblasts and myotubes.

IGF-1 or testosterone treatment (10ng/ml of IGF-1 or 10^{-5} M testosterone for 6 hours) did not affect the production of pandemic H1N1 virus from myoblasts (a-c) and myotubes (a'-c') infected at 0.1 MOI for 12, 24 and 36h of infection, compared with the vehicle only treated controls (10mM HCl + ethanol). ffu = foci forming units.

5.2.10 Ractopamine pre-treatment does not affect innate immune gene expression in myoblast or myotubes

Twenty hour ractopamine pre-treatment was shown to increase avian H2N3 virus production from myotubes (Figure 5.8.f) but not in myoblasts. Myoblasts and myotubes were infected with pandemic H1N1virus and swine H1N1viruse at MOI of

1.0. Comparable levels of M gene expression were detected for both myoblast and myotubes infected with pandemic or swine H1N1 virus (Figure 5.10.a and b). No significant difference in M gene expression observed between ractopamine treated cells to the DMSO control treatment. There was no difference in TNF-α expression between ractopamine treated and untreated myoblasts or myotubes in response to swine and pandemic H1N1 viruses (Figure 5.10.c and d). It is still notable that myoblasts had a higher level of TNF-α expression compared with myotubes regardless of infection. *Mx-1* is an inhibitor protein of negative stranded RNA viruses like influenza A and is induced by type I and type III interferons (Broni et al. 1990). Myoblasts and myotubes pre-treated with ractopamine and infected with swine H1N1 virus (Figure 5.10.c) and pandemic H1N1 virus (Figure 5.10 d) expressed *Mx1* mRNA comparable to corresponding vehicle only treated controls (Figure 5.10.e and f).

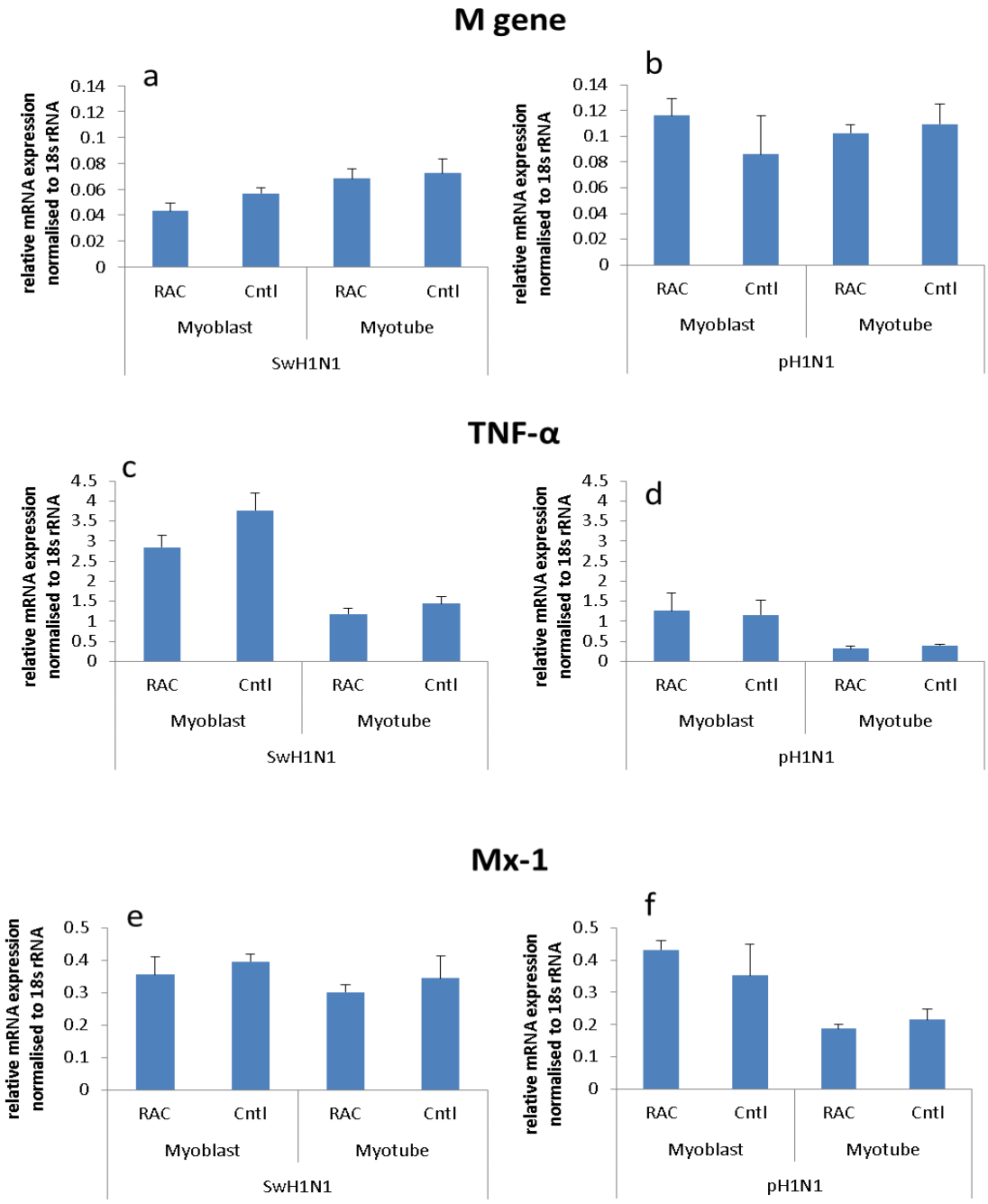

Figure 5.10 Ractopamine treatment did not affect innate immune gene expression or influenza M gene expression in myoblasts and myotubes infected with swine H1N1 or pandemic H1N1 virus

Myoblasts and myotubes pre-treated with ractopamine did not affect the M gene expression in comparison with vehicle only treated controls upon infection with swine H1N1 (a) or pandemic H1N1 (b) virus at 1.0 MOI. Myoblasts expressed higher basal levels of TNF-α than myotubes but no significant difference in expression was

observed between ractopamine treated and control samples. *Mx-1* expression in myoblasts and myotubes in response to infection was not affected by ractopamine pre-treatment (e and f). All expression values were normalised to 18S rRNA expression.

5.3 Discussion

This chapter aimed to establish porcine muscle cells as a suitable system to study the possible antiviral effects exerted by growth enhancers. Results confirm that porcine myoblasts and myotubes are susceptible to influenza virus infection and elicit a strong innate immune response against the infection. This study indicates that the growth enhancers such as ractopamine and IGF-1 may induce the replication of influenza virus in pig muscle cells.

Porcine muscle cells are susceptible and permissive to influenza A virus

Growth enhancers such as IGF-1, beta-adrenergic agonist ractopamine and testosterone(Basualto-Alarcón et al. 2014) contribute to growth (Laron 2001) and also to increase the protein to fat ratio in a farm animal production (Stoller et al. 2003). Although the underlying mechanisms of action of these factors are not fully understood, the potential to use them in growth promotion and disease resistance deserve utmost importance.

Since the RNA-seq and proteomics analyses predicted possible antiviral effect of these growth factors upon treating the porcine myotubes, the effects by of growth factor treatment on cell's innate immune ability was tested by using influenza virus infection as a model. Pigs serve as source of swine influenza which can cause human infections (Dowdle & Hattwick 1977). Influenza virus enters the host cell by binding to the sialic

acid receptors (SAα2,3-Gal and SAα2,6-Gal receptors) present on the cell surface, the virus bound on the membrane internalised by endocytosis (Chu & Whittaker 2004). Presence of these receptors is a critical factor for the entry of influenza virus into the cells(Suzuki et al. 2000). Previous research showed that the sialic acid receptors are present on several tissues including skeletal muscle of pigs (Nelli et al. 2010) but the in-vitro differentiated myotubes that were used in this study was not previously characterised for the expression of these receptors. Previous characterisation of the in-vitro myotubes confirmed that the myotubes express muscle proteins such as different myosin heavy chains which recapitulate adult muscle. Expression of SAα2,3-Gal and SAα2,6-Gal receptors on the cell surface of porcine myoblasts and myotubes were confirmed by sialic acid specific lectin staining. Since myotubes are expressed sialic acid receptors along with other muscle specific proteins, the choice of this cell type for this study was highly appropriate. Replication capacity of Low pathogenic avian influenza [LPAI] H2N3 was tested in porcine myotubes. Mammalian influenza viruses such as swine H1N1, human USSR H1N1 and pandemic H1N1 2009 successfully replicated in the myotubes (Figure 5.1 c-f).

Dynamics of influenza virus replication was analysed in porcine myoblast for swine H1N1 and pandemic H1N1. Detection of viral nucleoprotein by four hours of infection indicated that pandemic H1N1 can initiate the replication in porcine myoblasts cells faster than swine H1N1, which showed the viral NP detection only by 6 hours of infection (Figure 5.2). The time difference in viral NP detection between swine H1N1 and pandemic H1N1 was not very distinctive in the case of myotubes since viral NP was only detected by 6 hours of infection in myotubes. Expression of viral NP was detected by 6 hours of infection in human skeletal myotubes experimentally infected with influenza virus (Desdouits et al. 2013).

Influenza virus infection of porcine muscle cells produced infective virus particles in to the culture supernatant that were capable of infecting the MDCK cells. Number of infective virus particles present per millilitre of supernatant was calculated using focal forming unit measurements. The difference between porcine myoblasts and myotubes in their virus production capacity was very noticeable since myoblasts produced more virus particles than myotubes at almost every time point (10, 20 and 30 hours of infection) for both swine H1N1 and pandemic H1N1. Previous studies using chicken and duck muscle cells as an influenza virus target tissue, myotubes produced more virus progeny than myoblasts (Baquero-Perez et al. 2015). Similarly human skeletal myotubes produced more viral progeny than myoblasts (Desdouits et al. 2013).

One possible reason behind the reduced influenza virus replication in porcine myotubes than myoblasts may be the nuclear exclusion of viral NP observed in myotubes (Figure 5.5 and Figure 5.8). The myotubes used in this study was differentiated for seven days before the infection but in more mature myotubes, this nuclear exclusion phenomenon was more obvious since most of the nuclei were observed with almost no viral NP expression (data not shown). Since viral NP primarily localised in the cytosol, the replication efficiency may have been affected. This phenomenon was absent in myoblasts infected with influenza virus and also no similar effect was reported in any previous studies (Klavinskis et al. 1985; Cox et al. 1977) involving muscle cells infected with influenza virus.

Infection of porcine muscle cells with influenza virus resulted in an elevated host cell response by caspase 3/7 dependent apoptotic induction. Apoptosis happens in cells as a part of the homeostatic response to different injury stimuli or stress events such as infections, tissue damage and chemical stimuli. Cells undergoing apoptosis is characterised by the condensed cytoplasm and nuclear components in membrane

bound vesicles (Kerr et al. 1972). Sequential activation of a range of caspases is involved with the induction of apoptosis process. Caspases are proteolytic enzymes that reside in cells as inactive proenzymes. Upon activation of the apoptosis process these proenzymes get cleaved by other caspases or enzymes and become active. Caspase 7 is a downstream enzyme in the effector/execution phase of apoptosis and is cleaved to be activated by caspase 3 (Cohen 1997). Activated caspase 3/7 are the hallmarks of activated apoptosis. Skeletal muscle supports the apoptotic mechanism (Schwartz et al. 1993). Caspase 3 activation and increased apoptosis was observed in different muscular dystrophy condition (Sandri et al. 2001). Influenza virus infection caused apoptosis in cell cultures (Takizawa et al. 1996). Caspase 3 activation was observed in the cell infected with influenza virus followed by apoptosis (Takizawa et al. 1999).

Myoblasts showed an increased caspase activity than myotubes. A reduction in caspase3/7 activity was observed for pandemic H1N1 infection and also for the swine H1N1 at MOI of 0.1. When myotubes were infected with pandemic H1N1 or swine H1N1, a reduction in caspase 3/7 activity was observed except for the myotubes infected with swine H1N1 at MOI 1.0 (Figure 5.6 – f). This difference has correlated with the amount of virus replicated in the myotubes when infected with swine H1N1 at MOI of 1.0. As Figure 5.4.b indicates, myotubes infected with swine H1N1 at MOI of 1.0 resulted in a significantly greater number of virus output, where as myotubes or myoblasts infected with pandemic H1N1 at both MOI did not result in such an increase in virus output. Also swine H1N1 infected at MOI of 0.1 produced only significantly fewer viruses. Caspase activation was shown to facilitate influenza virus replication as the blockade of caspase 3 negatively affected the influenza A replication (Wurzer et al. 2003). Appropriately timed induction of apoptosis is required for the influenza

virus replication in cells (McLean et al. 2009). Bcl2- dependent Bax activation was required for apoptosis activation. Elevated level of caspase 3/7 activity was only observed in the myoblast infected with swine H1N1 at MOI of 1.0 at 10hpi. This activated caspase3/7 activity may account for the significantly higher levels of virus replication which was absent in lower MOI of swine H1N1 and also in the myoblasts or myotubes infected with pandemic H1N1.These results indicate that porcine muscle cells are suitable to use as a model system to study the replication of influenza virus and host innate immune responses.

Effect of growth factors in influenza virus replication in porcine muscle cells

This study utilised the porcine muscle cells as a model system to test the possible antiviral effects that can be attributed by the treatment of growth enhancers such as ractopamine, IGF-1 and testosterone.

Effect of ractopamine in influenza virus replication in pig cells

Since ractopamine treatment on myotubes predicted to induce possible antiviral effects, these effects were tested using an influenza virus infection model in porcine myotubes. Although skeletal muscle is the major target organ of ractopamine treatment, ractopamine residue accumulation or distribution was detected in other vital organs (Ho et al. 2014) even after several weeks of treatment (Pleadin et al. 2013). To take the tissue distribution of ractopamine into the consideration in a model system that uses influenza infection, skeletal muscle cells and tracheal epithelial cells, which is one of the most important targets of influenza virus infection was used in this study.

PTECs and NPTr cells were used in this study along with porcine myotubes. Experimental influenza infection in trachea was capable of spreading the virus particles to several other tissues upon infection with LPAI and HPAI (Mo et al.)

Ractopamine treatment did not elicit any significant effect on influenza virus replication in pig myoblasts and PTECs but NPTr cells showed increased permissiveness to influenza virus infection when the cells were pre-treated with ractopamine (Fig 5.2.7 a&b). Ractopamine is known to affect the gut microbial population in sheep(Thomas S Edrington et al. 2006) and increased the shedding of salmonella that was ingested experimentally salmonella in cattle(T. S. Edrington et al. 2006). The exact mechanism of ractopamine's action in the sheep and cattle system is not known and it may be not suitable to compare the increased influenza virus replication observed in this study to the results obtained by the study of Edrington et al. as the invitro infection model lack a lot of host innate immune mechanism to counter act the infection.

H2N3 infection in ractopamine treated myotubes resulted in an increased influenza virus replication (Fig 5.2.7- e &f). Although no evidence exist to support this finding, ractopamine's effect on intra cellular signalling cascade may have a supportive role in influenza virus replication in myotubes. Pandemic H1N1 influenza virus infected myoblast did not show any significant difference in virus replication by ractopamine treatment. Similar to the H2N3 infected myotubes, pandemic H1N1 virus infected myotubes showed a slight increase in virus replication in a ractopamine dependent manner though this difference was not enough to make significance in statistical analysis.

IGF-1 treatment on porcine myoblast and myotubes resulted in an increased pandemic H1N1 replication. Testosterone did not significantly affect the influenza virus replication in both myoblast and myotubes.

Although the expression of influenza-A M gene was not significantly different between ractopamine treated to the control muscle cells, the gene expression confirms that the virus successfully replicated in these cells. A previous study showed that myotubes accumulates higher levels of M gene than myoblasts in avian cells (Baquero-Perez et al. 2015) but in this study using porcine muscle cells, no significant difference in M gene accumulation was observed between myoblasts and myotubes. Influenza-A infection induce the expression of different interferon inducible genes including TNF-α and anti-influenza gene *Mx-1* (Mo et al.). Swine H1N1 induced higher levels of TNF-α expression than pandemic H1N1 and myoblasts had a higher level of TNF-α expression compared to myotubes. Pandemic H1N1 was previously shown to induce the interferons to a less extend (Osterlund et al. 2010). Different influenza viruses induce interferon inducible genes in a diverse pattern (Deng et al. 2012; Mussá et al. 2013). Expression of TNF-α and anti-influenza gene *Mx-1* expression indicates that skeletal muscle cells respond to the influenza infection by interferon induced mechanism and can be used as valid model to study the effect of growth enhancers and influenza virus infection study.

Chapter 6

Discussion

Skeletal muscle as the largest soft tissue in mammals deserves prime importance in its role as an innate immune organ and supportive tissue for structural maintenance and movements. Due to its importance in disease resistance and as a source of protein for human consumption, improvement in the quality and quantity of skeletal muscle through safe production methods is of the utmost importance. Such methods contribute to global food security and animal welfare. This research work aimed to develop and characterise an *in vitro* skeletal muscle system to reduce animal use in research and to improve the convenience and throughput of research applications. Since small animal models such as the mouse might not accurately translate the research findings into the target species, namely the pig, this study utilised porcine skeletal muscle cells. Pigs are considered to be similar to humans as disease models (Meurens et al. 2012) due to their similar physiological tissue functions and organ size. The pig is also an economically important food production farm animal species.

The role of skeletal muscle in innate immunity has been established by several studies. Early studies to identify the role of exercise in disease resistance showed that exercise can enhance the immune status of individuals by affecting different interleukins (IL) such as IL-1 (Simon 1984) and the inflammatory protein calprotectin which is released by neutrophils (Fagerhol et al. 2005). Exercise dependent changes in leukocytes' redistribution, temporal surface protein expression and functions suggest that the physiological state of skeletal muscle contributes to the immune status of the body (Freidenreich & Volek 2012). IL-6 has been identified as a cytokine produced by muscle upon exercise and proteins and peptides of other cytokines have been shown to affect the biological functions of muscle and other organs (Pedersen & Febbraio 2005). The research undertaken by this work succeeded in the development and characterisation of a prolonged 2D porcine myotube culture that functionally

resembled adult muscle fibres, could be maintained for several weeks and the fibres retained the MyHC isoform of adult muscle. In order to overcome the initial technical problems of the myotubes' limited differentiation capacity and rapid detachment from the culture plates, a combination of enhanced ECM coating conditions, better proliferation and differentiation media with necessary supplements and an elaborate method was developed. ECM provided a suitable microenvironment for the survival and functional maintenance of muscle cells and the fusion and maintenance of myotubes requires ECM (Gattazzo et al. 2014; Melo et al. 1996). The flexibility of the culture's microenvironment is a necessary feature of the ECM to support the growth of muscle cells and other cell types (Trensz et al. 2015).

Most of the reported myotube culture studies used a single ECM component such as collagen. The presence of long and thin collagen fibres in the endomysium and perimysium of skeletal muscle (Hantaï et al. 1985; Foidart et al. 1981) probably make it an attractive ECM component to use for muscle cell culture. The presence of collagen type-1 provided an elastic substrate for the maintenance of the skeletal muscle cells (Weist et al. 2013). Comparison of the myoblast proliferation rate on different extra cellular matrices in human showed that collagen type-1 provided an adequate ECM environment for the myoblast proliferation (Foidart et al. 1981). In another study, collagen was used in combination with biodegradable scaffolds in an attempt to generate transplantable muscle as a three dimensional tissue (Thorrez et al. 2008). Collagen type -1 coated three dimensional sheets were used to culture mouse C2C12 myoblasts to differentiate into myotubes (Sharples et al. 2012). In advanced 3D microfluidic channel muscle differentiation models, collagen-type 1 was used as the ECM and gelation agent (Shimizu et al. 2015). Type 1 collagen matrices were also used to generate electrospun fibres to mimic native ultrastructure of the cardiac muscle

tissue for the tissue engineering purpose (Elamparithi et al. 2015). There is therefore some justification for the inclusion of collagen type 1 in ECM media for porcine myoblast culture and differentiation.

Although several ECM proteins have been used to enable muscle cell growth *in vitro*, a recent study showed that ECM extracted from de-cellularised muscle led to better cell adhesion, proliferation and migration compared with single ECM components such as collagen or fibronectin (Chaturvedi et al. 2015). The preparation of such de-cellularised ECM is not easily repeatable thus alternative ECM components that reflect natural ECM of muscle cells are highly desirable. MaxGel ECM is a proprietary composition of extra cellular matrix components such as collagens, laminin, fibronectin, tenascin, elastin and a number of proteoglycans and glycosaminoglycans. The basis for these components originates from studies on different muscle diseases such as Duchenne's muscular dystrophy, congenital muscular dystrophies and congenital myopathies which showed that fibronectin, laminin, type I, III and IV collagens, all components of the Maxgel ECM, are present in muscle tissues (Hantaï et al. 1985). Maxgel has been used in cell culture to provide a 3 dimensional environment to enhance the growth and attempt to mimic the cells' growth environment *in vivo*. Maxgel has been used as a surface coating agent in cell proliferation assays (He et al. 2013). For example, Maxgel ECM was used to differentiate neural crest-like cells from human embryonic stem cells (Křivánek et al. 2014). In other experiments, Maxgel was used to differentiate keratinocytes into epidermal cells(Maas-Szabowski et al. 2005).

Since Maxgel and Collagen type-1 have been used in several skeletal muscle culture studies, the current study tested the effect of a collagen type-1 combined with Maxgel ECM on porcine skeletal muscle growth. Although the exact combination and relative

concentration of each component of Maxgel is not known due to its proprietary formulation, it contains several essential ECM components and clearly has some benefits as described earlier. Since both Maxgel and collagen are known to form gel-like 3D structures at high concentration (Rhim et al. 2007), it may be assumed that the combination of Maxgel with collagen made a supportive bed of ECM which is strong and flexible enough to maintain the proliferation and differentiation of muscle cells.

The MC+ mix (Maxgel and collagen typeI mix dried into the cell culture well) contains several of the natural ECM components. Using this ECM, the myoblasts adhered, proliferated and differentiated into myotubes which maintained their function. This was particularly noticeable in the twitching myotubes, where a flexible but strong sheath likes ECM Structure maintained the myotubes in place, but simultaneously allowed twitching (Additional video file in attached CD). The MC+ coating method included drying the ECM onto the culture plate surface, which presumably formed a better matrix on the surface of each culture plate well. This in turn, allowed the enhanced differentiation and prolonged maintenance of porcine myotubes in culture.

In addition to the use of MC+ ECM, additional culture conditions included modifications to the proliferation and differentiation media and maintenance of cultures in lower oxygen concentrations (Redshaw & Loughna 2012). This optimisation allowed the maintenance of myoblasts and retention of their myogenic potential for many passages. This is a major technical breakthrough in porcine in vitro skeletal myotube culture because previous attempts to culture porcine myotubes have resulted in a rapid reduction in myogenic potential after passaging (Machida et al. 2004). The current study also succeeded in maintaining the formed myotubes for more than 70 days although routine cultures were conducted for approximately four weeks where other reported culture methods allowed the maintenance of intact myotubes in

culture for about one week. In comparison to the existing cell culture models, especially for pigs compared with other mammalian and avian species, previous studies on porcine myoblast cells showed their lower differentiation capacity (Baquero-Perez et al. 2012).Along with the prolonged maintenance, this method resulted in the formation of myotubes with visible actin-myosin striations, which are indicative of functional myotubes. The detection of sarcomeric proteins such as α-actin and MyHC slow and fast twitch isoforms further validated the resemblance of these porcine myotubes to the *in vivo* myotubes which show a similar phenotype (Lefaucheur et al. 1998).

Recent experiments showed that the selectively isolated population of porcine skeletal muscle-derived, multipotent $PW1^{pos}/Pax7^{neg}$ interstitial cells maintained their proliferation capacity for several passages without losing their differentiation capacity. However, the differentiated myotubes were only maintained for five days and the study did not address the MyHC expression profile to indicate the functional similarity to an *in vivo* muscle (Lewis et al. 2014). Other studies showed the maintenance of porcine myotubes for 9 days but with limited fusion capacity (Perruchot et al. 2012). Another porcine myotube culture model was developed to study the glucose uptake mechanism. However, in this model there was with limited differentiation and the myotubes were used at two or three days of differentiation (Che et al. 2013).

The expression of MyHC isoforms in mammalian skeletal muscle is considered to be a continuum of pure and hybrid fibres containing slow and fast twitch isoforms, which exist in a reversible manner (Staron & Pette 1993; Pette & Staron 2000). However, post-natal pig skeletal muscle is predominantly composed of fast twitch type MyHCs isoforms, especially MyHC 2b (Toniolo et al. 2004).

A recent study showed that the MyHC isoform expression is restricted to the phenotype which resembles the muscle of origin (Zhu et al. 2013). In contrast, the work described in this thesis shows that MyHC isoform expression is regulated temporally and dependent on external stimuli such as ECM coatings, and culture medium. Co-expression of the embryonic form of MyHC (neonatal) was detected in *in vitro* porcine myotube cultures along with slow and fast twitch MyHC isoforms (Barjot et al. 1995). Furthermore, at early time points of myoblast fusion up to five days, embryonic MyHC and perinatal MyHC were expressed at the highest levels rather than other MyHC isoforms. Expression of MyHC slow and embryonic forms of MyHCs were detected as highest at seven days of differentiation with negligible amount of fast MyHCs. When the myotubes got more mature, the pattern of MyHC expression changed and a predominant MyHC 2x and 2b expression was detected in myotubes maintained in DM1 and MyHC 2a predominant expression was detected in myotubes maintained in DM2. This distinction in MyHC expression indicates that the expression of MyHCs is controlled in a temporal and external factor dependent manner rather than the muscle of origin. Since this work only utilised pig LD muscle, further work is needed to compare myoblasts isolated from other porcine muscle types. Since the *in vitro* generated myotubes recapitulates the MyHC expression profile of adult in vivo myotubes these myotubes are comparable to functional adult myotubes.

The porcine muscle culture system developed in this study was used to evaluate the effect of growth promoters, especially the beta agonist Ract on growth enhancement and selected cytokines associated with innate immune response. (The cytokines were chosen as potential molecular mediators involved with antiviral effects as predicted by bioinformatics programmes).

These SILAC based high throughput quantitative proteomics and phospho-proteomics analyses showed an increase in fatty acid turnover and glycogen synthesis following Ract treatment. This indicates that the Ract treatment of differentiated myotubes resulted in metabolic changes where increased fatty acid turn over and glycogen synthesis can be considered as a sign of lipolysis and growth promotion (Havel et al. 1963). Ract is known to induce lipolysis and inhibit lipogenesis (Hausman et al. 1989). Thus Ract may induce the use of stored lipids for energy needs and conversion to proteins. This correlates with the known action of Ract in pigs *in vivo* where Ract treated animals increased their total lean weight with reduction in fat content (Adeola et al. 1992; Quinn et al. 2008). Treatment with ractopamine resulted in lipolysis which increased the fatty acid turnover (Peterla & Scanes 1990). It is also known that Ractopamine treatment of gilts which are fed a high dietary protein resulted in an increased protein content at the finishing stage (Dunshea et al. 1993). This increase in protein content was mainly observed for the initial two to three weeks of Ract supplementation (Sainz et al. 1993). Treatment of Ract on *in vitro* cultured cells showed that $10^{(-5)}$ and $10^{(-6)}$ M Ract supplemented in porcine muscle cells resulted in a significant increase in protein and MyHC proteins (Anderson et al. 1990). The increase in protein synthesis was detected by the incorporation of radiolabelled amino acids as well as the amount of MyHC protein detected. Ractopamine treatment was shown to increase the transcription of myosin light chain 1 and 3 (S. B. Smith et al. 1989).

Another significant effect of Ract treated porcine myotubes was the activation of innate immune proteins. Ingenuity Pathway Analysis (IPA) analysis showed that the presence of several proteins associated with the host innate immune system were positively correlated with antiviral function. Proteins including STAT1, STAT6, Mx1,

IFITM3, RIG-I, IFIT5 and ISG15 were found to be upregulated by Ract treatment of porcine myotubes. Mx-1 is a known antiviral protein (Cai et al. 2013) and the expression of this protein inhibits influenza virus in cultured cells (Verhelst et al. 2012; Grimm et al. 2007) . Increased expression of RIG-I also helps control virus replication in cells (Takeuchi & Akira 2008). RIG-I also acts as anti-influenza factor (Xu et al. 2015). Due to the observed induction of many innate immune factors at the level of proteins well as their prediction by bioinformatics, it was hypothesised that Ract treatment of porcine myotubes will induce an antiviral effect. Thus the effect of Ract on selected genes involved in innate immune responses following influenza virus infection of porcine myotubes was tested.

Virus infections in humans are known to cause different muscle related diseases (Richardson et al. 1992; Why et al. 1994). However, the role of muscle as a target tissue following viral infection is not generally considered. In some cases of hepatitis C virus (HCV) infection, virus was detected in human muscle fibres. In such cases myositis was observed in patients (Ito et al. 2005). Coxsackievirus B was detected in the heart cells of patients who died from myocarditis and dilated cardiomyopathy (Gaaloul et al. 2014). Other studies showed that injection of Coxcackievirus into animals to induce antibody production resulted in the dissemination of these viruses to heart muscles along with other tissues (Semkow & Wilczyński 1979). These studies indicate the potential importance of viral infection of muscle tissue as a target of virus infection which may be particularly important in meat producing species such as the pig.

Influenza-associated myositis (IAM) is a clinical sign observed in influenza A infections in humans (Agyeman et al. 2004). This condition leads to elevated levels of blood creatine phosphokinase (CPK) which drives acute renal failure. Influenza

infected patients are sometimes observed with muscle pain and weakness which is generally caused by this myositis and also rhabdomyolysis which leads to the elevated CPK in blood and results in acute renal failure (Ozawa et al. 2000; Bove et al.). These clinical signs can be fatal (Abe et al. 2006). Similar clinical symptoms are also observed in elderly patients upon influenza A infection (Yoshino et al. 2000).

Influenza A virus (H5N1) has been isolated from fresh and frozen duck meat which suggests that influenza virus can spread to infect muscle (Lu et al. 2003) (Harder et al. 2009). This virus was also capable of growing in muscles and brain from ducks along with the respiratory tract (Tumpey et al. 2002). Recently, viable influenza virus was recovered from a different muscle of an infected chicken (Ejaz et al. 2007). Influenza virus H10N7 was isolated from duck carcasses (Serena Beato et al. 2006).

Experimental infection of chickens with HPAI (H5N2) via the intranasal route resulted in a systemic infection and very high titres of virus were detected in breast muscle. Chickens fed with the infected chicken muscle led to death of those animals (Swayne & Beck 2005). These studies indicate the potential risk of influenza virus infection of skeletal muscle, which is not only the largest mass of soft tissue in mammals but commonly eaten by people. This in turn raises concern about the security of food supply in the event of a large scale influenza infection of food production animals and the possibility of influenza transmission to humans via food.

It was previously shown that cultured human muscle cells can be infected with influenza virus (Armstrong et al. 1978), which resulted in cytopathic changes and the expression of viral proteins on host cells. and experimentally influenza virus strains successfully infected human muscle cells *in vitro* and released virus particles into the culture medium (Servidei et al. 1987). It was notable that CPK was detected in the culture media from six hours after infection. Thus it may be extrapolated that the

myositis and rhabdomyolysis observed in influenza infected patients may be due to the effects which follow infection of their muscle cells.

Since influenza virus infection causes myositis and other muscle diseases and subsequent renal failure *in vivo* in humans and muscle cells can be infected with influenza virus *in vitro,* it is reasonable to study the effects of influenza virus infection on porcine myotubes, including the impact on selected innate immune response genes. [Influenza virus was detected in the myocardium of infected turkey birds (McKenzie et al. 1972). Patients with acute Myoglobinurea were detected with acute myositis and virus particles were detected in myofibres which indicates that the (Fukuyama et al. 1977) virus infection of myofibres causes such clinical complications. *In vitro* cultured myotubes of chicken supported productive replication of influenza virus in a comparable level to the kidney cells infected with virus (Cox et al. 1977).

The current study showed that the *in vitro* cultured porcine myoblast and myotubes express both SAα2, 3Gal receptors and SAα2, 6Gal receptors. It also showed that the porcine myotubes support influenza virus production as evidenced by the expression of influenza virus protein by four hours of infection. This study also showed that the porcine myoblasts released more progeny virus particles into the culture supernatant than porcine myotubes, although both cell types showed cytopathic effects. This indicates that the *in vitro* generated porcine muscle cells are fully permissive to infection with different influenza viruses. Porcine muscle cells got active innate immune mechanism to response to virus infection as seen in in vivo condition. Subsequently infected muscle cells had an elevated caspase 3/7 activity, which indicates that the cells were committed to apoptosis. This evidence suggests that porcine muscle cells cultured using the conditions described can be used as a system to study the effects of influenza virus infection *in vitro*.

Cultured human skeletal muscle cells were detected to support the infection of two strains of influenza (H3N2) virus (Klavinskis et al. 1985). Although a study using rat muscle cell cultures showed that the influenza virus infection was abortive, since the infection did not spread to other myotubes (Nevalainen et al. 2010), other studies showed that chicken and duck myotubes are highly susceptible to influenza virus infection (Baquero-Perez et al. 2015). Human muscle cells also were found to be permissive to influenza virus infection which leads to the leakage of muscle proteins into the culture medium along with infective virus production (Desdouits et al. 2013).

This work found that (bioinformatics prediction) muscle cells treated with growth promoter Ract induced the expression of different anti-viral, particularly anti-influenza virus proteins. Despite of the predicted induced antiviral protein expression, the results showed that Ract treatment did not reduce the influenza virus production in porcine myoblasts or myotubes. This study utilised only a defined concentration (10^{-5}M) of Ract for either 6 hours or 20 hours of treatment prior to the influenza virus infection. Since Ract is known to have varied growth/ metabolic performance rate on treated animals in a manner dependent on treatment time (Almeida et al. 2013) it may be an effective approach to try different Ract treatment duration before influenza virus infection.

Gene expression study of the porcine muscle cells treated with Ract for 10 hours prior to swine H1N1 and pandemic H1N1 infection had no noticeable change in the influenza M gene expression compared with the vehicle only treated controls. Similarly the anti-influenza virus gene Mx-1 expression was also unaltered by Ract treatment. It was also notable that following influenza infection, the gene expression of TNF-α was higher in myoblasts than myotubes, which mirrors the cytopathic effects in these cells.

Weaknesses of the study design include a single concentration of ractopamine and the MOI of 0.1 or 1.0 MOI and only TNF-α and Mx-1 expression were evaluated Thus in the future, it may be necessary to analyse other pro-inflammatory cytokines and antiviral genes to test the predicted antiviral effects of Ract on porcine muscle cells more thoroughly. It was also noted that virus production from infected myoblasts and more evidently from myotubes reduced with time. Myotubes infected with influenza virus for 36 hours had lower amounts of viral NP in the nucleus and a subsequent reduction in virus production. Prominent viral NP nuclear exclusion was observed in more mature myotubes differentiated for over 12 days (data not presented). By comparison with myoblasts, myotubes may have some innate viral clearance mechanism which was not detected in the current study. A previous study showed that injection of influenza B virus into mouse muscle *in vivo* resulted in acute muscle damage but not all myonuclei were positive for virus proteins. There was a subsequent reduction in virus titre in the infected muscle cells which may suggest that the viruses are inactivated over time which results in the reduction of progeny release (Davis & Kornfeld 2001).

Results presented in this thesis support the hypothesis by successfully developing an *in vitro* porcine muscle culture system which can be maintained in culture for prolonged duration with high rate of differentiation. The myotubes resembles MyHC gene expression of adult myofibres by maintaining phenotypic plasticity with capacity to switch the MyHC gene expression profile based on different media supplement. Expression of influenza virus SAα2, 3 and SAα2, 6 receptors and full permissiveness to influenza virus infection makes the developed muscle cells comparable to in vivo muscle cells. Furthermore, these muscle cells displayed innate immune responses to influenza virus infection by innate immune gene expression and induction of apoptosis

similar to in vivo muscle cells. The porcine muscle cell culture model developed here can be used as a tool in biomedical research to study the muscle biology and innate immune response.

Future perspectives

In the future, efforts should continue to optimise the culture conditions of porcine myoblasts and myotubes to improve their relevance to *in vivo* muscle cells further, as well as improving attachment and conditions for relevant functions. This may include defining the optimum combination of ECM components and their relative quantities and medium supplements. Analysis of the ultrastructural details of MC+ coating using scanning electron microscopy (SEM) or atomic force microscopy (AFM) will provide more insights into the ECM structural arrangement including the size of formed fibres and their arrangement.

Usage of MC+ method improved the proliferation and differentiation capacity of other cells especially HSMM but the formed myotubes detached from plate. It may be because of the presence of some unwanted ECM components in MC+ coating or due to the lack of some key adhesion molecules (McDaneld 2006) in the HSMM myotubes. Further characterisation of the protein or gene expression profiles of porcine myotubes during the early differentiation stages may provide information about the expression of key ECM and cell adhesion component which positively affect the attachment of myotubes to the plate or ECM coating.

The molecular mechanisms involved in the differentiation of porcine myoblasts into myotubes were not addressed in this study. It was observed that myoblasts differentiated better in medium containing UG compared with horse serum Future comparison of gene and protein expression profiles during the differentiation process

will help to identify any novel targets (in addition to myogenic regulatory factors(Muroya et al. 2005)) to improve the efficiency of differentiation.

References

Aas, V. et al., 2013. Are cultured human myotubes far from home? *Cell and tissue research*, 354(3), pp.671–82. Available at: http://www.ncbi.nlm.nih.gov/pubmed/23749200 [Accessed September 6, 2015].

Abdul-Hussein, S., van der Ven, P.F.M. & Tajsharghi, H., 2012. Expression profiles of muscle disease-associated genes and their isoforms during differentiation of cultured human skeletal muscle cells. *BMC musculoskeletal disorders*, 13(1), p.262. Available at: http://www.biomedcentral.com/1471-2474/13/262 [Accessed September 6, 2015].

Abe, M. et al., 2006. Clinical study of influenza-associated rhabdomyolysis with acute renal failure. *Clinical nephrology*, 66(3), pp.166–70. Available at: http://www.ncbi.nlm.nih.gov/pubmed/16995338 [Accessed September 20, 2015].

Adeola, O., McBride, B.W. & Young, L.G., 1992. Metabolic responses induced by isoproterenol in ractopamine-fed pigs. *The Journal of nutrition*, 122(6), pp.1280–6. Available at: http://www.ncbi.nlm.nih.gov/pubmed/1588445 [Accessed September 20, 2015].

Agbulut, O. et al., 2003. Myosin heavy chain isoforms in postnatal muscle development of mice. *Biology of the Cell*, 95(6), pp.399–406. Available at: http://www.sciencedirect.com/science/article/pii/S024849000300087X [Accessed June 18, 2015].

Aguayo, J. et al., 1994. [Effect of insulin-like growth factor I on HLA-DR antigen

expression in cultured human thyrocytes: a component of the autoimmune process?]. *Revista médica de Chile*, 122(3), pp.248–52. Available at: http://www.ncbi.nlm.nih.gov/pubmed/7809513 [Accessed April 15, 2015].

Agyeman, P. et al., 2004. Influenza-associated myositis in children. *Infection*, 32(4), pp.199–203. Available at: http://www.ncbi.nlm.nih.gov/pubmed/15293074 [Accessed September 20, 2015].

Akira, S., Uematsu, S. & Takeuchi, O., 2006. Pathogen recognition and innate immunity. *Cell*, 124(4), pp.783–801. Available at: http://www.ncbi.nlm.nih.gov/pubmed/16497588 [Accessed July 9, 2014].

Allen, D.L. & Leinwand, L.A., 2001. Postnatal myosin heavy chain isoform expression in normal mice and mice null for IIb or IId myosin heavy chains. *Developmental biology*, 229(2), pp.383–95. Available at: http://www.sciencedirect.com/science/article/pii/S0012160600999743 [Accessed July 31, 2015].

Almeida, V. V et al., 2013. Time-response relationship of ractopamine feeding on growth performance, plasma urea nitrogen concentration, and carcass traits of finishing pigs. *Journal of animal science*, 91(2), pp.811–8. Available at: http://www.ncbi.nlm.nih.gov/pubmed/23307848 [Accessed September 21, 2015].

Alvarez, J. et al., 2015. Association of the presence of influenza A virus and porcine reproductive and respiratory syndrome virus in sow farms with post-weaning mortality. *Preventive veterinary medicine*. Available at: http://www.ncbi.nlm.nih.gov/pubmed/26210012 [Accessed August 8, 2015].

Anderson, P.T. et al., 1990. Ractopamine increases total and myofibrillar protein

synthesis in cultured rat myotubes. *The Journal of nutrition*, 120(12), pp.1677–83. Available at: http://europepmc.org/abstract/med/1979808 [Accessed September 19, 2015].

Andersson, S. et al., 2004. Effects of egg yolk testosterone on growth and immunity in a precocial bird. *Journal of evolutionary biology*, 17(3), pp.501–5. Available at: http://www.ncbi.nlm.nih.gov/pubmed/15149393 [Accessed April 15, 2015].

Anon, 2015. Caspase-Glo® 3/7 Assay Protocol. Available at: https://www.promega.co.uk/resources/protocols/technical-bulletins/101/caspase-glo-37-assay-protocol/ [Accessed March 28, 2015].

Armand, O. et al., 1983. Origin of satellite cells in avian skeletal muscles. *Archives d'anatomie microscopique et de morphologie expérimentale*, 72(2), pp.163–81. Available at: http://www.ncbi.nlm.nih.gov/pubmed/6651304 [Accessed June 15, 2015].

Armstrong, C.L. et al., 1978. Susceptibility of human skeletal muscle culture to influenza virus infection. I. Cytopathology and immunofluorescence. *Journal of the neurological sciences*, 35(1), pp.43–57. Available at: http://www.ncbi.nlm.nih.gov/pubmed/624960 [Accessed March 4, 2015].

Balan, O. V, Miuge, N.S. & Ozerniuk, N.D., 2009. [Analysis of expression of heavy myosin chains during in vitro differentiation of satellite cells and myoblasts derived from rat skeletal muscles]. *Izvestiia Akademii nauk. Seriia biologicheskaia / Rossiĭskaia akademiia nauk*, (3), pp.261–8. Available at: http://www.ncbi.nlm.nih.gov/pubmed/19551967 [Accessed July 21, 2015].

Balthazart, J., Schumacher, M. & Malacarne, G., 1984. Relative potencies of testosterone and 5 alpha-dihydrotestosterone on crowing and cloacal gland

growth in the Japanese quail (Coturnix coturnix japonica). *The Journal of endocrinology*, 100(1), pp.19–23. Available at: http://www.ncbi.nlm.nih.gov/pubmed/6690644 [Accessed August 7, 2015].

Baquero-Perez, B. et al., 2012. A simplified but robust method for the isolation of avian and mammalian muscle satellite cells. *BMC cell biology*, 13(1), p.16. Available at: http://www.biomedcentral.com/1471-2121/13/16 [Accessed July 26, 2015].

Baquero-Perez, B. et al., 2015. Chicken and duck myotubes are highly susceptible and permissive to influenza virus infection. *Journal of virology*, 89(5), pp.2494–506. Available at: http://www.pubmedcentral.nih.gov/articlerender.fcgi?artid=4325732&tool=pmcentrez&rendertype=abstract [Accessed February 11, 2015].

Baqureo-Perez, B. et al., 2012. A simplified but robust method for the isolation of avian and mammalian muscle satellite cells. *BMC Cell Biol.*, 13, p.16.

Barjot, C. et al., 1995. Expression of myosin heavy chain and of myogenic regulatory factor genes in fast or slow rabbit muscle satellite cell cultures. *Journal of Muscle Research and Cell Motility*, 16(6), pp.619–628. Available at: http://link.springer.com/10.1007/BF00130243 [Accessed July 11, 2015].

Barros, R. de A., Okoshi, M.P. & Cicogna, A.C., 1999. Beta-adrenergic pathway in healthy and hypertrophied hearts. *Arquivos Brasileiros de Cardiologia*, 72(5), pp.649–656. Available at: http://www.scielo.br/scielo.php?script=sci_arttext&pid=S0066-782X1999000500012&lng=en&nrm=iso&tlng=es [Accessed August 20, 2015].

Basualto-Alarcón, C. et al., 2014. Sarcopenia and Androgens: A Link between

Pathology and Treatment. *Frontiers in endocrinology*, 5, p.217. Available at: http://www.pubmedcentral.nih.gov/articlerender.fcgi?artid=4270249&tool=pmcentrez&rendertype=abstract [Accessed April 6, 2015].

Basuno, E., Yusdja, Y. & Ilham, N., 2010. Socio-economic impacts of avian influenza outbreaks on small-scale producers in Indonesia. *Transboundary and emerging diseases*, 57(1-2), pp.7–10. Available at: http://www.ncbi.nlm.nih.gov/pubmed/20537092 [Accessed August 1, 2015].

Baum, L.G. & Paulson, J.C., 1990. Sialyloligosaccharides of the respiratory epithelium in the selection of human influenza virus receptor specificity. *Acta histochemica. Supplementband*, 40, pp.35–8.

Bayne, E.K., Anderson, M.J. & Fambrough, D.M., 1984. Extracellular matrix organization in developing muscle: correlation with acetylcholine receptor aggregates. *The Journal of cell biology*, 99(4 Pt 1), pp.1486–501. Available at: http://www.pubmedcentral.nih.gov/articlerender.fcgi?artid=2113317&tool=pmcentrez&rendertype=abstract [Accessed July 19, 2015].

Beauchamp, J.R. et al., 1992. Expression and function of heterotypic adhesion molecules during differentiation of human skeletal muscle in culture. *The American journal of pathology*, 140(2), pp.387–401. Available at: http://www.pubmedcentral.nih.gov/articlerender.fcgi?artid=1886444&tool=pmcentrez&rendertype=abstract [Accessed September 28, 2015].

Benders, A.A.G.M. et al., 1991. The biochemical and structural maturation of human skeletal muscle cells in culture: the effect of the serum substitute Ultroser G. *Exp.Cell Res.*, 195(2), pp.284–294.

Beutler, B. et al., 2007. Genetic analysis of resistance to viral infection. *Nature*

reviews. Immunology, 7(10), pp.753–66. Available at: http://www.ncbi.nlm.nih.gov/pubmed/17893693 [Accessed August 7, 2015].

Biressi, S. & Rando, T.A., 2010. Heterogeneity in the muscle satellite cell population. *Seminars in cell & developmental biology*, 21(8), pp.845–54. Available at: http://www.pubmedcentral.nih.gov/articlerender.fcgi?artid=2967620&tool=pmcentrez&rendertype=abstract [Accessed July 27, 2015].

Bischoff, R., 1986a. A satellite cell mitogen from crushed adult muscle. *Developmental biology*, 115(1), pp.140–7. Available at: http://www.ncbi.nlm.nih.gov/pubmed/3699242 [Accessed June 14, 2015].

Bischoff, R., 1990. Cell cycle commitment of rat muscle satellite cells. *The Journal of cell biology*, 111(1), pp.201–7. Available at: http://www.pubmedcentral.nih.gov/articlerender.fcgi?artid=2116175&tool=pmcentrez&rendertype=abstract [Accessed June 15, 2015].

Bischoff, R., 1986b. Proliferation of muscle satellite cells on intact myofibers in culture. *Developmental biology*, 115(1), pp.129–39. Available at: http://www.ncbi.nlm.nih.gov/pubmed/3516758 [Accessed June 8, 2015].

Bischoff, R., 1975. Regeneration of single skeletal muscle fibers in vitro. *The Anatomical record*, 182(2), pp.215–35. Available at: http://www.ncbi.nlm.nih.gov/pubmed/168794 [Accessed May 26, 2015].

Blaauw, B., Schiaffino, S. & Reggiani, C., 2013. Mechanisms modulating skeletal muscle phenotype. *Comprehensive Physiology*, 3(4), pp.1645–87. Available at: http://www.ncbi.nlm.nih.gov/pubmed/24265241 [Accessed August 31, 2015].

Blanton, J.R. et al., 1999. Isolation of two populations of myoblasts from porcine

skeletal muscle. *Muscle & nerve*, 22(1), pp.43–50. Available at: http://www.ncbi.nlm.nih.gov/pubmed/9883856 [Accessed July 21, 2015].

Bove, K.E. et al., Morphology of acute myopathy associated with influenza B infection. *Pediatric pathology / affiliated with the International Paediatric Pathology Association*, 1(1), pp.51–66. Available at: http://www.ncbi.nlm.nih.gov/pubmed/6687269 [Accessed March 4, 2015].

Bowman, W., 1840. On the Minute Structure and Movements of Voluntary Muscle. *Philosophical Transactions of the Royal Society of London*, 130(0), pp.457–501. Available at: http://rstl.royalsocietypublishing.org/content/130/457.citation [Accessed July 28, 2015].

Brandan, E. & Inestrosa, N.C., 1987. Isolation of the heparan sulfate proteoglycans from the extracellular matrix of rat skeletal muscle. *Journal of neurobiology*, 18(3), pp.271–82. Available at: http://www.ncbi.nlm.nih.gov/pubmed/2955079 [Accessed July 19, 2015].

Brenner, B. & Eisenberg, E., 1987. The mechanism of muscle contraction. Biochemical, mechanical, and structural approaches to elucidate cross-bridge action in muscle. *Basic research in cardiology*, 82 Suppl 2, pp.3–16. Available at: http://www.ncbi.nlm.nih.gov/pubmed/2959261 [Accessed July 18, 2015].

Broni, B. et al., 1990. Parental influenza virion nucleocapsids are efficiently transported into the nuclei of murine cells expressing the nuclear interferon-induced Mx protein. *Journal of virology*, 64(12), pp.6335–40. Available at: http://www.pubmedcentral.nih.gov/articlerender.fcgi?artid=248816&tool=pmcentrez&rendertype=abstract [Accessed March 24, 2015].

Brooke, M.H. & Kaiser, K.K., 1970. Muscle fiber types: how many and what kind?

Archives of neurology, 23(4), pp.369–79. Available at: http://www.ncbi.nlm.nih.gov/pubmed/4248905 [Accessed May 30, 2015].

Buckingham, M. & Rigby, P.W.J., 2014. Gene regulatory networks and transcriptional mechanisms that control myogenesis. *Developmental cell*, 28(3), pp.225–38. Available at: http://www.ncbi.nlm.nih.gov/pubmed/24525185 [Accessed May 3, 2015].

Buller, A.J., ECCLES, J.C. & ECCLES, R.M., 1960. Interactions between motoneurones and muscles in respect of the characteristic speeds of their responses. *The Journal of physiology*, 150, pp.417–39. Available at: http://www.pubmedcentral.nih.gov/articlerender.fcgi?artid=1363172&tool=pmcentrez&rendertype=abstract [Accessed July 31, 2015].

Busquets, S. et al., 2004. Anticachectic effects of formoterol: a drug for potential treatment of muscle wasting. *Cancer research*, 64(18), pp.6725–31. Available at: http://www.ncbi.nlm.nih.gov/pubmed/15374990 [Accessed August 18, 2015].

van Buul-Offers, S.C. & Kooijman, R., 1998. The role of growth hormone and insulin-like growth factors in the immune system. *Cellular and molecular life sciences : CMLS*, 54(10), pp.1083–94. Available at: http://www.ncbi.nlm.nih.gov/pubmed/9817987 [Accessed July 31, 2015].

Cai, K.J. et al., 2013. Expression of bovine Mx1 protein inhibits the replication of foot-and-mouth disease virus in BHK-21 cells. *Acta virologica*, 57(4), pp.429–34. Available at: http://www.ncbi.nlm.nih.gov/pubmed/24294956 [Accessed September 20, 2015].

Cain, J.A., Solis, N. & Cordwell, S.J., 2014. Beyond gene expression: the impact of

protein post-translational modifications in bacteria. *Journal of proteomics*, 97, pp.265–86. Available at: http://www.ncbi.nlm.nih.gov/pubmed/23994099 [Accessed July 23, 2015].

Caiozzo, V.J. et al., 1994. Effect of spaceflight on skeletal muscle: mechanical properties and myosin isoform content of a slow muscle. *Journal of applied physiology (Bethesda, Md. : 1985)*, 76(4), pp.1764–73. Available at: http://www.ncbi.nlm.nih.gov/pubmed/8045858 [Accessed July 29, 2015].

Caiozzo, V.J. et al., 1996. Microgravity-induced transformations of myosin isoforms and contractile properties of skeletal muscle. *Journal of applied physiology (Bethesda, Md. : 1985)*, 81(1), pp.123–32. Available at: http://www.ncbi.nlm.nih.gov/pubmed/8828654 [Accessed July 23, 2015].

Campbell, N.A. & Reece, J.B., 2002. *Biology, Volume 1*, Benjamin Cummings. Available at: https://books.google.co.uk/books/about/Biology.html?id=9pqXQgAACAAJ&pgis=1 [Accessed September 29, 2015].

Cao, W. et al., 2015. A newly emerged swine origin A(H3N2)v influenza virus dampens host antiviral immunity but induces potent inflammasome activation. *The Journal of infectious diseases*. Available at: http://www.ncbi.nlm.nih.gov/pubmed/26068782 [Accessed August 8, 2015].

Capers, C.R., 1960. Multinucleation of skeletal muscle in vitro. *The Journal of biophysical and biochemical cytology*, 7, pp.559–66. Available at: http://www.pubmedcentral.nih.gov/articlerender.fcgi?artid=2224832&tool=pmcentrez&rendertype=abstract [Accessed September 6, 2015].

Carlson, B.M., 1973. The regeneration of skeletal muscle. A review. *The American*

journal of anatomy, 137(2), pp.119–49. Available at: http://www.ncbi.nlm.nih.gov/pubmed/4350147 [Accessed July 25, 2015].

Carlson, B.M. & Faulkner, J.A., 1983. The regeneration of skeletal muscle fibers following injury: a review. *Medicine and science in sports and exercise*, 15(3), pp.187–98. Available at: http://www.ncbi.nlm.nih.gov/pubmed/6353126 [Accessed July 25, 2015].

Castella, S. et al., 2015. Ilf3 and NF90 functions in RNA biology. *WIREs RNA*, 6, pp.243–256.

Centner, T.J., Alvey, J.C. & Stelzleni, A.M., 2014. Beta agonists in livestock feed: status, health concerns, and international trade. *Journal of animal science*, 92(9), pp.4234–40. Available at: http://www.ncbi.nlm.nih.gov/pubmed/25057027 [Accessed April 26, 2015].

Cerino, G. et al., 2015. Three dimensional multi-cellular muscle-like tissue engineering in perfusion-based bioreactors. *Biotechnology and bioengineering*. Available at: http://www.ncbi.nlm.nih.gov/pubmed/26126766 [Accessed September 6, 2015].

Chang, K.C., 2007. Key signalling factors and pathways in the molecular determination of skeletal muscle phenotype. , 1(05), pp.681–698. Available at: http://journals.cambridge.org/abstract_S1751731107702070 [Accessed July 31, 2015].

Chang, K.C. et al., 2003. Relationships of myosin heavy chain fibre types to meat quality traits in traditional and modern pigs. *Meat science*, 64(1), pp.93–103. Available at: http://www.ncbi.nlm.nih.gov/pubmed/22062667 [Accessed July 31, 2015].

Chang, K.C., Fernandes, K. & Dauncey, M.J., 1995. Molecular characterization of a developmentally regulated porcine skeletal myosin heavy chain gene and its 5' regulatory region. *Journal of cell science*, 108 (Pt 4, pp.1779–89. Available at: http://www.ncbi.nlm.nih.gov/pubmed/7615692 [Accessed September 6, 2015].

Chaturvedi, V. et al., 2015. Interactions between Skeletal Muscle Myoblasts and their Extracellular Matrix Revealed by a Serum Free Culture System. *PloS one*, 10(6), p.e0127675. Available at: http://www.pubmedcentral.nih.gov/articlerender.fcgi?artid=4450880&tool=pmcentrez&rendertype=abstract [Accessed July 23, 2015].

Che, B.N. et al., 2013. Phytanic acid stimulates glucose uptake in a model of skeletal muscles, the primary porcine myotubes. *Lipids in health and disease*, 12, p.14. Available at: http://www.pubmedcentral.nih.gov/articlerender.fcgi?artid=3606424&tool=pmcentrez&rendertype=abstract [Accessed September 6, 2015].

Chiakulas, J.J. & Pauly, J.E., 1965. A study of postnatal growth of skeletal muscle in the rat. *The Anatomical Record*, 152(1), pp.55–61. Available at: http://doi.wiley.com/10.1002/ar.1091520107 [Accessed July 27, 2015].

Chopra, A. et al., 2012. Reprogramming cardiomyocyte mechanosensing by crosstalk between integrins and hyaluronic acid receptors. *Journal of biomechanics*, 45(5), pp.824–31. Available at: http://www.pubmedcentral.nih.gov/articlerender.fcgi?artid=3386849&tool=pmcentrez&rendertype=abstract [Accessed September 6, 2015].

Chu, V.C. & Whittaker, G.R., 2004. Influenza virus entry and infection require host cell N-linked glycoprotein. *Proceedings of the National Academy of Sciences of*

the United States of America, 101(52), pp.18153–8. Available at: http://www.pnas.org/content/101/52/18153.full [Accessed April 18, 2015].

Church, J.C., 1970. Cell populations in skeletal muscle after regeneration. *Journal of embryology and experimental morphology*, 23(2), pp.531–7. Available at: http://www.ncbi.nlm.nih.gov/pubmed/5449488 [Accessed July 27, 2015].

Church, J.C.T., Noronha, R.F.X. & Allbrook, D.B., 1966. Satellite cells and skeletal muscle regeneration. *British Journal of Surgery*, 53(7), pp.638–642. Available at: http://doi.wiley.com/10.1002/bjs.1800530720 [Accessed May 27, 2015].

Cinnamon, Y., Kahane, N. & Kalcheim, C., 1999. Characterization of the early development of specific hypaxial muscles from the ventrolateral myotome. *Development (Cambridge, England)*, 126(19), pp.4305–15. Available at: http://www.ncbi.nlm.nih.gov/pubmed/10477298 [Accessed June 13, 2015].

Close, R., 1967. Properties of motor units in fast and slow skeletal muscles of the rat. *The Journal of physiology*, 193(1), pp.45–55. Available at: http://www.pubmedcentral.nih.gov/articlerender.fcgi?artid=1365581&tool=pmcentrez&rendertype=abstract [Accessed July 31, 2015].

Cohen, G.M., 1997. Caspases: the executioners of apoptosis. *The Biochemical journal*, 326 (Pt 1, pp.1–16. Available at: http://www.pubmedcentral.nih.gov/articlerender.fcgi?artid=1218630&tool=pmcentrez&rendertype=abstract [Accessed March 28, 2015].

Colbert, W.E., Williams, P.D. & Williams, G.D., 1991. Beta-adrenoceptor profile of ractopamine HCl in isolated smooth and cardiac muscle tissues of rat and guinea-pig. *The Journal of pharmacy and pharmacology*, 43(12), pp.844–7. Available at: http://www.ncbi.nlm.nih.gov/pubmed/1687583 [Accessed August

21, 2015].

da Costa, N. et al., 2002. Quantifying the temporospatial expression of postnatal porcine skeletal myosin heavy chain genes. *The journal of histochemistry and cytochemistry : official journal of the Histochemistry Society*, 50(3), pp.353–64. Available at: http://www.ncbi.nlm.nih.gov/pubmed/11850438 [Accessed September 6, 2015].

Cox, N.J., O'Neill, M.C. & Kendal, A.P., 1977. Replication of animal viruses in differentiating muscle cells: influenza virus A. *The Journal of general virology*, 37(1), pp.161–73. Available at: http://www.ncbi.nlm.nih.gov/pubmed/562389 [Accessed March 4, 2015].

D'Amico, A. et al., 2013. A new de novo missense mutation in MYH2 expands clinical and genetic findings in hereditary myosin myopathies. *Neuromuscular disorders : NMD*, 23(5), pp.437–40. Available at: http://www.pubmedcentral.nih.gov/articlerender.fcgi?artid=3639366&tool=pmcentrez&rendertype=abstract [Accessed September 6, 2015].

Davis, L.E. & Kornfeld, M., 2001. Experimental influenza B viral myositis. *Journal of the neurological sciences*, 187(1-2), pp.61–7. Available at: http://www.ncbi.nlm.nih.gov/pubmed/11440746 [Accessed March 4, 2015].

Demestre, M. et al., 2015. Formation and characterisation of neuromuscular junctions between hiPSC derived motoneurons and myotubes. *Stem cell research*, 15(2), pp.328–336. Available at: http://www.ncbi.nlm.nih.gov/pubmed/26255853 [Accessed September 6, 2015].

Deng, Y.-M. et al., 2012. Transmission of influenza A(H1N1) 2009 pandemic viruses in Australian swine. *Influenza and other respiratory viruses*, 6(3),

pp.e42–7. Available at: http://www.ncbi.nlm.nih.gov/pubmed/22336333 [Accessed March 22, 2015].

Depreux, F.F.S. et al., 2002. Paylean alters myosin heavy chain isoform content in pig muscle. *Journal of animal science*, 80(7), pp.1888–94. Available at: http://www.ncbi.nlm.nih.gov/pubmed/12162656 [Accessed August 21, 2015].

DeQuach, J.A. et al., 2010. Simple and high yielding method for preparing tissue specific extracellular matrix coatings for cell culture. *PloS one*, 5(9), p.e13039. Available at: http://www.pubmedcentral.nih.gov/articlerender.fcgi?artid=2946408&tool=pmcentrez&rendertype=abstract [Accessed July 19, 2015].

Desdouits, M. et al., 2013. Productive infection of human skeletal muscle cells by pandemic and seasonal influenza A(H1N1) viruses. *PloS one*, 8(11), p.e79628. Available at: http://www.pubmedcentral.nih.gov/articlerender.fcgi?artid=3818236&tool=pmcentrez&rendertype=abstract [Accessed March 4, 2015].

Devlin, R.B. & Emerson, C.P., 1978. Coordinate regulation of contractile protein synthesis during myoblast differentiation. *Cell*, 13(4), pp.599–611. Available at: http://www.ncbi.nlm.nih.gov/pubmed/657269 [Accessed June 15, 2015].

Dominguez, R. et al., 1998. Crystal Structure of a Vertebrate Smooth Muscle Myosin Motor Domain and Its Complex with the Essential Light Chain. *Cell*, 94(5), pp.559–571. Available at: http://www.sciencedirect.com/science/article/pii/S0092867400815986 [Accessed September 28, 2015].

Donoghue, P. et al., 2007. Proteomic profiling of chronic low-frequency stimulated

fast muscle. *Proteomics*, 7(18), pp.3417–30. Available at: http://www.ncbi.nlm.nih.gov/pubmed/17708595 [Accessed July 31, 2015].

Doumit, M.E. & Merkel, R.A., 1992. Conditions for isolation and culture of porcine myogenic satellite cells. *Tissue & cell*, 24(2), pp.253–62. Available at: http://www.ncbi.nlm.nih.gov/pubmed/1589873 [Accessed July 19, 2015].

Dowdle, W.R. & Hattwick, M.A., 1977. Swine influenza virus infections in humans. *The Journal of infectious diseases*, 136 Suppl, pp.S386–9. Available at: http://www.ncbi.nlm.nih.gov/pubmed/342616 [Accessed April 18, 2015].

Drexler, A. et al., 2013. Human IGF1 extends lifespan and enhances resistance to Plasmodium falciparum infection in the malaria vector Anopheles stephensi. *The Journal of experimental biology*, 216(Pt 2), pp.208–17. Available at: http://www.pubmedcentral.nih.gov/articlerender.fcgi?artid=3597202&tool=pmcentrez&rendertype=abstract [Accessed March 23, 2015].

Dunshea, F.R., King, R.H. & Campbell, R.G., 1993. Interrelationships between dietary protein and ractopamine on protein and lipid deposition in finishing gilts. *Journal of animal science*, 71(11), pp.2931–2941. Available at: https://dl.sciencesocieties.org/publications/jas/abstracts/71/11/2931 [Accessed September 19, 2015].

ECCLES, J.C., ECCLES, R.M. & LUNDBERG, A., 1958. The action potentials of the alpha motoneurones supplying fast and slow muscles. *The Journal of physiology*, 142(2), pp.275–91. Available at: http://www.pubmedcentral.nih.gov/articlerender.fcgi?artid=1356679&tool=pmcentrez&rendertype=abstract [Accessed July 31, 2015].

Ecob-Prince, M.S. et al., 1986. Neonatal and adult myosin heavy chain isoforms in a

nerve-muscle culture system. *The Journal of cell biology*, 103(3), pp.995–1005. Available at: http://www.pubmedcentral.nih.gov/articlerender.fcgi?artid=2114309&tool=pmcentrez&rendertype=abstract [Accessed July 31, 2015].

Edrington, T.S. et al., 2006. Effect of Ractopamine HCl Supplementation on Fecal Shedding of Escherichia coli O157:H7 and Salmonella in Feedlot Cattle. *Current Microbiology*, 53(4), pp.340–345. Available at: http://www.ncbi.nlm.nih.gov/pubmed/16972129 [Accessed March 10, 2015].

Edrington, T.S. et al., 2006. Effects of ractopamine HCl on Escherichia coli O157:H7 and Salmonella in vitro and on intestinal populations and fecal shedding in experimentally infected sheep and pigs. *Current microbiology*, 53(1), pp.82–8. Available at: http://www.ncbi.nlm.nih.gov/pubmed/16775793 [Accessed March 10, 2015].

Ejaz, R. et al., 2007. Chicken Meat as a Source of Avian Influenza Virus Persistence and Dissemination. *International Journal of Poultry Science*. Available at: http://agris.fao.org/agris-search/search.do?recordID=DJ2012052064 [Accessed September 20, 2015].

Elamparithi, A., Punnoose, A.M. & Kuruvilla, S., 2015. Electrospun type 1 collagen matrices preserving native ultrastructure using benign binary solvent for cardiac tissue engineering. *Artificial cells, nanomedicine, and biotechnology*, pp.1–8. Available at: http://www.ncbi.nlm.nih.gov/pubmed/25960178 [Accessed July 21, 2015].

Emmott, E. et al., 2010. Quantitative proteomics using SILAC coupled to LC-MS/MS reveals changes in the nucleolar proteome in influenza A virus-infected

cells. *Journal of Proteome Research*, 9, pp.5335–5345.

ENESCO, M. & PUDDY, D., 1964. INCREASE IN THE NUMBER OF NUCLEI AND WEIGHT IN SKELETAL MUSCLE OF RATS OF VARIOUS AGES. *The American journal of anatomy*, 114, pp.235–44. Available at: http://www.ncbi.nlm.nih.gov/pubmed/14131857 [Accessed May 6, 2015].

Errett, J.S. & Gale Jr, M., 2015. Emerging complexity and new roles for the RIG-I-like receptors in innate antiviral immunity. *Virologica Sinica*, 30(3), pp.163–173.

Fagerhol, M.K. et al., 2005. Increase in plasma calprotectin during long-distance running. *Scandinavian journal of clinical and laboratory investigation*, 65(3), pp.211–20. Available at: http://www.ncbi.nlm.nih.gov/pubmed/16095050 [Accessed September 18, 2015].

FAO, U.S.., 2012. FAO's Animal Production and Health Division: Meat & Meat Products. Available at: http://www.fao.org/ag/againfo/themes/en/meat/backgr_sources.html [Accessed September 29, 2015].

Feeley, E.M. et al., 2011. IFITM3 inhibits influenza A virus infection by preventing cytosolic entry. *PLoS Pathog*, 7(10), p.e1002337. Available at: http://dx.doi.org/10.1371%2Fjournal.ppat.1002337.

Ferrari, G., 1998. Muscle Regeneration by Bone Marrow-Derived Myogenic Progenitors. *Science*, 279(5356), pp.1528–1530. Available at: http://www.sciencemag.org/content/279/5356/1528.abstract [Accessed July 1, 2015].

Fitts, R.H. et al., 1980. Contractile, biochemical, and histochemical properties of

thyrotoxic rat soleus muscle. *The American journal of physiology*, 238(1), pp.C14–20. Available at: http://www.ncbi.nlm.nih.gov/pubmed/6444499 [Accessed July 29, 2015].

Fitts, R.H., Riley, D.R. & Widrick, J.J., 2001. Functional and structural adaptations of skeletal muscle to microgravity. *The Journal of experimental biology*, 204(Pt 18), pp.3201–8. Available at: http://www.ncbi.nlm.nih.gov/pubmed/11581335 [Accessed September 6, 2015].

Fitts, R.H. & Widrick, J.J., 1996. Muscle mechanics: adaptations with exercise-training. *Exercise and sport sciences reviews*, 24, pp.427–73. Available at: http://www.ncbi.nlm.nih.gov/pubmed/8744258 [Accessed July 28, 2015].

Foidart, M., Foidart, J.M. & Engel, W.K., 1981. Collagen localization in normal and fibrotic human skeletal muscle. *Archives of neurology*, 38(3), pp.152–7. Available at: http://www.ncbi.nlm.nih.gov/pubmed/7469848 [Accessed July 21, 2015].

Freidenreich, D.J. & Volek, J.S., 2012. Immune responses to resistance exercise. *Exercise immunology review*, 18, pp.8–41. Available at: http://www.ncbi.nlm.nih.gov/pubmed/22876721 [Accessed September 17, 2015].

Friedrich, B.M. et al., 2011. Striated acto-myosin fibers can reorganize and register in response to elastic interactions with the matrix. *Biophysical journal*, 100(11), pp.2706–15. Available at: http://www.pubmedcentral.nih.gov/articlerender.fcgi?artid=3117187&tool=pmcentrez&rendertype=abstract [Accessed September 28, 2015].

Frost, R.A. & Lang, C.H., 2012. Multifaceted role of insulin-like growth factors and

mammalian target of rapamycin in skeletal muscle. *Endocrinology and metabolism clinics of North America*, 41(2), pp.297–322, vi. Available at: http://www.pubmedcentral.nih.gov/articlerender.fcgi?artid=3376019&tool=pmcentrez&rendertype=abstract [Accessed April 15, 2015].

Fukuyama, Y., Ando, T. & Yokota, J., 1977. Acute fulminant myoglobinuric polymyositis with picornavirus-like crystals. *Journal of neurology, neurosurgery, and psychiatry*, 40(8), pp.775–81. Available at: http://www.pubmedcentral.nih.gov/articlerender.fcgi?artid=492834&tool=pmcentrez&rendertype=abstract [Accessed September 21, 2015].

Funk, W.D., Ouellette, M. & Wright, W.E., 1991. Molecular biology of myogenic regulatory factors. *Molecular biology & medicine*, 8(2), pp.185–95. Available at: http://www.ncbi.nlm.nih.gov/pubmed/1806761 [Accessed July 27, 2015].

Gaaloul, I. et al., 2014. Coxsackievirus B detection in cases of myocarditis, myopericarditis, pericarditis and dilated cardiomyopathy in hospitalized patients. *Molecular medicine reports*, 10(6), pp.2811–8. Available at: http://www.pubmedcentral.nih.gov/articlerender.fcgi?artid=4227425&tool=pmcentrez&rendertype=abstract [Accessed September 20, 2015].

Gattazzo, F., Urciuolo, A. & Bonaldo, P., 2014. Extracellular matrix: A dynamic microenvironment for stem cell niche. *Biochimica et biophysica acta*, 1840(8), pp.2506–2519. Available at: http://www.pubmedcentral.nih.gov/articlerender.fcgi?artid=4081568&tool=pmcentrez&rendertype=abstract [Accessed July 14, 2014].

Ge, R.-T. et al., 2015. Insulin-like growth factor-1 endues monocytes with immune suppressive ability to inhibit inflammation in the intestine. *Scientific reports*, 5,

p.7735. Available at: http://www.pubmedcentral.nih.gov/articlerender.fcgi?artid=4295102&tool=pmcentrez&rendertype=abstract [Accessed February 25, 2015].

Gillies, A.R. & Lieber, R.L., 2011. Structure and function of the skeletal muscle extracellular matrix. *Muscle & nerve*, 44(3), pp.318–31. Available at: http://www.pubmedcentral.nih.gov/articlerender.fcgi?artid=3177172&tool=pmcentrez&rendertype=abstract [Accessed July 19, 2015].

Glass, D.J., 2003. Signalling pathways that mediate skeletal muscle hypertrophy and atrophy. *Nature cell biology*, 5(2), pp.87–90. Available at: http://www.ncbi.nlm.nih.gov/pubmed/12563267 [Accessed September 6, 2015].

Glass, D.J., 2005. Skeletal muscle hypertrophy and atrophy signaling pathways. *The international journal of biochemistry & cell biology*, 37(10), pp.1974–84. Available at: http://www.ncbi.nlm.nih.gov/pubmed/16087388 [Accessed June 22, 2015].

Globus, R.K. et al., 1995. Integrin-extracellular matrix interactions in connective tissue remodeling and osteoblast differentiation. *ASGSB bulletin : publication of the American Society for Gravitational and Space Biology*, 8(2), pp.19–28. Available at: http://www.ncbi.nlm.nih.gov/pubmed/11538547 [Accessed September 6, 2015].

Goldspink, G., 1999. Changes in muscle mass and phenotype and the expression of autocrine and systemic growth factors by muscle in response to stretch and overload. *Journal of anatomy*, 194 (Pt 3, pp.323–34. Available at: http://www.pubmedcentral.nih.gov/articlerender.fcgi?artid=1467932&tool=pmcentrez&rendertype=abstract [Accessed July 29, 2015].

GOLDSPINK, G., 1970. The Proliferation of Myofibrils During Muscle Fibre Growth. *J. Cell Sci.*, 6(2), pp.593–603. Available at: http://jcs.biologists.org/content/6/2/593 [Accessed July 29, 2015].

Gonzalez, J.M. et al., 2007. Effect of ractopamine-hydrochloride and trenbolone acetate on longissimus muscle fiber area, diameter, and satellite cell numbers in cull beef cows. *Journal of animal science*, 85(8), pp.1893–901. Available at: http://www.ncbi.nlm.nih.gov/pubmed/17468415 [Accessed March 22, 2015].

Greenbaum, D. et al., 2003. Comparing protein abundance and mRNA expression levels on a genomic scale. *Genome biology*, 4(9), p.117. Available at: http://genomebiology.com/2003/4/9/117 [Accessed January 7, 2015].

Grimm, D. et al., 2007. Replication fitness determines high virulence of influenza A virus in mice carrying functional Mx1 resistance gene. *Proceedings of the National Academy of Sciences of the United States of America*, 104(16), pp.6806–11. Available at: http://www.pubmedcentral.nih.gov/articlerender.fcgi?artid=1871866&tool=pmcentrez&rendertype=abstract [Accessed September 20, 2015].

Gros, J. et al., 2005. A common somitic origin for embryonic muscle progenitors and satellite cells. *Nature*, 435(7044), pp.954–8. Available at: http://www.ncbi.nlm.nih.gov/pubmed/15843802 [Accessed May 29, 2015].

Gros, J., Scaal, M. & Marcelle, C., 2004. A two-step mechanism for myotome formation in chick. *Developmental cell*, 6(6), pp.875–82. Available at: http://www.ncbi.nlm.nih.gov/pubmed/15177035 [Accessed June 13, 2015].

Gry, M. et al., 2009. Correlations between RNA and protein expression profiles in 23 human cell lines. *BMC genomics*, 10(1), p.365. Available at:

http://www.biomedcentral.com/1471-2164/10/365 [Accessed July 28, 2015].

Gunawan, A.M. et al., 2007. Ractopamine induces differential gene expression in porcine skeletal muscles. *Journal Of Animal Science*, 85, pp.2115–2124.

Halevy, O. et al., 2004. Pattern of Pax7 expression during myogenesis in the posthatch chicken establishes a model for satellite cell differentiation and renewal. *Developmental dynamics : an official publication of the American Association of Anatomists*, 231(3), pp.489–502. Available at: http://www.ncbi.nlm.nih.gov/pubmed/15390217 [Accessed June 7, 2015].

Haller, O. et al., 2015. Mx GTPases: dynamin-like antiviral machines of innate immunity. *Trends in microbiology*, 23(3), pp.154–63. Available at: http://www.ncbi.nlm.nih.gov/pubmed/25572883 [Accessed June 16, 2015].

Haller, O., Frese, M. & Kochs, G., 1998. Mx proteins: mediators of innate resistance to RNA viruses. *Revue Scientifique Et Technique De L Office International Des Epizooties*, 17, pp.220–230.

Halsey, C.H.C. et al., 2011. The effect of ractopamine hydrochloride on gene expression in adipose tissues of finishing pigs. *Journal of animal science*, 89(4), pp.1011–9. Available at: http://www.ncbi.nlm.nih.gov/pubmed/21148782 [Accessed August 1, 2015].

Hantaï, D. et al., 1985. Fibronectin, laminin, type I, III and IV collagens in Duchenne's muscular dystrophy, congenital muscular dystrophies and congenital myopathies: an immunocytochemical study. *Connective tissue research*, 13(4), pp.273–81. Available at: http://www.ncbi.nlm.nih.gov/pubmed/3161692 [Accessed July 21, 2015].

Hanzlíková, V., Schiaffino, S. & Settembrini, P., 1970. Histochemical fiber types

characteristics in the normal and the persistent levator ani muscle of the rat. *Histochemie. Histochemistry. Histochimie*, 22(1), pp.45–50. Available at: http://www.ncbi.nlm.nih.gov/pubmed/4245675 [Accessed July 29, 2015].

Harder, T.C. et al., 2009. Highly pathogenic avian influenza virus (H5N1) in frozen duck carcasses, Germany, 2007. *Emerging infectious diseases*, 15(2), pp.272–9. Available at: http://www.pubmedcentral.nih.gov/articlerender.fcgi?artid=2657628&tool=pmcentrez&rendertype=abstract [Accessed September 20, 2015].

Harsha, H.C., Molina, H. & Pandey, A., 2008. Quantitative proteomics using stable isotope labeling with amino acids in cell culture. *Nature protocols*, 3(3), pp.505–16. Available at: http://www.ncbi.nlm.nih.gov/pubmed/18323819 [Accessed July 13, 2015].

Hausman, D.B. et al., 1989. Effect of ractopamine on insulin sensitivity and response of isolated rat adipocytes. *Journal of animal science*, 67(6), pp.1455–64. Available at: http://www.ncbi.nlm.nih.gov/pubmed/2670868 [Accessed September 19, 2015].

Havel, R.J., NAIMARK, A. & BORCHGREVINK, C.F., 1963. Turnover rate and oxidation of free fatty acids of blood plasma in man during exercise: studies during continuous infusion of palmitate-1-C14. *The Journal of clinical investigation*, 42, pp.1054–63. Available at: http://www.pubmedcentral.nih.gov/articlerender.fcgi?artid=289374&tool=pmcentrez&rendertype=abstract [Accessed September 20, 2015].

He, B. et al., 2013. Overexpression of LASP1 is associated with proliferation, migration and invasion in esophageal squamous cell carcinoma. *Oncology*

Reports, 29(3), pp.1115–1123. Available at: http://www.spandidos-publications.com/or/29/3/1115/abstract [Accessed July 21, 2015].

Hiscock, N. & Pedersen, B.K., 2002. Exercise-induced immunodepression- plasma glutamine is not the link. *Journal of applied physiology (Bethesda, Md. : 1985)*, 93(3), pp.813–22. Available at: http://www.ncbi.nlm.nih.gov/pubmed/12183472 [Accessed July 31, 2015].

Ho, J.-K. et al., 2014. Pharmacokinetics of ractopamine and its organ distribution in rats. *Journal of agricultural and food chemistry*, 62(38), pp.9273–8. Available at: http://www.ncbi.nlm.nih.gov/pubmed/25207456 [Accessed April 25, 2015].

Hoffmann, B. & Karg, H., 1976. Metabolic fate of anabolic agents in treated animals and residue levels in their meat. *Environmental quality and safety. Supplement*, (5), pp.181–91. Available at: http://www.ncbi.nlm.nih.gov/pubmed/782867 [Accessed July 31, 2015].

Hogan, E.L., Dawson, D.M. & Romanul, F.C., 1965. Enzymatic changes in denervated muscle. II. Biochemical studies. *Archives of neurology*, 13(3), pp.274–82. Available at: http://www.ncbi.nlm.nih.gov/pubmed/5832263 [Accessed July 31, 2015].

Hoh, J.F. & Yeoh, G.P., 1979. Rabbit skeletal myosin isoenzymes from fetal, fast-twitch and slow-twitch muscles. *Nature*, 280(5720), pp.321–3. Available at: http://www.ncbi.nlm.nih.gov/pubmed/460404 [Accessed July 31, 2015].

Holtzer, H. et al., 1960. THE LOSS OF PHENOTYPIC TRAITS BY DIFFERENTIATED CELLS IN VITRO, I. DEDIFFERENTIATION OF CARTILAGE CELLS. *Proceedings of the National Academy of Sciences of the United States of America*, 46(12), pp.1533–42. Available at:

http://www.pubmedcentral.nih.gov/articlerender.fcgi?artid=223078&tool=pmcentrez&rendertype=abstract [Accessed April 28, 2015].

Holtzer, H., MARSHALL, J.M. & FINCK, H., 1957. An analysis of myogenesis by the use of fluorescent antimyosin. *The Journal of biophysical and biochemical cytology*, 3(5), pp.705–24. Available at: http://www.pubmedcentral.nih.gov/articlerender.fcgi?artid=2224122&tool=pmcentrez&rendertype=abstract [Accessed June 13, 2015].

Huang, W. et al., 2012. [Effects of mechanical stretch with variant frequencies on alignment and differentiation of multilayer myotubes cultured in vitro]. *Zhongguo xiu fu chong jian wai ke za zhi = Zhongguo xiufu chongjian waike zazhi = Chinese journal of reparative and reconstructive surgery*, 26(6), pp.735–42. Available at: http://www.ncbi.nlm.nih.gov/pubmed/22792775 [Accessed September 7, 2015].

Hunt, P. & Eardley, D.D., 1986. Suppressive effects of insulin and insulin-like growth factor-1 (IGF1) on immune responses. *Journal of immunology (Baltimore, Md. : 1950)*, 136(11), pp.3994–9. Available at: http://www.ncbi.nlm.nih.gov/pubmed/3517163 [Accessed March 22, 2015].

Hutchinson, E.C. et al., 2010. Genome packaging in influenza A virus. *The Journal of general virology*, 91(Pt 2), pp.313–28. Available at: http://www.ncbi.nlm.nih.gov/pubmed/19955561 [Accessed August 1, 2015].

Ito, H. et al., 2005. In situ identification of hepatitis C virus RNA in muscle. *Neurology*, 64(6), pp.1073–5. Available at: http://www.ncbi.nlm.nih.gov/pubmed/15781833 [Accessed September 20, 2015].

Iwasaki, A. & Pillai, P.S., 2014. Innate immunity to influenza virus infection. *Nature reviews. Immunology*, 14(5), pp.315–28. Available at: http://www.pubmedcentral.nih.gov/articlerender.fcgi?artid=4104278&tool=pmcentrez&rendertype=abstract [Accessed July 9, 2014].

Jansen, K.M. & Pavlath, G.K., 2008. Molecular control of mammalian myoblast fusion. *Methods in molecular biology (Clifton, N.J.)*, 475, pp.115–33. Available at: http://www.ncbi.nlm.nih.gov/pubmed/18979241 [Accessed September 6, 2015].

Joseph Hill, E.O., 2012. Muscle 2-Volume Set, 1st Edition | Joseph Hill, Eric Olson | ISBN 9780123815101. Available at: http://store.elsevier.com/Muscle-2-Volume-Set/isbn-9780123815101/ [Accessed September 28, 2015].

Kahn, S.E., Hull, R.L. & Utzschneider, K.M., 2006. Mechanisms linking obesity to insulin resistance and type 2 diabetes. *Nature*, 444(7121), pp.840–6. Available at: http://www.ncbi.nlm.nih.gov/pubmed/17167471 [Accessed July 12, 2014].

Kakugawa, S. et al., 2009. Mitogen-activated protein kinase-activated kinase RSK2 plays a role in innate immune responses to influenza virus infection. *Journal of virology*, 83(6), pp.2510–7. Available at: http://www.pubmedcentral.nih.gov/articlerender.fcgi?artid=2648281&tool=pmcentrez&rendertype=abstract [Accessed March 31, 2015].

Käll, L. et al., 2008. Posterior error probabilities and false discovery rates: two sides of the same coin. *Journal of Proteome Research*, 7, pp.40–44.

Kalman, B. et al., 2015. Engineering human 3D micromuscles with co-culture of fibroblasts and myoblasts. *Computer methods in biomechanics and biomedical engineering*, pp.1–2. Available at:

http://www.ncbi.nlm.nih.gov/pubmed/26296042 [Accessed September 7, 2015].

Kang, Y.K. et al., 2011. Effects of myosin heavy chain isoforms on meat quality, fatty acid composition, and sensory evaluation in Berkshire pigs. *Meat science*, 89(4), pp.384–9. Available at: http://www.ncbi.nlm.nih.gov/pubmed/21636221 [Accessed July 31, 2015].

Karlsson, A.H., Klont, R.E. & Fernandez, X., 1999. Skeletal muscle fibres as factors for pork quality. *Livestock Production Science*, 60(2-3), pp.255–269. Available at: http://www.sciencedirect.com/science/article/pii/S0301622699000986 [Accessed July 29, 2015].

Karp, N.A. et al., 2010. Addressing accuracy and precision issues in iTRAQ quantification. *Mol.Cell.Proteomics*, 9(9), pp.1885–1897.

Katibah, G.E. et al., 2014. Broad and adaptable RNA structure recognition by the human interferon-induced tetratricopeptide repeat protein IFIT5. *Proc.Natl.Acad.Sci.U.S.A.*, 111(3), pp.12025–12030.

Katz, B., 1961. The Terminations of the Afferent Nerve Fibre in the Muscle Spindle of the Frog. *Philosophical Transactions of the Royal Society B: Biological Sciences*, 243(703), pp.221–240. Available at: http://rstb.royalsocietypublishing.org/content/243/703/221 [Accessed May 31, 2015].

Kelley, V.C. & Ruvalcaba, R.H., 1982. Use of anabolic agents in treatment of short children. *Clinics in endocrinology and metabolism*, 11(1), pp.25–39. Available at: http://www.ncbi.nlm.nih.gov/pubmed/7094391 [Accessed August 7, 2015].

Kerr, J.F., Wyllie, A.H. & Currie, A.R., 1972. Apoptosis: a basic biological phenomenon with wide-ranging implications in tissue kinetics. *British journal*

of cancer, 26(4), pp.239–57. Available at: http://www.pubmedcentral.nih.gov/articlerender.fcgi?artid=2008650&tool=pmcentrez&rendertype=abstract [Accessed January 14, 2015].

Kida, H. et al., 1994. Potential for transmission of avian influenza viruses to pigs. *The Journal of general virology*, 75 (Pt 9), pp.2183–8. Available at: http://www.ncbi.nlm.nih.gov/pubmed/8077918 [Accessed August 1, 2015].

Kim, D.-S. et al., 2014. Both α2,3- and α2,6-linked sialic acids on O-linked glycoproteins act as functional receptors for porcine Sapovirus. *PLoS pathogens*, 10(6), p.e1004172. Available at: http://www.pubmedcentral.nih.gov/articlerender.fcgi?artid=4047124&tool=pmcentrez&rendertype=abstract [Accessed September 29, 2015].

Kim, G.-D. et al., 2013. Relationship between pork quality and characteristics of muscle fibers classified by the distribution of myosin heavy chain isoforms. *Journal of animal science*, 91(11), pp.5525–34. Available at: http://www.ncbi.nlm.nih.gov/pubmed/23989883 [Accessed July 31, 2015].

Kim, J.H. et al., 2015. Mechanisms of myoblast fusion during muscle development. *Current opinion in genetics & development*, 32, pp.162–70. Available at: http://www.ncbi.nlm.nih.gov/pubmed/25989064 [Accessed September 6, 2015].

Kimble, B., Nieto, G.R. & Perez, D.R., 2010. Characterization of influenza virus sialic acid receptors in minor poultry species. *Virology journal*, 7, p.365. Available at: http://www.pubmedcentral.nih.gov/articlerender.fcgi?artid=3022680&tool=pmcentrez&rendertype=abstract [Accessed August 1, 2015].

Klavinskis, L.S. et al., 1985. Infection of cultured human muscle cells by influenza

virus. *The Journal of general virology*, 66 (Pt 11, pp.2335–45. Available at: http://www.ncbi.nlm.nih.gov/pubmed/3903046 [Accessed March 4, 2015].

Koerner, I. et al., 2007. Protective role of beta interferon in host defense against influenza A virus. *Journal of virology*, 81(4), pp.2025–30. Available at: http://www.pubmedcentral.nih.gov/articlerender.fcgi?artid=1797552&tool=pmcentrez&rendertype=abstract [Accessed August 7, 2015].

Koishi, K. et al., 1995. MyoD protein accumulates in satellite cells and is neurally regulated in regenerating myotubes and skeletal muscle fibers. *Developmental dynamics : an official publication of the American Association of Anatomists*, 202(3), pp.244–54. Available at: http://www.ncbi.nlm.nih.gov/pubmed/7780174 [Accessed July 27, 2015].

KONIGSBERG, I.R. et al., 1960. The dissociability of deoxyribonucleic acid synthesis from the development of multinuclearity of muscle cells in culture. *The Journal of biophysical and biochemical cytology*, 8, pp.333–43. Available at: http://www.pubmedcentral.nih.gov/articlerender.fcgi?artid=2224946&tool=pmcentrez&rendertype=abstract [Accessed June 15, 2015].

Krans, J.L., 2010. Sliding Filament Theory, Sarcomere, Muscle Contraction, Myosin. Available at: http://www.nature.com/scitable/topicpage/the-sliding-filament-theory-of-muscle-contraction-14567666 [Accessed September 29, 2015].

Křivánek, J. et al., 2014. Properties of neural crest-like cells differentiated from human embryonic stem cells. *Folia biologica*, 60 Suppl 1, pp.30–8. Available at: http://www.ncbi.nlm.nih.gov/pubmed/25369338 [Accessed July 21, 2015].

Kubis, H.P. et al., 1997. Adult fast myosin pattern and Ca2+-induced slow myosin pattern in primary skeletal muscle culture. *Proceedings of the National Academy of Sciences of the United States of America*, 94(8), pp.4205–10. Available at: http://www.pubmedcentral.nih.gov/articlerender.fcgi?artid=20604&tool=pmcentrez&rendertype=abstract [Accessed September 7, 2015].

Kuiper, H.A. et al., 1998. Illegal use of beta-adrenergic agonists: European Community. *Journal of animal science*, 76(1), pp.195–207. Available at: http://www.ncbi.nlm.nih.gov/pubmed/9464899 [Accessed July 31, 2015].

Kume, H. et al., 1994. Beta-adrenergic agonists regulate KCa channels in airway smooth muscle by cAMP-dependent and -independent mechanisms. *The Journal of clinical investigation*, 93(1), pp.371–9. Available at: http://www.pubmedcentral.nih.gov/articlerender.fcgi?artid=293787&tool=pmcentrez&rendertype=abstract [Accessed August 18, 2015].

Kurtz, A., Jelkmann, W. & Bauer, C., 1982. A new candidate for the regulation of erythropoiesis. Insulin-like growth factor I. *FEBS letters*, 149(1), pp.105–8. Available at: http://www.ncbi.nlm.nih.gov/pubmed/6759171 [Accessed March 23, 2015].

Kutzler, L.W. et al., 2011. Comparison of varying doses and durations of ractopamine hydrochloride on late-finishing pig carcass characteristics and meat quality. *Journal of animal science*, 89(7), pp.2176–88. Available at: http://www.ncbi.nlm.nih.gov/pubmed/21317349 [Accessed August 1, 2015].

Lakdawala, S.S. et al., 2013. Receptor specificity does not affect replication or virulence of the 2009 pandemic H1N1 influenza virus in mice and ferrets.

Virology, 446(1-2), pp.349–56. Available at: http://www.pubmedcentral.nih.gov/articlerender.fcgi?artid=3810034&tool=pmcentrez&rendertype=abstract [Accessed August 1, 2015].

Lamb, R.A. & Choppin, P.W., 1983. The gene structure and replication of influenza virus. *Annual review of biochemistry*, 52, pp.467–506. Available at: http://www.annualreviews.org/doi/abs/10.1146/annurev.bi.52.070183.002343 [Accessed August 1, 2015].

Laron, Z., 2001. Insulin-like growth factor 1 (IGF-1): a growth hormone. *Molecular pathology : MP*, 54(5), pp.311–6. Available at: http://www.pubmedcentral.nih.gov/articlerender.fcgi?artid=1187088&tool=pmcentrez&rendertype=abstract [Accessed April 18, 2015].

Larsen, M. et al., 2006. The matrix reorganized: extracellular matrix remodeling and integrin signaling. *Current opinion in cell biology*, 18(5), pp.463–71. Available at: http://www.ncbi.nlm.nih.gov/pubmed/16919434 [Accessed June 17, 2015].

Larsson, L. et al., 1994. Effects of thyroid hormone on fast- and slow-twitch skeletal muscles in young and old rats. *The Journal of physiology*, 481 (Pt 1, pp.149–61. Available at: http://www.pubmedcentral.nih.gov/articlerender.fcgi?artid=1155873&tool=pmcentrez&rendertype=abstract [Accessed July 29, 2015].

Lash, J.W., Holtzer, H. & Swift, H., 1957. Regeneration of mature skeletal muscle. *The Anatomical Record*, 128(4), pp.679–697. Available at: http://doi.wiley.com/10.1002/ar.1091280404 [Accessed June 15, 2015].

Lauren Cornall, D.H.M.M. and A.M., 2012. *Muscle Biopsy* C. Sundaram, ed., InTech. Available at: http://www.intechopen.com/books/muscle-

biopsy/generation-and-use-of-cultured-human-primary-myotubes [Accessed September 6, 2015].

Lee, J.C.-Y., 1958. Vascular patterns in the red and white muscles of the rabbit. *The Anatomical Record*, 132(4), pp.597–611. Available at: http://doi.wiley.com/10.1002/ar.1091320408 [Accessed September 29, 2015].

Lefaucheur, L., 2010. A second look into fibre typing--relation to meat quality. *Meat science*, 84(2), pp.257–70. Available at: http://www.ncbi.nlm.nih.gov/pubmed/20374784 [Accessed July 29, 2015].

Lefaucheur, L. et al., 1998. Evidence for three adult fast myosin heavy chain isoforms in type II skeletal muscle fibers in pigs. *Journal of animal science*, 76(6), pp.1584–93. Available at: http://www.ncbi.nlm.nih.gov/pubmed/9655578 [Accessed July 28, 2015].

Lefaucheur, L. et al., 2004. Myosin heavy chain composition of different skeletal muscles in Large White and Meishan pigs. *Journal of animal science*, 82(7), pp.1931–41. Available at: http://www.ncbi.nlm.nih.gov/pubmed/15309939 [Accessed July 31, 2015].

Lenoir, D. & Honegger, P., 1983. Insulin-like growth factor I (IGF I) stimulates DNA synthesis in fetal rat brain cell cultures. *Brain research*, 283(2-3), pp.205–13. Available at: http://www.ncbi.nlm.nih.gov/pubmed/6133596 [Accessed March 23, 2015].

Leung, H.S.Y. et al., 2012. Entry of influenza A Virus with a α2,6-linked sialic acid binding preference requires host fibronectin. *Journal of virology*, 86(19), pp.10704–13. Available at: http://www.pubmedcentral.nih.gov/articlerender.fcgi?artid=3457276&tool=pmc

entrez&rendertype=abstract [Accessed August 1, 2015].

Lewis, F.C. et al., 2014. Porcine skeletal muscle-derived multipotent PW1pos/Pax7neg interstitial cells: isolation, characterization, and long-term culture. *Stem cells translational medicine*, 3(6), pp.702–12. Available at: http://www.pubmedcentral.nih.gov/articlerender.fcgi?artid=4039454&tool=pmcentrez&rendertype=abstract [Accessed July 5, 2015].

Lewis, W.H. & Lewis, M.R., 1917. Behavior of cross striated muscle in tissue cultures. *American Journal of Anatomy*, 22(2), pp.169–194. Available at: http://doi.wiley.com/10.1002/aja.1000220202 [Accessed July 25, 2015].

Li, B.-J. et al., 2015. Isolation, Culture and Identification of Porcine Skeletal Muscle Satellite Cells. *Asian-Australasian journal of animal sciences*, 28(8), pp.1171–7. Available at: http://www.pubmedcentral.nih.gov/articlerender.fcgi?artid=4478486&tool=pmcentrez&rendertype=abstract [Accessed September 6, 2015].

Lin, Q. et al., 1997. Control of mouse cardiac morphogenesis and myogenesis by transcription factor MEF2C. *Science (New York, N.Y.)*, 276(5317), pp.1404–7. Available at: http://www.pubmedcentral.nih.gov/articlerender.fcgi?artid=4437729&tool=pmcentrez&rendertype=abstract [Accessed August 3, 2015].

Lu, X.H. et al., 2003. Pathogenesis of and immunity to a new influenza A (H5N1) virus isolated from duck meat. *Avian diseases*, 47(3 Suppl), pp.1135–40. Available at: http://www.ncbi.nlm.nih.gov/pubmed/14575129 [Accessed September 20, 2015].

Maas-Szabowski, N., Fusenig, N.E. & Stark, H.-J., 2005. Experimental models to

analyze differentiation functions of cultured keratinocytes in vitro and in vivo. *Methods in molecular biology (Clifton, N.J.)*, 289, pp.47–60. Available at: http://www.ncbi.nlm.nih.gov/pubmed/15502169 [Accessed July 21, 2015].

Machida, S., Spangenburg, E.E. & Booth, F.W., 2004. Primary rat muscle progenitor cells have decreased proliferation and myotube formation during passages. *Cell proliferation*, 37(4), pp.267–77. Available at: http://www.ncbi.nlm.nih.gov/pubmed/15245563 [Accessed September 19, 2015].

Masuda, K. et al., 2013. NF90 in posttranslational gene regulation and microRNA biogenesis. *International Journal of Molecular Sciences*, 14(8), pp.17111–17121.

Matrosovich, M., Herrler, G. & Klenk, H.D., 2015. Sialic Acid Receptors of Viruses. *Topics in current chemistry*, 367, pp.1–28. Available at: http://www.ncbi.nlm.nih.gov/pubmed/23873408 [Accessed August 1, 2015].

Matsakas, A. & Patel, K., 2009. Skeletal muscle fibre plasticity in response to selected environmental and physiological stimuli. *Histology and histopathology*, 24(5), pp.611–29. Available at: http://www.ncbi.nlm.nih.gov/pubmed/19283669 [Accessed September 29, 2015].

Mau, M., Oksbjerg, N. & Rehfeldt, C., 2008. Establishment and conditions for growth and differentiation of a myoblast cell line derived from the semimembranosus muscle of newborn piglets. *In vitro cellular & developmental biology. Animal*, 44(1-2), pp.1–5. Available at: http://www.ncbi.nlm.nih.gov/pubmed/18074188 [Accessed July 19, 2015].

Mauro, A., 1961. Satellite cell of skeletal muscle fibers. *The Journal of biophysical and biochemical cytology*, 9, pp.493–5. Available at: http://www.pubmedcentral.nih.gov/articlerender.fcgi?artid=2225012&tool=pmcentrez&rendertype=abstract [Accessed March 8, 2015].

Mauro, A. & Adams, W.R., 1961. The structure of the sarcolemma of the frog skeletal muscle fiber. *The Journal of biophysical and biochemical cytology*, 10(4)Suppl, pp.177–85. Available at: http://www.pubmedcentral.nih.gov/articlerender.fcgi?artid=2225102&tool=pmcentrez&rendertype=abstract [Accessed June 16, 2015].

McCubrey, J.A. et al., 2014. GSK-3 as potential target for therapeutic intervention in cancer. *Oncotarget*, 5(10), pp.2881–2911.

McDaneld, T.G., 2006. Ankyrin repeat and SOCS box protein 15 regulates protein synthesis in skeletal muscle. *AJP: Regulatory, Integrative and Comparative Physiology*, 290(6), pp.R1672–R1682. Available at: http://www.ncbi.nlm.nih.gov/pubmed/16424087 [Accessed September 22, 2015].

McKenzie, B.E., Easterday, B.C. & Will, J.A., 1972. Light and electron microscopic changes in the myocardium of influenza-infected turkeys. *The American journal of pathology*, 69(2), pp.239–54. Available at: http://www.pubmedcentral.nih.gov/articlerender.fcgi?artid=2032640&tool=pmcentrez&rendertype=abstract [Accessed March 4, 2015].

McLean, J.E. et al., 2009. Lack of Bax prevents influenza A virus-induced apoptosis and causes diminished viral replication. *Journal of virology*, 83(16), pp.8233–46. Available at: http://jvi.asm.org/content/83/16/8233.full [Accessed March

20, 2015].

Melo, F., Carey, D.J. & Brandan, E., 1996. Extracellular matrix is required for skeletal muscle differentiation but not myogenin expression. *Journal of cellular biochemistry*, 62(2), pp.227–39. Available at: http://www.ncbi.nlm.nih.gov/pubmed/8844403 [Accessed September 18, 2015].

Merceron, T.K. et al., 2015. A 3D bioprinted complex structure for engineering the muscle-tendon unit. *Biofabrication*, 7(3), p.035003. Available at: http://www.ncbi.nlm.nih.gov/pubmed/26081669 [Accessed September 6, 2015].

Meurens, F. et al., 2012. The pig: a model for human infectious diseases. *Trends in microbiology*, 20(1), pp.50–7. Available at: http://www.sciencedirect.com/science/article/pii/S0966842X11001958 [Accessed March 19, 2015].

Miller, J.B. & Stockdale, F.E., 1986. Developmental origins of skeletal muscle fibers: clonal analysis of myogenic cell lineages based on expression of fast and slow myosin heavy chains. *Proceedings of the National Academy of Sciences of the United States of America*, 83(11), pp.3860–4. Available at: http://www.pubmedcentral.nih.gov/articlerender.fcgi?artid=323624&tool=pmcentrez&rendertype=abstract [Accessed June 15, 2015].

Mitchell, K.J. et al., 2010. Identification and characterization of a non-satellite cell muscle resident progenitor during postnatal development. *Nature cell biology*, 12(3), pp.257–66. Available at: http://dx.doi.org/10.1038/ncb2025 [Accessed May 7, 2015].

Mo, I.P. et al., Comparative pathology of chickens experimentally inoculated with avian influenza viruses of low and high pathogenicity. *Avian diseases*, 41(1),

pp.125–36. Available at: http://www.ncbi.nlm.nih.gov/pubmed/9087329 [Accessed April 25, 2015].

Mocchegiani, E. et al., 1990. Influence of growth hormone on thymic endocrine activity in humans. *Hormone research*, 33(6), pp.248–55. Available at: http://www.ncbi.nlm.nih.gov/pubmed/2289783 [Accessed April 15, 2015].

Montarras, D., L'honoré, A. & Buckingham, M., 2013. Lying low but ready for action: the quiescent muscle satellite cell. *The FEBS journal*, 280(17), pp.4036–50. Available at: http://www.ncbi.nlm.nih.gov/pubmed/23735050 [Accessed April 5, 2015].

Mooij, P. et al., 2015. Pandemic Swine-Origin H1N1 Influenza Virus Replicates to Higher Levels and Induces More Fever and Acute Inflammatory Cytokines in Cynomolgus versus Rhesus Monkeys and Can Replicate in Common Marmosets. *PloS one*, 10(5), p.e0126132. Available at: http://www.pubmedcentral.nih.gov/articlerender.fcgi?artid=4422689&tool=pmcentrez&rendertype=abstract [Accessed September 6, 2015].

Moss, F.P. & Leblond, C.P., 1970. Nature of dividing nuclei in skeletal muscle of growing rats. *Journal of Cell Biology*, 44(2), pp.459–462. Available at: http://www.scopus.com/inward/record.url?eid=2-s2.0-0014739590&partnerID=tZOtx3y1.

Moss, F.P. & Leblond, C.P., 1971. Satellite cells as the source of nuclei in muscles of growing rats. *The Anatomical record*, 170(4), pp.421–35. Available at: http://www.ncbi.nlm.nih.gov/pubmed/5118594 [Accessed April 28, 2015].

Muroya, S. et al., 2005. Effect of phase limited inhibition of MyoD expression on the terminal differentiation of bovine myoblasts: no alteration of Myf5 or myogenin

expression. *Development, growth & differentiation*, 47(7), pp.483–92. Available at: http://www.ncbi.nlm.nih.gov/pubmed/16179075 [Accessed September 22, 2015].

Murray, M.R. & Pogogeff, I.A., 1946. Observations on adult mammalian skeletal muscle cultivated in vitro. *The Anatomical record*, 94, p.484. Available at: http://www.ncbi.nlm.nih.gov/pubmed/21066249 [Accessed September 6, 2015].

Mussá, T. et al., 2013. Swine, human or avian influenza viruses differentially activates porcine dendritic cells cytokine profile. *Veterinary immunology and immunopathology*, 154(1-2), pp.25–35. Available at: http://www.sciencedirect.com/science/article/pii/S0165242713001244 [Accessed April 25, 2015].

Nayak, D.P., Hui, E.K.-W. & Barman, S., 2004. Assembly and budding of influenza virus. *Virus research*, 106(2), pp.147–65. Available at: http://www.sciencedirect.com/science/article/pii/S0168170204003235 [Accessed July 18, 2015].

Nelli, R.K. et al., 2010. Comparative distribution of human and avian type sialic acid influenza receptors in the pig. *BMC veterinary research*, 6, p.4. Available at: http://www.pubmedcentral.nih.gov/articlerender.fcgi?artid=2832630&tool=pmcentrez&rendertype=abstract [Accessed April 19, 2015].

Nevalainen, M. et al., 2010. Influenza virus infection in multinucleated skeletal myofibers. *Experimental cell research*, 316(11), pp.1784–94. Available at: http://www.ncbi.nlm.nih.gov/pubmed/20362571 [Accessed March 4, 2015].

Ninomiya, A. et al., 2002. Seroepidemiological evidence of avian H4, H5, and H9 influenza A virus transmission to pigs in southeastern China. *Veterinary*

microbiology, 88(2), pp.107–14. Available at: http://www.ncbi.nlm.nih.gov/pubmed/12135631 [Accessed August 1, 2015].

Noda, T. et al., 2006. Architecture of ribonucleoprotein complexes in influenza A virus particles. *Nature*, 439(7075), pp.490–2. Available at: http://www.ncbi.nlm.nih.gov/pubmed/16437116 [Accessed August 1, 2015].

Noda, T., 2011. Native morphology of influenza virions. *Frontiers in microbiology*, 2, p.269. Available at: http://www.pubmedcentral.nih.gov/articlerender.fcgi?artid=3249889&tool=pmcentrez&rendertype=abstract [Accessed August 1, 2015].

Noda, T. & Kawaoka, Y., 2010. Structure of influenza virus ribonucleoprotein complexes and their packaging into virions. *Reviews in medical virology*, 20(6), pp.380–91. Available at: http://www.ncbi.nlm.nih.gov/pubmed/20853340 [Accessed August 1, 2015].

O'steen, W., 1963. The growth of human dystrophic skeletal muscle in diffusion chambers. *Subject Strain Bibliography 1963*, pp.369 – 379. Available at: http://mouseion.jax.org/ssbb1963/1267 [Accessed July 25, 2015].

Oldfors, A. & Lamont, P.J., 2008. Thick filament diseases. *Advances in experimental medicine and biology*, 642, pp.78–91. Available at: http://www.ncbi.nlm.nih.gov/pubmed/19181095 [Accessed July 28, 2015].

Ong, S.-E. et al., 2002. Stable isotope labeling by amino acids in cell culture, SILAC, as a simple and accurate approach to expression proteomics. *Molecular & cellular proteomics : MCP*, 1(5), pp.376–86. Available at: http://www.ncbi.nlm.nih.gov/pubmed/12118079 [Accessed January 6, 2015].

Opitz, B. et al., 2007. IFNbeta induction by influenza A virus is mediated by RIG-I

which is regulated by the viral NS1 protein. *Cellular microbiology*, 9(4), pp.930–8. Available at: http://www.ncbi.nlm.nih.gov/pubmed/17140406 [Accessed August 7, 2015].

Oplatka, A. et al., 1974. Demonstration of mechanochemical coupling in systems containing actin, atp and non-aggregating active myosin derivatives. *Journal of mechanochemistry & cell motility*, 2(4), pp.295–306. Available at: http://www.ncbi.nlm.nih.gov/pubmed/4277009 [Accessed September 29, 2015].

Osterlund, P. et al., 2010. Pandemic H1N1 2009 influenza A virus induces weak cytokine responses in human macrophages and dendritic cells and is highly sensitive to the antiviral actions of interferons. *Journal of virology*, 84(3), pp.1414–22. Available at: http://www.pubmedcentral.nih.gov/articlerender.fcgi?artid=2812319&tool=pmcentrez&rendertype=abstract [Accessed April 25, 2015].

Oustanina, S., Hause, G. & Braun, T., 2004. Pax7 directs postnatal renewal and propagation of myogenic satellite cells but not their specification. *The EMBO journal*, 23(16), pp.3430–9. Available at: http://www.pubmedcentral.nih.gov/articlerender.fcgi?artid=514519&tool=pmcentrez&rendertype=abstract [Accessed May 7, 2015].

Owens, J., Moreira, K. & Bain, G., 2013. Characterization of primary human skeletal muscle cells from multiple commercial sources. *In vitro cellular & developmental biology. Animal*, 49(9), pp.695–705. Available at: http://www.pubmedcentral.nih.gov/articlerender.fcgi?artid=3824271&tool=pmcentrez&rendertype=abstract [Accessed July 13, 2015].

Ozawa, H., Noma, S. & Nonaka, I., 2000. [Myositis and rhabdomyolysis with

influenza infection]. *Nihon rinsho. Japanese journal of clinical medicine*, 58(11), pp.2276–81. Available at: http://www.ncbi.nlm.nih.gov/pubmed/11225317 [Accessed September 20, 2015].

Pain, V.M., 1996. Initiation of protein synthesis in eukaryotic cells. *European journal of biochemistry / FEBS*, 236(3), pp.747–71. Available at: http://www.ncbi.nlm.nih.gov/pubmed/8665893 [Accessed September 26, 2015].

Pallafacchina, G., Blaauw, B. & Schiaffino, S., 2013. Role of satellite cells in muscle growth and maintenance of muscle mass. *Nutrition, metabolism, and cardiovascular diseases : NMCD*, 23 Suppl 1, pp.S12–8. Available at: http://www.ncbi.nlm.nih.gov/pubmed/22621743 [Accessed July 27, 2015].

Pandurangan, M. & Kim, D.H., 2015. A novel approach for in vitro meat production. *Applied microbiology and biotechnology*, 99(13), pp.5391–5. Available at: http://www.ncbi.nlm.nih.gov/pubmed/25971200 [Accessed September 6, 2015].

Pang, Y. et al., 2007. IGF-1 protects oligodendrocyte progenitors against TNFalpha-induced damage by activation of PI3K/Akt and interruption of the mitochondrial apoptotic pathway. *Glia*, 55(11), pp.1099–107. Available at: http://www.ncbi.nlm.nih.gov/pubmed/17577243 [Accessed March 31, 2015].

Park, S. et al., 2014. Mature IGF-I excels in promoting functional muscle recovery from disuse atrophy compared with pro-IGF-IA. *Journal of applied physiology (Bethesda, Md. : 1985)*, 116(7), pp.797–806. Available at: http://www.pubmedcentral.nih.gov/articlerender.fcgi?artid=3972750&tool=pmcentrez&rendertype=abstract [Accessed September 29, 2015].

Partridge, T.A., 2002. Cells that participate in regeneration of skeletal muscle. *Gene*

therapy, 9(11), pp.752–3. Available at: http://www.ncbi.nlm.nih.gov/pubmed/12032703 [Accessed August 7, 2015].

Partridge, T.A., 1997. Tissue culture of skeletal muscle. *Methods in molecular biology (Clifton, N.J.)*, 75, pp.131–44. Available at: http://www.ncbi.nlm.nih.gov/pubmed/9276265 [Accessed September 6, 2015].

Paula, F.M.M. et al., 2015. Exercise increases pancreatic β-cell viability in a model of type 1 diabetes through IL-6 signaling. *FASEB journal : official publication of the Federation of American Societies for Experimental Biology*, 29(5), pp.1805–16. Available at: http://www.ncbi.nlm.nih.gov/pubmed/25609426 [Accessed September 29, 2015].

Peake, J.M. et al., 2005. Exercise-induced muscle damage, plasma cytokines, and markers of neutrophil activation. *Medicine and science in sports and exercise*, 37(5), pp.737–45. Available at: http://www.ncbi.nlm.nih.gov/pubmed/15870626 [Accessed March 23, 2015].

Pedersen, B.K., 2011. Exercise-induced myokines and their role in chronic diseases. *Brain, behavior, and immunity*, 25(5), pp.811–6. Available at: http://www.ncbi.nlm.nih.gov/pubmed/21354469 [Accessed March 8, 2015].

Pedersen, B.K., 2013. Muscle as a secretory organ. *Comprehensive Physiology*, 3(3), pp.1337–62. Available at: http://www.ncbi.nlm.nih.gov/pubmed/23897689 [Accessed April 15, 2015].

Pedersen, B.K., 2011. Muscles and their myokines. *The Journal of experimental biology*, 214(Pt 2), pp.337–46. Available at: http://www.ncbi.nlm.nih.gov/pubmed/21177953 [Accessed May 29, 2015].

Pedersen, B.K., 2000. Special feature for the Olympics: effects of exercise on the

immune system: exercise and cytokines. *Immunology and cell biology*, 78(5), pp.532–5. Available at: http://dx.doi.org/10.1111/j.1440-1711.2000.t01-11-.x [Accessed July 31, 2015].

Pedersen, B.K., 2006. The anti-inflammatory effect of exercise: its role in diabetes and cardiovascular disease control. *Essays in biochemistry*, 42, pp.105–17. Available at: http://www.ncbi.nlm.nih.gov/pubmed/17144883 [Accessed July 31, 2015].

Pedersen, B.K. & Febbraio, M., 2005. Muscle-derived interleukin-6--a possible link between skeletal muscle, adipose tissue, liver, and brain. *Brain, behavior, and immunity*, 19(5), pp.371–6. Available at: http://www.ncbi.nlm.nih.gov/pubmed/15935612 [Accessed September 1, 2015].

Pende, M. et al., 2004. S6K1-/-/S6K2-/- Mice Exhibit Perinatal Lethality and Rapamycin-Sensitive 5'-Terminal Oligopyrimidine mRNA Translation and Reveal a Mitogen-Activated Protein Kinase-Dependent S6 Kinase Pathway. *Molecular and Cellular Biology*, 24(8), pp.3112–3124. Available at: http://mcb.asm.org/content/24/8/3112.long [Accessed September 26, 2015].

Penna, F. et al., 2010. Muscle wasting and impaired myogenesis in tumor bearing mice are prevented by ERK inhibition. *PloS One*, 5, p.e13604.

Pereira, D.S. et al., 2013. TNF-α, IL6, and IL10 polymorphisms and the effect of physical exercise on inflammatory parameters and physical performance in elderly women. *Age (Dordrecht, Netherlands)*, 35(6), pp.2455–63. Available at: http://www.pubmedcentral.nih.gov/articlerender.fcgi?artid=3824985&tool=pmcentrez&rendertype=abstract [Accessed September 15, 2015].

Perruchot, M.-H. et al., 2012. In vitro characterization of proliferation and

differentiation of pig satellite cells. *Differentiation; research in biological diversity*, 84(4), pp.322–9. Available at: http://www.ncbi.nlm.nih.gov/pubmed/23023068 [Accessed July 21, 2015].

Perry, R.L. & Rudnick, M.A., 2000. Molecular mechanisms regulating myogenic determination and differentiation. *Frontiers in bioscience : a journal and virtual library*, 5, pp.D750–67. Available at: http://www.ncbi.nlm.nih.gov/pubmed/10966875 [Accessed September 29, 2015].

Peter, J.B. et al., 1972. Metabolic profiles of three fiber types of skeletal muscle in guinea pigs and rabbits. *Biochemistry*, 11(14), pp.2627–2633. Available at: http://dx.doi.org/10.1021/bi00764a013 [Accessed July 29, 2015].

Peterla, T.A. & Scanes, C.G., 1990. Effect of beta-adrenergic agonists on lipolysis and lipogenesis by porcine adipose tissue in vitro. *Journal of animal science*, 68(4), pp.1024–9. Available at: http://www.ncbi.nlm.nih.gov/pubmed/1970556 [Accessed September 19, 2015].

Petersen, A.M.W. & Pedersen, B.K., 2005. The anti-inflammatory effect of exercise. *Journal of applied physiology (Bethesda, Md. : 1985)*, 98(4), pp.1154–62. Available at: http://www.ncbi.nlm.nih.gov/pubmed/15772055 [Accessed July 16, 2014].

Petruson, B., Hansson, H.A. & Petruson, K., 1988. Insulin-like growth factor I is a possible pathogenic mechanism in nasal polyps. *Acta oto-laryngologica*, 106(1-2), pp.156–60. Available at: http://www.ncbi.nlm.nih.gov/pubmed/3421095 [Accessed April 26, 2015].

Pette, D., 2002. The adaptive potential of skeletal muscle fibers. *Canadian journal of*

applied physiology = Revue canadienne de physiologie appliquée, 27(4), pp.423–48. Available at: http://www.ncbi.nlm.nih.gov/pubmed/12442355 [Accessed July 29, 2015].

Pette, D. & Staron, R.S., 2000. Myosin isoforms, muscle fiber types, and transitions. *Microscopy research and technique*, 50(6), pp.500–9. Available at: http://www.ncbi.nlm.nih.gov/pubmed/10998639 [Accessed July 29, 2015].

Phillips, P.J. et al., 1980. Metabolic and cardiovascular side effects of the beta 2-adrenoceptor agonists salbutamol and rimiterol. *British journal of clinical pharmacology*, 9(5), pp.483–91. Available at: http://www.pubmedcentral.nih.gov/articlerender.fcgi?artid=1429961&tool=pmcentrez&rendertype=abstract [Accessed September 29, 2015].

Picard, B. et al., 2002. Muscle fibre ontogenesis in farm animal species. *Reproduction, nutrition, development*, 42(5), pp.415–31. Available at: http://www.ncbi.nlm.nih.gov/pubmed/12537254 [Accessed September 29, 2015].

Pigsite, 2015. Diseases - The Pig Site. Available at: http://www.thepigsite.com/diseaseinfo/ [Accessed July 21, 2015].

Piralla, A. et al., 2015. Swine Influenza A(H3N2) Virus Infection in Immunocompromised Man, Italy, 2014. *Emerging infectious diseases*, 21(7), pp.1189–91. Available at: http://www.pubmedcentral.nih.gov/articlerender.fcgi?artid=4480377&tool=pmcentrez&rendertype=abstract [Accessed August 8, 2015].

Pleadin, J. et al., 2013. Comparison of ractopamine residue depletion from internal tissues. *Immunopharmacology and immunotoxicology*, 35(1), pp.88–92.

Available at: http://www.ncbi.nlm.nih.gov/pubmed/22758391 [Accessed April 25, 2015].

Poggi, C. et al., 1979. Effects and binding of insulin-like growth factor I in the isolated soleus muscle of lean and obese mice: comparison with insulin. *Endocrinology*, 105(3), pp.723–30. Available at: http://www.ncbi.nlm.nih.gov/pubmed/111916 [Accessed March 5, 2015].

Portiér, G.L. et al., 1999. Differentiation markers of mouse C2C12 and rat L6 myogenic cell lines and the effect of the differentiation medium. *In Vitro Cellular & Developmental Biology - Animal*, 35(4), pp.219–227. Available at: http://link.springer.com/10.1007/s11626-999-0030-8 [Accessed August 30, 2015].

Privalsky, M.L. & Penhoet, E.E., 1978. Influenza virus proteins: identity, synthesis, and modification analyzed by two-dimensional gel electrophoresis. *Proceedings of the National Academy of Sciences of the United States of America*, 75(8), pp.3625–9. Available at: http://www.pubmedcentral.nih.gov/articlerender.fcgi?artid=392838&tool=pmcentrez&rendertype=abstract [Accessed August 1, 2015].

Purslow, P.P. & Trotter, J.A., 1994. The morphology and mechanical properties of endomysium in series-fibred muscles: variations with muscle length. *Journal of muscle research and cell motility*, 15(3), pp.299–308. Available at: http://www.ncbi.nlm.nih.gov/pubmed/7929795 [Accessed July 19, 2015].

Quinn, L.S., Haugk, K.L. & Damon, S.E., 1997. Interleukin-15 stimulates C2 skeletal myoblast differentiation. *Biochemical and biophysical research communications*, 239(1), pp.6–10. Available at:

http://www.ncbi.nlm.nih.gov/pubmed/9345260 [Accessed August 8, 2015].

Quinn, L.S., Haugk, K.L. & Grabstein, K.H., 1995. Interleukin-15: a novel anabolic cytokine for skeletal muscle. *Endocrinology*, 136(8), pp.3669–72. Available at: http://www.ncbi.nlm.nih.gov/pubmed/7628408 [Accessed August 8, 2015].

Quinn, M.J. et al., 2008. The effects of ractopamine-hydrogen chloride (Optaflexx) on performance, carcass characteristics, and meat quality of finishing feedlot heifers. *Journal of Animal Science*, 86(4), pp.902–908. Available at: http://www.ncbi.nlm.nih.gov/pubmed/18192549 [Accessed September 20, 2015].

Ramsköld, D. et al., 2009. An abundance of ubiquitously expressed genes revealed by tissue transcriptome sequence data. *PLoS computational biology*, 5(12), p.e1000598. Available at: http://www.pubmedcentral.nih.gov/articlerender.fcgi?artid=2781110&tool=pmcentrez&rendertype=abstract [Accessed July 15, 2014].

Raschke, S. et al., 2013. Identification and validation of novel contraction-regulated myokines released from primary human skeletal muscle cells. *PloS one*, 8(4), p.e62008. Available at: http://journals.plos.org/plosone/article?id=10.1371/journal.pone.0062008 [Accessed July 13, 2015].

Redshaw, Z. & Loughna, P.T., 2012. Oxygen concentration modulates the differentiation of muscle stem cells toward myogenic and adipogenic fates. *Differentiation; research in biological diversity*, 84(2), pp.193–202. Available at: http://www.ncbi.nlm.nih.gov/pubmed/22790207 [Accessed September 19, 2015].

Rehwinkel, J. & Reis e Sousa, C., 2010. RIGorous detection: exposing virus through RNA sensing. *Science (New York, N.Y.)*, 327(5963), pp.284–6. Available at: http://www.ncbi.nlm.nih.gov/pubmed/20075242 [Accessed September 26, 2015].

Relaix, F. et al., 2005. A Pax3/Pax7-dependent population of skeletal muscle progenitor cells. *Nature*, 435(7044), pp.948–53. Available at: http://dx.doi.org/10.1038/nature03594 [Accessed April 7, 2015].

Rettew, J.A., Huet-Hudson, Y.M. & Marriott, I., 2008. Testosterone reduces macrophage expression in the mouse of toll-like receptor 4, a trigger for inflammation and innate immunity. *Biology of reproduction*, 78(3), pp.432–7. Available at: http://www.ncbi.nlm.nih.gov/pubmed/18003947 [Accessed April 15, 2015].

Rhim, C. et al., 2007. Morphology and ultrastructure of differentiating three-dimensional mammalian skeletal muscle in a collagen gel. *Muscle & nerve*, 36(1), pp.71–80. Available at: http://www.ncbi.nlm.nih.gov/pubmed/17455272 [Accessed September 19, 2015].

Richardson, P.J., Why, H.J. & Archard, L.C., 1992. Virus infection and dilated cardiomyopathy. *Postgraduate medical journal*, 68 Suppl 1, pp.S17–20. Available at: http://www.ncbi.nlm.nih.gov/pubmed/1329059 [Accessed September 20, 2015].

Rinderknecht, E. & Humbel, R.E., 1978. The amino acid sequence of human insulin-like growth factor I and its structural homology with proinsulin. *The Journal of biological chemistry*, 253(8), pp.2769–76. Available at: http://www.ncbi.nlm.nih.gov/pubmed/632300 [Accessed March 23, 2015].

Ringer, S., 1887. Regarding the Action of Lime Potassium and Sodium Salts on Skeletal Muscle. *The Journal of physiology*, 8(1), pp.20–4. Available at: http://www.pubmedcentral.nih.gov/articlerender.fcgi?artid=1485064&tool=pmcentrez&rendertype=abstract [Accessed March 29, 2015].

Roca, I. et al., 2015. Myogenic Precursors from iPS Cells for Skeletal Muscle Cell Replacement Therapy. *Journal of clinical medicine*, 4(2), pp.243–59. Available at: http://www.pubmedcentral.nih.gov/articlerender.fcgi?artid=4470123&tool=pmcentrez&rendertype=abstract [Accessed September 6, 2015].

Rønning, S.B. et al., 2013. The combination of glycosaminoglycans and fibrous proteins improves cell proliferation and early differentiation of bovine primary skeletal muscle cells. *Differentiation; research in biological diversity*, 86(1-2), pp.13–22. Available at: http://www.ncbi.nlm.nih.gov/pubmed/23933398 [Accessed July 19, 2015].

Roskoski, R., 2015. A historical overview of protein kinases and their targeted small molecule inhibitors. *Pharmacological research : the official journal of the Italian Pharmacological Society*, 100, pp.1–23. Available at: http://www.ncbi.nlm.nih.gov/pubmed/26207888 [Accessed July 25, 2015].

Rudnicki, M.A. et al., 1993. MyoD or Myf-5 is required for the formation of skeletal muscle. *Cell*, 75(7), pp.1351–9. Available at: http://www.ncbi.nlm.nih.gov/pubmed/8269513 [Accessed May 30, 2015].

Ryall, J.G., Schertzer, J.D. & Lynch, G.S., 2008. Cellular and molecular mechanisms underlying age-related skeletal muscle wasting and weakness. *Biogerontology*, 9(4), pp.213–28. Available at: http://www.ncbi.nlm.nih.gov/pubmed/18299960

[Accessed August 18, 2015].

Sainz, R. et al., 1993. Temporal changes in growth enhancement by ractopamine in pigs: performance aspects. *Australian Journal of Agricultural Research*, 44(7), p.1449. Available at: http://www.publish.csiro.au/view/journals/dsp_journal_fulltext.cfm?nid=40&f=AR9931449 [Accessed September 19, 2015].

Sakar, M.S. et al., 2012. Formation and optogenetic control of engineered 3D skeletal muscle bioactuators. *Lab on a chip*, 12(23), pp.4976–85. Available at: http://www.pubmedcentral.nih.gov/articlerender.fcgi?artid=3586563&tool=pmcentrez&rendertype=abstract [Accessed September 7, 2015].

Samji, T., 2009. Influenza A: understanding the viral life cycle. *The Yale journal of biology and medicine*, 82(4), pp.153–9. Available at: http://www.pubmedcentral.nih.gov/articlerender.fcgi?artid=2794490&tool=pmcentrez&rendertype=abstract [Accessed July 26, 2015].

Sandri, M. et al., 2001. Caspase 3 expression correlates with skeletal muscle apoptosis in Duchenne and facioscapulo human muscular dystrophy. A potential target for pharmacological treatment? *Journal of neuropathology and experimental neurology*, 60(3), pp.302–12. Available at: http://www.ncbi.nlm.nih.gov/pubmed/11245214 [Accessed March 28, 2015].

Santos-Rosa, H. & Caldas, C., 2005. Chromatin modifier enzymes, the histone code and cancer. *European Journal of Cancer*, 41, pp.2381–2402.

Schaefer, R. et al., 2015. A human-like H1N2 influenza virus detected during an outbreak of acute respiratory disease in swine in Brazil. *Archives of virology*, 160(1), pp.29–38. Available at:

http://www.ncbi.nlm.nih.gov/pubmed/25209152 [Accessed September 30, 2015].

Schalbruch, H. & Hellhammer, U., 1977. [Satellite cells as myogenic stem cells and their incidence in normal human skeletal muscles]. *Verhandlungen der Anatomischen Gesellschaft*, (71 Pt 2), pp.1251–8. Available at: http://www.ncbi.nlm.nih.gov/pubmed/610141 [Accessed September 6, 2015].

Schiaffino, S. et al., 2015. Developmental myosins: expression patterns and functional significance. *Skeletal muscle*, 5, p.22. Available at: http://www.ncbi.nlm.nih.gov/pubmed/26180627 [Accessed July 18, 2015].

Schiaffino, S. & Pierobon Bormioli, S., 1975. [Types of fibers in skeletal muscles of mammals: histochemical and ultrastructural characteristics in relation to their contractile properties]. *Rivista di istochimica, normale e patologica*, 19(1-4), pp.64–71. Available at: http://www.ncbi.nlm.nih.gov/pubmed/1233713 [Accessed July 28, 2015].

Schiaffino, S. & Reggiani, C., 2011. Fiber types in mammalian skeletal muscles. *Physiological reviews*, 91(4), pp.1447–531. Available at: http://www.ncbi.nlm.nih.gov/pubmed/22013216 [Accessed July 10, 2014].

Schiaffino, S. & Reggiani, C., 1994. Myosin isoforms in mammalian skeletal muscle. *Journal of applied physiology (Bethesda, Md. : 1985)*, 77(2), pp.493–501. Available at: http://www.ncbi.nlm.nih.gov/pubmed/8002492 [Accessed September 2, 2015].

Schindler, C. & Plumlee, C., 2008. Interferons pen the JAK-STAT pathway. *Seminars in Cell and Developmental Biology*, 19, pp.311–318.

Schreiber, T.B. et al., 2008. Quantitative phosphoproteomics - an emerging key

technology in signal-transduction research. *PROTEOMICS*, 8(21), pp.4416–4432. Available at: http://www.ncbi.nlm.nih.gov/pubmed/18837465 [Accessed September 23, 2015].

Schultz, E., 1996. Satellite cell proliferative compartments in growing skeletal muscles. *Developmental biology*, 175(1), pp.84–94. Available at: http://www.ncbi.nlm.nih.gov/pubmed/8608871 [Accessed June 15, 2015].

Schultz, E. & McCormick, K.M., 1994. Skeletal muscle satellite cells. *Reviews of physiology, biochemistry and pharmacology*, 123, pp.213–57. Available at: http://www.ncbi.nlm.nih.gov/pubmed/8209136 [Accessed June 15, 2015].

Schwartz, L.M. et al., 1993. Selective repression of actin and myosin heavy chain expression during the programmed death of insect skeletal muscle. *Developmental biology*, 158(2), pp.448–55. Available at: http://www.ncbi.nlm.nih.gov/pubmed/8344462 [Accessed March 28, 2015].

Seale, P. et al., 2000. Pax7 is required for the specification of myogenic satellite cells. *Cell*, 102(6), pp.777–86. Available at: http://www.ncbi.nlm.nih.gov/pubmed/11030621 [Accessed March 4, 2015].

Sebastian, S. et al., 2015. Extended 2D myotube culture recapitulates postnatal fibre type plasticity. *BMC Cell Biology*, 16(1), p.23. Available at: http://www.biomedcentral.com/1471-2121/16/23 [Accessed September 17, 2015].

Semkow, R. & Wilczyński, J., 1979. Detection and tissue localization of components of the immune complex in animals infected and immunized with influenza virus. *Acta virologica*, 23(1), pp.52–8. Available at: http://www.ncbi.nlm.nih.gov/pubmed/35959 [Accessed September 20, 2015].

Serena Beato, M. et al., 2006. Isolation and characterization of an H10N7 avian influenza virus from poultry carcasses smuggled from China into Italy. *Avian pathology : journal of the W.V.P.A*, 35(5), pp.400–3. Available at: http://www.ncbi.nlm.nih.gov/pubmed/16990150 [Accessed September 20, 2015].

Servidei, S., Miranda, A.F. & Gamboa, E.T., 1987. Infectivity of influenza B virus in cultured human muscle. *Acta neuropathologica*, 73(1), pp.67–76. Available at: http://www.ncbi.nlm.nih.gov/pubmed/3300131 [Accessed March 4, 2015].

Shafiq, S.A., Gorycki, M.A. & Milhorat, A.T., 1967. An electron microscopic study of regeneration and satellite cells in human muscle. *Neurology*, 17(6), pp.567–74 passim. Available at: http://www.ncbi.nlm.nih.gov/pubmed/6067392 [Accessed July 27, 2015].

Sharples, A.P. et al., 2012. Modelling in vivo skeletal muscle ageing in vitro using three-dimensional bioengineered constructs. *Aging cell*, 11(6), pp.986–95. Available at: http://www.ncbi.nlm.nih.gov/pubmed/22882433 [Accessed July 21, 2015].

Shaul, Y.D. & Seger, R., 2007. The MEK/ERK cascade: from signaling specificity to diverse functions. *Biochim.Biophys.Acta*, 1773, pp.1213–1226.

Shi, H. et al., 2007. Extracellular signal-regulated kinase pathway is differentially involved in b-agonist induced hypertrophy in slow and fast muscles. *American Journal of Physiology -Cell Physiology*, 292, pp.C1681–C1690.

Shimizu, K. et al., 2015. Microfluidic devices for construction of contractile skeletal muscle microtissues. *Journal of bioscience and bioengineering*, 119(2), pp.212–6. Available at: http://www.ncbi.nlm.nih.gov/pubmed/25085533

[Accessed July 20, 2015].

Simon, H.B., 1984. The immunology of exercise. A brief review. *JAMA : the journal of the American Medical Association*, 252(19), pp.2735–2738.

Smith, S.B., Garcia, D.K. & Anderson, D.B., 1989. Elevation of a Specific mRNA in Longissimus Muscle of Steers Fed Ractopamine. *Journal of Animal Science*, 67(12), pp.3495–3502. Available at: https://dl.sciencesocieties.org/publications/jas/abstracts/67/12/JAN0670123495 [Accessed September 19, 2015].

Smith, A.S.T. et al., 2012. Characterization and optimization of a simple, repeatable system for the long term in vitro culture of aligned myotubes in 3D. *Journal of cellular biochemistry*, 113(3), pp.1044–53. Available at: http://www.ncbi.nlm.nih.gov/pubmed/22065378 [Accessed September 7, 2015].

Smith, D.J. & Shelver, W.L., 2002. Tissue residues of ractopamine and urinary excretion of ractopamine and metabolites in animals treated for 7 days with dietary ractopamine. *Journal of animal science*, 80(5), pp.1240–9. Available at: http://www.ncbi.nlm.nih.gov/pubmed/12019611 [Accessed September 29, 2015].

Smith, S.B. et al., 1989. Elevation of a specific mRNA in longissimus muscle of steers fed ractopamine. *Journal of animal science*, 67(12), pp.3495–502. Available at: http://www.ncbi.nlm.nih.gov/pubmed/2613589 [Accessed March 17, 2015].

So, B. et al., 2014. Exercise-induced myokines in health and metabolic diseases. *Integrative Medicine Research*, 3(4), pp.172–179. Available at: http://www.sciencedirect.com/science/article/pii/S2213422014000705

[Accessed April 26, 2015].

Somlyo, A.P. & Somlyo, A. V, 1994. Signal transduction and regulation in smooth muscle. *Nature*, 372(6503), pp.231–6. Available at: http://www.ncbi.nlm.nih.gov/pubmed/7969467 [Accessed September 28, 2015].

Srinivas, B.P. et al., 2007. A conserved molecular pathway mediates myoblast fusion in insects and vertebrates. *Nature genetics*, 39(6), pp.781–6. Available at: http://www.ncbi.nlm.nih.gov/pubmed/17529975 [Accessed September 6, 2015].

Staron, R.S. & Pette, D., 1993. The continuum of pure and hybrid myosin heavy chain-based fibre types in rat skeletal muscle. *Histochemistry*, 100(2), pp.149–53. Available at: http://www.ncbi.nlm.nih.gov/pubmed/8244766 [Accessed September 19, 2015].

Stephany, R.W., 2010. Hormonal growth promoting agents in food producing animals. *Handbook of experimental pharmacology*, (195), pp.355–67. Available at: http://www.ncbi.nlm.nih.gov/pubmed/20020373 [Accessed September 29, 2015].

Stites, C.R. et al., 1991. The effect of ractopamine hydrochloride on the carcass cutting yields of finishing swine. *Journal of animal science*, 69(8), pp.3094–101. Available at: http://www.ncbi.nlm.nih.gov/pubmed/1680116 [Accessed March 22, 2015].

Stoller, G.M. et al., 2003. The effect of feeding ractopamine (Paylean) on muscle quality and sensory characteristics in three diverse genetic lines of swine. *Journal of animal science*, 81(6), pp.1508–16. Available at: http://www.ncbi.nlm.nih.gov/pubmed/12817499 [Accessed April 18, 2015].

Sultan, K.R. et al., 2006. Quantification of hormone-induced atrophy of large

myotubes from C2C12 and L6 cells: atrophy-inducible and atrophy-resistant C2C12 myotubes. *American Journal of Physiology -Cell Physiology*, 290(2), pp.C650–C659.

Suzuki, S. et al., 2014. Inhibition of the insulin-like growth factor system is a potential therapy for rheumatoid arthritis. *Autoimmunity*, pp.1–8. Available at: http://www.ncbi.nlm.nih.gov/pubmed/25352179 [Accessed April 15, 2015].

Suzuki, Y. et al., 2000. Sialic acid species as a determinant of the host range of influenza A viruses. *Journal of virology*, 74(24), pp.11825–31. Available at: http://www.pubmedcentral.nih.gov/articlerender.fcgi?artid=112465&tool=pmcentrez&rendertype=abstract [Accessed April 19, 2015].

Swayne, D.E. & Beck, J.R., 2005. Experimental study to determine if low-pathogenicity and high-pathogenicity avian influenza viruses can be present in chicken breast and thigh meat following intranasal virus inoculation. *Avian diseases*, 49(1), pp.81–5. Available at: http://www.ncbi.nlm.nih.gov/pubmed/15839417 [Accessed September 20, 2015].

Szepsenwol, J., 1946. A comparison of growth, differentiation, activity and action currents of heart and skeletal muscle in tissue culture. *The Anatomical record*, 95, pp.125–46. Available at: http://www.ncbi.nlm.nih.gov/pubmed/20990819 [Accessed September 6, 2015].

Takeuchi, O. & Akira, S., 2008. MDA5/RIG-I and virus recognition. *Current opinion in immunology*, 20(1), pp.17–22. Available at: http://www.ncbi.nlm.nih.gov/pubmed/18272355 [Accessed September 19, 2015].

Takizawa, T. et al., 1999. Recruitment of apoptotic cysteine proteases (caspases) in influenza virus-induced cell death. *Microbiology and immunology*, 43(3), pp.245–52. Available at: http://www.ncbi.nlm.nih.gov/pubmed/10338194 [Accessed March 28, 2015].

Takizawa, T., Ohashi, K. & Nakanishi, Y., 1996. Possible involvement of double-stranded RNA-activated protein kinase in cell death by influenza virus infection. *Journal of virology*, 70(11), pp.8128–32. Available at: http://www.pubmedcentral.nih.gov/articlerender.fcgi?artid=190888&tool=pmcentrez&rendertype=abstract [Accessed March 28, 2015].

Tapscott, S.J. et al., 1988. MyoD1: a nuclear phosphoprotein requiring a Myc homology region to convert fibroblasts to myoblasts. *Science (New York, N.Y.)*, 242(4877), pp.405–11. Available at: http://www.ncbi.nlm.nih.gov/pubmed/3175662 [Accessed May 21, 2015].

Thorrez, L. et al., 2008. Growth, differentiation, transplantation and survival of human skeletal myofibers on biodegradable scaffolds. *Biomaterials*, 29(1), pp.75–84. Available at: http://www.pubmedcentral.nih.gov/articlerender.fcgi?artid=2275665&tool=pmcentrez&rendertype=abstract [Accessed July 21, 2015].

Tong, S. et al., 2013. New world bats harbor diverse influenza A viruses. *PLoS pathogens*, 9(10), p.e1003657. Available at: http://journals.plos.org/plospathogens/article?id=10.1371/journal.ppat.1003657 [Accessed July 2, 2015].

Toniolo, L. et al., 2004. Fast fibres in a large animal: fibre types, contractile properties and myosin expression in pig skeletal muscles. *The Journal of*

experimental biology, 207(Pt 11), pp.1875–86. Available at: http://www.ncbi.nlm.nih.gov/pubmed/15107442 [Accessed September 19, 2015].

Torphy, T.J., 1994. Beta-adrenoceptors, cAMP and airway smooth muscle relaxation: challenges to the dogma. *Trends in pharmacological sciences*, 15(10), pp.370–4. Available at: http://www.ncbi.nlm.nih.gov/pubmed/7809952 [Accessed August 18, 2015].

Trensz, F. et al., 2015. Increased microenvironment stiffness in damaged myofibers promotes myogenic progenitor cell proliferation. *Skeletal muscle*, 5, p.5. Available at: http://www.pubmedcentral.nih.gov/articlerender.fcgi?artid=4343274&tool=pmcentrez&rendertype=abstract [Accessed September 18, 2015].

Trotter, J.A. & Purslow, P.P., 1992. Functional morphology of the endomysium in series fibered muscles. *Journal of morphology*, 212(2), pp.109–22. Available at: http://www.ncbi.nlm.nih.gov/pubmed/1608046 [Accessed July 19, 2015].

Tumpey, T.M. et al., 2002. Characterization of a Highly Pathogenic H5N1 Avian Influenza A Virus Isolated from Duck Meat. *Journal of Virology*, 76(12), pp.6344–6355. Available at: http://jvi.asm.org/content/76/12/6344.long [Accessed September 20, 2015].

Valtorta, A. et al., 1990. [In vitro effects of GH and IGF-1 on natural cytostatic activity]. *Medicina (Florence, Italy)*, 10(2), pp.149–50. Available at: http://www.ncbi.nlm.nih.gov/pubmed/2273948 [Accessed March 23, 2015].

VanderWal, P., 1976. General aspects of the effectiveness of anabolic agents in increasing protein production in farm animals, in particular in bull calves.

Environmental quality and safety. Supplement, (5), pp.60–78. Available at: http://www.ncbi.nlm.nih.gov/pubmed/782873 [Accessed July 31, 2015].

Velle, W., 1976. Endogenous anabolic agents in farm animals. *Environmental quality and safety. Supplement*, (5), pp.159–70. Available at: http://www.ncbi.nlm.nih.gov/pubmed/782866 [Accessed July 31, 2015].

Venters, S.J. & Ordahl, C.P., 2002. Persistent myogenic capacity of the dermomyotome dorsomedial lip and restriction of myogenic competence. *Development (Cambridge, England)*, 129(16), pp.3873–85. Available at: http://www.ncbi.nlm.nih.gov/pubmed/12135925 [Accessed June 13, 2015].

Verhelst, J. et al., 2012. Interferon-inducible protein Mx1 inhibits influenza virus by interfering with functional viral ribonucleoprotein complex assembly. *Journal of virology*, 86(24), pp.13445–55. Available at: http://www.pubmedcentral.nih.gov/articlerender.fcgi?artid=3503048&tool=pmcentrez&rendertype=abstract [Accessed September 20, 2015].

Voorma, H.O., Thomas, A.A. & Van Heugten, H.A., 1994. Initiation of protein synthesis in eukaryotes. *Molecular biology reports*, 19(3), pp.139–45. Available at: http://www.ncbi.nlm.nih.gov/pubmed/7969102 [Accessed September 26, 2015].

Wakeford, S., Watt, D.J. & Partridge, T.A., 1991. X-irradiation improves mdx mouse muscle as a model of myofiber loss in DMD. *Muscle & nerve*, 14(1), pp.42–50. Available at: http://www.ncbi.nlm.nih.gov/pubmed/1992296 [Accessed August 7, 2015].

Weintz, G. et al., 2010. The phosphoproteome of toll-like receptor-activated macrophages. *Molecular systems biology*, 6, p.371. Available at:

http://www.pubmedcentral.nih.gov/articlerender.fcgi?artid=2913394&tool=pmcentrez&rendertype=abstract [Accessed September 23, 2015].

Weist, M.R. et al., 2013. TGF-β1 enhances contractility in engineered skeletal muscle. *Journal of tissue engineering and regenerative medicine*, 7(7), pp.562–71. Available at: http://www.pubmedcentral.nih.gov/articlerender.fcgi?artid=4035810&tool=pmcentrez&rendertype=abstract [Accessed July 21, 2015].

Wells, J.B., 1965. Comparison of mechanical properties between slow and fast mammalian muscles. *The Journal of Physiology*, 178(2), pp.252–269. Available at: http://doi.wiley.com/10.1113/jphysiol.1965.sp007626 [Accessed September 29, 2015].

Whalen, R.G. et al., 1981. Three myosin heavy-chain isozymes appear sequentially in rat muscle development. *Nature*, 292(5826), pp.805–809. Available at: http://dx.doi.org/10.1038/292805a0 [Accessed July 31, 2015].

Why, H.J. et al., 1994. Clinical and prognostic significance of detection of enteroviral RNA in the myocardium of patients with myocarditis or dilated cardiomyopathy. *Circulation*, 89(6), pp.2582–9. Available at: http://www.ncbi.nlm.nih.gov/pubmed/8205668 [Accessed September 20, 2015].

Wiese, S. et al., 2007. Protein labeling by iTRAQ: a new tool for quantitative mass spectrometry in proteome research. *Proteomics*, 7(3), pp.340–350.

Wilschut, K.J., Haagsman, H.P. & Roelen, B.A.J., 2010a. Extracellular matrix components direct porcine muscle stem cell behavior. *Experimental cell research*, 316(3), pp.341–52. Available at: http://www.ncbi.nlm.nih.gov/pubmed/19853598 [Accessed July 19, 2015].

Wilschut, K.J., Haagsman, H.P. & Roelen, B.A.J., 2010b. Extracellular matrix components direct porcine muscle stem cell behavior. *Experimental cell research*, 316(3), pp.341–52. Available at: http://www.sciencedirect.com/science/article/pii/S0014482709004431 [Accessed July 19, 2015].

Wilson, J., 1809. A description of two Muscles surrounding the membranous part of the Urethra. *Medico-chirurgical transactions*, 1, pp.175–82. Available at: http://www.pubmedcentral.nih.gov/articlerender.fcgi?artid=2128799&tool=pmcentrez&rendertype=abstract [Accessed March 29, 2015].

Wimmers, K. et al., 2008. Relationship between myosin heavy chain isoform expression and muscling in several diverse pig breeds. *Journal of animal science*, 86(4), pp.795–803. Available at: http://www.ncbi.nlm.nih.gov/pubmed/18156349 [Accessed September 2, 2015].

Wolff, T. et al., 2008. Sabotage of antiviral signaling and effectors by influenza viruses. *Biological chemistry*, 389(10), pp.1299–305. Available at: http://www.ncbi.nlm.nih.gov/pubmed/18713015 [Accessed August 7, 2015].

Wurzer, W.J. et al., 2003. Caspase 3 activation is essential for efficient influenza virus propagation. *The EMBO journal*, 22(11), pp.2717–28. Available at: http://www.pubmedcentral.nih.gov/articlerender.fcgi?artid=158404&tool=pmcentrez&rendertype=abstract [Accessed March 6, 2015].

Xu, W. et al., 2015. Pigeon RIG-I Function in Innate Immunity against H9N2 IAV and IBDV. *Viruses*, 7(7), pp.4131–51. Available at: http://www.pubmedcentral.nih.gov/articlerender.fcgi?artid=4517142&tool=pmcentrez&rendertype=abstract [Accessed September 20, 2015].

Yaeger, M.J. et al., 2012. Myocardial toxicity in a group of greyhounds administered ractopamine. *Veterinary pathology*, 49(3), pp.569–73. Available at: http://www.ncbi.nlm.nih.gov/pubmed/21997565 [Accessed April 26, 2015].

Yoshida, T. et al., 2010. IGF-1 prevents ANG II-induced skeletal muscle atrophy via Akt- and Foxo-dependent inhibition of the ubiquitin ligase atrogin-1 expression. *American journal of physiology. Heart and circulatory physiology*, 298(5), pp.H1565–70. Available at: http://www.pubmedcentral.nih.gov/articlerender.fcgi?artid=2867436&tool=pmcentrez&rendertype=abstract [Accessed September 29, 2015].

Yoshino, M. et al., 2000. High incidence of acute myositis with type A influenza virus infection in the elderly. *Internal medicine (Tokyo, Japan)*, 39(5), pp.431–2. Available at: http://www.ncbi.nlm.nih.gov/pubmed/10830190 [Accessed September 20, 2015].

Yousry, C. & Kanitakis, J., 1991. [Non-immunologic effects of cyclosporins]. *Pathologie-biologie*, 39(4), pp.293–9. Available at: http://www.ncbi.nlm.nih.gov/pubmed/2062556 [Accessed July 31, 2015].

Yu, M. et al., 2015. Insulin-like growth factor-1 (IGF-1) promotes myoblast proliferation and skeletal muscle growth of embryonic chickens via the PI3K/Akt signalling pathway. *Cell biology international*. Available at: http://www.ncbi.nlm.nih.gov/pubmed/25808997 [Accessed April 26, 2015].

Zhang, L.J. et al., 2015. Testosterone regulates thyroid cancer progression by modifying tumor suppressor genes and tumor immunity. *Carcinogenesis*, 36(4), pp.420–8. Available at: http://www.ncbi.nlm.nih.gov/pubmed/25576159 [Accessed April 15, 2015].

Zhang, Y. et al., 2009. Tissue-specific extracellular matrix coatings for the promotion of cell proliferation and maintenance of cell phenotype. *Biomaterials*, 30(23-24), pp.4021–8. Available at: http://www.ncbi.nlm.nih.gov/pubmed/19410290 [Accessed July 19, 2015].

Zhang, Y.-H. et al., 2011. Substrate stiffness regulates apoptosis and the mRNA expression of extracellular matrix regulatory genes in the rat annular cells. *Matrix biology : journal of the International Society for Matrix Biology*, 30(2), pp.135–44. Available at: http://www.ncbi.nlm.nih.gov/pubmed/21055467 [Accessed September 6, 2015].

Zhao, Y. et al., 2009. Fabrication of skeletal muscle constructs by topographic activation of cell alignment. *Biotechnology and bioengineering*, 102(2), pp.624–31. Available at: http://www.pubmedcentral.nih.gov/articlerender.fcgi?artid=3825623&tool=pmcentrez&rendertype=abstract [Accessed September 7, 2015].

Zhu, H. et al., 2013. Porcine satellite cells are restricted to a phenotype resembling their muscle origin. *Journal of animal science*, 91(10), pp.4684–91. Available at: https://www.animalsciencepublications.org/publications/jas/articles/91/10/4684 [Accessed July 21, 2015].

Zierath, J.R. & Hawley, J.A., 2004. Skeletal muscle fiber type: influence on contractile and metabolic properties. *PLoS biology*, 2(10), p.e348. Available at: http://www.pubmedcentral.nih.gov/articlerender.fcgi?artid=521732&tool=pmcentrez&rendertype=abstract [Accessed September 6, 2015].

Sebastian et al. BMC Cell Biology (2015) 16:23
DOI 10.1186/s12860-015-0069-1

BMC Cell Biology

METHODOLOGY ARTICLE Open Access

Extended 2D myotube culture recapitulates postnatal fibre type plasticity

Sujith Sebastian, Leah Goulding, Suresh V. Kuchipudi and Kin-Chow Chang*

Abstract

Background: The traditional problems of performing skeletal muscle cell cultures derived from mammalian or avian species are limited myotube differentiation, and transient myotube persistence which greatly restricts the ability of myotubes to undergo phenotypic maturation. We report here on a major technical breakthrough in the establishment of a simple and effective method of extended porcine myotube cultures (beyond 50 days) in two-dimension (2D) that recapitulates key features of postnatal fibre types.

Results: Primary porcine muscle satellite cells (myoblasts) were isolated from the *longissimus dorsi* of 4 to 6 weeks old pigs for 2D cultures to optimise myotube formation, improve surface adherence and characterise myotube maturation. Over 95 % of isolated cells were myoblasts as evidenced by the expression of Pax3 and Pax7. Our relatively simple approach, based on modifications of existing surface coating reagents (Maxgel), and of proliferation and differentiation (Ultroser G) media, typically achieved by 5 days of differentiation fusion index of around 80 % manifested in an abundance of discrete myosin heavy chain (MyHC) slow and fast myotubes. There was little deterioration in myotube viability over 50 days, and the efficiency of myotube formation was maintained over seven myoblast passages. Regular spontaneous contractions of myotubes were frequently observed throughout culture. Myotubes in extended cultures were able to undergo phenotypic adaptation in response to different culture media, including the adoption of a dominant postnatal phenotype of fast-glycolytic *MyHC 2x* and *2b* expression by about day 20 of differentiation. Furthermore, fast-glycolytic myotubes coincided with enhanced expression of the putative porcine long intergenic non-coding RNA (*linc-MYH*), which has recently been shown to be a key coordinator of *MyHC 2b* expression *in vivo*.

Conclusions: Our revised culture protocol allows the efficient differentiation and fusion of porcine myoblasts into myotubes and their prolonged adherence to the culture surface. Furthermore, we are able to recapitulate in 2D the maturation process of myotubes to resemble postnatal fibre types which represent a major technical advance in opening access to the *in vitro* study of coordinated postnatal muscle gene expression.

Keywords: Postnatal, Myosin heavy chain, Differentiation, Fusion, Contraction, Fibre type switching, Porcine, Myotubes, Six1, lincRNA, Linc-MYH, Coordinated expression, Fast glycolytic, Oxidative

Background

Skeletal muscle satellite cells as progenitor cells of multi-nucleated muscle fibres are one of the earliest recognised cells with stem cell-like properties [1]. Isolated satellite cells in culture are activated to undergo rapid proliferation as myoblasts which then differentiate and fuse to form post-mitotic myotubes as early muscle fibres. Muscle fibres *in vivo* are highly adapted to undergo phenotypic changes in size (hypertrophy or atrophy) and metabolic capacity (ranging from highly oxidative to enhanced glycolytic fibre type) to meet changes in physiological demands or in response to disease [2]. Newly formed myotubes undergo a maturation process of hypertrophy and metabolic remodelling during which the initial dominant embryonic and perinatal (neonatal) myosin heavy chain (MyHC) isoforms are replaced with the four main postnatal MyHC isoforms of slow, 2A, 2X and 2B, each sequentially corresponding to a fibre type of increasing glycolytic and decreasing oxidative capacity.

Although muscle satellite cells of different host species have been used in adherent two-dimension (2D) cultures for many years, to date such cultures can primarily only recapitulate the early stages of myogenesis and myotube

* Correspondence: kin-chow.chang@nottingham.ac.uk
School of Veterinary Medicine and Science, University of Nottingham, Sutton Bonington LE12 5RD, UK

BioMed Central

© 2015 Sebastian et al. **Open Access** This article is distributed under the terms of the Creative Commons Attribution 4.0 International License (http://creativecommons.org/licenses/by/4.0/), which permits unrestricted use, distribution, and reproduction in any medium, provided you give appropriate credit to the original author(s) and the source, provide a link to the Creative Commons license, and indicate if changes were made. The Creative Commons Public Domain Dedication waiver (http://creativecommons.org/publicdomain/zero/1.0/) applies to the data made available in this article, unless otherwise stated.

formation [3–5]. Myoblasts often show limited efficiency of differentiation and fusion. Furthermore, as myotubes in cultures are prone to rapid loss, presumably through spontaneous contractions, their replacement by more newly-formed myotubes perpetuates an immature phenotype in culture [6]. As a consequence to such technical limitations, muscle culture experiments are typically performed on immature myotubes over a narrow window of 3 to 7 days of differentiation [3, 7]. A variety of culture media and extracellular matrices, including the use of electrospun polycaprolactone polymer coating [8], have been reported to facilitate, with limited success, myoblast differentiation and fusion, and myotube attachment. Other attempts to extend the transient persistence of myotubes included the use of three-dimension (3D) cultures of murine C2C12 muscle cells on silicon wafers [9], rat myoblasts in cantilever arrays [10], and primary rabbit muscle cells on gelatin microbeads in suspension that allowed prolonged myotube adherence and fibre maturation for up to 5 weeks with the expression of adult fast MyHCs (2A, 2X and/or 2B isoform) [6]. The use of 3D collagen mould in a chamber slide also improved primary rat myotube formation and reduced loss over a 3-week period [11]. However, such culture methods and other similar approaches have limited practicalities requiring specialised culture platforms with reduced flexibility to conduct routine cellular manipulations.

We report on a major technical breakthrough in the long term culture of myotubes. We developed a simple and highly reproducible method for the extended 2D culture of myotubes based on the strategic use of primary porcine myoblasts; the pig is an excellent model species, owing to its physiological similarity to human and relative availability, and its own importance as target species. Our method, based on modified use of surface coating reagents (Maxgel), and of proliferation and differentiation (Ultroser G) media, allowed efficient differentiation and fusion of myoblasts into myotubes that remained adherent to the culture surface for over 7 weeks of differentiation. To our knowledge, we are able for the first time to recapitulate *in vitro* the maturation process of myotubes in 2D to resemble postnatal fibre types which is a major technical advance in the ability to study phenotype plasticity.

Methods

Culture of porcine myoblasts and myotubes

Porcine muscle satellite cells (myoblasts) were isolated from skeletal muscles (*longissimus dorsi*) of 4 to 6 weeks old commercial Large White-cross pigs as previously described [12]. This work was approved by the School of Veterinary Medicine and Science ethical committee. Pigs were humanely euthanased according to Schedule 1 to the Animals (Scientific Procedures) Act 1986. All myoblasts and myotubes were grown on optimised coated surfaces. Into each well of a 12-well plate was applied 400 μl of 0.22 μm filter sterilised Maxgel coating mixture (MC+), comprising a 1:1 mix ratio of 1 % Maxgel ECM solution (Sigma-Aldrich, E0282-1ML; 1 in a 100 dilution with Dulbecco's modified Eagle's medium [DMEM]) and 2 % rat type I collagen solution (Sigma Aldrich, C3867; 1 ml rat collagen solution in 49 ml phosphate buffered saline [PBS]), which was left to fully dry overnight in a cell culture cabinet and rinsed with PBS before use. For other size plates or flasks, the volume of MC+ used was proportionally scaled.

Newly harvested satellite cells were grown in proliferation medium (PM), comprising SKGM-2 medium (Lonza, CC-3245) with added 10 % heat inactivated fetal calf serum (FCS) (Invitrogen, 10500–064), 2 % chick embryo extract (EGG Tech, 60650) and 1 % penicillin-streptomycin (P/S) (Invitrogen 15140-122), in a 37 °C incubator with gas mixture of 5 % CO2 and 5 % O2, with complete replacement of PM every 2 days. Myoblasts were passaged once at a ratio of 1:3 in PM before freezing in a mixture of 50 % FCS, 10 % dimethylsulphoxide and 40 % PM, and storing in liquid nitrogen. Depending on seeding density of thawed myoblasts, 0.5 million cells in a T75 flask should reach 60 to 70 % confluence by 3-4 days of culture.

At around 80 to 90 % confluence, the cells were rinsed and replaced with differentiation medium 1 (DM1) comprising DMEM high glucose (Invitrogen, 41965–039) with 0.4 % Ultroser G (Pall Corporation, 15950–017) and 1 % P/S. Ultroser G is a proprietary serum replacement containing a cocktail of undisclosed growth factors. Extensive myotubes should form by 3 to 4 days of differentiation. For long-term maintenance of the myotubes, from day 5–7 of differentiation, 25 % volume of the original DM1 was replaced every third day with fresh DM1, or differentiation medium 2 (DM2, DMEM high glucose with 2 % horse serum [Gibco, 26050-088] and 1 % P/S). In this way, good myotube integrity was readily maintained for several weeks.

Cell viability

Measurement of mitochondrial activity in myotubes, as an indication of cell viability, was performed in a 96-well format with a CellTiter 96 AQueous Non-Radioactive Cell Proliferation Assay (MTS) kit (Promega) according to the manufacturer's instructions. The MTS kit is composed of solutions of a novel tetrazolium compound [3-(4,5-dimethylthiazol-2-yl)-5-(3-carboxymethoxyphenyl)-2-(4-sulfophenyl)-2H-tetrazolium, inner salt; MTS] and an electron coupling reagent (phenazine methosulfate). MTS is bioreduced by cells into a formazan product that is soluble in cell culture medium. The conversion of MTS (measured at 490 nm absorbance) into the aqueous soluble formazan product is accomplished by dehydrogenase enzymes found in metabolically active cells. The quantity of formazan

product is directly proportional to the number or activity of living cells in culture.

Real time PCR

RNA extraction from myoblasts and myotubes was performed with an RNeasy fibrous tissue mini kit (Qiagen). TaqMan real-time PCR was used to quantify the expression of six porcine MyHC gene isoforms (*MyHC embryonic*, *MyHC perinatal*, *MyHC slow/I*, *MyHC 2a*, *MyHC2x* and *MyHC 2b*) using primers and TaqMan probes as previously described [13–15]. Forward and reverse primers for the SYBR Green detection of putative porcine *long intergenic non-coding* (*linc*)-*MYH* (exon 5) are 5′-GAGGCTCG GGAAGGAATCC-3′ and 5′-TGCCCTCTGGTGGTAAA AGC-3′. Forward and reverse primers for porcine *Six1* and *Eya1* detection are 5′-GTTCAAGAACCGAAGGCAAC-3′ and 5′-CCCCTTCCAGAGGAGAGAGT-3′, and 5′-C AGCTCTCCATATCCAGCACATT-3′ and 5′-TTTGTGG ACGGCGTCGTA-3′ respectively. A relative standard curve was used to quantify the expression of each gene normalised to its corresponding 18S rRNA expression.

Results

Culture of primary porcine muscle cells

Greater than 95 % of isolated porcine muscle cells, derived from the *longissimus dorsi* of 4 to 6 weeks old pigs, expressed transcription factors Pax3 and Pax7 (Fig. 1a) indicating that the isolated cells were highly enriched for muscle satellite cells [16, 17]. Porcine myoblasts were grown in PM in culture plates or flasks coated with a specified volume of MC+ that was fully dried overnight (see Methods). When myoblasts reached around 80 %

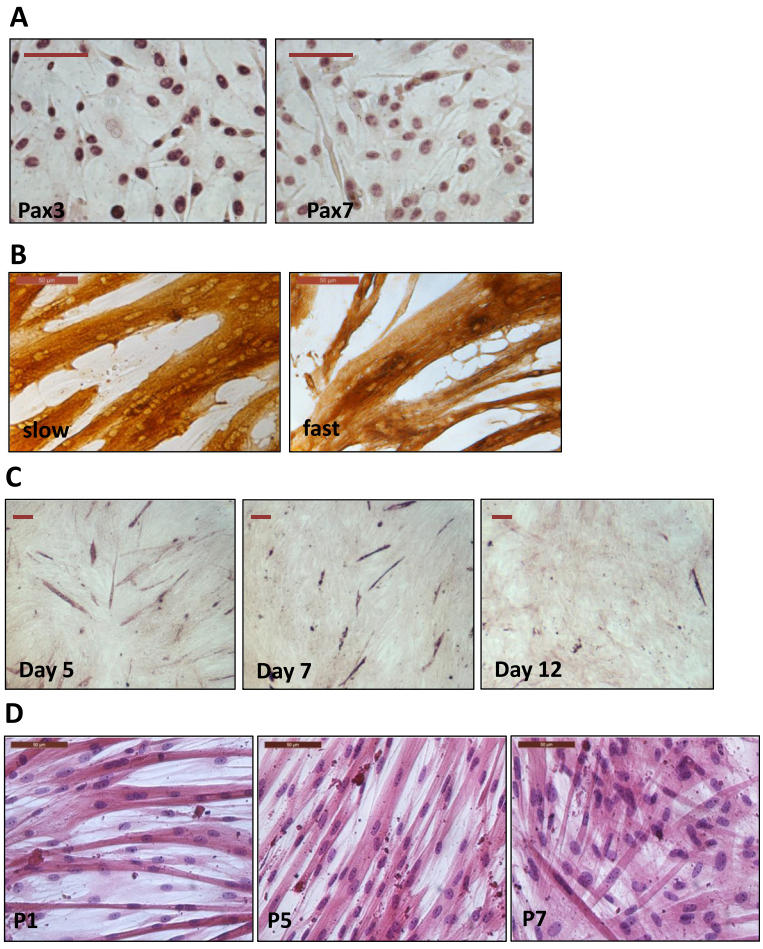

Fig. 1 Characterisation of primary porcine muscle cells. **a** Highly enriched myoblasts were isolated from 4 to 6 week old muscles (*longissimus dorsi*), as evidenced by nuclear detection of Pax3 and Pax7 (both antibodies from R&D Systems, 1:100 dilution). **b** Extensive discrete immunodetection of MyHC slow (Sigma, M8421, 1:4000 dilution) and fast (Sigma, M4276, 1:400 dilution) in myotubes at day 5 differentiation. **c** By contrast, myotube formation was typically low using standard media (in this case MEM with 10 % fetal bovine serum and 1 % penicillin-streptomycin (P/S) as proliferation medium, and MEM with 2 % horse serum and 1 % P/S as differentiation medium [12, 19]). Immunodetection of α-actin was confined to a limited number of myoblasts/myotubes over 12 days of differentiation. Day = days of differentiation. **d** Present protocol conferred comparably high levels of myotube formation over 7 passages (P) of porcine myoblasts. Hematoxylin and eosin (H&E) stained myotubes at day 3 differentiation from P1, P5 and P7

confluence, usually by day 3 or 4 of culture from frozen stock, PM was replaced with differentiation medium containing Ultroser G (DM1). By 5 days of differentiation, we typically detected an abundance of discrete MyHC slow and fast myotubes (Fig. 1b) which was in marked contrast to conventional cultures for porcine myotubes where few myotubes were found (Fig. 1c). With our improved protocol, the efficiency of myotube formation remained unaffected over seven myoblast passages (Fig. 1d).

Enhanced myotube differentiation and sustained viability

With our approach, by day 5 of differentiation, fusion index was typically around 80 % (Fig. 2a). To maintain myotube integrity over several weeks, from day 5 to 7 of differentiation, a quarter of DM1 was replaced with fresh DM1 or DM2 (with horse serum) at every third day of culture. There was little deterioration in myotube viability based on mitochondrial activity (MTA assays) over 50 days of differentiation, and morphological appearance (Fig. 2b and c). Myotubes transduced at day 8 with replication-defective adenovirus expressing green fluorescence protein (GFP) were found to persist in culture for at least 28 days of differentiation which demonstrated that the culture conditions applied were conducive to extended myotube survival, a requisite for myotube maturation (Fig. 2d). Formed myotubes throughout the differentiation period manifestly possessed lateral striations characteristic of sarcomeres which remained visible throughout several rounds of myoblast passages (Fig. 3).

Extended myotube culture displayed phenotypic plasticity and postnatal phenotype

An exciting observation made on extended myotube cultures over 28 days of differentiation was that the choice of DM could profoundly affect the profiles of *MyHC* expression. Despite absence of innervation, myotube cultures by 21 days in DM1 (with Ultroser G) underwent fast phenotypic changes of raised fast *MyHC 2x* and *2b* expression (Fig. 4a) which resembled the relative expression pattern of *MyHCs* in *longissimus dorsi* (fast) muscle of a 22 week old pig (Fig. 4b). Interestingly, testosterone was one ingredient identified by high throughput metabolomic analysis in the proprietary serum substitute Ultroser G (data not shown) but its influence on postnatal MyHC expression is unclear. The use of DM2 (with horse serum), by contrast, appeared to maintain a phenotype of sustained *MyHC embryonic* and *perinatal* expression, and preferentially up-regulated the expression of the oxidative *MyHC slow* and *2a* genes (Fig. 4a). These results demonstrated the plasticity of myotubes in being able to undergo phenotypic changes in response to different culture media. Furthermore, regular spontaneous contractions of myotubes were frequently observed throughout much of the extended culture period; contractions appeared earlier, more vigorous and extensive with the use DM1. Additional movie files (see Additional file 1, Additional file 2, Additional file 3, Additional file 4 and Additional file 5) show contracting myotubes in DM1 or DM2 at 4, 8, 9, 27 and 60 day differentiation respectively. Thus, with relatively simple but significant culture modifications, we were able to induce extensive myotube formation, and maintain myotube attachment and viability for several weeks of differentiation. These results were particularly gratifying as porcine myoblasts have been recognised to be least efficient amongst the commonly used host species (rodents, rabbit, chicken, duck and human) to differentiate into myotubes [12, 18, 19].

Rising putative *linc-MYH* expression coincided with accumulation of *MyHC 2x* and *2b* in myotubes

Expression of the long intergenic non-coding gene, *linc-MYH*, located in the 70 kb intergenic region between *Myh3* (*MyHC embryonic*) and *Myh2* (*MyHC 2a*) of the skeletal *MyHC* cluster, was recently shown to confer the coordinated adult fast-type (in particular *MyHC 2b*) and prevent the slow-type programme in murine *tibialis anterior* muscle [20]. Interestingly, the promoters of *linc-MYH*, *MyHC 2b* and *2x* are controlled in common by a Six1-dependent enhancer located at the immediate 5′-end of the *linc-MYH* gene within the murine *Myh3-Myh2* intergenic region [20]. Six1, a homeobox transcription factor, along with its cofactor Eya1, also activates the adult fast-twitch and represses the slow-twitch programme in muscle fibres [21, 22]. By sequence alignment (EMBOSS Matcher) of the 73 kb porcine *Myh3-Myh2* intergenic region with the murine *linc-MYH* RNA (2310065F04Rik), we identified all 5 putative porcine *linc-MYH* exons at modest similarities (as expected) of 58 to 67 % with corresponding murine exons [23]. We compared the expression of *linc-MYH*, *Six1* and *Eya1* in our extended myotube cultures to determine their possible involvement in fast phenotype determination (Fig. 5). Beyond 10 days of differentiation, *linc-MYH* expression was much more highly up-regulated in DM1 than DM2 (Fig. 5a) which corresponded with the much higher expression of *MyHC 2x* and *2b* in DM1 myotubes (Fig. 4a and b). *Six1* and *Eya1*, on the other hand, showed sharp reduction in expression from day 1 of differentiation in both DM1 and DM2 cultures (Fig. 5b and c). *Linc-MYH* and *Six1*, as predicted, were more highly expressed in the fast *longissimus dorsi* than slow *psoas* muscle of 22-week-old pigs (Fig. 5). Therefore, the fast postnatal MyHC phenotype in extended DM1 cultures strongly correlated with enhanced *linc-MYH* expression but not with *Six1* expression.

Discussion

The usefulness of myotubes in cultures to examine muscle gene regulation or response to external stimuli has hitherto been limited by the immature state of myotubes derived

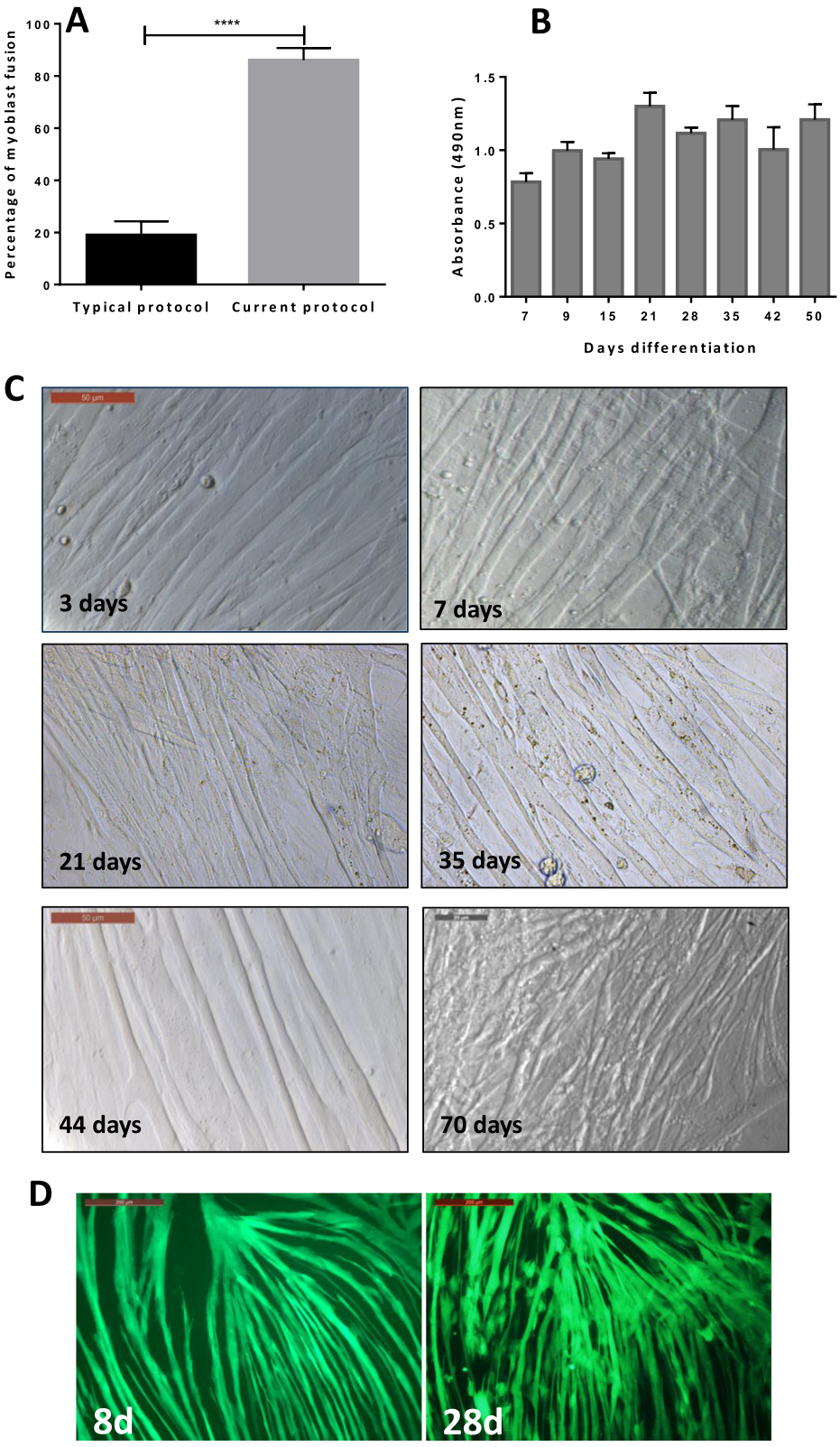

Fig. 2 (See legend on next page.)

(See figure on previous page.)
Fig. 2 Enhanced myotube formation and viability. **a** Present culture protocol conferred highly efficient myotube formation relative to typical cultures [12, 19]. About 80 % of fusion could be typically achieved by day 5 of differentiation (error bars = standard deviation, **** = $P \leq 0.0001$ based on two-sample unpaired *t* test). **b** Myotube mitochondrial activity as determined by MTS assays remained relatively unchanged over a period of 50 days of differentiation. **c** From day 5 of differentiation, 25 % of DM1 was replaced with DM2 every third day for extended myotube maintenance to at least day 50 of differentiation (bar = 200 μm). **d** Porcine myotubes transduced with GFP-expressing non-replicating adenovirus at day 8 remained largely intact at day 28 of differentiation based on persistence of green fluorescence which was indicative of extended myotube survival in culture (bar = 200 μm)

from a range of mammalian (human, pig, rabbit, cow, horse, mouse and rat) [3, 4, 6, 7, 12, 18, 19] and avian (chicken and duck) [5, 12] species. Most published experiments on myotubes are performed within about a week of differentiation, at a stage when adult MyHCs (namely MyHC 2X and 2B) are largely lacking. The principal reasons for this predicament are limited efficiency in myotube formation and continual loss of newly formed myotubes. The ability to culture myotubes long term in 2D to resemble the postnatal phenotype is of high biomedical value. The most important biomedical or veterinary muscle conditions (such as muscle hypertrophic growth [24], muscle wasting or atrophy [25], changes in fibre type composition affecting muscle performance [26] or even meat quality [27], and obesity-related insulin resistance [28, 29]) all involve skeletal muscle in the postnatal fibre state. To have a suitable *in vitro* platform to examine such basic underlying changes is clearly advantageous. Until now such a platform has been elusive in that myotube differentiation and maturation were major limiting factors. The present paper reports on such a technical breakthrough that promotes myotube differentiation and accommodates spontaneous myotube contractions without detachment which would facilitate the *in vitro* study of all aspects of postnatal muscle fibre biology.

In the first weeks of postnatal development in rats and mice, there is typically progressive loss of embryonic and perinatal MyHCs and accumulation of MyHC 2A, 2X and 2B isoforms in designated fast fibre populations [2]. Our extended porcine myotube cultures in DM1 showed

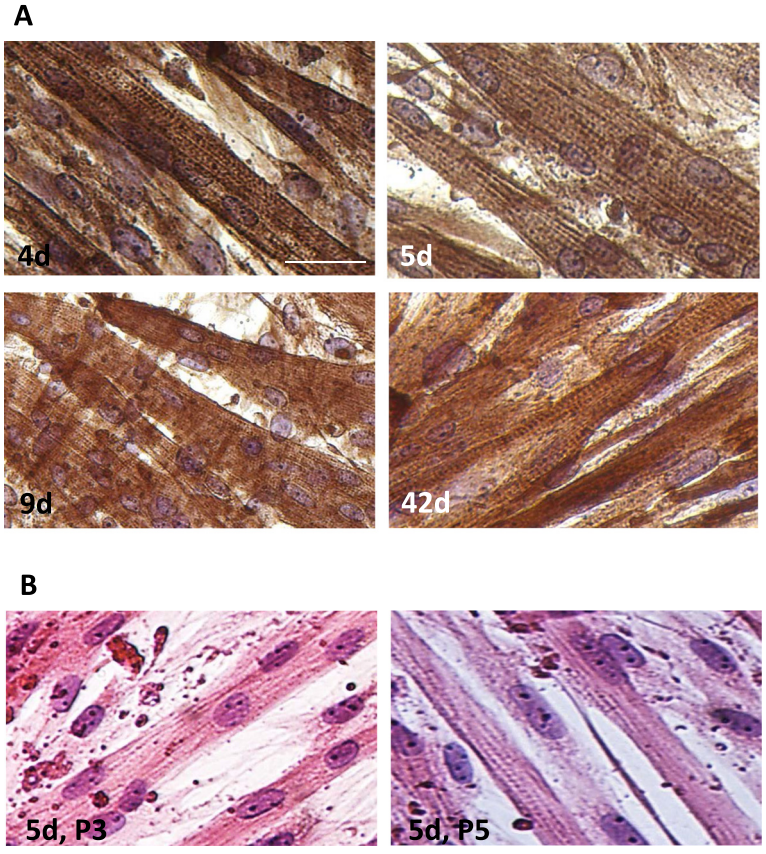

Fig. 3 Myotube formation was accompanied by the observation of lateral striations indicative of sarcomeric structures. **a** Myotubes at 4d, 5d, 9d (DM1) and 42d (DM1) of differentiation were immunostained for the presence of sarcomeric α-actin (Sigma A2172, 1:500 dilution). **b** Sarcomeric lateral striations were visible in H&E stained myotubes differentiated for 5d, derived from P3 and P5 *longissimus dorsi* myoblasts. Bar = 50 μm for all panels

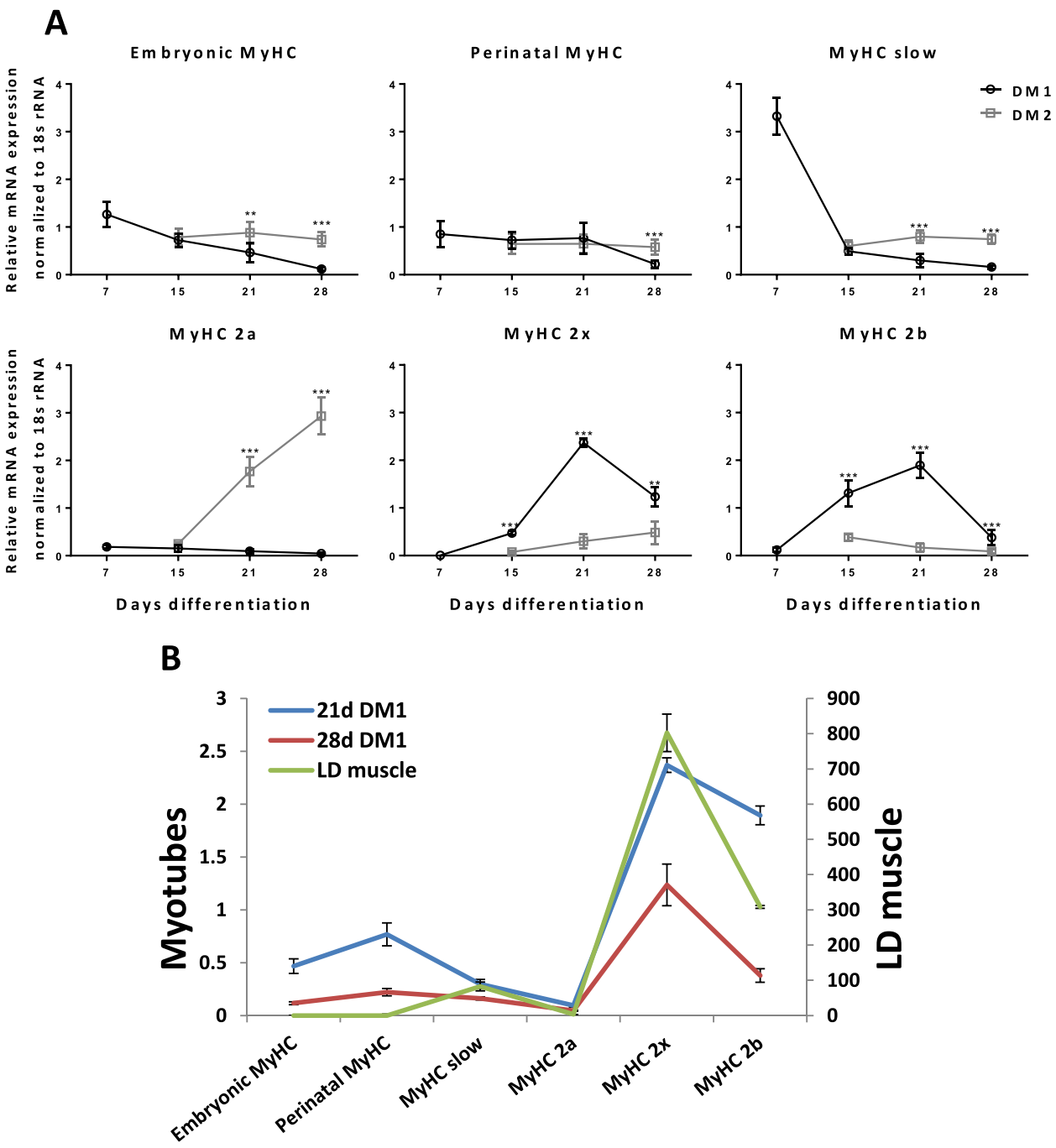

Fig. 4 Extended myotube cultures exhibited phenotype plasticity and postnatal fibre phenotype. **a** Full complement of pre- and post-natal *MyHC* RNA isoforms in myotubes at 7, 15, 21 and 28 days of differentiation were quantified by real-time PCR (normalised to 18S rRNA). Use of DM1 (with Ultroser G) and DM2 (with horse serum) resulted in divergent *MyHC* profiles from day 15 of differentiation. *MyHC* profiles shown are a representative set of three independent experiments. **b** The use of DM1, but not DM2, promoted myotube transition towards a fast-glycolytic *MyHC* profile that resembled postnatal *longissimus dorsi* (LD) muscle of a 22-week-old Duroc pig. Error bars = standard deviation; ** = $P \leq 0.01$, *** = $P \leq 0.001$ based on two-sample unpaired t test at indicated time points

similar changes where reduction in *embryonic* and *perinatal MyHC* expression was accompanied by dominant expression of *MyHC 2x* and *2b* (Fig. 3a). Furthermore, the pattern of relative *MyHC* expression at day 21 and 28 of differentiation in DM1 showed resemblance to the *MyHC* expression profile of a 22 week old pig *longissimus dorsi* muscle (Fig. 4b) [14]. The divergence in *MyHC* profiles between DM1 and DM2 is biologically

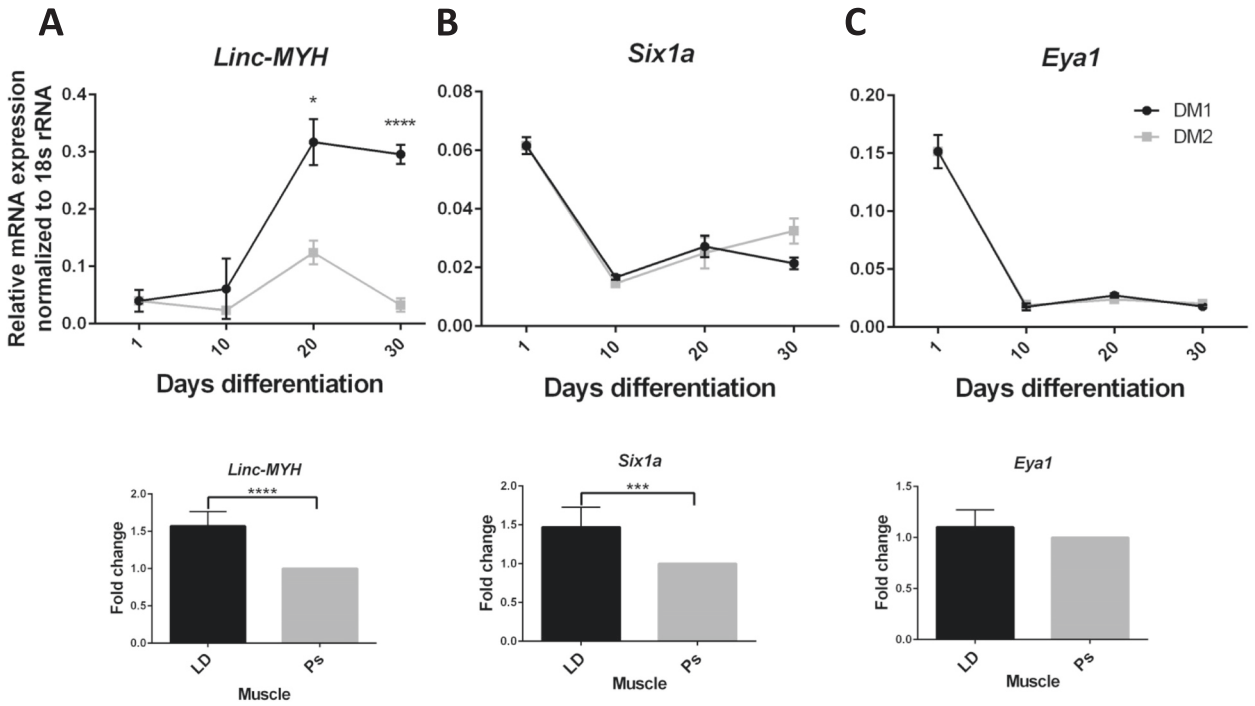

Fig. 5 Induction of *linc-MYH* expression paralleled elevated expression of fast MyHC 2x and 2b in myotubes. The expression of *linc-MYH* (**a**), *Six1* (**b**) and *Eya1* (**c**) was determined by real-time PCR (normalised to 18S rRNA) in extended myotube cultures in DM1 (with Ultroser G) and DM2 (with horse serum), and skeletal muscles: fast *longissimus dorsi* (LD) and slow *psoas* (Ps). Skeletal muscle data shown are the combined results of three sets of LD and Ps from three 22-week-old pigs. Error bars = standard deviation; * = $P \leq 0.05$, *** = $P \leq 0.001$, **** = $P \leq 0.0001$ based on two-sample unpaired t test at indicated time point

significant as it demonstrated the expression plasticity of postnatal *MyHC* genes through the use of different culture media. *In vivo*, early postnatal changes in *MyHC* gene expression that lead to the formation of adult fibre types are dependent on the establishment of corresponding fast and slow motor units, load bearing after birth, and thyroid hormone surge in the case of fast MyHC induction [2]. The ability of our myotubes to adopt fast or slow *MyHC* profile in the absence of innervation indicates that the choice of particular culture conditions is also an important phenotype determinant. DM1 myotube culture over several weeks recapitulated a fast-like postnatal pattern of *MyHC* expression. We have therefore established a 2D culture platform that is conducive to the study of coordinated gene changes that govern fibre type and associated phenotypic alterations.

Acquiring a fundamental understanding of preferential up- or down-regulation of specific MyHC isoforms *in vitro* could facilitate our ability to manipulate phenotypic changes *in vivo* for beneficial biomedical and veterinary outcomes. The present culture platform opens up a convenient controlled environment to investigate a range of mechanisms and factors that are involved in the coordinated expression of muscle gene isoforms, such as the roles of transcription factors like NFATc1 [30], microRNAs [31–33], and anti-sense [34] and linc [20] RNAs in the differential regulation of *MyHC* and other fibre type-specific genes. We can systematically interrogate the role or effectiveness of individual genes or compounds on coordinated MyHC isoform switching or myotube development. As an exemplification, we found that the fast glycolytic myotube phenotype of elevated *MyHC 2x* and *2b* expression (under DM1 culture condition) closely mirrored the rising profile of putative porcine *linc-MYH* RNA expression but not with that of *Six1* and *Eya1*. In muscle, on the other hand, the fast phenotype has been shown to correlate with the up-regulation of *linc-MYH* [20] and the presence or over-expression of Six1 [21, 22, 35]. Our finding of an inverse relationship between *linc-MYH* RNA and *Six1* expression (Fig. 5) suggests that factors other than Six1 could be responsible for the induction of *linc-MYH* RNA in growing myotubes.

Another research opportunity is to examine *in vitro* the role of thyroid hormone and other growth factors in the programming of fast phenotype to dissect the qualitative and quantitative changes of orchestrated gene expression during the transition [34, 36]. Access to largely pure cultures of myotubes of a particular phenotype would also make the isolation of myonuclei and subsequent study of

chromatin modifications much simpler than the use of whole muscle tissues. Finally, extended myotube cultures would allow us to better scrutinise whether there are intrinsic differences in the conferment of myotube phenotype between satellite cells of fast and slow muscles from the same animal or between animals of different ages.

Conclusion

In conclusion, we have made a major technical breakthrough to be able to culture well differentiated porcine myotubes in 2D over an extended period of at least 50 days. Furthermore, we showed that cultured myotubes could be made to adopt a fast adult phenotype of dominant *MyHC 2x* and *2b* expression. For the first time, to our knowledge, we are able to recapitulate the maturation process of myotubes *in vitro*, opening new opportunities to study coordinated postnatal muscle gene expression.

Additional files

Additional file 1: 4 day differentiation LD.avi. Contracting myotubes in DM1 at 4 day differentiation. (AVI 6059 kb)

Additional file 2: 8 day differentiation LD.mp4. Contracting myotubes in DM2 at 8 day differentiation. (MP4 56597 kb)

Additional file 3: 9 day differentiation LD.avi. Contracting myotubes in DM2 at 9 day differentiation. (AVI 182623 kb)

Additional file 4: 27 day differentiation LD.mp4. Contracting myotubes in DM1 at 27 day differentiation. (MP4 3834 kb)

Additional file 5: 60 day differentiation LD.wmv. Contracting myotubes in DM1 at 60 day differentiation. (WMV 2609 kb)

Abbreviations

2D: Two-dimension; MyHC: Myosin heavy chain; linc: Long intergenic non-coding; 3D: Three-dimension; MC+: Maxgel coating mixture; PM: Proliferation medium; DM: Differentiation medium; GFP: Green fluorescence protein; LD: *Longissimus dorsi*.

Competing interests

The authors declare no competing interests. Zoetis Inc. part funded the studentships of SS and LG.

Authors' contributions

KCC and SS conceived and initiated the project. KCC and SVK supervised, designed and technically assisted SS and LG who jointly conducted all the experiments. All authors contributed to the writing and proof reading of the manuscript and approved its submission.

Acknowledgements

SS was supported by a PhD studentship jointly funded by University of Nottingham and Zoetis Inc. LG was supported by a Biotechnology and Biological Sciences Research Council-Zoetis CASE PhD studentship. We thank Zoe Redshaw and Paul Loughna for assistance in Pax immunocytochemistry and primary myoblasts isolation.

Received: 28 July 2015 Accepted: 8 September 2015
Published online: 17 September 2015

References

1. Goldring K, Partridge T, Watt D. Muscle stem cells. J Pathol. 2002;197:457–67.
2. Schiaffino S, Reggiani C. Fiber types in mammalian skeletal muscles. Physiol Rev. 2011;91:1447–531.
3. Cornall L, Hryciw D, Mathai M, McAinch A. Generation and use of cultured human primary myotubes. In: Sundaram C, editor. Muscle biopsy. 1st ed. Croatia: InTech; 2012.
4. Owens J, Moreira K, Bain G. Characterization of primary human skeletal muscle cells from multiple commercial sources. In Vitro Cell Dev Biol. 2013;49:695–705.
5. Partridge TA. Tissue culture of skeletal muscle. Basic cell culture protocols edition. In: Pollard JW, Walker JM, editors. Methods in molecular biology. Totowa, NJ: Humana Press Inc; 1997. p. 131–44.
6. Kubis HP, Haller EA, Wetzel P, Gros G. Adult fast myosin pattern and Ca^{2+} -induced slow myosin pattern in primary skeletal muscle culture. Proc Natl Acad Sci U S A. 1997;94:4205–10.
7. Abdul-Hussein S, van der Vwn PFM, Tajsharghi H. Expression profiles of muscle disease-asociated genes and their isoforms during differentiation of cultured human skeletal muscle cells. BMC Musculoskelet Disord. 2012;13:262.
8. Guex AG, Kocher FM, Fortunato G, Körner E, Hegemann D, Carrel TP, et al. Fine-tuning of substrate architecture and surface chemistry promotes muscle tissue development. Acta Biomater. 2012;8:1481–9.
9. Sakar MS, Neal D, Boudou T, Borochin MA, Li Y, Weiss R, et al. Formation and optogenetic control of engineered 3D skeletal muscle bioactuators. Lab Chip. 2012;12:4976–85.
10. Das M, Wilson K, Molnar P, Hickman JJ. Differentiation of skeletal muscle and integration of myotubes with silicon microstrutures using serum-free medium and a synthetic silane substrate. Nat Protoc. 2007;2:1795–801.
11. Smith AST, Passey S, Greensmith L, Mudera V, Lewis MP. Characterization and optimization of a simple repeatable system for the long term in vitro culture of aligned myotubes in 3D. J Cell Biochem. 2012;113:1044–53.
12. Baqureo-Perez B, Kuchipudi SV, Nelli RK, Chang KC. A simplified but robust method for the isolation of avian and mammalian muscle satellite cells. BMC Cell Biol. 2012;13:16.
13. da Costa N, Beuzen N, Johnston I, McGillivray C, Sun YM, Chang KC. The 5′-end of the porcine perinatal myosin heavy chain gene shows alternative splicing and is clustered with repeat elements. J Muscle Res Cell Motil. 2000;21:183–8.
14. da Costa N, Blackley R, Alzuherri H, Chang KC. Quantifying the temporo-spatial expression of porcine postnatal skeletal myosin heavy chain genes. J Histochem Cytochem. 2002;50:353–64.
15. Sun YM, da Costa N, Birrell R, Archibald AL, Alzuherri H, Chang KC. Molecular and quantitative characterisation of the porcine embryonic myosin heavy chain gene. J Muscle Res Cell Motil. 2001;22:317–27.
16. von Maltzahn J, Jones AE, Parks RJ, Rudnicki MA. Pax7 is critical for the normal function of satellite cells in adult skeletal muscle. Proc Natl Acad Sci U S A. 2013;110:16474–9.
17. Young AP, Wagers AJ. Pax3 induces differentiation of juvenile skeletal muscle stem cells without transcriptional upregulation of canonical myogenic regulatory factors. J Cell Sci. 2010;123:2632–9.
18. Doumit ME, Merkel RA. Conditions for isolation and culture of porcine myogenic satellite cells. Tissue Cell. 1992;24:253–62.
19. Zhu H, Park S, Scheffler JM, Kuang S, Grant AL, Gerrard DE. Porcine satellite cells are restricted to a phenotype resembling their muscle of origin. J Anim Sci. 2013;91:4684–91.
20. Sakakibara I, Santolini M, Ferry A, Hakim V, Maire P. Six homeoproteins and a linc-RNA at the fast MYH locus lock fast myofiber terminal phenotype. PLoS Genet. 2014;10:e1004386.
21. Grifone R, Laclef C, Spitz F, Lopez S, Demignon J, Guidotti JE, et al. Six1 and Eya1 expression can reprogram adult muscle from the slow-twitch phenotype into the fast-twitch phenotype. Mol Cell Biol. 2004;24:6253–67.
22. Hetzler KL, Collins BC, Shanely RA, Sue H, Kostek MC. The homeobox gene *SIX1* alters myosin heavy chain isoform expression in mouse skeletal muscle. Acta Physiol. 2014;210:415–28.
23. Ulitsky I, Bartel DP. lincRNAs: genomics, evolution and mechanisms. Cell. 2013;154:26–46.
24. Glass DJ. Skeletal muscle hypertrophy and atrophy signaling pathways. Int J Biochem Cell Biol. 2005;37:1974–84.
25. Glass DJ. Signalling pathways that mediate skeletal muscle hypertrophy and atrophy. Nat Cell Biol. 2003;5:87–90.
26. Chang KC. Key signalling factors and pathways in the molecular determination of skeletal muscle phenotype. Animal. 2007;1:681–98.
27. Chang KC, da Costa N, Blackley R, Southwood O, Evans G, Plastow G, et al. Relationships of myosin heavy chain fibre types to meat quality traits in traditional and modern pigs. Meat Sci. 2003;64:93–103.

28. Zierath JR, Hawley JA. Skeletal muscle fiber type: influence on contractile and metabolic properties. PLoS Biol. 2004;2:e348.
29. Kahn SE, Hull RL, Utzschneider KM. Mechanisms linking obesity to insulin resistance and type 2 diabetes. Nature. 2006;444:840–6.
30. Ehlers ML, Celona B, Black BL. NFATc1 controls skeletal muscle fiber type and is a negative regulator of MyoD activity. Cell Rep. 2014;8:1639–48.
31. An D, Lessard SJ, Toyoda T, Lee MY, Koh HJ, Qi L, et al. Overexpression of TRB3 in muscle alters muscle fiber type and improves exercise capacity in mice. Am J Physiol Regul Integr Comp Physiol. 2014;306:R925–33.
32. Yeung F, Chung E, Guess MG, Bell ML, Leinwand LA. Myh7b/miR-499 gene expression is transcriptionally regulated by MRFs and Eos. Nucleic Acids Res. 2012;40:7303–18.
33. Sharma M, Juvvuna PK, Kukreti H, McFarlene C. Mega roles of microRNAs in regulation of skeletal muscle health and disease. Front Physiol. 2014;5:239.
34. Pandorf CE, Jiang W, Qin AX, Bodell PW, Baldwin KM, Haddad F. Regulation of an antisense RNA with transition of neonatal to IIb myosin heavy chain during postnatal development and hypothyroidism in rat skeletal muscle. Am J Physiol Regul Integr Comp Physiol. 2012;302:R854–67.
35. Wu W, Ren Z, Zhang L, Liu Y, Li H, Xiong Y. Overexpression of *Six1* gene supresses proliferation and enhances expression of fast-type muscle genes in C2C12 myoblasts. Mol Cell Biochem. 2013;380:23–32.
36. Russell SD, Cambon N, Nadal-Ginard B, Whalen RG. Thyroid hormone induces a nerve-independent precocious expression of fast myosin heavy chain mRNA in rat hindlimb skeletal muscle. J Biol Chem. 1988;263:6370–4.

Submit your next manuscript to BioMed Central and take full advantage of:

- **Convenient online submission**
- **Thorough peer review**
- **No space constraints or color figure charges**
- **Immediate publication on acceptance**
- **Inclusion in PubMed, CAS, Scopus and Google Scholar**
- **Research which is freely available for redistribution**

Submit your manuscript at
www.biomedcentral.com/submit

BioMed Central